Localization and Trafficking of the Death-Inducing Fas Ligand Protein in Cytotoxic T Lymphocytes

by

Ana Laura Clementin

A thesis submitted in partial fulfillment of the requirements for the degree of

Doctor of Philosophy

in

IMMUNOLOGY

Department of Medical Microbiology and Immunology
University of Alberta

ABSTRACT

Cytotoxic T lymphocytes (CTL) can kill tumor cells and cells infected with intracellular pathogens. Their two major killing mechanisms are the degranulation pathway and the Fas-FasL pathway. The degranulation process consists of the release of cytolytic perforin and granzyme molecules that are stored within lysosomal granules. The cytolytic components of granules contain sorting signals within their sequences that act as signals to direct their transport to lysosomes after their biosynthesis. When CTL become stimulated after encountering their target cells, the granules move along microtubules to the contact point with the target cell where a set of vesicle trafficking proteins mediate the specific fusion of the granules with the plasma membrane allowing the release of their cytolytic contents. The Fas-FasL pathway consists of the expression of Fas ligand (FasL) on the surface of CTL, which after binding to its receptor (Fas), triggers the apoptotic death of the Fas-expressing target cells. Previous experiments from our laboratory have shown that target-cell engagement leads to two "waves" of FasL surface expression on CTL. The first is thought to result from the rapid translocation of stored molecules and the second is believed to be product of the surface transport of newly synthesized proteins. The research objective for this work was to identify the storage compartment that harbors FasL in unstimulated CTL and to determine the trafficking route that the pre-synthesized stored pool of FasL molecules follow to reach their storage compartment.

Using confocal microscopy colocalization analysis, I demonstrated that FasL is stored in intracellular vesicles that also contain the proteins Syntaxin 3, Munc18-2 and Rab32 and that these compartments are distinct from the lysosomal granules. Moreover, I found that FasL is endocytosed from the plasma membrane using a signal in its cytoplasmic tail and from there targeted to its storage vesicle via a tri-lysine motif. Furthermore, I found evidence that the motor protein myosin and the SNARE protein Syntaxin 3 affect the translocation of FasL to the surface.

The findings presented in this report strongly indicated that the storage vesicle of FasL is distinct from lysosomal granules and suggested that it must thus be differentially regulated. It also provided markers for the FasL storage vesicle, and insight into the trafficking mechanism of this protein. Understanding how FasL trafficking is regulated will allow the manipulation of this killing pathway and to decipher its contribution during an immune response.

PREFACE

Figure 5.13 in chapter 5 is a collaborative work. I designed the experiments but data collection was performed by Colleen Reid under my supervision.

ACKNOWLEDGMENTS

Many people have contributed to my overall technical and conceptual formation and many more people have contributed to generating a friendly working environment that overall allowed me to complete this thesis. Although a detailed enumeration of their names would be too extensive, I would like to give special thanks to:

My supervisor, Dr. Ostergaard, for her constant encouragement and guidance.

The members of my supervisory committee, Drs. Rob Ingham and Troy Baldwin, for their advice and feedback.

My labmates from the Ostergaard and Kane labs, for their technical assistance as well as for their moral support.

My friends, some of which even helped me with scientific discussions.

And most importantly, my parents and my husband for their incredible patience and caring support.

TABLE OF CONTENTS

CHAPTER 1: Introduction 1

1.1. Overview of the Immune System 1

1.2. Biology of T cells 2

1.2.1. Activation and differentiation of T cells 2

1.2.2. CTL activation signals 3

1.3. CTL killing mechanisms 5

1.3.1. Degranulation pathway 5

1.3.2. Fas-FasL pathway 7

1.3.3. TNF-α 7

1.4. Fas-FasL pathway 8

1.4.1. Functions of the Fas-FasL pathway 8

1.4.2. Fas-FasL as the trigger of apoptosis 11

1.4.3. FasL structure 12

1.4.4. Regulation of FasL 14

1.4.4.1. Transcriptional regulation of FasL 14

1.4.4.2. Post-translational regulation of FasL 15

1.4.5. FasL localization 16

1.5. Vesicle transport 17

1.5.1. Vesicle budding 18

1.5.2. Vesicle tethering: Rab proteins 20

1.5.3. Vesicle fusion: SNAREs 22

1.6. Trafficking of cytolytic granule components 23

1.6.1. Targeting to cytolytic granules 23

1.6.2. Trafficking to the surface 24

1.7. Hypothesis and objectives 26

CHAPTER 2: Materials and Methods 27

2.1. Cells 27

2.2. Antibodies 27

2.3. Reagents 28

2.4. Mutagenesis of FasL *30*
2.4.1. Deletion mutagenesis of FasL 30
2.4.2. Site-directed mutagenesis of FasL 31
2.5. CTL stimulation with PMA and ionomycin *32*
2.6. Transient transfection of CTL *33*
2.7. Transient transfection of COS-1 cells *33*
2.8. Cell lysis and immunoprecipitation *34*
2.9. Pull-down assay *34*
2.10. SDS-PAGE and Coomasie Blue Staining *35*
2.11. Mass spectrometry *35*
2.12. Western Blotting *36*
2.13. Flow cytometry analysis *36*
2.14. Active Caspase 3 assay for FasL-mediated cytotoxicity *36*
2.15. Confocal microscopy analysis *37*
2.16. Endocytosis microscopy assay *38*
2.17. Statistical analysis *39*

CHAPTER 3: Identification and Characterization of the Storage Vesicle for FasL in Cytotoxic T Lymphocytes 40

3.1. Introduction *40*
3.2. Results *41*
3.2.1. FasL is not stored in late endosomes or lysosomal granules 41
3.2.2. FasL is not stored with TNF-α or PD-1 44
3.2.3. FasL appears to be located near MAMs 48
3.2.4. FasL is stored with Rab32 51
3.2.5. FasL is stored with Syntaxin 3 and Munc18-2 51
3.2.6. The FasL storage vesicle is distinct from the cytolytic granules 53
3.2.7. FasL cannot be detected in molecular complexes with Stx3, Rab32 or Munc18-2 59
3.2.8. FasL is stored in $Stx3^{+}$ $Munc18\text{-}2^{+}$ $Rab32^{+}$ $LAMP\text{-}1^{-}$ $perforin^{-}$ vesicles in CTL Clone 11 cells 64
3.2.9. FasL is stored in $Stx3^{+}$ $LAMP\text{-}1^{-}$ vesicles in CTL CTLL-2 cells 70

3.2.10. The stored pool of FasL remains in the same vesicle after stimulation 70
3.3. Discussion *74*

CHAPTER 4: Characterization of the FasL trafficking route in Cytotoxic T lymphocytes 81
4.1. Introduction *81*
4.2. Results *83*
4.2.1. FasL is located on the surface in COS-1 cells 83
4.2.2. FasL is endocytosed from the cell surface 89
4.2.3. Cycling of FasL between the surface and its storage vesicle 91
4.2.4. FasL has no detectable association with components of the recycling pathway 93
4.2.5. Syntaxin 3 affects FasL localization in COS-1 cells 98
4.2.6. Syntaxin 3 affects FasL trafficking in CTL 102
4.2.7. Rab32 has no detectable effect on FasL trafficking 104
4.2.8. Myosin affects FasL translocation to the surface after stimulation 109
4.3. Discussion *110*

CHAPTER 5: Identification of FasL sequences important for trafficking in Cytotoxic T Lymphocytes 118
5.1. Introduction *118*
5.2. Results *121*
5.2.1. Both the N-terminal and C-terminal ends of FasL contain important trafficking sequences 121
5.2.2. The self-assembly domain is necessary for translocation after stimulation 132
5.2.3. Glycosylation is important for FasL trafficking 134
5.2.4. N-terminal domain of FasL is important for endocytosis and targeting to FSVs in CTL 143
5.2.5. Lysines 71, 72 and 73 are important for FasL targeting to FSVs ... 148
5.2.6. FasL has no detectable ubiquitin or SUMO modifications 151
5.3. Discussion *160*

CHAPTER 6: General Discussion 169
6.1. Summary of Results 169
6.2. Components of the FasL storage vesicle 172
6.2.1. Syntaxin 3 172
6.2.2. Munc18-2 174
6.2.3. Rab32 175
6.2.4. Markers of the FSV 176
6.2.5. FSVs are distinct from lysosomal granules 177
6.3. Trafficking of FasL in CTL 178
6.3.1. Targeting to FSVs 178
6.3.2. Trafficking to the surface upon stimulation 182
6.4. Model of FasL trafficking 183
6.5. Future directions 186
6.5.1. Trafficking to FSVs 186
6.5.2. Trafficking to the surface upon stimulation 188
REFERENCES 190
APPENDIX 222

LIST of FIGURES

Figure 1.1. Illustration of FasL domains and motifs. *13*
Figure 1.2. General steps of vesicle transport. *19*
Figure 1.3. Cycles for membrane association/dissociation and GTP hydrolysis of Rab proteins. *21*

Figure 3.1. FasL is not stored in late endosomes *43*
Figure 3.2. FasL is not stored in lysosomal granules. *45*
Figure 3.3. TNF-α is expressed after stimulation and is not found with FasL. *47*
Figure 3.4. FasL is not stored with PD-1. ..... *49*
Figure 3.5. FasL is stored near the mitochondria. *50*
Figure 3.6. FasL is stored near the mitochondria-associated membranes. *50*
Figure 3.7. FasL is stored with Rab32. ..... *52*
Figure 3.8. FasL is stored with Stx3 and Munc18-2. ..... *54*
Figure 3.9. Stx3 is stored with Rab32 and Munc18-2. ..... *56*
Figure 3.10. Stx3 and Rab32 are not stored in lysosomal granules. *58*
Figure 3.11. FasL has no detectable association with Stx3 or Rab32. ..... *62*
Figure 3.12. FasL has no detectable association with Munc18-2. ..... *63*
Figure 3.13. FasL is stored with Stx3, Munc18-2 and Rab32 in Clone 11 cells. . *66*
Figure 3.14. FasL is not stored in cytolytic granules in Clone 11 cells. *67*
Figure 3.15. Stx3 is stored with Munc18-2 and Rab32 in vesicles distinct from lysosomal granules in Clone 11 cells. *69*
Figure 3.16. FasL and Stx3 are stored together in vesicles distinct from lysosomal granules in CTLL-2 cells. *72*
Figure 3.17. FasL is stored with Stx3 and Rab32 in CTL Clone 3/4 cells after stimulation. *73*
Figure 3.18. FasL is stored with Stx3 and Rab32 in CTL Clone 11 cells after stimulation. *75*

Figure 4.1. Transfected DsRed-FasL is predominantly located on the surface of COS-1 cells. *84*

Figure 4.2. Transfected DsRed-FasL is located in Stx3$^+$ LAMP-1$^-$ intracellular vesicles in CTL Clone 3/4. ..... *86*
Figure 4.3. Transfected DsRed-FasL is located in Stx3$^+$ LAMP-1$^+$ intracellular vesicles in CTL Clone 11. ..... *87*
Figure 4.4. Transfected DsRed-FasL is located in Stx3$^+$ LAMP-1$^+$ intracellular vesicles in CTLL-2 cells. *88*
Figure 4.5. General alternatives for FasL trafficking in CTL. *90*
Figure 4.6. Antibodies against FasL are endocytosed from the cell surface. *92*
Figure 4.7. Protein synthesis is not necessary for FasL surface detection, endocytosis and FSV targeting. *94*
Figure 4.8. FasL does not colocalize with Rab4. ..... *96*
Figure 4.9. FasL does not colocalize with Rab4, Rab11, Rab5 and Rab8. ..... *97*
Figure 4.10. Stx3 has no detectable effect on surface FasL expression in COS-1 cells. *99*
Figure 4.11. Stx3 affects the localization of FasL in COS-1 cells. *101*
Figure 4.12. Stx3 has no detectable effect on surface FasL expression in stimulated CTL. *103*
Figure 4.13. Stx3 increases surface FasL expression in unstimulated CTL. *105*
Figure 4.14. Rab32 has no detectable effect on surface FasL expression in unstimulated CTL. *107*
Figure 4.15. Rab32 has no detectable effect on surface FasL expression in stimulated CTL. *108*
Figure 4.16. Myosin affects FasL surface expression after stimulation. *112*

Figure 5.1. Sequence of the N-terminal end of mouse FasL. *120*
Figure 5.2. Structure of the DsRed-tagged chimeras of FasL and Ly49A. *122*
Figure 5.3. The FasL chimeras have no detectable defect in expression, localization or function in COS-1 cells. *124*
Figure 5.4. DsRed-Ly49A is located on the surface of CTL. *126*
Figure 5.5. DsRed-FasL/Ly49A and DsRed-Ly49A/FasL are located on the surface and intracellular vesicles in CTL. *128*

Figure 5.6. Colocalization scoring criteria. *130*
Figure 5.7. Intracellular DsRed-FasL/Ly49A is located in Stx3$^-$ LAMP-1$^-$ vesicles and DsRed-Ly49A/FasL is located in Stx3$^-$ LAMP-1$^+$ vesicles. *131*
Figure 5.8. Structure of the DsRed-tagged FasL C-terminal mutant constructs. *133*
Figure 5.9. DsRed-FasL ΔSA is located in intracellular Stx3$^+$ LAMP-1$^-$ vesicles. *136*
Figure 5.10. DsRed-FasL ΔSA is not translocated to the surface after stimulation. *137*
Figure 5.11. DsRed-FasL N117Q and N258Q are in intracellular vesicles while DsRed-FasL N182Q is located on the surface and intracellular vesicles. *139*
Figure 5.12. DsRed-FasL N117Q and N258Q are in Stx3$^+$ LAMP-1$^-$ vesicles while intracellular DsRed-FasL N182Q is located in Stx3$^-$ LAMP-1$^+$ vesicles. *142*
Figure 5.13. Glycosylation in N258 affects FasL surface expression in COS-1 cells. *144*
Figure 5.14. Structure of the DsRed-tagged FasL N-terminal deletion mutant constructs. *145*
Figure 5.15. DsRed-FasL Δ2-43, ΔPRD, and Δ3K are located on the surface and intracellular vesicles in CTL. *147*
Figure 5.16. Intracellular DsRed-FasL Δ2-43 and ΔPRD are located in Stx3$^+$ LAMP-1$^-$ vesicles while Δ3K is found in Stx3$^-$ LAMP-1$^+$ vesicles. *150*
Figure 5.17. Structure of the DsRed-tagged FasL lysine mutant constructs. *152*
Figure 5.18. DsRed-FasL K71A, K72A and K73A are located on the surface and in intracellular vesicles in CTL. *153*
Figure 5.19. Intracellular DsRed-FasL K71A, K72A and K73A are located in Stx3$^-$ LAMP-1$^+$ vesicles. *155*
Figure 5.20. Ubiquitination of FasL was not detected in CTL Clone 3/4 or CTLL-2 cells. *158*
Figure 5.21. SUMOylation of endogenous FasL was not detected in CTL Clone 3/4 or CTLL-2 cells. *161*
Figure 5.22. Model for trafficking of FasL mutant constructs in CTL. *167*

Figure 6.1. Lysines 71, 72 and 73 are exposed to the solvent. *181*
Figure 6.2. LIGHT and TWEAK contain 3-4 positively charged residues near the transmembrane domain, similar to FasL. *181*
Figure 6.3. Model for trafficking of FasL in CTL. *184*
Figure 6.4. Model for trafficking of FasL in COS-1 cells. *185*

Appendix Figure 1. Rab32 has no detectable effect on FasL localization. *222*
Appendix Figure 2. GFP-FasL is not stored in Stx3$^+$ vesicles. *222*

LIST OF TABLES

Table 2.1. Primers used in the construction of deletion mutants..... 31

Table 2.2. Primers used in the site-directed mutagenesis of FasL 32

LIST OF ABBREVIATIONS

AC8	adenylyl cyclase 8
AICD	activation-induced cell death
AP	adaptor protein
AP-1	activator protein 1
Apaf-1	apoptotic protease activating factor 1
APC	antigen-presenting cell
APLS	autoimmune lymphoroliferative syndrome
APRIL	a proliferation-inducing ligand
ARF	ADP-ribosylation family
BACE1	β-site amyloid precursor protein-cleaving enzyme
BAFF	B cell activating factor
Bak	Bcl-2 homologous antagonist/killer
Bax	Bcl-2 associated X protein
BCR	B cell receptor
Bid	BH3 interacting-domain death agonist
BiP	Binding immunoglobulin protein
BSA	bovine serum albumin
CHX	cyclohexamide
CI-MPR	cation-independent mannose-6-phsophate receptor
CKI	casein kinase I
CLN5	Ceroid lipofuscinosis neuronal protein 5
COP	coat protein
cSMAC	central supramolecular activation complex
CTL	cytotoxic T lymphocyte
CTLA-4	Cytotoxic T-Lymphocyte Antigen 4
DAG	diacylglycerol
DC	dendritic cell
dCS	defined bovine calf serum
DD	death domain
DED	death-effector domain
DISC	death-inducing signaling complex
DMEM	Dulbecco's modified Eagle's medium
DMSO	dimethyl sulfoxide
DNA	deoxyribonuclein acid
dSMAC	distal supramolecular activation complex
DsRed	*Discosoma* sp. red fluorescent protein
ECL	enhanced chemioluminisence
EDTA	ethylenediaminetetracetic acid
Egr	early growth response
EGTA	ethylene glycol tetra-acetic acid
ERK	extracellular signal-regulated kinase
FADD	Fas-associated DD containing protein
FasL	Fas ligand
FBS	fetal bovine serum

FHL	familial haemophagocytic lymphohistiocytosis
FSC	fetal calf serum
FSV	FasL storage vesicle
GADS	Grb2-related adaptor downstream of Shc
GAP	GTPase-activating protein
GDF	GDI displacement factor
GDI	GDP dissociation inhibitor
GDP	guanine 5'-diphsophate
GEF	guanine exchange factor
GFP	green fluorescent protein
GITRL	glucocorticoid-induced TNFR family related ligand
GluR6	flutamate receptor subunit 6
Grb2	growth factor receptor-bound protein 2
GST	gluthatione S-transferase
GTP	guanine 5'-triphsophate
His	histidine
HRP	horseradish peroxidase
IC	isotype control
ICER	inducible cyclic adenosine monophosphate early repressor
IFN	interferon
IL	interleukin
IP	immunoprecipitation
IP3	inositol-1,4,5-triphosphate
IPTG	Isopropyl β-D-1-thiogalactopyranoside
IRAP	Insulin-responsive aminopeptidase
IRF-1	Interferon regulating factor-1
Itk	interleukin-2-inducible T cell kinase
IV	intracellular vesicles
JNK	c-Jun N-terminal kinase
KO	knock-out
LAMP-1	lysosomal-associated membrane protein
LAT	linker for activation of T cells
Lck	lymphocyte-specific protein tyrosine kinase
LPS	lipopolysaccharide
M	membrane
M + IV	membrane and intracellular vesicles
M_1	Manders coefficient
M6P	mannose-6-phsophate
M6PR	mannose-6-phosphate receptor
MAM	mitochondria-associated membrane
mFasL	membrane-bound FasL
MHC	major histocompatibility complex
MTOC	microtubule-organizing center
NF-κB	nuclear factor kappa B
NFAT	nuclear factor of activated T cells
NK	natural killer

NP	nucleoprotein
NP-40	nonidet P-40
NS	not significant
NSF	N-ethylmaleimide-sensitive factor
PAMP	pathogen-associated molecular pattern
PBS	phosphate-buffered saline
PCR	polymerase chain reaction
PD-1	programmed-death 1
PE	phycoerythrin
PIP2	phosphatidylinositol-4,5-biphosphate
PKC	protein kinase C
PMA	phorbol 12-myristate 13-acetate
PRD	proline-rich domain
PRR	pattern-recognition receptor
PS	pre-imune control sera
pSMAC	peripheral supramolecular activation complex
r	Pearson coefficient
RB	receptor-binding site
RPMI	Roswell Park Memorial Institute
SA	self-assembly
SDS-PAGE	sodium dodecyl sulphate polyacrylamide gel electrophoresis
sFasL	soluble FasL
SLP	synaptogamin-like protein
SLP-76	SH2 domain-containing leukocyte protein 76
SM	Sec/Munc-like
SNAP	synaptosomal associated protein
SNARE	soluble NSF attachement receptor
SOS	son of sevenless homologue
SUMO	small ubiquitin-like modifier
t-SNARE	target-SNARE
TACE	TNF-α converting enzyme
TAE	Tris-acetate EDTA
TAPI	TNF-α processing inhibitor
TCR	T cell receptor
TfR	transferrin receptor
TGF-β	transforming growth factor β
TGN	trans-Golgi network
THD	TNF homology domain
TM	transmembrane
TNF	tumor necrosis factor
TNFR	tumor necrosis factor receptor
TRAIL	TNF-related apoptosis inducing ligand
TRPM8	Transient receptor potential cation channel subfamily M member 8
TWEAK	TNF-related weak inducer of apoptosis
Uq	ubiquitin
v-SNARE	vesicle-SNARE

VAMP	vesicle-associated membrane protein
VIP36	vesicular integral membrane protein of 36 kDa
WB	Western Blot
WT	wild type
ZAP-70	zeta-associated protein 70

CHAPTER 1: Introduction

1.1. Overview of the Immune System

The main function of the immune system is to protect organisms from potential harm. Its major task consists of destroying invading microorganisms, such as viruses, bacteria and parasites; but it also has a fundamental importance in combating cancer cells. The immune system is composed of two branches: innate and adaptive immunity. Some of the cellular components of innate immunity are macrophages, dendritic cells, neutrophils, monocytes, eosinophil and natural killer (NK) cells. These cells provide the first line of defense after a microorganism breaches the anatomical barriers of the organism. They detect structures common to numerous microbes, known as pathogen-associated molecular patterns (PAMPs), using pattern-recognition receptors (PRR) (Janeway and Medzhitov 2002). This interaction triggers a signaling cascade within the immune cells that results in their activation. Activated innate immune cells secrete antimicrobial peptides, which directly kill pathogens in different ways, as well as cytokines and chemokines to aid in the recruitment, activation and differentiation of other components of the immune system (Mogensen 2009). Moreover, activation of macrophages and dendritic cells increases their migration to lymph nodes where they act as antigen-presenting cells (APCs) and activate components of the adaptive immune system (Iwasaki and Medzhitov 2004).

Cells of the adaptive immune system can recognize a vast repertoire of pathogenic structures, and in contrast to innate immunity, it provides an enhanced "adapted" response upon repeat exposure to the same antigen. The major components of the adaptive immune system are B and T cells. They contain similar receptors in their surface, B cell receptors (BCRs) and T cell receptors (TCRs), that are generated by somatic recombination and provide these cells with the ability to recognize a large number of pathogenic protein and carbohydrate structures resulting in the initiation of an immune response upon recognition. After they are generated in the bone marrow and before they are allowed to

circulate through the organism, cells undergo positive and negative selection processes. Through positive selection, T cells with TCRs able to bind to MHC-peptide complexes survive the process of elimination. However, T cells that recognize "self" proteins with high affinity are eliminated through negative selection. This latter process, known as central tolerance, helps to avoid the response against structures present within the proteins of the host itself, which would result in autoimmunity.

1.2. Biology of T cells

1.2.1. Activation and differentiation of T cells

After being educated and selected in the thymus, naïve T cells migrate through the blood to secondary lymphoid tissues and recirculate via the lymphatic system searching for their cognate antigen. There are two major types of T cells, those that express the CD4 co-receptor and those that express CD8. If an intracellular pathogen invades an organism, naïve $CD8^+$ T cells bearing TCRs that can bind to the MHC I-bound antigenic peptides interact with APCs presenting peptides from the invading pathogens on their surface within the context of major histocompatibility complex type I (MHC I) molecule. These cells interact through the TCR:MHC/peptide complex aided by the CD8 co-receptor that also binds to MHC I. This interaction triggers an intracellular signaling cascade that provides the first T cell activation signal. Activated APCs also upregulate the costimulatory surface molecule B7 which binds to the T cell surface protein CD28, serving as the second activation signal. Cytokines provide the third signal for T cell activation and allow for their differentiation (Curtsinger and Mescher 2010).

Extracellular pathogens are usually endocytosed and degraded intracellularly by APCs. The products of this degradation, antigenic peptides, are loaded on MHC class II molecules, expressed on the surface and presented for recognition by T cells that express the CD4 co-receptor. As with $CD8^+$ T cells, the

TCR/CD4 interaction provides the first activation signal and interaction with CD28 then further allows for the full activation of $CD4^+$ T cells.

T cell activation leads to their differentiation into effector cells. Effector T cells express different chemokine receptors that drive them to various tissues where they exert their functions. $CD4^+$ T cells become T helper cells that aid in the activation of B cells and secrete cytokines to amplify and regulate the immune response. $CD8^+$ T cells differentiate into cytotoxic T lymphocytes (CTL), which are in a primed state that allows them to efficiently kill their targets after receiving only the first activation signal. That is, target cells bearing the appropriate antigenic peptide on the context of their surface MHC I are killed within minutes after CTL recognize them through their TCR. After inducing target cell apoptosis, CTL can disengage and continue searching for additional targets.

1.2.2. CTL activation signals

CTL migration ceases upon its interaction with their target cell. This allows for the recruitment of receptors and signaling molecules to the point of contact, forming immunological synapses (Dustin and Long 2010). This antigen-specific cell-to-cell conjugation has a very specific conformation with a shape of a bull's eye and has been described in detail for the T cell-APC interaction involved in naïve T cell activation. The receptors involved in target recognition, such as the TCR and CD8, are mainly focused in a central supramolecular activation complex (cSMAC) while the molecules responsible for the adhesion of the T cell and the target cell are located on an outer concentric ring denominated the peripheral supramolecular activation complex (pSMAC) (Monks et al. 1998). Large molecules such as CD45, a phosphatase involved in regulating the TCR, are excluded to the outer ring of the distal supramolecular activation complex (dSMAC) (Huppa and Davis 2003). Cytotoxic synapses have a similar shape, with the additional presence of a "secretory domain" within the cSMAC (Stinchcombe et al. 2001b). TCR engagement triggers a cascade of signaling events that results in protein phosphorylation, increase in Ca^{++} levels, cytoskeleton rearrangements,

and the activation of transcriptional factors. The TCR complex includes the TCR α and β chains that confer antigen recognition and the associated CD3 complex that, upon TCR engagement, becomes rapidly phosphorylated by members of the Src family of protein tyrosine kinases (Straus and Weiss 1992). The kinase ZAP-70 then associates with the phosphorylated residues of CD3 and phosphorylates the adapter molecules LAT and SLP-76 which allow for the generation of a protein complex that includes Grb2, GADS, SOS, Vav-1 and the kinase Itk (Samelson 2002). Activation of phospholipase Cγ1, via phosphorylation by Itk, results in hydrolysis of membrane-bound phosphatidylinositol-4,5-biphosphate (PIP_2) into inositol-1,4,5-triphosphate (IP_3), and diacylglycerol (DAG). Both of these products have important roles in the activation signaling cascade of T cells. IP_3 triggers the release of Ca^{++} from intracellular ER stores that leads to the opening of calcium-release-activated channels in the plasma membrane to promote the entry of extracellular Ca^{++} (Acuto and Cantrell 2000). The increase in the level of intracellular Ca^{++} is translated by calmodulin into the activation of the phosphatase calcineurin that dephosphorylates NFAT family transcription factors allowing their translocation to the nucleus to exert its function. DAG, the other hydrolysis product of PIP2, activates protein kinase C that regulates various downstream targets resulting in cytoskeletal changes and activation of transcription factors (Cronin and Penninger 2007). DAG also activates RasGRP leading to the activation of Ras and the downstream Erk/MAP kinase pathway, which can regulate numerous other pathways including the activation of transcription factors (Roose et al. 2005). The sum of these events leads to the activation of CTL.

Additionally, TCR ligation also triggers the re-orientation of the microtubule-organizing center (MTOC), from which microtubules grow. The MTOC dissociates form its position near the nuclear membrane and moves toward the TCR (Dustin and Long 2010). This polarization of the cytoskeleton allows for the efficient release of cytolytic molecules within the CTL towards the "secretory domain" in the synapse and the site of contact with the target cell (Stinchcombe and Griffiths 2007).

1.3. CTL killing mechanisms

CTL-mediated lysis of target cells can occur by two general mechanisms: the degranulation of cytolytic molecules, and the expression of Fas ligand (FasL). In addition, the secretion of TNF-α has also been shown to be a part of the death-inducing activity of CTL (Guidotti et al. 1996, Lee et al. 1996, Suk et al. 2001).

1.3.1. Degranulation pathway

The degranulation process involves the release of cytolytic molecules stored in specialized vesicles denominated "granules". Granules are dual-function organelles derived from lysosomes. They contain lysosomal proteins as well as the cytolytic components. These organelles have an acidic pH and perform the degradative functions of the cells (Burkhardt et al. 1990). However, unlike regular lysosomes, they fuse with the plasma membrane upon T cell activation. They share characteristics with other "secretory lysosomes" that secrete their contents to the extracellular environment in response to external stimuli (Blott and Griffiths 2002). Such specialized organelles exist in different cell types, such as melanosomes in melanocytes, platelet dense granules, basophil granules and neutrophil azurophil granules, among others (Dell'Angelica et al. 2000). The importance of storing cytolytic molecules resides in the ability of the T cell to precisely control the time and place of their release, triggered only at the time of target cell encounter and solely at the point of contact between the target and the T cell.

The granules have two major cytolytic components: perforin and granzymes. Perforin has been shown to play an important part in T cell-mediated cytotoxicity as evidenced by perforin knock out (KO) mice that display defects in *in vitro* cytotoxicity assays as well as *in vivo* resistance to viral and intracellular bacterial infections and tumor clearance (Catalfamo and Henkart 2003). Moreover, patients with human familial haemophagocytic lymphohistiocytosis type 1 (FHL1) have perforin mutations leading to defective cytotoxic lymphocyte

function (Stepp 1999). However, the exact mechanism of cytotoxicity employed by perforin remains controversial. It was originally believed that perforin induced lysis by punching holes on the membrane of the target cell. Electron microscopy experiments showed that isolated perforin oligomerizes on the target cell membrane to form pores (Podack et al. 1985). It was then hypothesized that these pores allowed for the delivery of granzymes inside the target cell, which then triggered target cell apoptosis (Barry and Bleackley 2002, Catalfamo and Henkart 2003). However, it was later shown that granzyme B could enter target cells in the absence of perforin (Shi et al. 1997) thus challenging the original postulation for perforin-mediated delivery. It was then postulated that membrane damage caused by perforin could trigger target-cell mediated repair mechanisms that would result in the internalization of both perforin and granzymes and that subsequently, perforin would have a role in releasing the granzymes from the target endocytic compartments (Thiery et al. 2011). Recently, however, this hypothesis has also been questioned by the analysis of the crystal structure of perforin that suggests it is unlikely that perforin creates small pores and advocates for a mechanism where plasma membrane pores formed by perforin allow for passive diffusion of granzymes (Lopez et al. 2012). Although the controversy is still unresolved, these alternatives for the function of perforin may not be mutually exclusive.

T lymphocytes also contain at least eleven different serine esterases denominated granzymes A-M (Barry and Bleackley 2002). Of these, granzymes A and B are the best characterized. Granzyme B cleaves target-cell caspases 3 and 8 at internal aspartate residues (Harris et al. 1998). Cleavage of caspases activates them and induces apoptosis. Granzyme B can also initiate caspase-independent apoptosis by cleaving the pro-apoptotic protein Bid which translocates to the mitochondria and activates the pro-apoptotic regulators Bax and Bak, resulting in the release of cytochrome c and apoptosis induction (Barry and Bleackley 2002). Granzyme A initiates a caspase-independent cell death pathway, causing nicks in single-stranded DNA and preventing cellular repair, consequently forcing the cells to undergo apoptosis (Beresford et al. 2001). As discussed before, the mechanism by which granzymes reach the inside of target cells is still uncertain.

Besides the various perforin-mediated mechanisms mentioned above, granzyme B has been shown to bind the cation-independent mannose-6-phosphate receptor (CI-MPR) on the surface of target cells (Motyka et al. 2000) although CI-MPR-independent granzyme-mediated cell death suggests this pathway may be sufficient but not necessary for cytotoxicity (Dressel et al. 2004).

After CTL encounter their target cells bearing the appropriate peptide-MHC complexes, cytolytic granules move along microtubules to the contact point where a fraction of the granules fuse with the plasma membrane and the contents are directionally released to the target cell resulting in rapid target cell death (Trambas and Griffiths 2003).

1.3.2. Fas-FasL pathway

Before the identification of FasL, it was observed that T cells could kill target cells using a Ca^{++}-independent pathway distinct from the degranulation pathway (Ostergaard et al. 1987, Trenn et al. 1987). This killing mechanism was later shown to be the Fas-FasL pathway (Rouvier et al. 1993).

The FasL-mediated killing pathway involves the interaction of Fas ligand, expressed on the surface of T cells with the Fas receptor on the surface of the target cell. This interaction leads to the activation of an intracellular signaling cascade that results in the apoptotic death of the target cell. Because Fas is constitutively expressed on a variety of tissues (Watanabe-Fukunaga et al. 1992b), the expression of FasL on CTL must be tightly regulated to avoid non-specific target cell killing. FasL is the focus of this thesis, therefore, its functions, structure, and regulation is discussed in further detail in section 1.4.

1.3.3. TNF-α

CTL can also secrete cytokines, such as TNF-α, to induce target cell killing (Ratner and Clark 1993, Lee et al. 1996, Suk et al. 2001, Sabri et al. 2003). TNF-α binds to its receptors TNFR1 or 2 on target cells and induces caspase-

mediated apoptosis (Baker and Reddy 1998). This killing mechanism is believed to have a major importance in the non-specific destruction of virus-infected cells that have escaped CTL detection by down-regulating MHC I expression on their surface (Wohlleber et al. 2012).

1.4. Fas-FasL pathway

1.4.1. Functions of the Fas-FasL pathway

The Fas-FasL pathway is mostly known for its role as a CTL cytotoxicity mechanism that functions in conjunction with the degranulation pathway to induce target cell death. Although the differential roles of these pathways in killing specific targets are not clear yet, it is believed that FasL may be required for clearing persistent infections (Rode et al. 2004, Zelinskyy et al. 2004, Shrestha and Diamond 2007) and that it contributes to virus clearance and selection of CTL escape variants of Influenza virus (Price et al. 2005). Regarding tumor clearance, publications suggest FasL-mediated lysis may be important for the regression or elimination of some tumors *in vivo* (Seki et al. 2002, Caldwell et al. 2003, Dobrzanski et al. 2004).

Besides the canonical function of the Fas-FasL pathway in CTL-mediated induction of apoptosis of infected and tumor cells, this pathway has been shown to have multiple additional roles in different aspects of the immune system. The relevant role of the Fas-FasL pathway in immune homeostasis and prevention of autoimmunity became apparent after the analysis of naturally occurring mutant mice carrying mutations in Fas and FasL. Lymphoproliferative disorder (*lpr*) mice have a retroviral transposon in the *fas* gene that reduces the expression of Fas (Watanabe-Fukunaga et al. 1992a). Generalized lymphoproliferative disorders (*gld*) mice have a single point mutation in the *fasL* gene causing the synthesis of a mutant FasL protein unable to bind to Fas (Takahashi et al. 1994). These mutations cause the accumulation of potentially autoreactive T cells, lymphadenopathy and splenomegaly. They develop arthritis or nephritis and die at

around 5 months of age (Watanabe-Fukunaga et al. 1992a, Takahashi et al. 1994). In humans, a similar disease, the autoimmune lymphoproliferative syndrome (ALPS) has also been associated with defects in Fas and FasL (Rieux-Laucat et al. 2003, Del-Rey et al. 2006, Magerus-Chatinet et al. 2013). ALPS patients have massive lymphadenopathy and splenomegaly and increased numbers of circulating $CD3^+$ $CD4^-$ $CD8^-$ T cells (Sneller et al. 1997). *fasl* KO mice display a severe autoimmune phenotype more pronounced than in *gld* mice (Karray et al. 2004) but human FasL mutations are rare. It has therefore been proposed that a FasL defect would not be compatible with life (Rieux-Laucat et al. 2003).

The mechanism of autoimmunity in Fas and FasL deficient mice and humans is not fully clear. However, the Fas-FasL pathway has a role in activation-induced cell death (AICD) of T cells (Green et al. 2003). This mechanism induces apoptosis and contraction of activated effector T cells after antigen clearance to terminate the immune response and in ALPS patients, it is thought to be important for eliminating auto-reactive peripheral T cells (Rieux-Laucat et al. 2003). FasL is thought to mediate AICD in a cell-autonomous manner and in a fratricide manner. For suicide, although not clear, FasL may be released within the membrane of microvesicles from activated CTL, and from there, it may interact with membrane-bound Fas receptors of the same secreting cell (Monleon et al. 2001). Surprisingly, however, fratricide killing does not seem to be mediated by FasL molecules expressed on neighbor CTL. Adoptive transfer experiments showed that wild-type T cells were not deleted in *gld* recipients, whereas *gld* T cells contracted normally in wild-type recipients. These results suggested FasL-mediated induction of apoptosis was triggered from nonlymphoid tissue cells, particularly intestinal epithelial cells (Pinkoski et al. 2002, Brunner 2003). Nonetheless, other studies have shown that contraction after acute virus infection of Fas-deficient T cells was identical to that of T cells expressing Fas (Zimmermann et al. 1996, Reich et al. 2000). These findings indicate that FasL is probably not the only death-inducing pathway in T cell homeostasis.

Besides its role in peripheral deletion, FasL has been proposed to mediate both negative and positive selection in central thymic tolerance. The contribution

of the Fas-FasL pathway to negative selection is controversial. While T cell selection has been reported to proceed normally in *gld* and *lpr* mice (Sidman et al. 1992, Singer and Abbas 1994), Kishimoto et al. suggested clonal deletion of T cells is Fas-independent at low antigen doses but Fas-dependent at higher doses (Kishimoto et al. 1998). On the other hand, Boursalian et al. propose that Fas molecules expressed on thymic epithelial cells bind to FasL on thymoctes and initiate a positive reverse signal through FasL that enhances positive selection of thymocytes expressing MHC-I and MHC II-restricted TCRs of moderate affinity for MHC/self-peptide complexes (Boursalian and Fink 2003).

Using a similar mechanism of reverse signaling capacity, FasL has also been described to have a role in a drastically different function by aiding in the co-stimulation for T cell activation *in vitro* and *in vivo*. Alloantigen-specific proliferation is reduced in $CD8^+$ *gld* CTL cells compared to their wild-type counterparts (Suzuki and Fink 2000). Moreover, $CD8^+$ CTL cells have a significantly higher expansion compared to CTL from *gld* donors when adoptively transferred into WT hosts and their proliferation requires Fas expression on the recipient (Suzuki et al. 2000). The signaling cascade downstream of FasL that gives it this proliferation-enhancing function, is not fully understood. However, FasL costimulation has been reported to correlate with phosphorylation of FasL in serine residues, the activation of Akt, ERK1/2 and JNK, the activation and nuclear translocation of the transcription factors NFAT and AP-1 and the enhancement of IFN-γ production (Sun et al. 2006).

FasL has also been proposed to contribute to the immune-privileged status of the testes, the placenta and the eye (Bellgrau et al. 1995, Griffith et al. 1995, Hunt et al. 1997). FasL is constitutively expressed at these sites and it kills Fas-expressing infiltrating lymphocytes. Similarly, some tumors have been suggested to constitutively express FasL to attack the components of immune surveillance and potentially kill tumor-infiltrating lymphocytes generating a “tumor immune privilege site”. This is known as the “tumor counterattack” model (O'Connell et al. 1999). However, several investigators have challenged this model. They report that transplantation of FasL-expressing tumors, results in rapid neutrophil

infiltration, induction of inflammation and rejection (Igney and Krammer 2005). In conclusion, the interaction of Fas and FasL seems to play several roles that provide significance to the in depth study of this pathway.

1.4.2. Fas-FasL as the trigger of apoptosis

Despite being a multifunctional pathway whose roles are not yet fully understood, the activity of the Fas-FasL pathway in activated T cells as a cytotoxic apoptosis-inducing mechanism is well described. Cell death is induced through the action of caspases that are highly conserved cysteine proteases thought of as the central executioners of apoptosis (Hengartner 2000).

Binding of FasL to Fas triggers the formation of a death-inducing signaling complex (DISC) of proteins that associate with Fas on the target cell (Peter and Krammer 2003). First, the Fas-associated DD containing protein (FADD) binds through the interaction of its death domain (DD) with the DD domain of Fas (Chinnaiyan et al. 1996). FADD also contains a death-effector domain (DED) that allows it to interact with DED-containing procaspase-8 molecules which are thus recruited to the DISC (Muzio et al. 1996). The high local concentration of caspase-8 is believed to result in the autoproteolytic cleavage and activation of caspase 8, which is the main initiator caspase in Fas signaling (Medema et al. 1997). The pathway at this point diverges in different cells, denominated type I and type II, but ultimately converges in the activation of caspase-3 leading to the execution of apoptosis (Scaffidi et al. 1998). In type I cells, production of large amounts of caspase-8 results in the direct cleavage and activation of caspase-3. In type II cells, the DISC complex is not so efficiently formed, and fewer FADD and caspase 8 molecules are recruited. In these cells, the caspase cascade is amplified via the mitochondria (Krammer 2000). Caspase-8 cleaves the Bcl-2 family member Bid yielding a truncated fragment, known as t-Bid, which then causes the aggregation of Bax and Bak on the surface of the mitochondria and triggers the release of cytochrome c (Luo et al. 1998). Cytochrome c then associates with Apaf-1 and procaspase-9 to form the

"apoptosome". Activated caspase-9 then cleaves and activates caspase-3 (Li et al. 1997). Bid deficient mice are resistant to Fas-induced hepatocellular damage and show no evidence of caspase-3 activation, while their thymphocytes are not protected from Fas-mediated apoptosis (Yin et al. 1999). These results suggest thymocytes are type I and hepatocytes are type II cells.

1.4.3. FasL structure

FasL is a type II transmembrane glycoprotein that belongs to the TNF superfamily, that also includes TNF-α, lymphotoxin α, 4-1BB ligand, CD40 ligand, and TRAIL, among others (Suda et al. 1993, Bodmer et al. 2002). It contains 281 amino acids in humans and 279 amino acids in mice. Human and murine FasL share 76.9% of sequence identity and, as described above, mutations in either one lead to similar functional defects.

Its N-terminal cytoplasmic tail is the longest of the TNF ligands. It contains a proline-rich domain (PRD) that has been suggested to be implicated in directing FasL to its storage compartment (Blott et al. 2001) and is involved in the interaction with proteins with SH3 or WW domains. Some of the proteins described to interact with human FasL are: Fyn, Lyn, Lck, Hck, Fgr, Src, Abl (Src-related kinases) Grb2, Gads, Nck, CIP4, FBP1, PACSIN and sortin nexins 9, 18 and 33 (adapter proteins) (Lettau et al. 2011). The FasL cytoplasmic tail also contains two conserved motifs for the binding of casein kinase I (CKI) that mediates serine/threonine phosphorylation (Watts et al. 1999). This domain is thought to be involved in the costimulatory function of FasL.

The C-terminal extracellular domain of FasL contains a self-assembly (SA) domain, which allows for the trimerization of FasL, a TNF homology domain (THD) with a Fas receptor-binding site (RB) at the very C-terminal part of the molecule (**Figure 1.1**) that mediates binding to cysteine-rich regions of the Fas receptor (Orlinick et al. 1997a, Orlinick et al. 1997b). Within its external domain, FasL also contains three putative N-glycosylation sites in human and four in mice, but their role in FasL expression or function remains unknown.

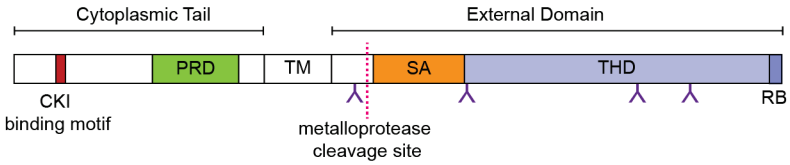

Figure 1.1. Illustration of FasL domains and motifs.
In its N-terminal cytoplasmic tail it contains two casein kinase I (CKI) binding motifs and a proline rich domain (PRD). In its C-terminal external domain it contains a self-assembly (SA) domain and a tumor necrosis factor homology domain (THD) with a Fas-receptor binging (RB) site. It also contains three (in human) or four (in mice) glycosylation sites. The putative metalloprotease cleavage site is also depicted.

The membrane bound FasL (mFasL) can undergo metalloprotease-mediated proteolytic processing in its extracellular domain resulting in the release of soluble FasL (sFasL). The putative cleavage site has been mapped to Ser126/Leu127 in human FasL and to Lys129/Gln130 in mouse FasL (Schneider et al. 1998); since the processing site is located upstream of the SA domain, sFasL may still form trimers. sFasL is thought to counteract the action of mFasL in triggering apoptosis (Suda et al. 1997, Schneider et al. 1998, Tanaka et al. 1998, Hohlbaum et al. 2000, LA et al. 2009) and has also been described to have chemotactic activity for neutrophils (Seino et al. 1998, Ottonello et al. 1999). Full-length FasL can also be released as a membrane component of exosomes, in which it efficiently triggers apoptosis (Martinez-Lorenzo et al. 1999, Frangsmyr et al. 2005, Koncz et al. 2012).

1.4.4. Regulation of FasL

Since Fas is constitutively expressed on several cell types, and because of its crucial function in triggering cell death, FasL surface expression on T cells must be tightly regulated to prevent unwanted damage. This regulation can be accomplished through different mechanisms.

1.4.4.1. Transcriptional regulation of FasL

Interaction of the TCR with the correct peptide/MHC complex leads to the stimulation of T cells and induces FasL transcription. Several transcription factors have been reported to mediate TCR-triggered FasL transcription: NFAT, NF-κB, c-myc, IRF-1, Egr2, Egr3 and SP-1 (Li-Weber and Krammer 2003). FasL expression can also be induced by stress and through cytokines. Environmental stress-induced FasL transcription is dependent on the activation of the AP-1 transcription factor (Faris et al. 1998). IL-2 is also thought to induce the transcription of *fasl* via the SP-1 and NFAT binding motifs (Xiao et al. 1999).

FasL transcription can also be negatively regulated by retinoic acid, nitric oxide, vitamin D_3 and ICER. Retinoic acid blocks the translocation of NFAT from the cytosol to the nucleus (Lee et al. 2002); nitric oxide interferes with the ability of AP-1 to induce *fasl* expression (Melino et al. 2000); vitamin D_3-mediated inhibition was shown to be mediated by a non-canonical c-myc binding element (Cippitelli et al. 2002); while formation of a ternary complex between ICER and NFAT leads to the down-regulation of NFAT-mediated *fasl* transcription (Bodor et al. 2002).

1.4.4.2. Post-translational regulation of FasL

Several post-translational modifications have been described for FasL (Voss et al. 2008). As mentioned above, it has several putative N-glycosylation sites in its C-terminal external domain. However, whether FasL is in fact glycosylated in T cells or other cell types, or what role glycosylation may play in the biology or function of the protein, has not been determined yet. In addition, human, but not murine FasL, contains three tyrosine residues Y7, Y9 and Y13 on its N-terminal end that have been shown to be important for the mono-ubiquitination of lysines 72 and 73, which are thought to have a role in FasL intracellular trafficking (Zuccato et al. 2007). Moreover, CKI-mediated serine phosphorylation on the N-terminal domain has been implicated in reverse signaling and stimulation of $CD8^+$ T cells (Sun et al. 2007).

One of the better-studied aspects of post-translational regulation of FasL is its intracellular storage and rapid release upon TCR engagement. Although early studies reported that FasL mediated cytotoxicity was performed by *de novo* synthesized FasL (Walsh et al. 1994, Vignaux et al. 1995, Glass et al. 1996), several studies have now confirmed that there is a preformed pool of FasL stored inside the CTL in addition to the FasL molecules that are synthesized in response to TCR engagement (Li et al. 1998, Bossi and Griffiths 1999, Kojima et al. 2002, He and Ostergaard 2007). Stimulation of CTL with target cells triggers two waves of FasL surface expression. The early wave, peaking within 10-20 min after

stimulation, results from the rapid translocation of proteins stored inside the cell, while the later wave, that peaks around 2 hours after stimulation, results from transcriptional induction of FasL expression, translation and translocation to the surface (He and Ostergaard 2007). The early wave of surface FasL expression requires intracellular Ca^{++} but does not require extracellular Ca^{++}, as evidenced by comparable surface expression levels in the presence of the Ca^{++} chelator EGTA (He and Ostergaard 2007). In contrast, the later phase of FasL expression does requires extracellular Ca^{++} for optimal levels and is completely inhibited with the protein synthesis inhibitor cyclohexamide, which does not affect the early surface expression phase (He and Ostergaard 2007). These results indicated the later wave, but not the early wave, is dependent on protein translation and comes after the *de novo* synthesis of molecules. They also indicated these two phases of expression have different Ca^{++} requirements and are thus probably independently regulated. Consistently, early-translocated FasL requires a lower threshold of activation and is rapidly cleared from the surface (He et al. 2010). On the other hand, *de novo* synthesized FasL, but not stored translocated FasL, mediates bystander killing of non-antigen-bearing cells (He et al. 2010).

1.4.5. FasL localization

The early wave of surface FasL expression comes from a pool of molecules that is stored in intracellular vesicles in order to rapidly translocate to the surface upon CTL stimulation (He and Ostergaard 2007). The identity of the intracellular storage vesicles that hold pre-synthesized proteins is controversial. Several authors argue that it is stored in lysosomal granules together with perforin and granzymes (Bossi and Griffiths 1999, Lettau et al. 2004, Qian et al. 2006). However, other authors and previous results from our laboratory have found separate locations for the degranulation components and FasL (He and Ostergaard 2007, Kassahn et al. 2009, Schmidt et al. 2011a). In support of the latter, the regulation of both pathways has also been shown to be different. The absence of Ca^{++} dependency first suggested there was a degranulation-independent pathway

(Ostergaard et al. 1987), which is now known to be the Fas/FasL pathway (Rouvier et al. 1993). Further evidence supported this theory since CTL from *ashen* mice, which are defective in degranulation, are still able to kill via the FasL pathway (Haddad et al. 2001). To examine the distinctions between these two pathways our laboratory examined whether different thresholds of signal led to different outcomes. By using peptide-specific CTL clones and different concentrations of peptides, it was demonstrated that the threshold of activation for the delivery of stored FasL to the cell surface was lower compared to the degranulation of cytolytic molecules (He et al. 2010). Moreover, treatment with colchicine did not inhibit rapid FasL surface delivery but impaired degranulation suggesting granules move towards the immunological synapse via microtubules but not the FasL-containing vesicles (He and Ostergaard 2007). These results favour the proposal that T cells have two distinct storage compartments for the degranulation of cytolytic molecules and for FasL, and that these are separately regulated resulting in distinguishable functions. However, the field lacks the tools to fully differentiate between these two cytotoxic mechanisms and their relative contributions to immune responses.

1.5. Vesicle transport

Vesicles transport proteins and lipids via two major pathways: the outwards, secretory pathway, and the inwards, endocytic pathway. The endocytic pathway is required for the uptake of nutrients or internalization of surface-expressed molecules that are transported to the early endosome. Proteins destined for recycling are sorted to recycling endosomes and then returned to the plasma membrane, whereas proteins destined for degradation are transported to late endosomes and subsequently to lysosomes. Conversely, the secretory pathway sorts newly synthesized proteins from the ER, through the trans-Golgi network (TGN) directly to their final destination at the lysosome or plasma membrane (Maxfield and McGraw 2004).

Proteins destined for secretion can be transported through the constitutive or the regulated pathways for exocytosis. Proteins leaving the cell by the constitutive pathway are not concentrated in secretory granules for storage in the cytoplasm but instead are constantly secreted. In contrast, proteins secreted by the regulated exocytosis pathway are pooled in a storage vesicle and only released when they receive an appropriate signal (Burgess and Kelly 1987). The degranulation of lysosomally-derived granules in CTL is an example of regulated exocytosis (Stinchcombe and Griffiths 1999).

The overall mechanism of membrane traffic can be divided into five general steps. First, proteins are "sorted" or selectively incorporated into forming vesicles; second, transport vesicles bud from the "donor" compartment; third, vesicles are specifically targeted to an "acceptor" compartment; forth, vesicles dock onto the target membrane; and lastly, membranes from the acceptor compartment and the vesicles fuse resulting in relocation of the cargo proteins (Bonifacino and Glick 2004) (**Figure 1.2**). Typically, the ARF family of proteins are involved in the budding steps, the Rab family of proteins are involved in vesicle targeting steps, and SNARE proteins mediate membrane docking and fusion of the vesicles.

1.5.1. Vesicle budding

The ADP-ribosylation factor (ARF) family of proteins belongs to the Ras superfamily of small GTPases. They are usually found in their GDP-bound state in the cytosol. The loading of GTP on ARF proteins is mediated by guanine exchange factors (GEFs) that are located on specific membranes where they activate specific ARF proteins. The binding of GTP causes the ARF proteins to expose its myristoyl tail that inserts it into the "donor" lipid membrane (D'Souza-Schorey and Chavrier 2006). Activated ARFs then recruit coat proteins, such as COP I, COP II or clathrin, that interact and specifically recognize "sorting motifs" on the cargo proteins and coat a section of the membrane causing it to deform and

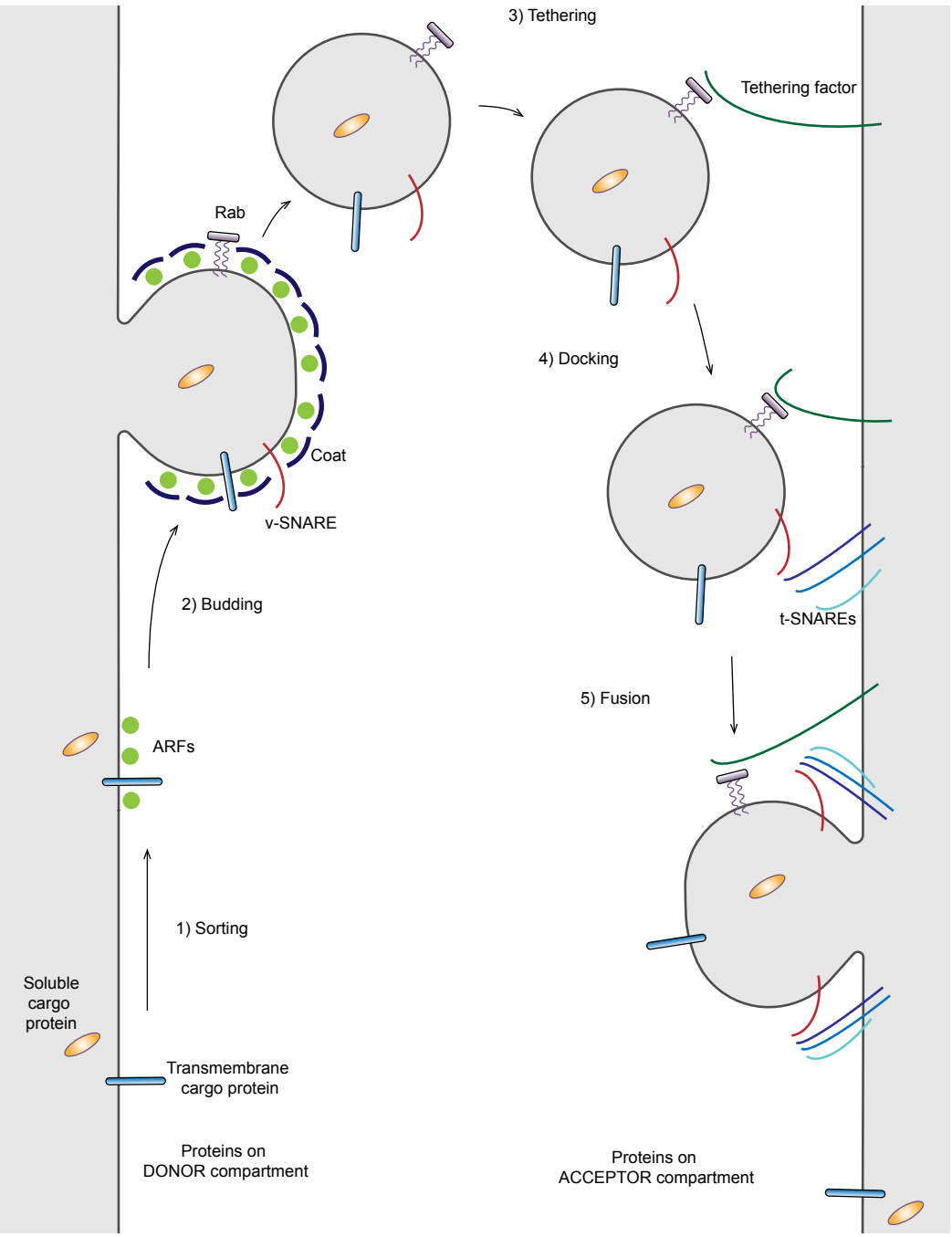

Figure 1.2. General steps of vesicle transport.
Sorting. AFP-ribosylation factor (ARF) proteins recognize sorting motifs on cargo proteins located on the DONOR compartment. *2) Budding*. The recruitment of coat proteins deforms the membrane and allows for the budding of vesicles. *3) Tethering*. Rab proteins on the vesicles recognize and bind to a tethering factor on the ACCEPTOR compartment allowing for initial attachment to the membrane. *4) Docking*. v-SNAREs on the vesicle binds to t-SNAREs on the ACCEPTOR compartment. *5) Fusion*. SNAREs on the vesicle and on the target membrane associate into a core complex that generates a force pushing the lipid bilayers together and forcing them to fuse.

form vesicles. ARFs also recruit adaptor proteins which act as bridges between some cargo and coat proteins (van Vliet et al. 2003).

1.5.2. Vesicle tethering: Rab proteins

Rabs are also a family of small Ras-like GTPases that oscillate between GTP- and GDP- bound conformations. The GTP-bound state is considered "active" as this is the form that interacts with soluble factors that act as "effectors" to transduce the signal of the Rab GTPase in the transport mechanism (Stenmark and Olkkonen 2001). This switch is controlled by GEFs that promote dissociation of GDP, and GTPase-activating proteins (GAPs) which accelerate hydrolysis of GTP to GDP. Rabs also undergo a membrane insertion and extraction cycle. Membrane insertion requires the modification of two cysteines near the C-terminus with geranyl lipid groups. A chaperone called GDP dissociation inhibitor (GDI) binds to the GDP-bound Rabs and masks their isoprenyl anchor preventing the insertion or extracting inserted Rabs. When a GDP-bound Rab protein finds its "donor" compartment, the dissociation of GDI is catalyzed by a GDI displacement factor (GDF). The resulting membrane-associated GDP-bound Rab protein can then interact with GEF and since the intracellular concentration of GTP is higher than GDP, the empty Rab protein binds GTP. This "active" form of the Rab protein is then able to bind to its effector(s). The transport vesicle with the Rab protein on its surface travels to the target compartment, where additional rounds of nucleotide exchange and hydrolysis occur to recruit effector tethering proteins that allow for an initial attachment of vesicles to membranes. The GDP-bound Rab on the "acceptor" compartment is then extracted by GDI for recycling back to the "donor" membrane (Tuvim et al. 2001, Pfeffer and Aivazian 2004). These cycles are depicted in **Figure 1.3**.

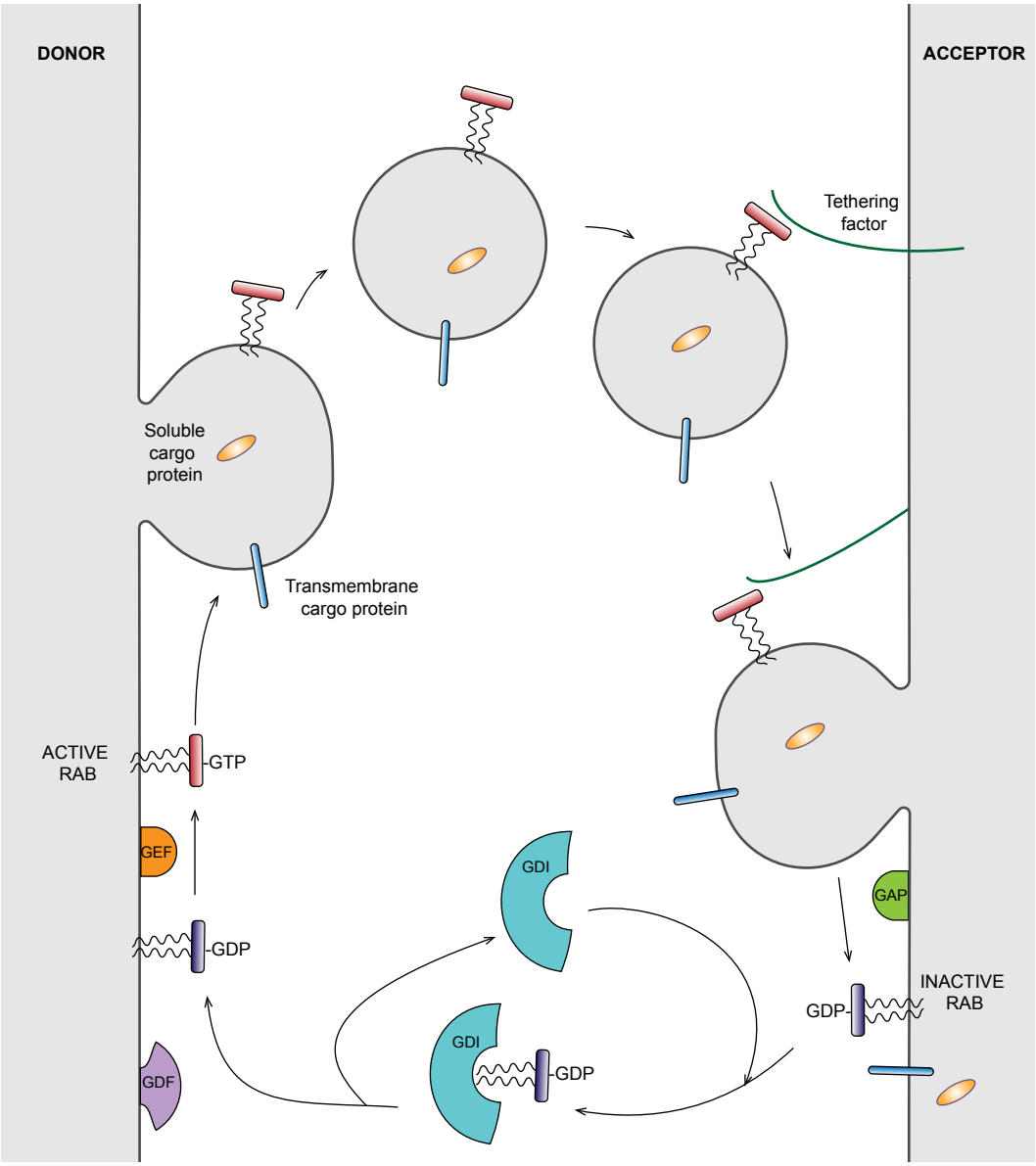

Figure 1.3. Cycles for membrane association/dissociation and GTP hydrolysis of Rab proteins.
GDP dissociation inhibitors (GDI) bind to inactive Rabs and mask their isoprenyl anchor. On the donor compartment, GDI displacement factors (GDFs) catalyze the displacement of GDIs. Guanine exchange factors (GEFs) promote dissociation of GDP allowing the binding of GTP. Active Rabs are transported within the transport vesicles and bind to their effector tethering proteins to promote initial attachment of the vesicle. This is linked to the hydrolysis of GTP mediated by GTPase-activating proteins (GAPs). GDIs then extract inactive Rabs from the acceptor compartment and recycle it back to the donor compartment.

1.5.3. Vesicle fusion: SNAREs

After a vesicle is tethered to the acceptor compartment, if the target and vesicle membranes have compatible fusion markers, they will interact leading to the docking of the vesicle. The fusion machinery will then bring the membranes together and promote their fusion. The fusion machinery is mainly composed of soluble N-ethylmaleimide-sensitive factor (NSF) attachment receptors (SNAREs) proteins.

SNAREs are a superfamily of small proteins that contain a common "SNARE motif". This motif, found near their membrane region, consists of heptad repeat sequences that are unstructured when SNAREs are monomeric. However, when appropriate groups of SNAREs associate, the motifs form helices (Jahn and Scheller 2006). SNAREs can be classified for their location, as v-SNAREs for those proteins found on vesicles originating from "donor" compartments and t-SNAREs located on the target membrane compartment. They can also be classified based on their structure: R-SNAREs contain arginine and Q-SNAREs contain glutamine on central residues of their SNARE motif. The R-SNAREs usually correspond to the v-SNAREs and the Q-SNAREs usually correspond to the t-SNAREs (Jahn and Scheller 2006). SNARE proteins associate into core complexes using their helix domains. The zippering model states that three SNARE helices on the target membrane assemble with a v-SNARE helix on the vesicle forming a highly stable quaternary complex that is known as the *trans*-SNARE complex. The zippering starts on the N-terminal end of the SNARE motifs toward the C-terminal membrane anchor and generates a force that pushes the lipid bilayers together forcing them to fuse. After fusion occurs, the helices are completely assembled, the force disappears and the SNAREs in this low-energy conformation are said to be in a *cis*-SNARE complex, since they are all located on the same membrane. The specialized ATPase NSF and its adaptor protein SNAP disassemble this complex to restart the SNARE cycle (Chen and Scheller 2001, Sudhof and Rothman 2009).

The Sec/Munc-like (SM) proteins also have an essential role in membrane fusion. They are composed of a 600-amino acid sequence that folds into an arch-shaped "clasp" structure and they associate with SNARE proteins in at least two different ways. They can bind individual SNARE proteins forming an inactive or "closed" complex that includes part of the SNARE motif and disables the formation of SNARE complexes. This inhibitory role would allow them to provide an additional step in regulating the time and place of membrane fusion. Moreover, they can also bind an N-terminal peptide of the SNARE protein and use their arch-shaped domain to stabilize the four helices in the SNARE complex and favor membrane fusion (Sudhof and Rothman 2009, Carr and Rizo 2010).

1.6. Trafficking of cytolytic granule components

1.6.1. Targeting to cytolytic granules

After being synthesized, the cytotoxic components of granules, perforin and granzymes, are transported to the lysosomal granules. Granzymes move along the ER and Golgi organelles of the secretory pathway as zymogens where they are modified with mannose-6-phosphate (M6P) residues. M6P receptors recognize these residues and direct the glycoproteins to the lysosomal granules via endosomes (Griffiths and Isaaz 1993). In the lysosome, they are processed by cathepsin C, and cathepsin H in the case of granzyme B, and stored as active proteinases (Pham and Ley 1999, D'Angelo et al. 2010). Perforin is efficiently and rapidly exported from the ER directed by a signal in the C-terminal tail, specifically the last residue (W555), which ensures its safe delivery to the acidic environment of the lysosome where it remains inactive (Brennan et al. 2011). The mechanism and machinery for this transport remain to be elucidated. The stimulation of CTL after interacting with the proper MHC/peptide combination leads to their release towards the target cell.

1.6.2. Trafficking to the surface

The release of the cytotoxic components in the degranulation pathway is accomplished through the regulated exocytosis of lysosomal granules, which consists of the targeting, docking and fusion of these vesicles with the plasma membrane. Human diseases and their mouse models giving rise to defects in secretory lysosomes have been used to decipher the mechanism by which the cytolytic granules move, dock and fuse with the plasma membrane (Stinchcombe et al. 2004). To date, the only Rab protein identified to be exclusively involved in the fusion of secretory lysosomes with the plasma membrane is Rab27a (Stinchcombe et al. 2001a). It is absent in patients suffering from Griscelli's syndrome that exhibit defects in lymphocyte cytotoxicity (Menasche et al. 2000). Studies using CTL from the Rab27a deficient mice *ashen*, show that while the granules can move along the microtubules and accumulate at the MTOC near the contact site with the target cell, they are unable to dock at the plasma membrane (Haddad et al. 2001, Stinchcombe et al. 2001a). The effectors of Rab27a that mediate tethering with the plasma membrane are the synaptogamin-like proteins SLP1 and SLP2 (Holt et al. 2008, Menasche et al. 2008).

Another protein shown to be essential for CTL degranulation is Munc13-4 (Feldmann et al. 2003). This protein belongs to the family of MS proteins and its absence causes FHL3 resulting from defects in NK and T cytotoxicity. The docking of granules from Munc13-4 deficient CTL seems to be unaffected, however, they are unable to fuse with the plasma membrane (Feldmann et al. 2003). Similarly, Munc13-4 has been shown to control granule exocytosis in mast cells and neutrophils (Neeft et al. 2005, Brzezinska et al. 2008, Pivot-Pajot et al. 2008). Cytolytic granules have been proposed to have an intermediate maturation step in which they fuse with an endosomal compartment that contains the exocytic machinery (Rab27a and Munc13-4) and Munc13-4 is thought to allow for the merging of these compartments (Menager et al. 2007). Additionally, by analogy with the mechanism of action of Munc13-1, Munc13-4 is thought to "prime" the target SNARE protein on the plasma membrane by switching its conformation

from an inactive closed shape to an open conformation that associates with the v-SNARE on the granules and promotes its fusion (Hong 2005).

Syntaxin 11 has been proposed to be one of the SNARE proteins involved in the membrane fusion of cytotoxic granules. Syntaxin 11 is thought to be stored in late endosomes and transported to the plasma membrane independently from the granules (Dabrazhynetskaya et al. 2012, Halimani et al. 2013). Loss of Syntaxin 11 is the cause of FHL4 and its deficiency impairs granule exocytosis in NK and CTL without affecting granule polarization, suggesting it plays a role in a downstream step (Bryceson et al. 2007). Mutations in the gene encoding for Munc18-2 were recently shown to result in FHL5, with a similar phenotype to Syntaxin 11-deficient FHL4 patients. Because Munc18-2 can bind to Syntaxin 11, these two proteins have been postulated to regulate granule docking and initiation of SNARE complex formation to fuse cytolytic granules with the plasma membrane (Cote et al. 2009, zur Stadt et al. 2009).

As discussed above, the identity of the FasL storage vesicle is controversial and thus so is its trafficking. The authors claiming that FasL is stored together with the degranulation effectors within cytolytic granules maintain that FasL is delivered and incorporated on the plasma membrane as part of the same process. However, previous results from our laboratory and others suggest FasL is stored in a separate compartment (He and Ostergaard 2007, Kassahn et al. 2009, Schmidt et al. 2011a), therefore indicating that there might be an independent trafficking mechanism of which nothing is yet known.

1.7. Hypothesis and objectives

The underlying hypothesis for this thesis is that the storage compartment, the trafficking pathway and the surface expression of FasL are differentially regulated and independent from the degranulation pathway of CTL-mediated killing.

The principal aim of this study is to examine the storage and trafficking of FasL in CTL. The specific questions to be addressed are as follows:

1. Where is FasL stored in CTL? Is the storage vesicle a separate compartment from the cytolytic granules?

2. What is the trafficking route FasL utilizes to reach its storage compartment?

3. What sequences of the FasL protein are important for its trafficking?

In this thesis I will present data that demonstrates that FasL is stored in a unique compartment, together with Rab32 and Syntaxin 3, that segregates from the cytolytic granules. I will show that FasL is endocytosed from the surface in a process signaled by the N-terminal cytoplasmic tail of the protein and that three cytoplasmic lysines mediate its targeting to the intracellular storage vesicle in unstimulated conditions.

These results will contribute to the general knowledge of FasL trafficking and will allow for a better distinction of the CTL killing pathways. Understanding the mechanisms of FasL storage, trafficking and surface expression will provide the means to better differentiate contributions of each lytic pathway during an immune response, which may allow for future manipulation of CTL in the treatment of cancer and infection.

CHAPTER 2: Materials and Methods

2.1. Cells

The murine alloreactive $CD8^+$ CTL Clone 11 ($H\text{-}2^k$ anti-$H\text{-}2^b$) and the murine peptide-specific CTL Clone 3/4 that recognizes $H\text{-}2D^b$-restricted $NP_{366\text{-}374}$ peptide (ASNENMETM) derived from the nucleoprotein of the A/PR/8/34 (H1N1) influenza virus were described previously (Kane et al. 1989, Kane and Mescher 1993). CTL clones were maintained by weekly stimulation with irradiated (2500 rad) C57BL/6 splenocytes alone (for Clone 11) or pulsed with 200μg/ml $NP_{366\text{-}374}$ peptide (for Clone 3/4) and 10 U/ml murine recombinant IL-2. CTL clones were cultured in RPMI 1640 supplemented with 10% fetal calf serum (FCS), 2mM L-glutamine, 100 μg/ml penicillin/streptomycin, 0.1 mM nonessential amino acids, 1mM sodium pyruvate and 53 nM 2-mercaptoethanol.

CTLL-2 cells were cultured in RPMI 1640 supplemented with 4% FCS, 4% Fetalclone I, 2mM L-glutamine, 100 μg/ml penicillin/streptomycin, 0.1 mM nonessential amino acids, 1 mM sodium pyruvate and 53 nM 2-mercaptoethanol and 6 U/ml recombinant IL-2.

The L1210 lymphoma cell line expressing Fas (L.Fas) was a gift from Dr. Kevin Kane (University of Alberta, Alberta, Canada). It was grown in DMEM supplemented with 8% defined fetal calf serum (dCS).

COS-1 cells were a gift from Dr. J. Elliott (University of Alberta, Alberta, Canada) and were grown in DMEM supplemented with 10% fetal bovine serum (FBS).

2.2. Antibodies

Anti-FasL antiserum used for immunoprecipitations was developed in our laboratory from rabbits injected with a purified GST-conjugated polypeptide of the cytoplasmic tail of FasL (corresponding to amino acids 1 - 78). PE-conjugated anti-FasL (MFL3), PE-conjugated hamster IgG isotype control, biotin-conjugated

anti-FasL (MFL3), biotin-conjugated isotype control, anti-LAMP-1 (1D4B), anti-perforin (H-315), anti-TNF (MP6-XT22), anti-GM-130 (35/GM130) and anti-active caspase-3 (C92-605) were purchased from BD Pharmigen (San Jose, California, USA). Anti-FasL antibody (clone 101626) was purchased from R&D Systems (Minneapolis, Minnesota, USA). Anti-DsRed polyclonal antibody was purchased from Clontech (Mountain View, California, USA). Anti-CD63 (M-13), anti-cathepsin D (G-19), anti-PD-1 (E-18), goat anti-syntaxin 3 (N-17) and anti-Myc (9E10) were purchased from Santa Cruz Biotechnology (Santa Cruz, California, USA). Anti-Rab4 antibody was purchased from Sigma Aldrich (St. Louis, Missouri, USA). Anti-cytochrome c (7H8) and PE-conjugated donkey anti-rabbit IgG were purchased from eBioscience (San Diego, California, USA). Anti-Grp78 serum was purchased from Enzo Life Biosciences (Farmingdale, New York, USA). Rabbit anti-Syntaxin 3, anti-Munc18-2 and anti-SUMO-1 were purchased from Synaptic Systems (Goettingen, Germany). Anti-HA (HA-7) was purchased from Abcam (Cambridge, United Kingdom). Anti-Rab32 was a gift from Dr. Thomas Simmen (University of Alberta, Alberta, Canada). A1 antibody that recognizes Ly49A was a gift from Dr. Kevin Kane (University of Alberta, Alberta, Canada, (Nagasawa et al. 1987). Anti-rat IgG-HRP, anti-mouse IgG-HRP and anti-rabbit IgG-HRP were purchased from Jackson ImmunoResearch Laboratories (West Grove, Pennsylvania, USA). Anti-GFP (3E6), Alexa Fluor 555- Alexa Fluor 594-, Alexa Fluor 488- and Alexa Fluor 647-conjugated streptavidin and secondary antibodies were purchased from Life Technologies (Carlsbad, California, USA).

2.3. Reagents

Protein A-coupled sepharose, FCS, dCS and FBS were purchased from GE Healthcare (Piscataway, New Jersey, USA). PE-Cy5-conjugated streptavidin was purchased from BD Pharmigen (San Jose, California, USA). NeutrAvidin and streptavidine agarose were purchased from Thermo Fisher Scientific Inc (Waltham, Massachusetts, USA). Cyclohexamide (CHX), blebbistatin, poly-L

lysine solution, phorbol 12-myristate 13-acetate (PMA), dimethyl sulfoxide (DMSO) Hybri-Max, doxycycline hyclate, N-ethylmaleimide (NEM), Histopaque-1077, ampicillin, kanamycin, glutation sepharose 4B, Isopropyl β-D-1-thiogalactopyranoside (IPTG) and bovine serum albumin (BSA) were purchased from Sigma-Aldrich (St. Louis, Missouri, USA). Ionomycin, TAPI and saponin were purchased from Calbiochem (San Diego, California, USA). Cell Tracker Orange CMRA was purchased from Life Technologies (Carlsbad, California, USA). Normal donkey serum was purchased from Jackson ImmunoResearch Laboratories (West Grove, Pennsylvania, USA). $NP_{366-374}$ peptide (ASNENMETM) was synthesized by GenScript (Piscataway, New Jersey, USA). SUMO 1 control peptide was purchased form Synaptic Systems (Goettingen, Germany). MG-132 was purchased from EMD Millipore (Chicago, Illinois, USA). The protease inhibitor cocktail capsules were purchased from Roche (Indianopolis, Indiana, USA). Bio-Safe Coomasie G-250 stain and Immun-Blot PVDF were purchased from Bio-Rad (Hercules, California, USA). The pEGFP/Rab32 WT and pEGFP/Rab32 T39N plasmids were a gift from Dr. Thomas Simmen (Bui et al. 2010). The pEGFP/Rab8A (31803) and the pCDNA4/Stx3-Myc-Myc-His (12372) plasmids were purchased from Addgene (Sharma et al. 2006, Guizetti et al. 2011). The GFP-tagged Rab4, Rab5 and Rab11 plasmids (pEGFP-c2/Rab4, pEGFP-c2/Rab5 and pEGFP-c2/Rab11) were a gift from Dr. Stephen Ferguson (London, Ontario, Canada). The pCDNA/HA-Ubiquitin plasmid was a gift from Dr. Robert Inhgam (University of Alberta, Canada). Full length FasL was cloned in pC1-neo and in pDsRed by Dr. Jinshu He. Full length Ly49A, and the FasL/Ly49A chimeras were cloned in pDsRed by Nancy Hu. pDsRed/FasL was mutated into Δ3K and N182Q by Peter Hwang. Colleen Reid cloned the N-terminal cytoplasmic tail of FasL in the pGEX4T3 plasmid and transformed One Shot BL21 Star (DE3) competent *Escherichia coli* cells (Life technologies, Carlsbad, California, USA).

2.4. Mutagenesis of FasL

2.4.1. Deletion mutagenesis of FasL

Under my supervision, Colleen Reid constructed the deletion mutants FasL Δ2-43, ΔPRD and ΔSA. All of them were constructed using pDsRed-FasL as the template for PCR. FasL Δ2-43 was constructed using a forward primer that contained a restriction site for *KpnI*, the initial ATG codon and a few codons for the sequence of FasL starting in residue 44. The C-terminal reverse primer contained a restriction site for *BamHI*. The resulting product was purified using the Quiaquick PCR purification kit (Qiagen, Missisagua, Ontario, Canada) and digested with *KpnI* and *BamHI* for 2.5 hs at 37°C.

FasL ΔPRD and ΔSA were constructed via a step-wise PCR method using the Pfu Turbo DNA polymerase (Life technologies, Carlsbad, California, USA). The N-terminal fragment was amplified using a reverse primer that contained a short 11 bp bridge sequence complementary to the C-terminal fragment. After the C-terminal fragment was amplified independently from the N-terminal fragment, these sequences were separated by electrophoresis in 0.75% agarose gels in 1mM guanosine TAE buffer (40mM Tris-acetate 1mM EDTA in water) and bands of the correct size were excised and purified. The fragments were mixed for a third PCR reaction and the resulting product was purified and digested with *KpnI* and *BamHI*.

The primers used for the reactions described above are listed in Table 1.2 and were purchased from Sigma-Aldrich (St. Louis, Missouri, USA).

Construct	Primer	Sequence (5'- 3')
Δ2-43	Forward	CTTCTGGTACCATGAGACCGCCACCTCCA
	Reverse	TCTCTGGATCCTTAAAGCTTATACAAGC
ΔPRD	Forward (N fragment)	TCTCTGGTACCATGCAGCAGCCCATGAATTAC
	Reverse (N fragment)	GTTGTGGTCCTTCTTCCTTTGGTCCGGCCCTCTAGG
	Forward (C fragment)	GGACCAAAGGAAGAAGGACCACAACACAAATCTG
	Reverse (C fragment)	TCTCTGGATCCTTAAAGCTTATACAAGC
ΔSA	Forward (N fragment)	TCTCTGGTACCATGCAGCAGCCCATGAATTAC
	Reverse (N fragment)	AACGAAACTGGGTTCTACTTCGTG
	Forward (C fragment)	CCAGTTTCGTTTCTACTGGGGTTGGCTAT
	Reverse (C fragment)	TCTCTGGATCCTTAAAG-CTTATACAAGC

Table 2.1. Primers used in the construction of deletion mutants.

The resulting products were cloned into pDsRed (Clontech, Mountain View, California, USA) previously digested with *KpnI* and *BamHI* incubating with the T4 DNA ligase (Life technologies, Carlsbad, California, USA) overnight at 16°C.

Transformation of the construct into Library Efficient DH5α competent *Escherichia coli* cells (Life technologies, Carlsbad, California, USA) was done following the instructions from the manufacturer. Endotoxin-free DNA preparations were made using the Endo-free Plasmid Maxi Kit (Qiagen, Missisagua, Ontario, Canada) and the resulting plasmids were sequenced (using the TAGC Applied Genomic Core in the University of Alberta).

2.4.2. Site-directed mutagenesis of FasL

Under my supervision Colleen Reid constructed the mutants FasL N117Q, N258Q, K71A, K72A and K73A. Site-directed mutagenesis was performed by

PCR using primers that contained the mutation as well as 9 bp not overlapping, as reported by Zheng et al. (Zheng et al. 2004). pDsRed-FasL was used as a template and the resulting PCR product was purified and treated with *DpnI* (Life technologies, Carlsbad, California, USA) to destroy the template plasmid. The construct was then transformed into Library Efficient DH5α competent cells, purified using the Endo-free Plasmid Maxi Kit and sequenced to ensure successful mutation.

The primers used for the reactions described above are shown in Table 2.2 and were purchased from Sigma-Aldrich (St. Louis, Missouri, USA).

Construct	Primer	Sequence (5'- 3')
N117Q	Forward	CTGGCAGAACTCCGTGAGTTCACCCAGCAAAG CCTTAAAGTA
	Reverse	AAAAGATGATACTTTAAGGCTTTGCTGGGTGA ACTCACGGAG
N258Q	Forward	ACCAGTGCTGACCATTTATATGTCCAAATATCT CAACTCTCT
	Reverse	ATTGATCAGAGAGAGTTGAGATATTTGGACAT ATAAATGGTC
K71A	Forward	CCACTGCCGCCACTGACCCCTCTAGCGAAGAA GGACCACAAC
	Reverse	CAGATTTGTGTTGTGGTCCTTCTTCGCTAGAGC GGTCAGTGG
K72A	Forward	CTGCCGCCACTGACCCCTCTAAAGGCGAAGGA CCACAACACA
	Reverse	CCACAGATTTGTGTTGTGGTCCTTCGCCTTTAG AGGGGTCAG
K73A	Forward	CCGCCACTGACCCCTCTAAAGAAGGCGGACCA CAACACAAAT
	Reverse	TAGCCACAGATTTGTGTTGTGGTCCGCCTTCTT TAGAGGGGT

Table 2.2. Primers used in the site-directed mutagenesis of FasL

2.5. CTL stimulation with PMA and ionomycin

CTL were harvested, washed with PBS and resuspended at a concentration of 2 x 10^7 cells/ml in cold RPMI 1640 supplemented with 2% dCS. PMA and

ionomycin were added at a concentration of 5 ng/ml and 0.5 μM, respectively. CTL were then incubated at 37°C for the length of time indicated in the legends.

2.6. Transient transfection of CTL

Live cells were enriched by density centrifugation. Histopaque-1077 was added to the bottom of the tube containing harvested CTL and centrifugated at 800xg for 15 min at room temperature. The intermediate cell layer was collected and washed with RPMI 1640 supplemented with 10% FCS, 2mM L-glutamine, 100 μg/ml penicillin/streptomycin, 0.1 mM nonessential amino acids, 1mM sodium pyruvate and 53 nM 2-mercaptoethanol. After washing with PBS, cells were resuspended in PBS and 5 x 10^6 cells were dispensed in separate tubes for each sample. Cells were centrifugated at 0.8 rpm for 10 min. The supernatant was discarded and the pellets were resuspended in 50 μl of Nucelofector Solution from the Mouse T cell Nucelofector Kit from Lonza (Basel, Switzerland), which were promptly mixed with 50 μl of Nucelofector Solution previously mixed with 2μg of plasmid DNA. Cells were nucleofected using the X-01 program of the Amaxa nucleofector I (Lonza, Basel, Switzerland) and then immediately supplemented with 0.5 ml of Nucleofector Solution. After 10 min of incubation in this media, cells were transferred to 12-well plates containing 1.5 ml of Nucelofector Solution previously incubated at least 30 min at 37°C in the incubator. After 18 hours of nucleofection, cells were used for various experiments.

2.7. Transient transfection of COS-1 cells

COS-1 cells were transfected using the Effectene transfection kit purchased from Qiagen (Mississauga, ON) according to the instructions from the manufacturer. 24 hours after the transfection, cells were washed with PBS and fresh DMEM media supplemented with 10% FCS was added. After 48 hours of transfection, media from the plates was aspirated and replaced by cold PBS

supplemented with 4mM EDTA. After 10 min of incubation, cells were harvested and used for further experiments.

2.8. Cell lysis and immunoprecipitation

1 x 10^7 CTL or 1 x 10^6 COS-1 cells were lysed by incubation with 1ml of 1% NP-40 lysis buffer (1% NP-40, 150 mM NaCl, 10 mM Tris pH 7.6, 1 mM sodium orthovanadate and protein inhibitor cocktail) at 4°C for 20 min. Lysates were then centrifuged at 13,000 rpm for 5 min at 4°C. For post-nuclear lysate controls 40 µl of CTL lysates (corresponding to 8 x 10^5 cells) and 40 µl of COS-1 lysates (corresponding to 4 x 10^4 cells) were set aside. For immunoprecipitations post-nuclear lysates were incubated with 8 µl of anti-FasL antiserum, or pre-immune serum as a control, for 1 hour at 4°C, followed by incubation with 30 µl of a 50% slurry of protein A sepharose beads for 1 hour at 4°C with rotation. Alternatively, lysates were immunoprecipitated with 1 µg of biotin-conjugated anti-FasL antibody or biotin-conjugated Armenian hamster isotype control for 1h in ice followed by incubation with 25 µl of a 50% Streptavidin Agarose slurry for 2 hours at 4°C with rotation. Beads were pelleted and washed three times with NP-40 lysis buffer and then prepared for SDS-PAGE by addition of 60 µl of 1X Laemmli reducing sample buffer and boiling for 5 min.

For the analysis of ubiquitination, cells were pre-incubated with 5 µM MG-132 for 4 hours prior to lysis. For the analysis of ubiquitination and SUMOylation, lysis was performed in the presence of 1% freshly prepared NEM.

2.9. Pull-down assay

Cultures of BL21 Star (DE3) competent cells transformed with the pGEX4T3 vector or pGEX4T3/$FasL_{Cyto}$ were grown in 1L of LB with 50µl/ml ampicillin at 37°C with rotation until the absorbance at 600 nm was about 1.8 units. Expression of the GST-tagged construct was induced by addition of 0.2 mM IPTG and incubation for 3 hours at 37°C with rotation. Bacteria were then

pelleted, resuspended in 50 ml of cold PBS and disrupted by sonication (5 pulses of 30 sec with 30 sec intervals). Triton X-100 was then added at final concentration of 1 %v/v and gently mixed for 30 min at room temperature. After centrifugation at 10,000 rpm for 10 min at 4 °C, 1 ml of a 50% slurry of glutathione sepharose 4B was added to sonicates and they were incubated at room temperature with gentle agitation for 30 min. GST-containing proteins were sedimented by centrifugation at 2500 rpm for 5 min at 4 °C, washed 6 times with 6x NaCl PBS and resuspended in 2 ml of cold PBS. 100 µl of the suspension containing the GST-$FasL_{Cyto}$ polypeptide (and 100 µl of the suspension containing GST as a control) were incubated overnight at 4 °C with rotation with 1 ml of CTL or COS-1 lysates corresponding to 1 x 10^7 or 1 x 10^6 cells, respectively. Beads were pelleted and washed three times with NP-40 lysis buffer and then prepared for SDS-PAGE by addition of 60 µl of 1X Laemmli reducing sample buffer and boiling for 5 min.

2.10. SDS-PAGE and Coomasie Blue Staining

Cell lysates, IPs and pull-downs were analyzed by electrophoresis on 8.5% acrylamide SDS-PAGE gels. Some of these gels were stained with Bio-Safe Coomasie G-250 stain (Bio-Rad, Hercules, California, USA) using the instructions from the manufacturer.

2.11. Mass spectrometry

Bands were excised from the polyacrylamide gels stained with Coomasie Blue and sent for mass spectrometry sequencing and analysis at the Mass Spectrometry Facility of the University of Alberta.

2.12. Western Blotting

Proteins from some of the polyacrylamide gels were transferred to polyvinylidene difluoride (PVDF) membranes (Bio-Rad, Hercules, California, USA) and blocked with 5 % milk powder in washing buffer (0.01M Tris, 0.15 NaCl pH 7.6 0.1% Tween-20). Western Blots were performed using the indicated primary and appropriate HRP-coupled secondary antibodies and visualized by enhanced chemiluminisence (ECL) reagents (PerkinElmer Life Science Products, Boston, Massachusetts, USA). When sequential Western Blots were needed, antibodies were stripped off the membrane with a buffer containing β-mercaptoethanol, SDS and Tris-HCl pH 6.7 at 56 °C for 30 min.

2.13. Flow cytometry analysis

For surface staining cells were washed with cold 5 mM EDTA PBS and incubated with the indicated antibodies or the corresponding isotype controls in 100 µl of cold PBS supplemented with 5 mM EDTA and 4% dCS for 30 min in ice. For detection of total protein levels (surface and intracellular), cells were fixed with 2 % paraformaldehyde for 20 min at room temperature, then washed with 1 % dCS PBS and finally stained in 100 µl of PBS supplemented with 0.2 % saponin and 4 % dCS with the indicated antibodies and the appropriate isotype controls. After washing with 0.2 % saponin 4 % dCS PBS and PBS cells were resuspended in 0.1 % formaldehyde PBS for flow cytometry analysis. Cells were analyzed in the BD FACS Calibur or BD LSR II flow cytometers (BD Biosciences, San Jose, California, USA) and data was analyzed in the FCS Express software (De Novo Software, Los Angeles, California, USA).

2.14. Active Caspase 3 assay for FasL-mediated cytotoxicity

L.Fas cells were harvested, washed with PBS, resuspended in 10 ml of RPMI 1640 and incubated with 1 µl of Cell Tracker Orange CMRA for 30 min at

37 °C. Cells were then centrifuged, resuspended in 10 ml of RPMI 1640 and incubated another 30 min at 37 °C. After washing, labeled cells were resuspended in cold RPMI 1640 supplemented with 4% dCS at $1x10^6$ cells/ml and combined at 4:1 ratio (COS-1: L.Fas) with COS-1 cells transfected with FasL. Cells were centrifugated at 200 g for 3 min at 4 °C and incubated for 2 hs at 37 °C. After vortexing, cells were permeabilized and stained for intracellular active Caspase 3 analysis by flow cytometry as described above. The percentage of cells expressing active caspase 3 was determined after gating on the stained L.Fas population.

2.15. Confocal microscopy analysis

Cells were harvested, washed with PBS and resuspended in PBS at 3 x 10^6 cells/ml. 200 µl were then incubated with coverslips (previously incubated with poly-L-lysine overnight) for 10 min at room temperature and then fixed with 1 ml of methanol for 10 at -20 °C. Cells were washed with PBS and blocked with blocking buffer (PBS supplemented with 2% donkey serum and 1 % BSA) for 30 min at room temperature. Staining was conducted with a 1/100 or 1/50 dilution of the indicated primary antibodies in blocking buffer for 30 min at room temperature in a dark chamber. After washing, staining with the appropriate secondary antibodies was conducted using 1/400 or 1/500 dilutions on blocking buffer. When biotinylated antibodies were employed, blocking and staining steps were conducted with 0.1 mg/ml NeutrAvidin 1% BSA in PBS. For double or three-color staining, each antibody was added and incubated independently in separate steps. Stained coverslip were finally mounted onto microscope slide with ProLong antifade reagent (Life technologies, Carlsbad, California, USA). Samples were examined with a Zeiss LSM710 confocal microscope at the Imaging Facility of the Cross Cancer Institute. Plan Apochromat 40x/1.3 oil DIC objective lens was used. Z-stack images (interval 0.2 µm) were acquired and subjected to deconvolution using the Huygens Essential software (Scientific Volume Imaging, Hilversum, The Netherlands). Three-dimensional reconstruction and Z projections were done using Imaris software (BitPlane, Zurich,

Switzerland) and the ImarisColoc application was utilized to analyse colocalization. This software allowed me to create a three-dimensional color channel containing the colocalization results and it provided me with the Manders coefficient. The fluorescent intensity profiles were obtained using the ZEN software. The corresponding Pearson coefficients were calculated using Excel (Microsoft, Washington, USA). In all cases, staining with secondary antibodies without the primary antibody staining led to negligible background. For untransfected samples, three areas under the microscope were randomly acquired in each of the independent experiments. Each area contained between 3 to 10 cells. For transfected samples, 4-7 areas where transfected cells could be seen, were acquired in each of the independent experiments. Each imaged area contained 1 to 3 cells. Unless otherwise stated in the corresponding legend all the data shown in this report is representative of at least 3 independent experiments.

The scoring system to classify the location of transfected proteins is based on the analysis of three dimensional confocal microscopy images. If the fluorescent staining of the protein was observed as an outline perfectly coinciding with the edge of the cell, I categorized that as a membrane (M) localization. If the fluorescent staining of the protein was detected as spots within the cell, I classified that as intracellular vesicles (IV) localization. Finally, if the protein could be simultaneously be detected both on the surface as well as within intracellular vesicles in the same cell, I scored that protein to have a membrane + intracellular vesicle (M+ IV) localization in that particular cell. Analysis of the localization of the same protein in several cells allowed me to determine the trend for localization in the majority of the studied cells.

2.16. Endocytosis microscopy assay

CTL were harvested, washed with PBS and resuspended in 1% BSA PBS at 3 x 10^6 cells/ml. 200 µl were then incubated with coverslips (previously incubated with poly-L-lysine overnight) for 10 min at room temperature and blocked with NeutrAvidin 0.1 mg/ml. After washing three times with PBS, cells

were incubated with biotin-conjugated anti-FasL, or biotin-isotype control for 4 hours at 37 °C. After being thoroughly washed, they were permeabilized with methanol, stained with appropriate secondary antibodies and analyzed by confocal microscopy as described above.

In the experiments assessing FasL recycling (shown in Figure 4.7) a pre-incubation with CHX was added to the protocol as follows. CTL were harvested, washed with PBS and resuspended in 1% BSA PBS at 3 x 10^6 cells/ml. Half of them were incubated with 10 μg/ml CHX and all of them were incubated for 3.5 hours at 37 °C. During the last 30 min, NeutrAvidin was added at 0.1 mg/ml. After washing three times with PBS, cells were resuspended in 1 % BSA PBS. The portion of cells that had been pre-incubated with CHX was further divided in two and incubated with biotin-conjugated anti-FasL, or biotin-isotype control, together with CHX. Cells not pre-incubated with CHX were also divided in two and incubated with biotin-conjugated anti-FasL or biotin-conjugated isotype control. They were all incubated 13 hours at 37 °C. After being thoroughly washed, they were fixed onto coverslips, permeabilized with methanol, stained with appropriate secondary antibodies and analyzed by confocal microscopy as described above.

2.17. Statistical analysis

Statistical analysis of results was done using unpaired Student *t* test with the Prism software (GraphPad Software, La Jolla, California, USA).

CHAPTER 3: Identification and Characterization of the Storage Vesicle for FasL in Cytotoxic T Lymphocytes

3.1. Introduction

Stimulation of cytotoxic T lymphocytes results in the production of newly synthesized FasL molecules (He and Ostergaard 2007). However, constitutive expression generates a baseline pool of pre-formed FasL proteins that remain stored within the killer cells in order to respond to the stimulation signal triggered by the encounter of a target cell and rapidly translocate to the cell surface where FasL can induce target-cell apoptotic death (Kessler et al. 1998, Li et al. 1998). FasL is stored in intracellular vesicles in different cell types, such as T cells, NK cells, monocytes and tumor cells (Kiener et al. 1997, Bossi and Griffiths 1999, Blott et al. 2001, Andreola 2002, Kojima et al. 2002, Smith et al. 2003, Lettau et al. 2004, Qian et al. 2006, He and Ostergaard 2007, Zuccato et al. 2007, Kassahn et al. 2009, Schmidt et al. 2011a, Schmidt et al. 2011b). The identity of the storage vesicle in CTL, however, remains controversial. Bossi et al. showed by confocal microscopy analysis that FasL colocalized with typical components of the cytolytic granules (perforin, cathepsin D and granzyme B) in the human NK cell line YT, as well as in the human $CD8^+$ CTL clone $GC8^+$e cells. Furthermore, GFP-tagged FasL transfected into the rat basophil leukemia cell line RBL colocalized with the lysosomal protein lgp100 (Bossi and Griffiths 1999) and with cathepsin D (Qian et al. 2006). Similarly, endogenous FasL colocalized with cathepsin D in human $CD4^+$and $CD8^+$ CTL clone cells (Lettau et al. 2004). On the other hand, subcellular fractionation of human T cells, revealed FasL and granzyme B were enriched in separate density fractions (Schmidt et al. 2011a) and confocal microscopy analysis of murine T cell blasts showed no colocalization between endogenous FasL and the lysosomal granule marker lysosomal-associated membrane protein 1 (LAMP-1) (Kassahn et al. 2009). Moreover, previous results from our laboratory have shown that endogenous FasL does not colocalize with cathepsin D, LAMP-1, granzyme B or perforin in murine CTL

clone cells (He and Ostergaard 2007) and in human CTL (He and Ostergaard, unpublished data) analyzed by confocal microscopy.

Previous experiments from our laboratory (He and Ostergaard, unpublished data) also showed that FasL did not colocalize with the ER markers calnexin and β-COP (Wada et al. 1991, Oprins et al. 1993) and the Golgi marker 58K (Gao 1998). Nonetheless, the composition of the storage vesicle for FasL remains unknown and further experiments are required to identify the compartment in which FasL is stored in cytotoxic T lymphocytes.

In this chapter, through confocal microscopy studies I identified three markers of the FasL storage vesicle: Syntaxin 3, Munc18-2 and Rab32. I demonstrated that the components of the FasL vesicle differ from those of lysosomal granules further validating that FasL is not stored in granules and instead located in a vesicle of unique composition. I showed the composition of the vesicle was consistent in several T cell types and indicated the vesicle may be found near the ER and mitochondria, suggesting a strategic location for sensing the intracellular Ca^{++} flux triggered within the T cell upon TCR engagement with the specific peptide-MHC complex on the target cell.

3.2. Results

3.2.1. FasL is not stored in late endosomes or lysosomal granules

To identify the components of the FasL storage vesicle I used confocal microscopy to examine the colocalization of FasL with known markers of different subcellular structures or organelles by confocal microscopy. CD63 is a tetraspanin protein typically described to be in late endosomes and lysosomes (Kobayashi et al. 2000). However, Schmidt et al. showed that FasL was co-enriched with CD63 in the same fraction from an iodixanol gradient (Schmidt et al. 2011a) suggesting it could be in the FasL storage vesicle in T cells. To evaluate this possibility, I stained unstimulated Clone 3/4 cells (non-transformed peptide-specific CTL clones) for FasL and CD63 for confocal microscopy

analysis. Acquisition of Z-stack images, followed by deconvolution and three-dimensional reconstruction of the acquired images, showed that FasL is located in intracellular vesicles, as previously described, but overlapping of FasL and CD63 images showed no colocalization of the vesicles (**Figure 3.1**, third panel). I further studied colocalization by generating a "colocalization" image (**Figure 3.1**, forth panel) which only shows signal where the fluorescent signals for FasL and CD63 overlap, clearly indicating the spots in the three dimensional cell where the proteins coexist, which in this case were few. I also determined the Manders coefficient (M_1) that indicates the percentage of overlap between two fluorescent signals. The coefficient ranges from 0: no overlap, to 1: complete colocalization. The low value of M_1 corresponding to the overlap of FasL and CD63 reflected the poor colocalization of these proteins. However, false positives could arise from partially overlapping vesicles that fortuitously collide in the small cytosolic space of T lymphocytes. To reduce the possibility of an erroneous analysis and validate the reported results, I analyzed the fluorescent intensity profile by tracing a line over the image with merged signals, attempting to include maximums for both, and I graphed the profile for both signals for every spot on that line (**Figure 3.1**, second row). If the peaks for each intensity profile are found on the same spot, this suggests true colocalization. I also calculated the Pearson coefficient (r) for the two intensity functions in the graph. This coefficient indicates correlation between two variables and ranges from -1: completely independent, to 1: perfect correlation. For FasL and CD63, the peaks did not coincide and the Pearson coefficient was 0.08, a low value, further corroborating my conclusion that FasL and CD63 do not colocalize.

As discussed above, the colocalization of FasL with markers of the lysosomal granules has remained controversial over many years. Early studies advocated FasL was stored with degranulation proteins in secretory lysosomes (Bossi and Griffiths 1999, Lettau et al. 2004, Qian et al. 2006). Later studies, however, showed it localized in a different compartment, not yet characterized (He and Ostergaard 2007, Kassahn et al. 2009, Schmidt et al. 2011a). In order to evaluate whether or not FasL was localized in lysosomal granules, I applied the

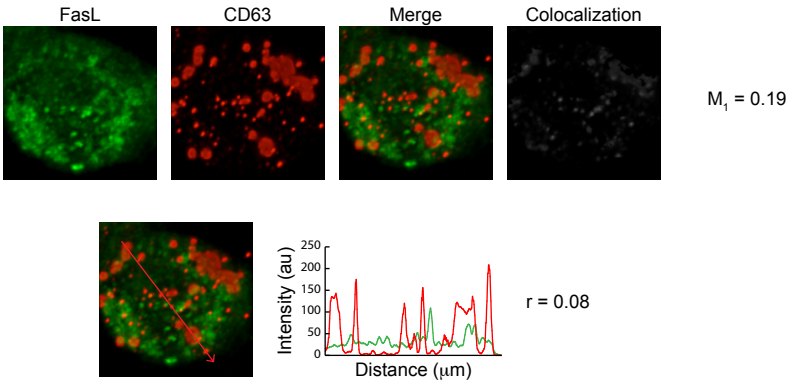

Figure 3.1. FasL is not stored in late endosomes
Clone 3/4 CTL cells were stained with antibodies specific for FasL and CD63, as well as the appropriate secondary antibodies and analyzed by confocal microscopy. Z-stack images were acquired (interval, 0.2μm) and subjected to deconvolution and three-dimensional reconstruction. Representative projections of the reconstructed images are shown. Colocalization images were created displaying only the regions where the two channels colocalize and the corresponding Manders coefficients (M_1) were calculated. Lines were drawn across the merged images attempting to include maximums from both channels, the fluorescent intensity profiles over that line were graphed and Pearson coefficients (r) were calculated for each pair of profiles. Data is representative of 2 independent experiments corresponding to at least 30 cells.

detailed colocalization analysis described above in cells stained with antibodies specific for perforin and LAMP-1. Perforin is a cytolytic molecule while LAMP-1 is a lysosomal protein and they are both found in secretory lysosomes in T cells (Carlsson et al. 1988, Peters et al. 1991). I stained CTL Clone 3/4 cells with anti-FasL and anti-perforin as well as with anti-FasL and anti-LAMP-1 antibodies. The analysis showed that FasL did not colocalize with perforin or LAMP-1 (**Figure 3.2 A and B**) corroborating later studies that FasL is not stored within the granules. As a control, I analyzed the colocalization of LAMP-1 and cathepsin D, a protease also used as a marker of lysosomal granules. These two proteins are indisputably considered to reside in the same vesicle (Bucci et al. 2000, Blott and Griffiths 2002, He and Ostergaard 2007, Appelqvist et al. 2013) and the antibodies used for staining exhibit negligible background and strong signal. The high colocalization displayed by the colocalization analysis (**Figure 3.2 C**) serves as a control for the analysis itself and confirms that the lytic granules remain intact in the CTL used in this study.

Overall, the lack of colocalization of FasL with CD63, perforin and LAMP-1 indicate that FasL is not stored in late endosomes or lysosomal granules. Together with previous results that indicated that FasL is not stored in the ER or Golgi compartments, they emphasize the uniqueness of the FasL storage compartment.

3.2.2. FasL is not stored with TNF-α or PD-1

Since FasL failed to colocalize with typical components of common ubiquitous vesicles and organelles, I next attempted to determine if FasL was stored together with other proteins with prominent roles in cytotoxic T cells. TNF-α is a cytokine, and like FasL, belongs to the TNF ligand superfamily and is responsible for inducing cytotoxicity (Lee et al. 1996). Moreover, in macrophages TNF-α is stored in vesicles that colocalize with vesicle-associated membrane protein 3 (VAMP-3) and upon stimulation with LPS it is quickly transported to

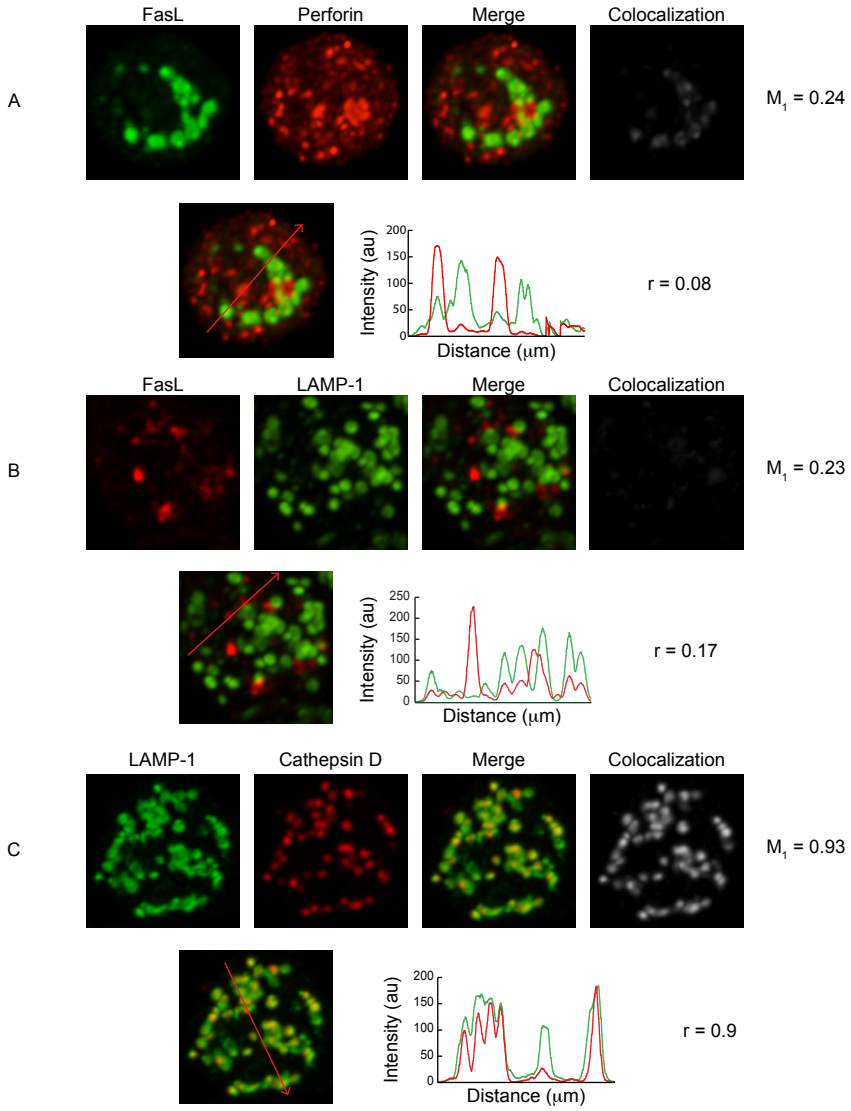

Figure 3.2. FasL is not stored in lysosomal granules.
Clone 3/4 CTL cells were stained with antibodies specific for FasL and perforin **(A)** or LAMP-1 **(B)** and for cathepsin D and LAMP-1 **(C)** as well as the appropriate secondary antibodies, and subsequently analyzed by confocal microscopy. Z-stack images were acquired (interval, 0.2μm) and subjected to deconvolution and three-dimensional reconstruction. Representative projections of the reconstructed images are shown. Colocalization images were created displaying only the regions where the two channels colocalize and the corresponding Manders coefficients (M_1) were calculated. Lines were drawn across the merged images attempting to include maximums from both channels, the fluorescent intensity profiles over that line were graphed and Pearson coefficients (r) were calculated for each pair of profiles. Data is representative of 3 independent experiments corresponding to at least 27 cells.

the cell surface for secretion at the site of the phagocytic cup formation (Murray et al. 2005). Due to their sequence homology, and their functional similarity in their cytotoxic abilities, I postulated that TNF-α and FasL would be stored in the same vesicle in CTLs and that they would colocalize. I stained unstimulated CTL Clone 3/4 cells for FasL and TNF-α and analyzed the results by confocal microscopy. Because I was unable to detect TNF-α in this condition (**Figure 3.3 A**), I stimulated the Clone 3/4 cells with phorbol 12-myristate 13-acetate (PMA) and ionomycin for 2 hours. These two chemicals result in PKC activation and intracellular Ca^{++} flux, replicating the signals T cells receive after TCR engagement (Berrebi et al. 1987). In macrophages, detection of surface accumulation of TNF-α by confocal microscopy, involves treatment of the cells with a TNF-α processing inhibitor (TAPI) that inhibits the action of the surface TNF-α converting enzyme (TACE) and blocks the proteolytic release of TNF-α (Black et al. 1997). I adopted this method in my experiment and included samples treated (1) only with DMSO (as a carrier control), (2) treated with 10 μM TAPI, (3) treated with DMSO, PMA and ionomycin, or (4) treated with TAPI, PMA and ionomycin. Upon analysis of the confocal images obtained, I concluded that TNF-α seems to be expressed in stimulated T cells only and that its localization is different from that of FasL (**Figure 3.3**).

I also explored the possibility of FasL being found in the same vesicle as other TNF superfamily members. I assayed for colocalization with CD40L, a member of the TNF ligand superfamily shown to be stored in intracellular vesicles distinct from the lytic granules in $CD4^+$ T cells (Koguchi et al. 2011). I also tried to study the colocalization with CD27 and 41BB, which are members of the TNF receptor superfamily and are expressed in T cells (Croft 2003). However, I was unable to detect these proteins by confocal microscopy. I then proceeded to assess if FasL colocalized with VAMP-3 or CTLA-4. VAMP-3 colocalizes with TNF-α in macrophages and mediates the fusion of its storage vesicle to the cell surface (Murray et al. 2005) and CTLA-4 is stored intracellularly in T cells (Leung et al. 1995). However, I was unable to detect any of the listed proteins by confocal microscopy. Possible reasons for this failure of detection could include

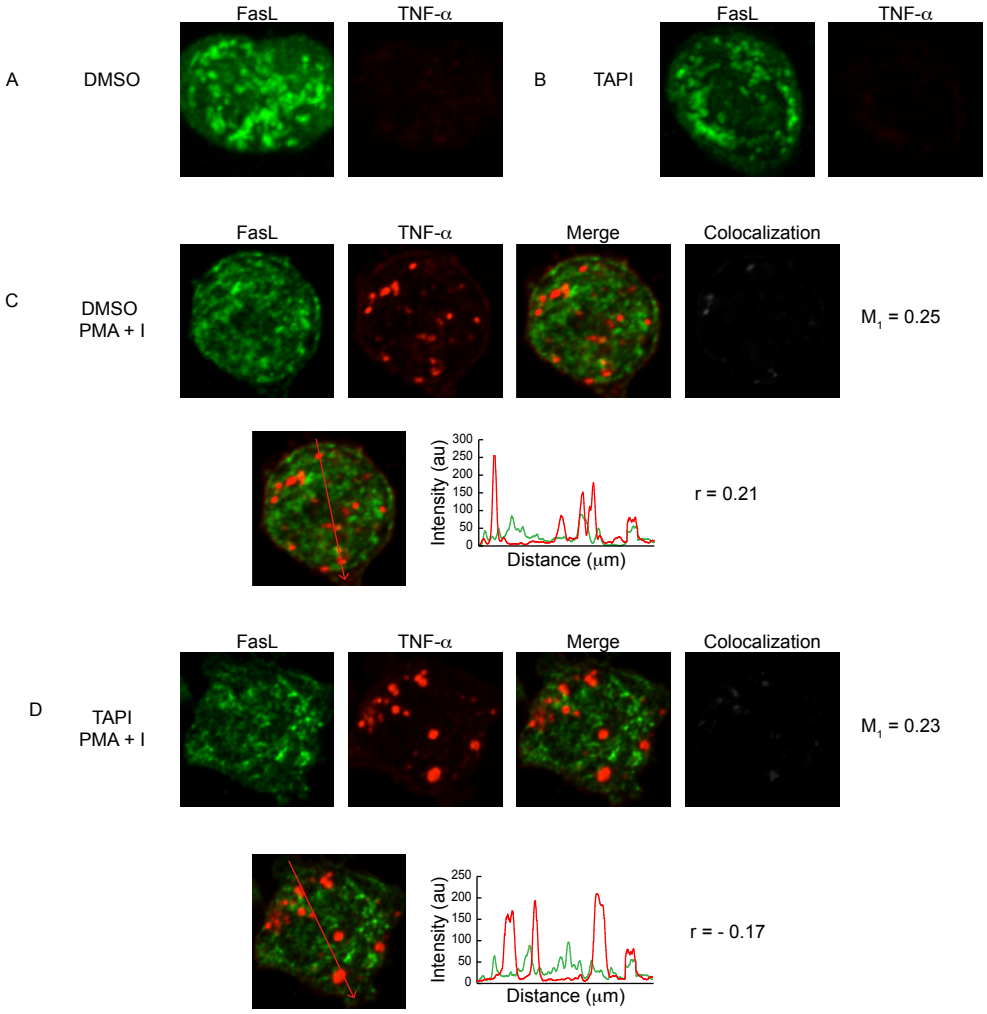

Figure 3.3. TNF-α is expressed after stimulation and is not found with FasL. Clone 3/4 CTL cells were treated with DMSO (as a carrier control) **(A)** TAPI **(B)**, DMSO, PMA and Ionomycin (I) **(C)** or TAPI PMA and Ionomycin **(D)** for 2 hours. Subsequently treated cells were stained with antibodies specific for FasL and TNF-α as well as the appropriate secondary antibodies and analyzed by confocal microscopy. Z-stack images were acquired (interval, 0.2μm) and subjected to deconvolution and three-dimensional reconstruction. Representative projections of the reconstructed images are shown. **(C and D)** Colocalization images were created displaying only the regions where the two channels colocalize and the corresponding Manders coefficients (M_1) were calculated. Lines were drawn across the merged images attempting to include maximums from both channels, the fluorescent intensity profiles over that line were graphed and Pearson coefficients (r) were calculated for each pair of profiles. Data is representative of 2 independent experiments corresponding to at least 12-36 cells.

that the proteins are not expressed at high enough levels for detection or that the antibodies employed did not recognize their target proteins under the conditions used for my studies.

Lastly, I stained CTL Clone 3/4 cells for FasL and programmed death-1 (PD-1). PD-1 is a ligand stored in intracellular vesicles in T cells and lacked colocalization with markers of Golgi, recycling endosomes, and lysosomal granules in a recent study (Pentcheva-Hoang et al. 2007). However, my results do not support FasL colocalization with PD-1 (**Figure 3.4**), indicating these proteins are not stored in the same vesicle.

3.2.3. FasL appears to be located near MAMs

Previous experiments in our laboratory suggested FasL was closely associated with the ER and the mitochondria (He and Ostergaard, unpublished data). To further investigate these observations, I analyzed the colocalization of FasL and cytochrome C by confocal microscopy. The presence of yellow spots on the merged image and of white vesicle-shaped spots on the "colocalization" channel as well as the intermediate value of the Manders coefficient ($M_1 = 0.43$) suggested there was a partial colocalization between these proteins (**Figure 3.5**, top row). Moreover, the intensity profile analysis of the merged image showed that some of the peaks coincided and some of them were slightly out of phase (**Figure 3.5**, bottom row) further substantiating the partial colocalization of the two proteins and suggesting close proximity of FasL to the mitochondria.

Mitochondria-associated membranes (MAMs) are zones of close contact between the mitochondria and the ER that allow for efficient lipid and Ca^{++} exchange (Giorgi et al. 2009). Glucose regulated protein 78 (Grp78), also known as Binding immunoglobulin protein (BiP), is an ER chaperone enriched in the MAMs of human embryonic kidney 293 cells (Gilady et al. 2010). Interestingly, analysis of FasL colocalization with Grp78 also showed partial overlay of the two proteins and examination of the intensity versus distance profile revealed mostly non-overlapping peaks and some FasL maximums slightly shifted with respect to

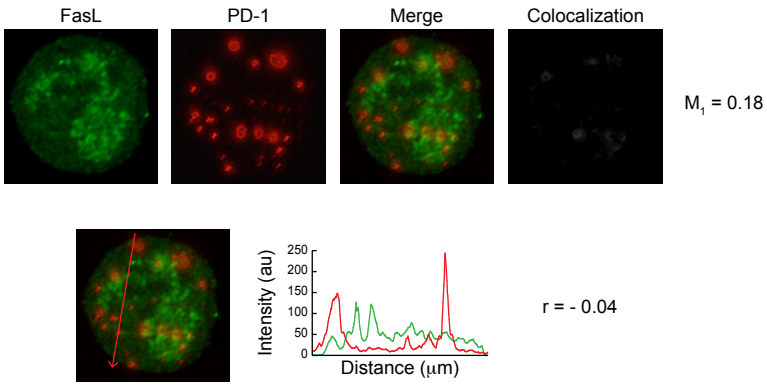

Figure 3.4. FasL is not stored with PD-1.
Clone 3/4 CTL cells were stained with antibodies specific for FasL and PD-1, as well as the appropriate secondary antibodies, and analyzed by confocal microscopy. Z-stack images were acquired (interval, 0.2μm) and subjected to deconvolution and three-dimensional reconstruction. Representative projections of the reconstructed images are shown. Colocalization images were created displaying only the regions where the two channels colocalize and the corresponding Manders coefficients (M_1) were calculated. Lines were drawn across the merged images attempting to include maximums from both channels, the fluorescent intensity profiles over that line were graphed and Pearson coefficients (r) were calculated. Data is representative of 6 independent experiments corresponding to at least 54 cells.

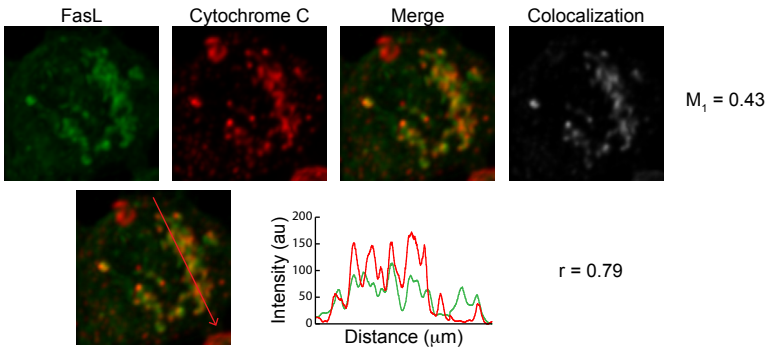

Figure 3.5. FasL is stored near the mitochondria.
Clone 3/4 CTL cells were stained with antibodies specific for FasL and cytochrome C, as well as the appropriate secondary antibodies, and analyzed by confocal microscopy. Z-stack images were acquired (interval, 0.2μm) and subjected to deconvolution and three-dimensional reconstruction. Representative projections of the reconstructed images are shown. Colocalization images were created displaying only the regions where the two channels colocalize and the corresponding Manders coefficients (M_1) were calculated. Lines were drawn across the merged images attempting to include maximums from both channels, the fluorescent intensity profiles over that line were graphed and Pearson coefficients (r) were calculated. Data is representative of 3 independent experiments corresponding to at least 27 cells.

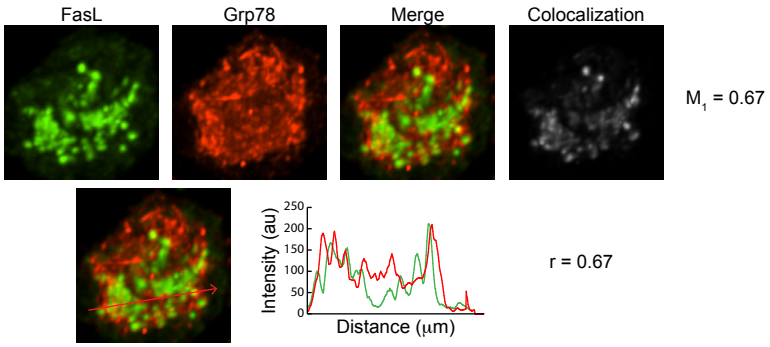

Figure 3.6. FasL is stored near the mitochondria-associated membranes.
Clone 3/4 CTL cells were stained with antibodies specific for FasL and Grp78, as well as the appropriate secondary antibodies, and analyzed by confocal microscopy. Z-stack images were acquired (interval, 0.2μm) and subjected to deconvolution and three-dimensional reconstruction. Representative projections of the reconstructed images are shown. Colocalization images were created displaying only the regions where the two channels colocalize and the corresponding Manders coefficients (M_1) were calculated. Lines were drawn across the merged images attempting to include maximums from both channels, the fluorescent intensity profiles over that line were graphed and Pearson coefficients (r) were calculated. Data is representative of 5 independent experiments corresponding to at least 45 cells.

the Grp78 peaks (**Figure 3.6**). Overall, the results from these two experiments support previous observations from our laboratory and reinforce the hypothesis that FasL is stored in a compartment near the MAMs. This location would allow FasL to efficiently sense the Ca^{++} ions released from the ER after stimulation before they are sequestered by the mitochondria.

3.2.4. FasL is stored with Rab32

Rab32 is a Rab protein that regulates the composition of MAMs in human epithelial HeLa cells (Bui et al. 2010). Due to its close association with MAMs, I hypothesized FasL would colocalize with Rab32. To test this hypothesis, I stained CTL Clone 3/4 cells for FasL and Rab32 and assessed their colocalization by confocal microscopy. The analysis revealed that these two proteins had a high level of colocalization (**Figure 3.7 A**). To further support my conclusion, I calculated the M_1 values corresponding to cells from three separate acquisitions taken in three independent experiments and compared their distribution relative to positive and negative controls. I chose the colocalization M_1 values of LAMP-1 and cathepsin D (Figure 3.2) as a positive control and of FasL and PD-1 (Figure 3.4) as a negative control. Since the M_1 values for the colocalization of FasL and Rab32 were distributed in a similar range as the positive control (**Figure 3.7 B**), I concluded that FasL is stored in the same vesicle with Rab32 in CTL.

3.2.5. FasL is stored with Syntaxin 3 and Munc18-2

After identifying Rab32 and FasL as residents of the same storage vesicle in CTLs, I wanted to investigate additional potential markers of the FasL storage vesicle. I looked into protein trafficking mediators as potential candidates. A recent study in human cytotoxic T lymphocytes showed that of the 17 SNARE proteins tested, Syntaxin 3 (Stx3) and Syntaxin 11 (Stx11) were localized in intracellular vesicles and showed no colocalization with perforin (Pattu et al. 2012). Given that in my investigation I observed that FasL was also localized in

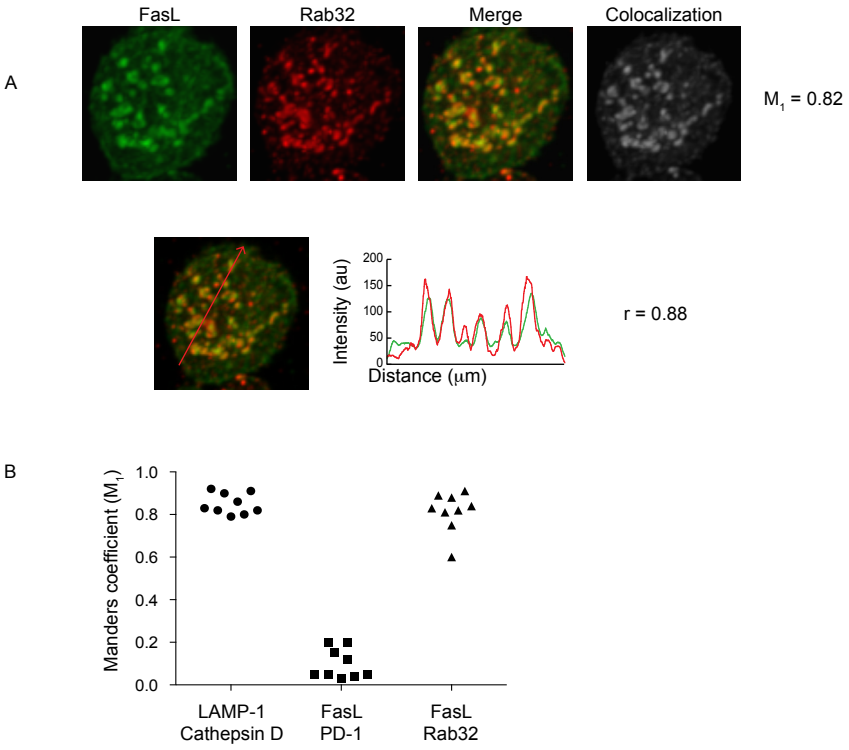

Figure 3.7. FasL is stored with Rab32.
Clone 3/4 CTL cells were stained with antibodies specific for FasL and Rab32, as well as the appropriate secondary antibodies, and analyzed by confocal microscopy. Z-stack images were acquired (interval, 0.2μm) and subjected to deconvolution and three-dimensional reconstruction. **(A)** Representative projections of the reconstructed images are shown. Colocalization images were created displaying only the regions where the two channels colocalize and the corresponding Manders coefficients (M_1) were calculated. Lines were drawn across the merged images attempting to include maximums from both channels, the fluorescent intensity profiles over that line were graphed and Pearson coefficients (r) were calculated. Data is representative of 4 independent experiments corresponding to at least 36 cells. **(B)** M_1 coefficients corresponding to cells from three separate acquisitions taken in three independent experiments of samples stained for LAMP-1 and cathepsin D (positive control – 1st set), FasL and PD-1 (negative control – 2nd set) and FasL and Rab32 (3rd set).

intracellular vesicles that did not localize with perforin, I sought out to determine if the SNARE proteins Stx3 and Stx11 were on the same storage vesicle as FasL. To test this hypothesis, I analyzed colocalization by confocal microscopy. Although staining for Stx11 resulted in no detection of the protein, the analysis of FasL colocalization with Stx3 by confocal microscopy resulted in a high level of colocalization (**Figure 3.8 A**). Stx3 is a SNARE protein involved in the fusion step of vesicle trafficking and has been shown to participate in a number of different processes in neuronal cells (Jurado et al. 2013), mast cells (Tadokoro et al. 2007, Brochetta et al. 2014), melanocytes (Yatsu et al. 2013), pancreatic beta cells (Zhu et al. 2013), epithelial cells (Sharma et al. 2006), acinar cells (Hansen 1999) and macrophages (Hackam et al. 1996). However, its localization or function has not been described in T cells. Interestingly, Stx3 has been shown to interact with Munc18-2 (Hata and Sudhof 1995, Martin-Verdeaux 2002). Munc18-2 belongs to the family of SM (Sec/Munc-like) proteins which function as regulators of SNARE complex assembly (Sudhof and Rothman 2009, Carr and Rizo 2010). Because of the reported association of Stx3 with Munc18-2, and the high colocalization of FasL with Stx3, I hypothesized that FasL would reside with Munc18-2 in the same vesicles. I stained CTL Clone 3/4 cells for FasL and Munc18-2 and analyzed their colocalization by confocal microscopy. I concluded that FasL colocalized with Munc18-2 (**Figure 3.8 B**). The examination of M_1 values that reflect the overlap of FasL with Stx3 and of FasL with Munc18-2, together with the comparison to positive and negative controls (**Figure 3.8 C**), further supports the conclusion that FasL is stored with Stx3 and Munc18-2.

3.2.6. The FasL storage vesicle is distinct from the cytolytic granules

The strong degree of colocalization of FasL with Rab32 (Figure 3.7), Stx3 and Munc18-2 (Figure 3.8) could signify that FasL is stored in vesicles that contain all of these proteins or it could also mean that it is stored in several vesicles that contain each of these proteins or a combination of them. To determine which of the two possibilities defines the FasL storage vesicles, I

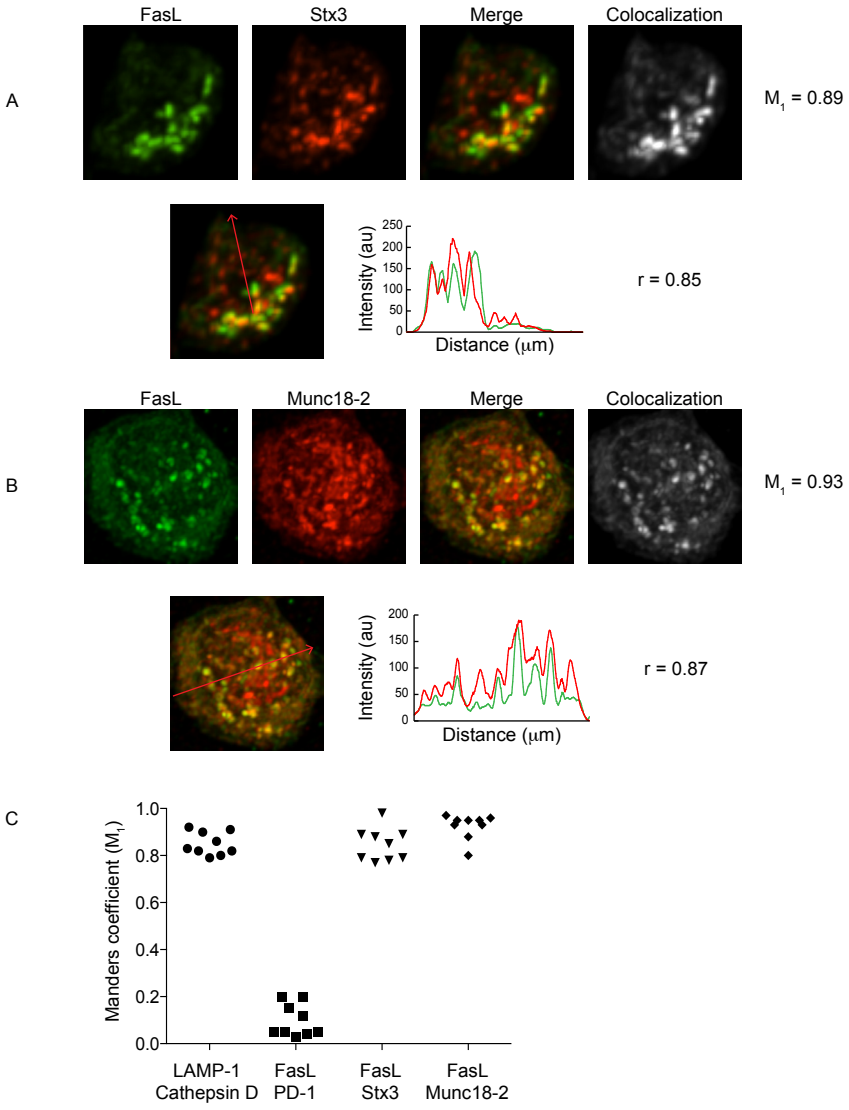

Figure 3.8. FasL is stored with Stx3 and Munc18-2.
Clone 3/4 CTL cells were stained with antibodies specific for FasL and Stx3 **(A)** or Munc18-2 **(B)**, as well as the appropriate secondary antibodies, and analyzed by confocal microscopy. Z-stack images were acquired (interval, 0.2μm) and subjected to deconvolution and three-dimensional reconstruction. Data is representative of 4 independent experiments corresponding to at least 36 cells. **(A and B)** Colocalization was analyzed and displayed as explained in Figure 3.7. **(C)** M_1 coefficients corresponding to cells from three separate acquisitions taken in three independent experiments of samples stained for LAMP-1 and cathepsin D (positive control – 1st set), FasL and PD-1 (negative control - 2nd set), FasL and Stx3 (3rd set) and FasL and Munc18-2 (4th set).

assessed the localization of Stx3 relative to Rab32 and Munc18-2 in CTL Clone 3/4 cells. Analysis of the colocalization of Stx3 with Rab32 indicated that there was high colocalization of the two proteins, although there were some $Stx3^+$ $Rab32^-$ and some $Rab32^+$ $Stx3^-$ vesicles (**Figure 3.9 A**). Similarly, most of the $Stx3^+$ vesicles seemed to colocalize with Munc18-2 (**Figure 3.9 B**). In **Figure 3.9 C**, I plotted the M_1 coefficients corresponding to cells stained for Stx3 and Rab32 and stained for Stx3 and Munc18-2, and compared them to positive and negative controls previously described above. The distribution of the M_1 values in this graph indicated Stx3 is likely in the same vesicles as Munc18-2 and in most of the $Rab32^+$ vesicles. Overall these results suggest that FasL is in $Rab32^+$ $Stx3^+$ $Munc18\text{-}2^+$ vesicles.

FasL colocalized with Rab32, Stx3 and Munc18-2 (Figures 3.7 and 3.8) and it did not colocalize with perforin or LAMP-1 (Figure 3.2), suggesting the FasL storage vesicle has a different composition from the cytolytic granules. If this premise was correct, none of the FasL storage vesicle components would colocalize with members of the cytolytic granules. To test this hypothesis, I stained CTL Clone 3/4 cells with Stx3 and perforin and analyzed their colocalization by confocal microscopy. As expected, Stx3 did not overlap with perforin (**Figure 3.10 A**). I also analyzed the colocalization of Stx3 with LAMP-1 and concluded they did not colocalize either (**Figure 3.10 B**). Furthermore, Rab32 also displayed a low level of colocalization with LAMP-1 (**Figure 3.10 C**). Although the M_1 coefficient corresponding to the colocalization image could have suggested a minimal partial colocalization, the intensity vs. distance profile revealed that the intensity peaks did not align and the seemingly partial colocalization observed is probably due to the high background staining of the Rab32 antibody. Overall comparison of the distribution of M_1 coefficients with respect to positive and negative controls supported the conclusion that Stx3 and Rab32 did not colocalize with perforin and LAMP-1 (**Figure 3.10 D**). These results further support that FasL storage vesicles are distinct in composition to the cytolytic granules.

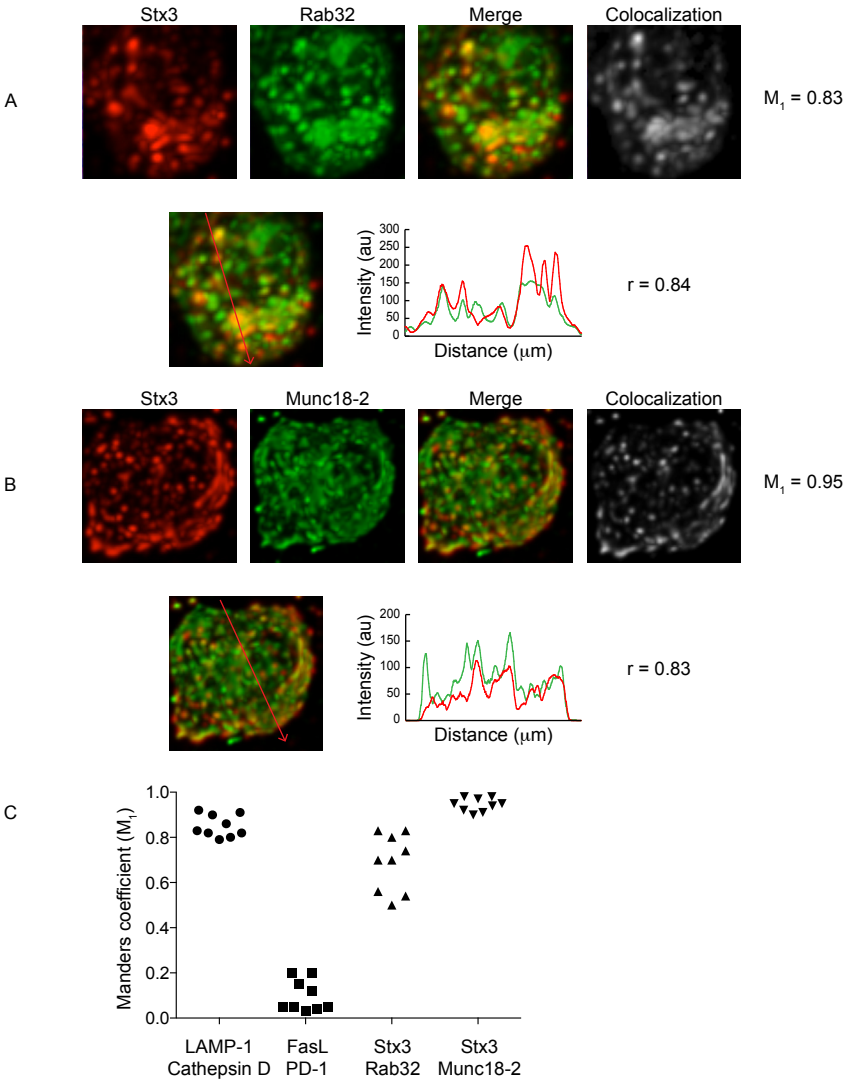

Figure 3.9. Stx3 is stored with Rab32 and Munc18-2.
Clone 3/4 CTL cells were stained with antibodies specific for Stx3 and Rab32 **(A)** or Munc18-2 **(B)**, as well as the appropriate secondary antibodies, and analyzed by confocal microscopy. Z-stack images were acquired (interval, 0.2μm) and subjected to deconvolution and three-dimensional reconstruction. Data is representative of 3 independent experiments corresponding to at least 27 cells. **(A and B)** Colocalization was analyzed and displayed as explained in Figure 3.7. **(C)** M_1 coefficients corresponding to cells from three separate acquisitions taken in three independent experiments of samples stained for LAMP-1 and cathepsin D (positive control – 1st set), FasL and PD-1 (negative control – 2nd set), Stx3 and Rab32 (3rd set) and Stx3 and Munc18-2 (4th set).

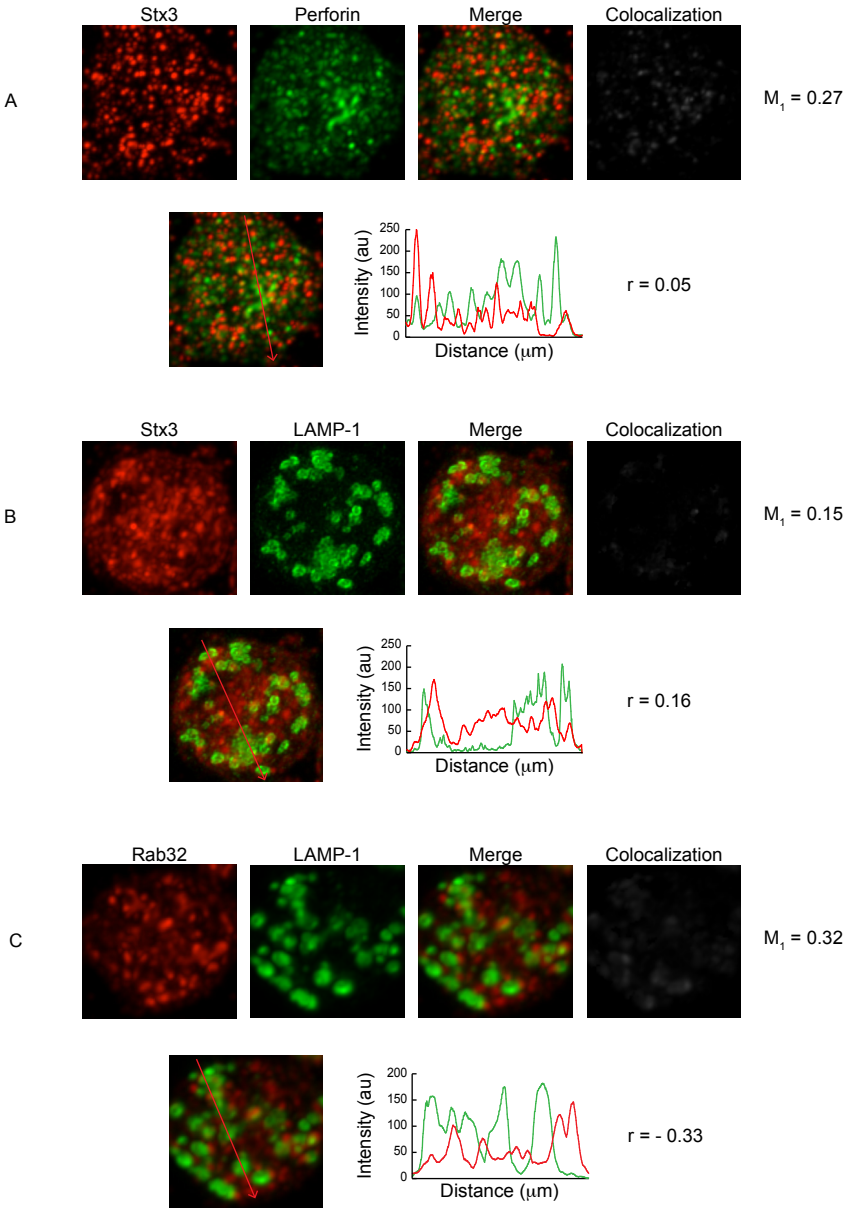
A
Stx3
Perforin
Merge
Colocalization
M1 = 0.27
Intensity (au)
250
200
150
100
50
0
Distance (μm)
r = 0.05
B
Stx3
LAMP-1
Merge
Colocalization
M1 = 0.15
Intensity (au)
250
200
150
100
50
0
Distance (μm)
r = 0.16
C
Rab32
LAMP-1
Merge
Colocalization
M1 = 0.32
Intensity (au)
200
150
100
50
0
Distance (μm)
r = - 0.33

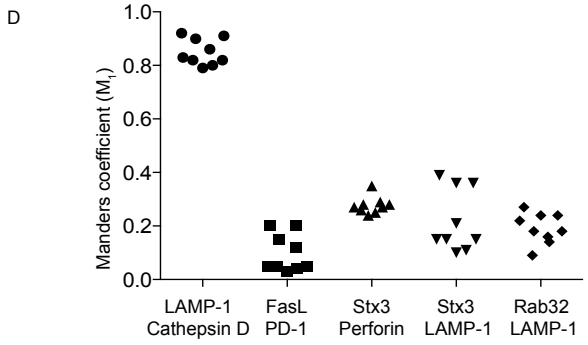

Figure 3.10. Stx3 and Rab32 are not stored in lysosomal granules.
Clone 3/4 CTL cells were stained with antibodies specific for Stx3 and perforin **(A)**, Stx3 and LAMP-1 **(B)** or Rab32 and LAMP-1 **(C)** as well as the appropriate secondary antibodies. Z-stack images were acquired (interval, 0.2μm) and subjected to deconvolution and three-dimensional reconstruction. Data is representative of 3 independent experiments corresponding to at least 27 cells. **(A-C)** Representative projections of the reconstructed images are shown. Colocalization images were created displaying only the regions where the two channels colocalize and the corresponding Manders coefficients (M_1) were calculated. Lines were drawn across the merged images attempting to include maximums from both channels, the fluorescent intensity profiles over that line were graphed and Pearson coefficients (r) were calculated. **(D)** M_1 coefficients corresponding to cells from three separate acquisitions taken in three independent experiments of samples stained for LAMP-1 and cathepsin D (positive control – 1st set), FasL and PD-1 (negative control – 2nd set), Stx3 and perforin (3rd set), Stx3 and LAMP-1 (4th set) and Rab32 and LAMP-1 (5th set).

3.2.7. FasL cannot be detected in molecular complexes with Stx3, Rab32 or Munc18-2

To evaluate whether FasL associated in a complex with the proteins it is stored with, I immunoprecipitated FasL from whole cell lysates of CTL Clone 3/4 cells and I assessed its association with Stx3 and Rab32 by SDS-PAGE and Western Blot. Neither Stx3 nor Rab32 were detected in immunoprecipitates of FasL (**Figure 3.11 A**). To verify that the FasL antibody used for immunoprecipitation was indeed able to pull down the protein, samples were probed against FasL. A set of bands corresponding to the different post-translational modifications of FasL was detected in the lane corresponding to FasL immunoprecipitates but not on the control immunoprecipitates. To control that the antibodies used for Western blotting were able to detect the proteins, monkey fibroblast COS-1 cells were transfected with DsRed-tagged FasL, with a Stx3 construct containing two C-terminal tags of Myc and one hexa-histidine tag, as well as with GFP-tagged Rab32. Post-nuclear cell lysates of the transfected COS-1 cells were run together with the CTL immunoprecipitated samples and revealed that FasL, Stx3 and Rab32 could be recognized by Western blot. COS-1 cells do not express FasL, as evidenced by the lack of signal on the lane corresponding to untransfected COS-1 cells. However, bands corresponding to the predicted molecular weight of endogenous Stx3 and Rab32 could be observed in all of the lanes corresponding to COS-1 lysates. Nonetheless, Stx3 and Rab32 could not be detected in lysates from CTL Clone 3/4 cells, possibly due to low levels of expression that fall under the threshold of detection of this method. This low level of detection could also provide an alternative explanation as to the lack of Stx3 and Rab32 bands on the FasL immunoprecipitates. To reduce the possibility that low protein amounts would interfere with the analysis of association, I transfected COS-1 cells with FasL and Stx3 or FasL and Rab32 and immunoprecipitated FasL from post-nuclear lysates. The high transfection efficiency of these cells and the high level of expression of transfected proteins observed in Figure 3.11 A, indicated these cells could be used to test the

association of FasL with Rab32 and Stx3. However, neither Stx3 nor Rab32 were detected in FasL-transfected or double transfected immunoprecipitated samples (**Figure 3.11 B**), indicating that these proteins do not associate with FasL. As a control, lysates from transfected cells were immunoprecipitated with a control antibody that did not immunoprecipitate FasL. Moreover, Stx3 and Rab32 could be detected in lysates from single and double-transfected cells indicating the proteins were indeed present in the lysates and could be recognized with the antibodies employed. As a clarification, the bands on the Rab32 Western blot on the FasL and control immunoprecipitated samples that migrated with similar elecrophoretic mobility to that of GFP-Rab32, correspond to the immunoglobulin heavy chain from the antibodies used to perform the immunoprecipitations. Taken together these experiments strongly suggest FasL does not associate in a complex with Rab32 or Stx3 under the conditions used for the experiment. However, the possibility that the method is unable to detect low levels of FasL-associating proteins cannot be excluded. This possibility is less likely when using COS-1 cells that overexpress the transfected protein to high levels but given that FasL is not endogenously expressed in these cells, the presence of the FasL storage vesicles is improbable and it could explain why these proteins do not associate in this cell type.

The co-immunoprecipitation of Munc18-2 was not evaluated in the experiment corresponding to Figure 3.11 A because this protein migrates between the 48 and 58 kDa molecular weight markers and may not have been visible under the broad band formed by the heavy chain. To overcome this difficulty, FasL was immunoprecipitated using a biotin-conjugated hamster antibody that would not be recognized by the secondary anti-rabbit antibody used for immunoblotting. Even though Munc18-2 could be visualized in the lane corresponding to CTL Clone 3/4 lysates, it was not detected in the FasL immunoprecipitate (**Figure 3.12**). This experiment does not support association between FasL and Munc18-2 although the method may not have the sufficient sensitivity to detect low levels of protein association.

A

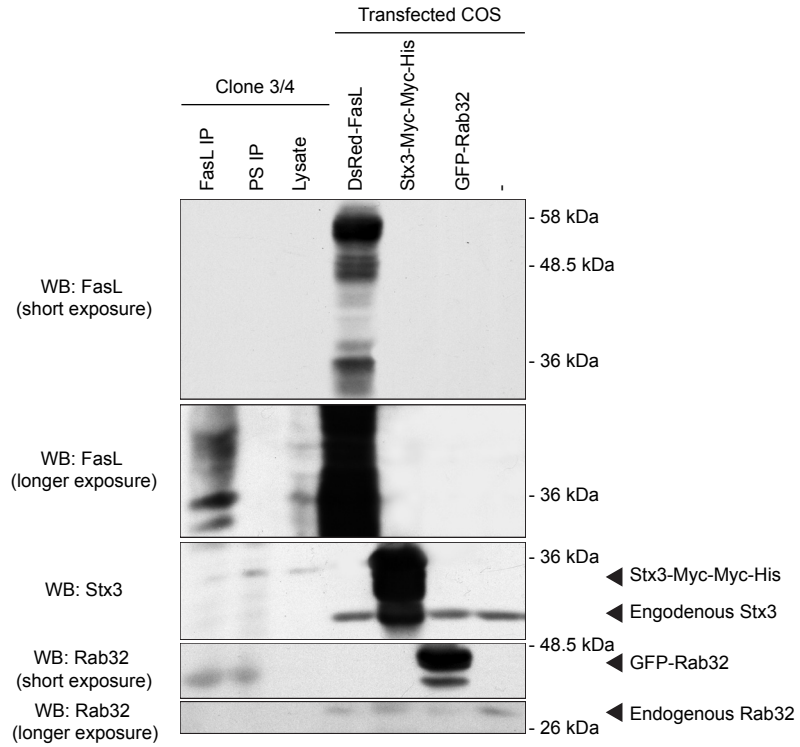
Transfected COS
Clone 3/4
FasL IP
PS IP
Lysate
DsRed-FasL
Stx3-Myc-His
GFP-Rab32
-
WB: FasL
(short exposure)
WB: FasL
(longer exposure)
WB: Stx3
WB: Rab32
(short exposure)
WB: Rab32
(longer exposure)
- 58 kDa
- 48.5 kDa
- 36 kDa
- 36 kDa
- 36 kDa
- 48.5 kDa
- 26 kDa
Stx3-Myc-Myc-His
Engodenous Stx3
GFP-Rab32
Endogenous Rab32

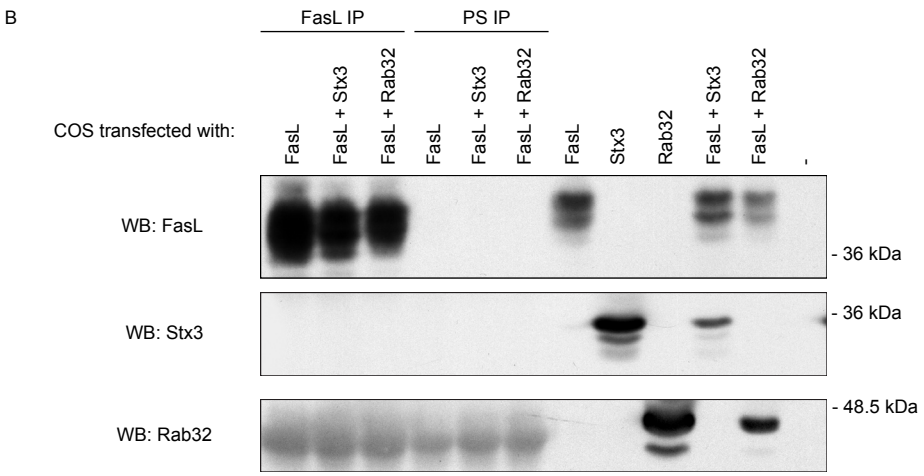

Figure 3.11. FasL has no detectable association with Stx3 or Rab32.
(A) $2x10^7$ Clone 3/4 post-nuclear cell lysates were immunoprecipitated with antisera specific for FasL (FasL IP) or pre-immune control sera (PS IP). A non-immunoprecipitated lysate control corresponding to $8x10^5$ cells was also included. $4x10^4$ COS-1 cells transfected with DsRed-FasL, Stx3-Myc-Myc-His, GFP-Rab32 or left untransfected (-) were lysed and run in an SDS-PAGE. Immunoblotting was performed for FasL (top two panels), Stx3 (third panel) and Rab32 (4^{th} and 5^{th} panels). Longer exposure times are displayed for FasL and Rab32 immunoblots to show the endogenous proteins. **(B)** $1x10^6$ COS-1 cells transfected with FasL, FasL and Stx3-Myc-Myc-His, or FasL and GFP-Rab32 were lysed and immunoprecipitated with antisera specific for FasL (FasL IP) or pre-immune control sera (PS IP). $4x10^4$ COS-1 cells transfected with FasL, Stx3-Myc-Myc-His, GFP-Rab32, FasL and Stx3-Myc-Myc-His, FasL and GFP-Rab32 or left untransfected (-) were lysed and run in an SDS-PAGE. Immunoblotting was performed for FasL (top panel), Stx3 (middle panel) and Rab32 (bottom panel).

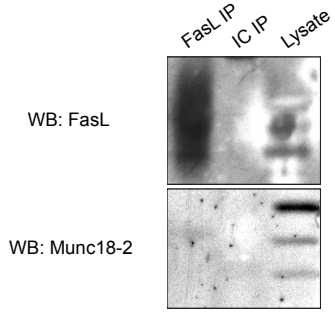

Figure 3.12. FasL has no detectable association with Munc18-2.
(A) $2x10^7$ Clone 3/4 post-nuclear cell lysates were immunoprecipitated with antibodies specific for FasL (FasL IP) or isotype control antibodies (IC IP). A non-immunoprecipitated lysate control corresponding to $1x10^6$ cells was also included in the SDS-PAGE. Immunoblotting was performed for FasL (top panel) and Munc18-2 (bottom panel).

3.2.8. FasL is stored in Stx3$^+$ Munc18-2$^+$ Rab32$^+$ LAMP-1$^-$ perforin$^-$ vesicles in CTL Clone 11 cells

In order to confirm that the localization results showed above for Clone 3/4 cells were not cell type-specific, I studied FasL intracellular distribution and colocalization with several proteins in different CTL cells. I first used non-transformed alloreactive CTL Clone 11 cells, which have also been shown to store FasL in intracellular vesicles (He and Ostergaard 2007). I stained these cells for FasL and Stx3, for FasL and Munc18-2 and for FasL and Rab32. In every case, analysis of colocalization by confocal microscopy showed a strong colocalization (**Figure 3.13**), indicating that FasL is stored with Stx3, Munc18-2 and Rab32 in CTL Clone 11 cells. Colocalization of FasL with LAMP-1 and perforin was also evaluated in these cells. From the lack of colocalization obtained (**Figure 3.14**) it can be concluded that FasL is not stored with perforin or LAMP-1.

Furthermore, the localization of each of the identified FasL storage vesicle components relative to each other was also examined. I stained CTL Clone 11 cells for Stx3, Munc18-2 and FasL. The images of merged Stx3 and Munc18-2 staining as well as the colocalization image and the corresponding M_1 coefficient, all reflected a high level of colocalization of these proteins (**Figure 3.15 A**, top row **and D**). Moreover, the fluorescence intensity profiles across the line drawn over the image of merged Stx3, Munc18-2 and FasL three-color staining clearly depicted the overlapping peaks of fluorescence intensity for all three proteins (**Figure 3.15 A**, second row). The high colocalization of Stx3 and Rab32 (**Figure 3.15 B and D**) further supported the conclusion that Stx3 is stored with Munc18-2 and Rab32. In addition, the distinctiveness of the FasL storage vesicle relative to the lysosomal granules was confirmed by the weak colocalization of Stx3 and LAMP-1 (**Figure 3.15 C and D**)

Overall, the results from these experiments indicate that in CTL Clone 11 cells, FasL is stored in vesicles that also contain the proteins Stx3, Munc18-2 and Rab32 and that these vesicles are distinct from LAMP-1$^+$ cytolytic granules.

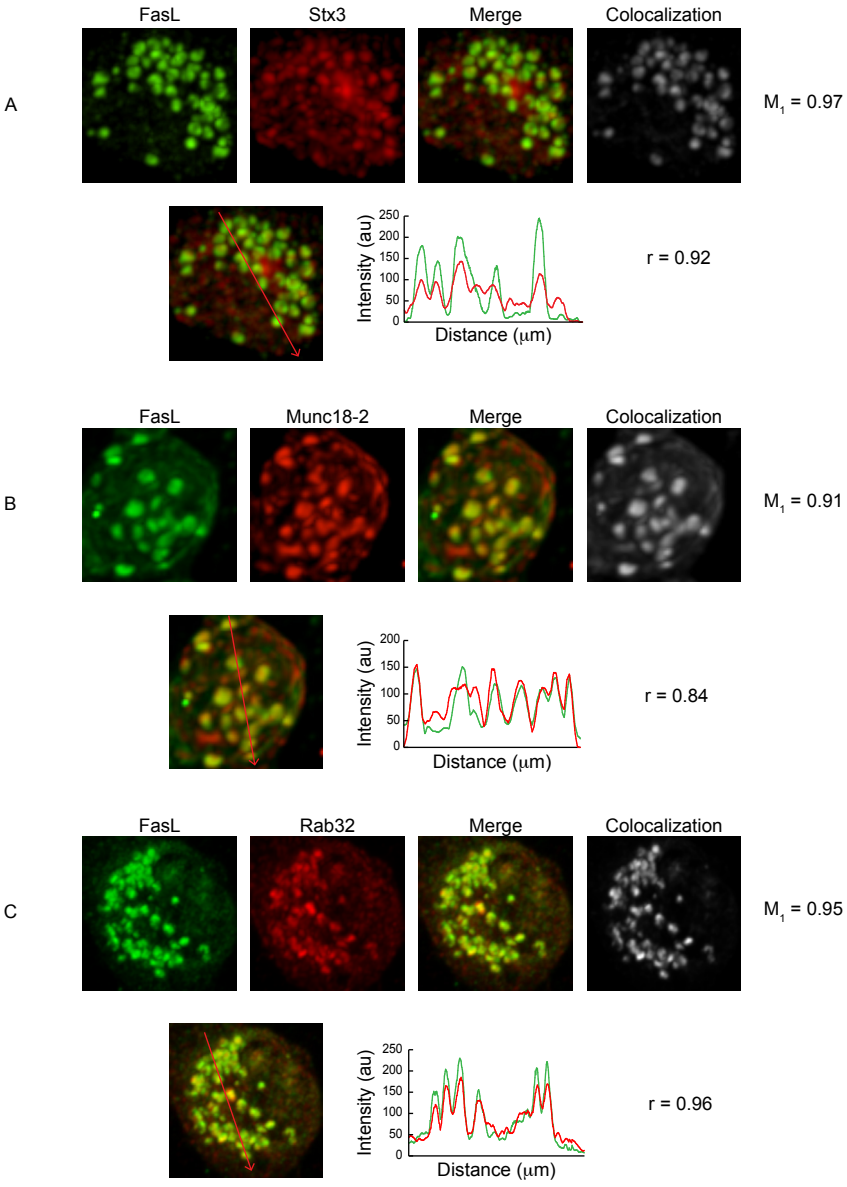
A
FasL
Stx3
Merge
Colocalization
M1 = 0.97
Intensity (au)
250
200
150
100
50
0
Distance (μm)
r = 0.92
B
FasL
Munc18-2
Merge
Colocalization
M1 = 0.91
Intensity (au)
200
150
100
50
0
Distance (μm)
r = 0.84
C
FasL
Rab32
Merge
Colocalization
M1 = 0.95
Intensity (au)
250
200
150
100
50
0
Distance (μm)
r = 0.96

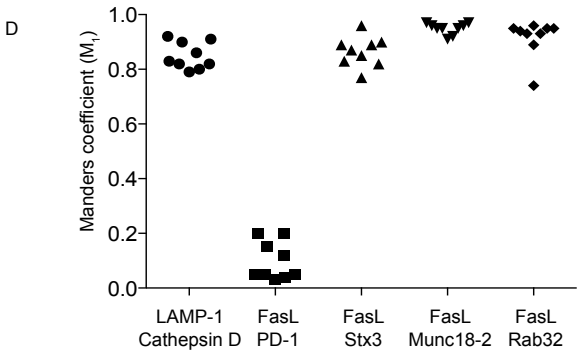

Figure 3.13. FasL is stored with Stx3, Munc18-2 and Rab32 in Clone 11 cells. CTL Clone 11 cells were stained with antibodies specific for FasL and Stx3 **(A)**, Munc18-2 **(B)** or Rab32 **(C)** as well as the appropriate secondary antibodies, and analyzed by confocal microscopy. Z-stack images were acquired (interval, 0.2μm) and subjected to deconvolution and three-dimensional reconstruction. Data is representative of 3 independent experiments corresponding to at least 27 cells. **(A-C)** Representative projections of the reconstructed images are shown. Colocalization images were created displaying only the regions where the two channels colocalize and the corresponding Manders coefficients (M_1) were calculated. Lines were drawn across the merged images attempting to include maximums from both channels, the fluorescent intensity profiles over that line were graphed and Pearson coefficients (r) were calculated. **(D)** M_1 coefficients corresponding to cells from three separate acquisitions taken in three independent experiments of samples stained for LAMP-1 and cathepsin D (positive control – 1st set), FasL and PD-1 (negative control – 2nd set), FasL and Stx3 (3rd set), FasL and Munc18-2 (4th set) and FasL and Rab32 (5th set).

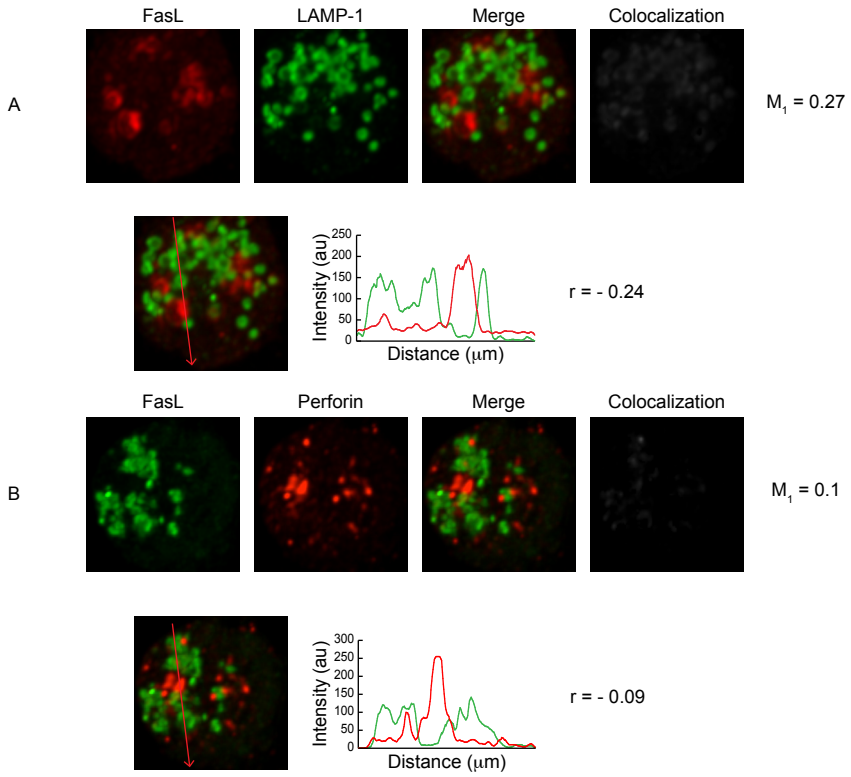

Figure 3.14. FasL is not stored in cytolytic granules in Clone 11 cells.
CTL Clone 11 cells were stained with antibodies specific for FasL and LAMP-1 **(A)**, or perforin **(B)** as well as the appropriate secondary antibodies, and analyzed by confocal microscopy. Z-stack images were acquired (interval, 0.2μm) and subjected to deconvolution and three-dimensional reconstruction. Representative projections of the reconstructed images are shown. Colocalization images were created displaying only the regions where the two channels colocalize and the corresponding Manders coefficients (M_1) were calculated. Lines were drawn across the merged images attempting to include maximums from both channels, the fluorescent intensity profiles over that line were graphed and Pearson coefficients (r) were calculated for each pair of profiles. Data is representative of 3 independent experiments corresponding to at least 27 cells.

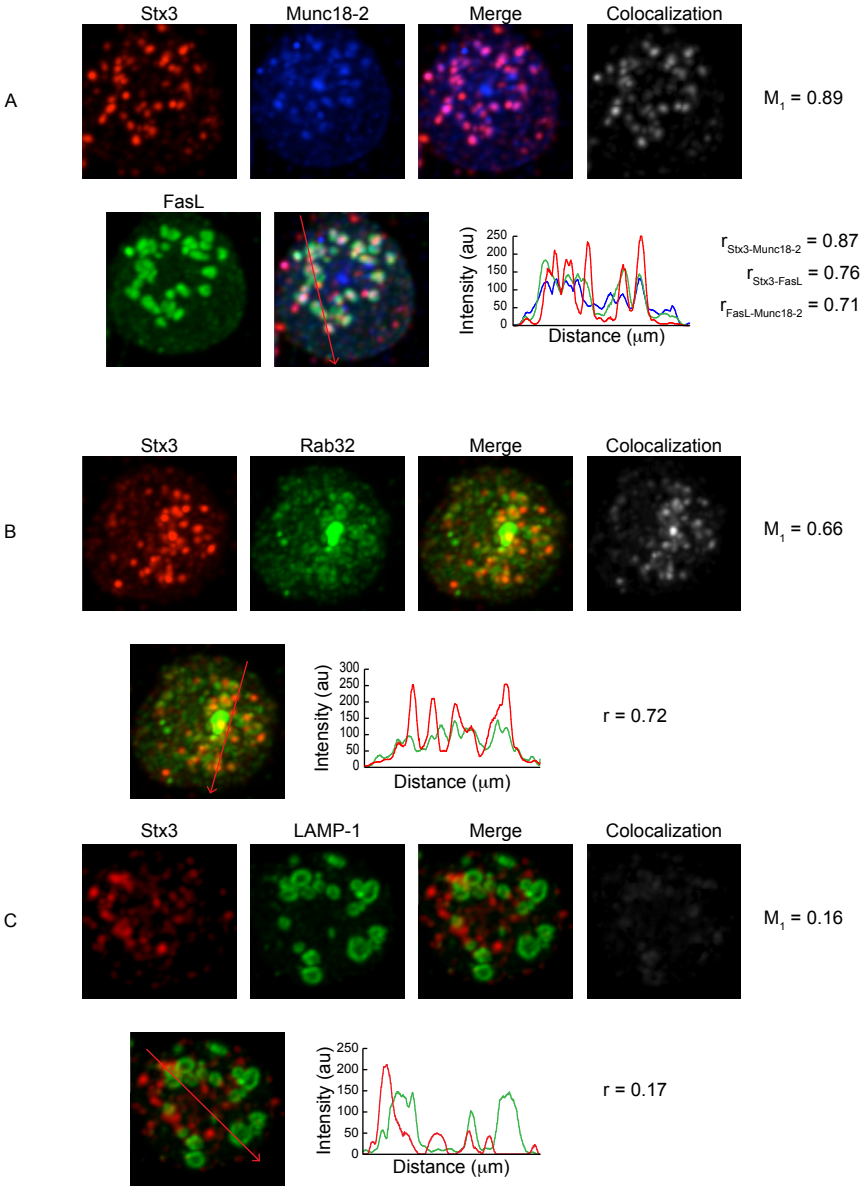
A
Stx3
Munc18-2
Merge
Colocalization
M1 = 0.89
FasL
Intensity (au)
250
200
150
100
50
0
Distance (μm)
rStx3-Munc18-2 = 0.87
rStx3-FasL = 0.76
rFasL-Munc18-2 = 0.71
B
Stx3
Rab32
Merge
Colocalization
M1 = 0.66
Intensity (au)
300
250
200
150
100
50
0
Distance (μm)
r = 0.72
C
Stx3
LAMP-1
Merge
Colocalization
M1 = 0.16
Intensity (au)
250
200
150
100
50
0
Distance (μm)
r = 0.17

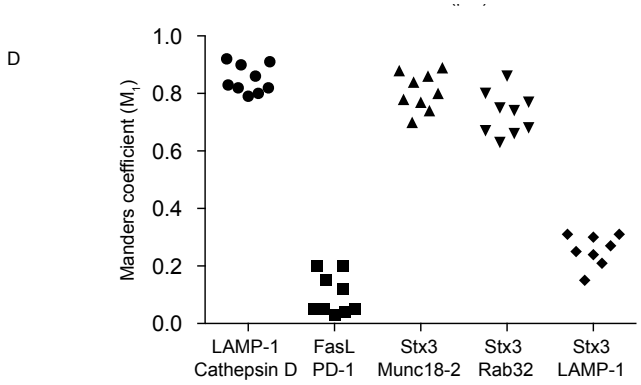

Figure 3.15. Stx3 is stored with Munc18-2 and Rab32 in vesicles distinct from lysosomal granules in Clone 11 cells.
CTL Clone 11 cells were stained with antibodies specific for Stx3 and Munc18-2 **(A)**, Rab32 **(B)** or LAMP-1 **(C)** as well as the appropriate secondary antibodies, and analyzed by confocal microscopy. Z-stack images were acquired (interval, 0.2μm) and subjected to deconvolution and three-dimensional reconstruction. Data is representative of 3 independent experiments corresponding to at least 27 cells. **(A-C)** Representative projections of the reconstructed images are shown. Colocalization images were created displaying only the regions where the two channels colocalize and the corresponding Manders coefficients (M_1) were calculated. Lines were drawn across the merged images attempting to include maximums from both channels, the fluorescent intensity profiles over that line were graphed and Pearson coefficients (r) were calculated for each pair of profiles. **(D)** M_1 coefficients corresponding to cells from three separate acquisitions taken in three independent experiments of samples stained for LAMP-1 and cathepsin D (positive control - 1st set), FasL and PD-1 (negative control – 2nd set), Stx3 and Munc18-2 (3rd set), Stx3 and Rab32 (4th set) and Stx3 and LAMP-1 (5th set).

3.2.9. FasL is stored in Stx3$^+$ LAMP-1$^-$ vesicles in CTL CTLL-2 cells

For further confirmation of the composition of the FasL storage vesicle, I stained CTLL-2 cells, another IL-2-dependent CTL clone, with antibodies specific for Stx3 and FasL and I analyzed their colocalization by confocal microscopy (**Figure 3.16 A and D**). The high level of colocalization of these two proteins confirmed FasL is stored with Stx3.

To determine if FasL was stored in vesicles separate from the cytolytic granules in this cell type as observed in the other tested CTL, I stained CTLL-2 cells for FasL and LAMP-1 and for Stx3 and LAMP-1. Neither FasL nor Stx3 colocalized with LAMP-1 (**Figure 3.16 B, C and D**). Overall, these results support the findings in CTL Clone 3/4 and Clone 11 cells and demonstrate that FasL is stored with Stx3 in a vesicle independent from the LAMP-1$^+$ lytic granules.

3.2.10. The stored pool of FasL remains in the same vesicle after stimulation

In unstimulated T cells, FasL is found in intracellular vesicles. When T cells encounter their target and TCRs recognize their specific antigen in the proper MHC context, some of the FasL molecules stored within the cells are translocated to the cell surface where they can bind to the Fas receptors on the target cells and induce apoptosis. However, intracellular staining and flow cytometry analysis of FasL (He and Ostergaard, unpublished data) has suggested that some of the FasL molecules remain inside the cell. This led me to question whether the remaining intracellular FasL proteins stayed in the same vesicles or if they moved to a different compartment, which could have provided a clue about the FasL trafficking route to the surface after stimulation. I therefore stained CTL Clone 3/4 cells previously stimulated for 30 min with PMA and ionomycin, with antibodies specific for FasL and Stx3, and for FasL and Rab32. I then analyzed their colocalization by confocal microscopy. The results obtained indicated that FasL colocalized with Stx3 and Rab32 in stimulated CTL cells (**Figure 3.17**).

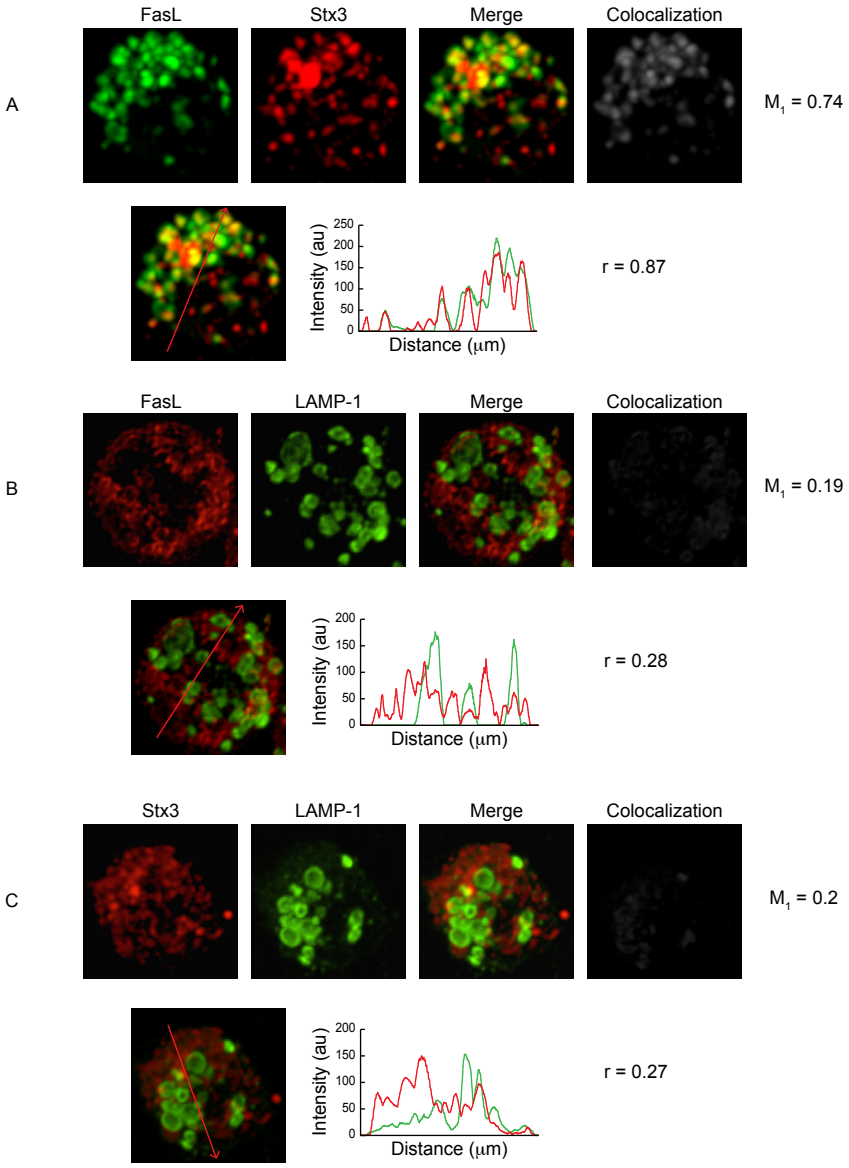
A
FasL
Stx3
Merge
Colocalization
M1 = 0.74
Intensity (au)
250
200
150
100
50
0
Distance (μm)
r = 0.87
B
FasL
LAMP-1
Merge
Colocalization
M1 = 0.19
Intensity (au)
200
150
100
50
0
Distance (μm)
r = 0.28
C
Stx3
LAMP-1
Merge
Colocalization
M1 = 0.2
Intensity (au)
200
150
100
50
0
Distance (μm)
r = 0.27

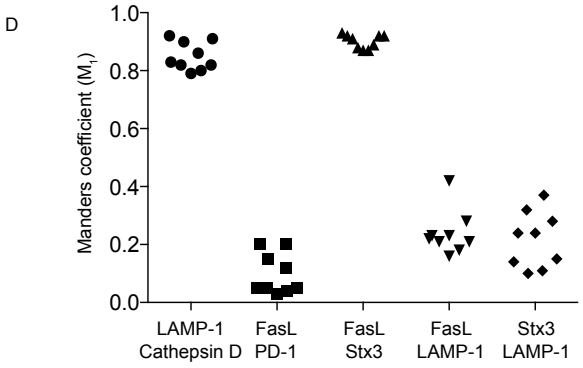

Figure 3.16. FasL and Stx3 are stored together in vesicles distinct from lysosomal granules in CTLL-2 cells.
CTL Clone 11 cells were stained with antibodies specific for FasL and Stx3 **(A)**, FasL and LAMP-1 **(B)** or Stx3 and LAMP-1 **(C)** as well as the appropriate secondary antibodies. Z-stack images were acquired (interval, 0.2μm) and subjected to deconvolution and three-dimensional reconstruction. Data is representative of 3 independent experiments corresponding to at least 27 cells. **(A-C)** Representative projections of the reconstructed images are shown. Colocalization images were created displaying only the regions where the two channels colocalize and the corresponding Manders coefficients (M_1) were calculated. Lines were drawn across the merged images attempting to include maximums from both channels, the fluorescent intensity profiles over that line were graphed and Pearson coefficients (r) were calculated for each pair of profiles. **(D)** M_1 coefficients corresponding to cells from three separate acquisitions taken in three independent experiments of samples stained for LAMP-1 and cathepsin D (positive control – 1st set), FasL and PD-1 (negative control – 2nd set), FasL and Stx3 (3rd set), FasL and LAMP-1 (4th set) and Stx3 and LAMP-1 (5th set).

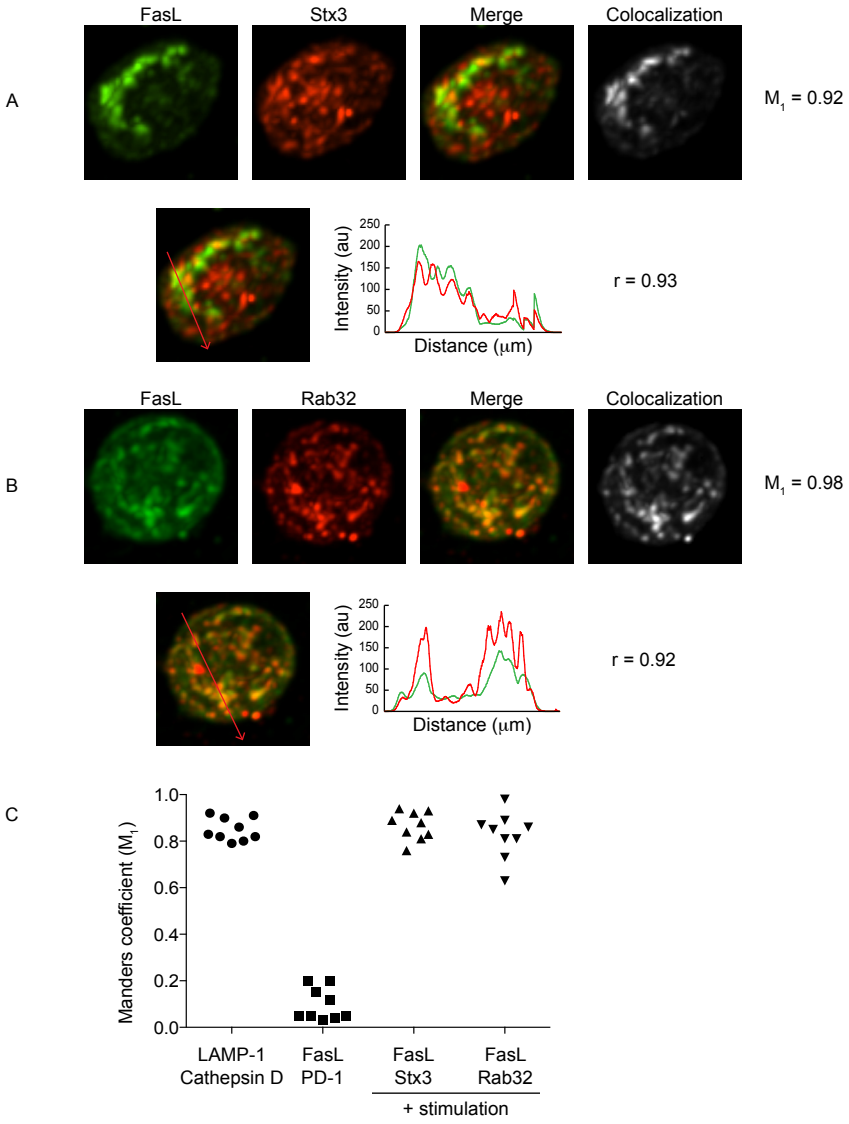

Figure 3.17. FasL is stored with Stx3 and Rab32 in CTL Clone 3/4 cells after stimulation.

CTL Clone 3/4 cells previously incubated with PMA and Ionomycin for 30 min were stained with antibodies specific for FasL and Stx3 **(A)**, or Rab32 **(B)** as well as the appropriate secondary antibodies, and analyzed by confocal microscopy. Z-stack images were acquired (interval, 0.2μm) and subjected to deconvolution and three-dimensional reconstruction. Data is representative of 3 independent experiments corresponding to at least 27 cells. **(A and B)** Colocalization was analyzed and displayed as explained in Figure 3.16. **(C)** M_1 coefficients corresponding to cells from three separate acquisitions taken in three independent experiments of samples stained for LAMP-1 and cathepsin D (positive control – 1st set), FasL and PD-1 (negative control – 2nd set), FasL and Stx3 (3rd set) and FasL and Rab32 (4th set).

I extended the FasL localization studies in stimulated cells to CTL Clone 11 cells. Confocal microscopy analysis of cells treated with PMA and ionomycin confirmed that FasL colocalized with Stx3 and Rab32 in stimulated Clone 11 cells (**Figure 3.18**). In summary, these results demonstrate that FasL remains in the same $Stx3^+$ $Rab32^+$ vesicles after stimulation in CTL Clone 3/4 and Clone 11 cells.

3.3. Discussion

The series of experiments presented in this chapter describe for the first time the components of the FasL storage vesicle. Using confocal microscopy analysis I determined that FasL colocalizes with the proteins Stx3, Munc18-2 and Rab32 in three different CTL types. I also demonstrated that FasL, Stx3 and Rab32 failed to colocalize with perforin and LAMP-1, which confirmed that the storage vesicle for FasL is distinct from the cytolytic granules.

I chose to use physiologically relevant peptide-specific CTL clone cells. These CTL clones were previously shown to express FasL in vesicles and were identical compared to *ex vivo* CTL in all tested aspects related to FasL, (He and Ostergaard 2007, He et al. 2010). I endeavored to determine the localization of endogenous FasL. This approach has the disadvantage of lower affinity and higher background antibodies compared to the alternative approach of using transfected tagged FasL that would permit the use of antibodies specific for the tag, which are generally of much better quality compared to the few, low quality antibodies against FasL. However, this strategy favors the authenticity of the results since it is not based on the assumption that the overexpressed proteins are being transported to the correct location. I chose to use confocal microscopy imaging because it allows for direct visualization of the localization of the stained proteins and the acquisition of Z-stack images enables the generation of three-dimensional reconstructions of the cells and a more clear interpretation of the results. To support the visual assessment of colocalization, I generated a "colocalization" image and its corresponding Manders coefficient and a profile of

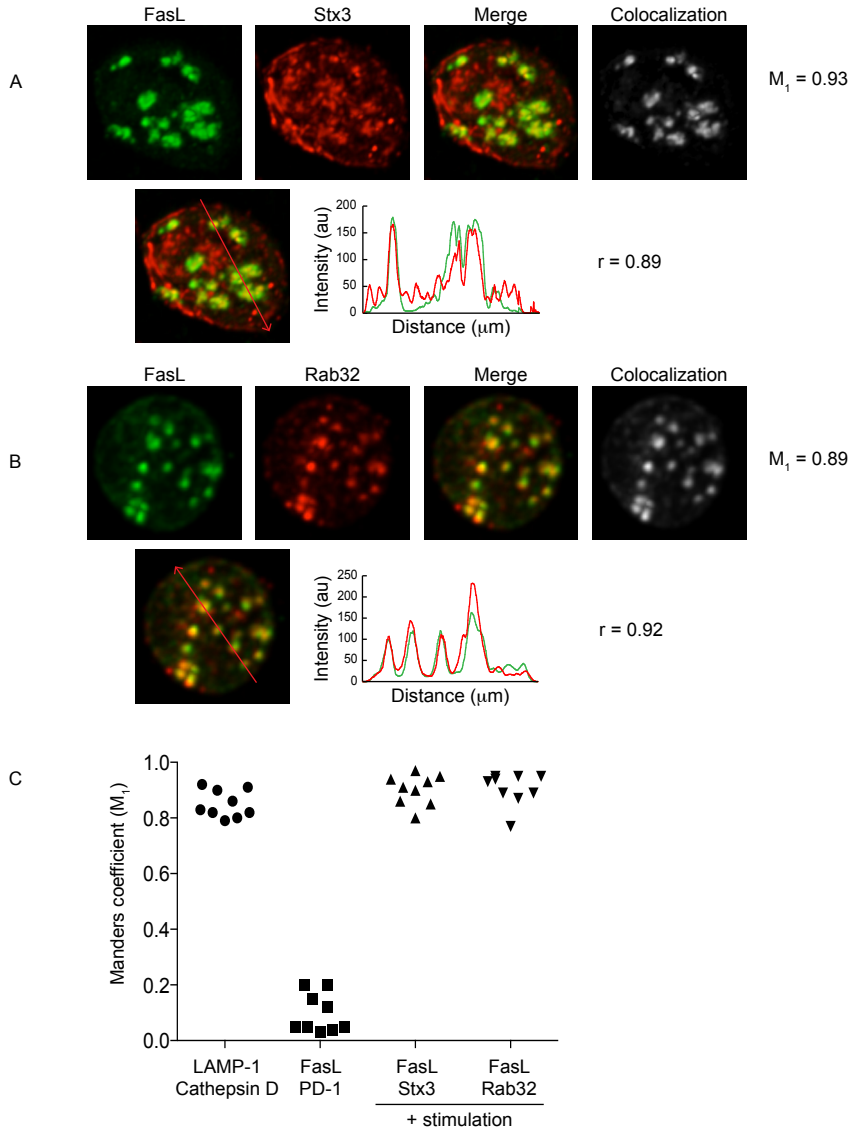

Figure 3.18. FasL is stored with Stx3 and Rab32 in CTL Clone 11 cells after stimulation.

CTL Clone 11 cells previously incubated with PMA and Ionomycin for 30 min were stained with antibodies specific for FasL and Stx3 **(A)**, or Rab32 **(B)** as well as the appropriate secondary antibodies, and analyzed by confocal microscopy. Z-stack images were acquired (interval, 0.2μm) and subjected to deconvolution and three-dimensional reconstruction. **(A and B)** Colocalization was analyzed and displayed as explained in Figure 3.16. **(C)** M_1 coefficients corresponding to cells from three separate acquisitions taken in three independent experiments of samples stained for LAMP-1 and cathepsin D (positive control – 1st set), FasL and PD-1 (negative control – 2nd set), FasL and Stx3 (3rd set) and FasL and Rab32 (4th set). Data is representative of 3 independent experiments corresponding to at least 27 cells.

the fluorescence intensity for the stained proteins over a line drawn above their maximums on a projection image.

Confocal microscopy analysis showed that FasL did not colocalize with the ER markers calnexin and β-COP, the Golgi 58K marker (He and Ostergaard, unpublished data), the late endosomes marker CD63 (Figure 3.1) or the lysosomal granules markers perforin and LAMP-1 (Figure 3.2). Overall this suggests FasL is not stored in any of the known cytosolic organelles and hints that it must be stored in a specialized secretory vesicle. Examples of proteins with specialized storage vesicles in T cells are RANTES (Catalfamo et al. 2004) CXCR1 (Gasser et al. 2005) and PD-1 (Pentcheva-Hoang et al. 2007). However, the presence of specialized secretory vesicles of different composition and regulation is not unique to T lymphocytes. Mast cells possess vesicles containing histamine and TNF-α and separate granules that harbor serotonin which are differentially regulated (Puri and Roche 2008). Neutrophils contain at least four types of granules: primary or azurophilic granules where defensins and cathepsin G among others are stored, secondary or specific granules, which hold lactoferrin, tertiary or gelatinase granules that store metalloprotease 9 and secretory vesicles rich in alkaline phosphatase (Lacy 2006).

I attempted to discover the identity of the FasL storage vesicle by examining the localization of FasL in relation to other proteins expressed in T cells, which, similarly to FasL, are presented on the surface of the cell upon stimulation indicating they could be under similar regulation. I was only able to successfully stain for TNF-α and PD-1, but neither of these proteins was stored in the same compartment with FasL (Figures 3.3 and 3.4). TNF-α was only detected after incubating the CTL with PMA and ionomycin for 2 hours, which could have allowed for *de novo* protein synthesis, indicating it is not stored intracellularly in T cells. The mechanism for TNF-α production, storage and secretion has not been described for T cells, even though it is a relevant killing mechanism employed by these cells (Ratner and Clark 1993, Lee et al. 1996). Thus, it would be interesting to study its regulation and compare it to the FasL and degranulation pathways.

The partial colocalization of FasL with cytochrome C and Grp78 (Figures 3.5 and 3.6) indicated FasL is probably stored in a compartment near the MAMs, a specialized section of ER-mitochondria interconnected membranes that allows for efficient Ca^{++} exchange between the two organelles. The advantage of such an association would be that, upon TCR engagement, the signaling cascade that leads to Ca^{++} release from the ER, could be readily sensed by the unknown mechanism that triggers FasL translocation to the surface. This would be consistent and could provide an explanation to previous studies from our laboratory showing that stored FasL translocation is independent of extracellular Ca^{++} but requires intracellular Ca^{++} (He and Ostergaard 2007); the close proximity to the MAM would allow for high enough concentrations of Ca^{++} that would make extracellular Ca^{++} unnecessary.

The major contribution of this chapter is the identification of three novel markers of the FasL storage vesicle, which I will refer to as FSV. Where none was known before, the field can now use Stx3, Munc18-2 or Rab32 to determine if different treatments or mutations affect the localization of FasL. Moreover, because these proteins are SNARE, SM and Rab proteins respectively, all of which are usually involved in protein trafficking, they may provide insight into the FasL trafficking route to or from its vesicle. Stx3 has been shown to participate in the fusion step of a number of different processes, such as neurotransmitter receptor exocytosis in neuronal cells (Jurado et al. 2013), degranulation in mast cells (Tadokoro et al. 2007, Brochetta et al. 2014), protein traffic to melanosomes in melanocytes (Yatsu et al. 2013), insulin-containing granules to granule fusion in pancreatic beta cells (Zhu et al. 2013), chemokine release by mast cells (Frank et al. 2011), targeting of apical proteins in epithelial cells (Sharma et al. 2006), zymogen granule to granule fusion in acinar cells (Hansen 1999) and phagosomal maturation in macrophages (Hackam et al. 1996). The involvement of Syntaxin3 in FasL trafficking will be discussed in chapter 4.

Munc18-2, as other members of the SM family, can function both as a regulator of SNARE complex assembly and as part of the machinery necessary for SNARE-mediated membrane fusion (Sudhof and Rothman 2009, Carr and

Rizo 2010). Munc18-2 can interact with Syntaxins 1, 2, 3 and 11 (Hata and Sudhof 1995, Martin-Verdeaux 2002, Cote et al. 2009, zur Stadt et al. 2009). It is involved in platelet secretion (Al Hawas et al. 2012), apical membrane trafficking in epithelial cells (Riento 2000), insulin secretion from pancreatic beta cells (Mandic et al. 2011) and degranulation from mast cells and neutrophils (Martin-Verdeaux 2002, Brochetta et al. 2008, Brochetta et al. 2014). Most relevantly, mutations in Munc18-2 that impair its binding to Stx11 have been recently described to cause familial hemophagocytic lymphohistiocytosis type 5 (FHL5) and cytotoxicity defects in NK and T cells (Cote et al. 2009, zur Stadt et al. 2009). Although degranulation was shown to be defective in these studies, FasL-mediated cytotoxicity has not been evaluated. After the T cell encounters a target cell, Munc18-2 could be involved in the fusion of FSVs with the plasma membrane. Moreover, Munc18-2 could act as a negative regulator, binding to Stx3 or other SNAREs in FSVs to prevent SNARE complex formation in a similar way to Munc18-1-mediated inhibition of Syntaxin 1 (Dulubova et al. 1999, Misura et al. 2000, Yang et al. 2000) ensuring SNARE complexes are formed in the correct location and time.

Rab32 localizes to and regulates the composition of mitochondria-associated membranes (MAMs) (Bui et al. 2010). The colocalization of FasL with Rab32 supports the notion that FSVs are located near MAMs, and because it is a protein involved in protein trafficking, it also suggests it could be involved in FasL trafficking to its storage compartment. This possibility will be explored in chapter 4.

My studies showed that Stx3 colocalized with Munc18-2 and Rab32, both in CTL Clone 3/4 and Clone 11 cells (Figures 3.9 and 3.15), strongly indicating FasL is stored together in the same vesicle with these two proteins. Ideally, four-color staining and confocal microscopy analysis of the colocalization of these proteins would prove their co-existence in the same vesicle but unfortunately, the antibodies at our disposal do not allow for such a staining. Nonetheless, if FasL colocalizes with Stx3, Munc18-2 and Rab32, and if Stx3 colocalizes with Munc18-2 and Rab32, it is logical to conclude they must all be in the same

vesicle. The microscopy images showed the colocalization was not always completely overlapping, leaving for example some $Stx3^+$ $FasL^-$, $Rab32^+$ $FasL^-$, or $Stx3^-$ $Rab32^+$ vesicles, even a few $Stx3^-$ $FasL^+$ vesicles. This could imply that Stx3 Rab32 and Munc18-2 are not exclusive to the FasL vesicle. These observations could also mean that FasL is not always in the company of all of the three proteins. However, there is also the possibility that the amount of these proteins in some of the vesicles is below the detection threshold or at background levels.

While I showed that FasL co-resided in intracellular vesicles with Stx3, Munc18-2 and Rab32, both before (Figures 3.7 and 3.8) and after stimulation (Figure 3.17), I found no evidence of complex formation with these proteins (Figures 3.11 and 3.12). This is not unexpected, since SNARE and Rab proteins have not been shown to interact directly with the proteins in the vesicles they tether or fuse. The study of FasL-interacting proteins will be further discussed in chapter 4 (Figure 4.17).

Several authors argue that FasL is stored in cytolytic granules (Bossi and Griffiths 1999, Lettau et al. 2004, Qian et al. 2006, Schmidt et al. 2011b). In contrast, I showed that FasL is not stored with perforin or LAMP-1 (Figure 3.2) The lack of colocalization of other components of the FSVs, Stx3 and Rab32, with perforin and LAMP-1 (Figure 3.10) reinforced the disparity of the composition of these two vesicles. This thorough colocalization analysis proves that the FasL storage vesicle and the cytolytic granules are two distinct specialized vesicles with different components. Some of the opposing publications that claim FasL is stored in cytolytic granules used transfected FasL constructs and transformed non-T lymphocyte cell lines (Bossi and Griffiths 1999, Qian et al. 2006). A possible explanation for the different interpretations regarding FasL localization could result from aberrant trafficking of the overexpressed tagged proteins. Such a possibility could be reassessed using the FSV markers I have identified to verify the correct localization of the transfected proteins.

However, the colocalization studies that show colocalization of endogenous FasL with lytic granules suggest a more complex scenario may be possible; depending on the activation status, the strength of the received activation signal and the cell type, FSVs and granules could potentially merge together and traffic to the plasma membrane through an intermediate vesicle containing proteins from both compartments. Consistent with this unifying theory, recent reports have shown that some of the proteins that are found within the lytic granules when fusing with the plasma membrane are not found in this compartment prior to stimulation. Translocation and fusion of the cytolytic granules with the cell surface is dependent on Rab27a, Munc13-4 and Stx11. Rab27a allows tethering of the cytolytic granules to the plasma membrane (Haddad et al. 2001, Stinchcombe et al. 2001a), Munc13-4 is thought to prime the docked granules to enable fusion with the plasma membrane (Feldmann et al. 2003) and Syntaxin 11 has been shown to be important for granule exocytosis (Bryceson et al. 2007). Interestingly, these proteins are stored in separate compartments and converge at the immunological synapse after activation of T and NK cells (Menager et al. 2007, de Saint Basile et al. 2010, Dabrazhynetskaya et al. 2012). Thus, in certain cells and under given conditions, FSVs could potentially fuse with cytolytic granules before fusing with the plasma membrane. In these hypothetical circumstances, FasL would appear to colocalize with components of the lysosomal granules.

CHAPTER 4: Characterization of the FasL trafficking route in Cytotoxic T lymphocytes

4.1. Introduction

Non-stimulated resting cytotoxic T lymphocytes produce FasL molecules and store them intracellularly in a compartment distinct from the ER and Golgi (He and Ostergaard, unpublished data), which I showed to have a unique composition in the previous chapter. This suggests that FasL exits the ER-Golgi organelles, where it is produced, and traffics to its FSV after its synthesis. Moreover, if and when CTL encounter a target, pre-synthesized FasL molecules stored in intracellular vesicles are rapidly translocated to the surface where they can exercise their target-killing function (He and Ostergaard 2007). Therefore, trafficking of FasL has an important role for the function of this protein in CTL.

Transmembrane proteins, such as FasL, are co-translationally transported into the ER. Proteins not destined to reside in the ER move along the biosynthetic-secretory pathway towards the *cis*-Golgi first and the *trans*-Golgi later. From here proteins can either be secreted to the plasma membrane, following a default constitutive secretion route, or they can be directed towards their specific organelle (Mellman and Warren 2000). Sorting of proteins from the *trans*-Golgi network (TGN) is well understood for lysosomal proteins. Cathepsins, for example, are directly transported to lysosomes in vesicles budding from the TGN (Hasilik et al. 1980). LAMP-1, on the other hand, although it can traffic through the intracellular endocytic pathway, in certain cells, it follows the default secretion pathway to the surface where it is recognized for endocytosis and carried to the lysosomes (Carlsson and Fukuda 1992). Similarly, components of specialized secretory vesicles can follow different routes to their destination. Granzymes A and B are targeted to cytolytic granules through the intracellular endocytic pathway, while the cytotoxic T cell antigen 4 (CTLA-4), traffics through the constitutive secretion pathway to the surface from where it is internalized and delivered to its intracellular storage vesicle (Griffiths and Isaaz

1993, Qureshi et al. 2012). However, the route FasL travels post-synthesis to reach its destination vesicle remains unclear.

After they receive a stimulating signal, secretory cells discharge the components of their specialized secretory vesicles into the extracellular medium or the plasma membrane where the secreted molecules can execute their function (Burgess and Kelly 1987). In CTLs, for example, after the TCR recognizes the appropriate peptide-MHC complex, the microtubule organizing center (MTOC) polarizes towards the interface with the target cell allowing lytic granules to move along this microtubule network to reach the immunological synapse (Stinchcombe and Griffiths 2007). Similarly, the transport of secretory vesicles in activated mast cells has been shown to be microtubule-dependent (Smith et al. 2003). In melanocytes, however, melanin-filled melanosomes travel to the cell surface using members of the myosin family as motor proteins to propel them over the actin cytoskeleton (Wu et al. 1997). The mechanisms involved in FasL trafficking to the surface after T cell stimulation are not well understood. FasL surface delivery was not inhibited in the presence of colchicine, which blocks microtubule polymerization and impairs degranulation (He and Ostergaard 2007). This observation indicates different mechanisms, still unknown, may be at play in the surface translocation of FasL after CTL stimulation.

In this chapter I describe several aspects of the FasL trafficking route. Using an endocytosis confocal microscopy assay I demonstrated that FasL trafficked to the cell surface, became endocytosed and targeted to the FSV. In contrast, I showed that transfected FasL was mainly found on the surface of non-hematopoietic COS-1 cells, suggesting these cells lack the necessary mechanisms for FasL endocytosis and intracellular targeting. Moreover, flow cytometry experiments suggested Stx3 influences FasL trafficking and provided evidence that supports a role for myosin-mediated movement in the surface translocation of FasL after CTL stimulation.

4.2. Results

4.2.1. FasL is located on the surface in COS-1 cells

Although FasL is found in intracellular vesicles in T cells, NK cells and monocytes (Kiener et al. 1997, Bossi and Griffiths 1999, Kojima et al. 2002, Lettau et al. 2004, He and Ostergaard 2007, Kassahn et al. 2009), when transfected into epithelial HeLa cells, FasL is observed predominantly on the cell surface (Bossi and Griffiths 1999, Blott et al. 2001, Qian et al. 2006). Authors claimed this difference in localization was due to differences in trafficking mechanisms in hematopoietic versus non-hematopoietic cell types. However, these authors also claimed that FasL was stored in LAMP-1^+ lysosomal granules in hematopoietic cells. Because my results (discussed in chapter 3) indicated FasL is stored in LAMP-1^- vesicles in CTL, I decided to evaluate the localization of FasL in non-hematopoietic COS-1 cells.

COS-1 is an African green monkey kidney fibroblast-like cell line that does not express endogenous FasL (Suda et al. 1993). Consistently, I detected no FasL in untransfected COS-1 cells by flow cytometry (**Figure 4.1 A**), confocal microscopy (data not shown) or in lysates by Western Blot (Figure 3.11). Therefore, I studied FasL localization in COS-1 cells transfected with a DsRed-tagged FasL construct. Surface staining with antibodies specific for FasL and flow cytometry analysis revealed a high level of surface FasL expression (**Figure 4.1 B**). I confirmed this observation by staining transfected COS-1 cells for DsRed and analyzing them by confocal microscopy. Acquisition of Z-stack images, deconvolution and three-dimensional reconstruction indicated that FasL was mostly found on the surface of the cells with minor intracellular localization. The surface localization was more evidently observed in the slice images of the three-dimensational reconstruction (**Figure 4.1 C**).

To compare the localization of FasL in non-hematopoietic COS-1 cells versus hematopoietic CTL under identical experimental conditions, I transfected Clone 3/4, Clone 11 and CTLL-2 cells, the same cell types employed in chapter 3,

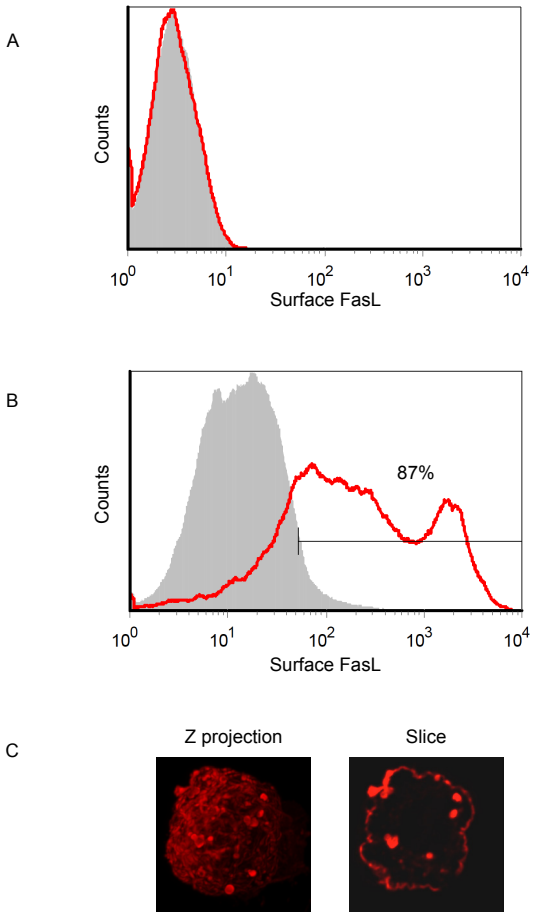

Figure 4.1. Transfected DsRed-FasL is predominantly located on the surface of COS-1 cells.
(A) Total FasL expression was determined on COS-1 cells by flow cytometry (red) and compared to isotype control (gray). **(B and C)** COS-1 cells were transfected with DsRed-FasL. Surface FasL expression was determined by flow cytometry (red) and compared to isotype controls (gray) **(B)** and intracellular distribution was assessed on permeabilized cells by confocal microscopy after staining for DsRed and the appropriate secondary antibodies **(C)**. Z-stack images were acquired (interval, 0.2µm) and subjected to deconvolution and three-dimensional reconstruction. Representative projections of the reconstructed images as well as a single optical slice are shown. In A and B data is representative of at least 3 independent experiments. In C data is representative of at least 30 cells.

with the DsRed-tagged FasL construct. I stained transfected CTL Clone 3/4 cells for surface FasL and analyzed them by flow cytometry. Although slightly higher compared to mock transfected cells, FasL surface expression was low in CTL Clone 3/4 cells (**Figure 4.2 A**). Confocal microscopy analysis of transfected Clone 3/4 cells stained for DsRed showed that FasL had no detectable expression on the surface but was instead found in intracellular vesicles (**Figure 4.2 B**). Confocal microscopy is probably a less sensitive detection method compared to flow cytometry, explaining why low levels of surface expression were not detected. To determine whether transfected DsRed-tagged FasL localized to endogenous FasL vesicles, I used the FSV marker Stx3 identified in chapter 3 and tested if it colocalized with transfected FasL using confocal microscopy. Analysis of Clone 3/4 cells stained for DsRed and Stx3 showed that transfected FasL had a high degree of colocalization with Stx3 (**Figure 4.2 C**). Moreover, confocal microscopy analysis of DsRed-FasL transfected Clone 3/4 cells stained for DsRed and LAMP-1 showed that DsRed-FasL colocalized poorly with the cytolytic granule marker LAMP-1 (**Figure 4.2 D**). Overall, these results indicated that transfected DsRed-FasL trafficked to intracellular $Stx3^{+}$ $LAMP^{-}$ vesicles, as reported in chapter 3 for endogenous FasL.

Confocal microscopy analysis of transfected CTL Clone 11 cells also showed intracellular localization of DsRed-FasL (**Figure 4.3 A**). Surprisingly, however, even though DsRed-FasL displayed a strong colocalization with Stx3, it also colocalized to a high degree with LAMP-1 in transfected CTL Clone 11 cells (**Figure 4.3 B**). Moreover, merged images of Clone 11 cells stained for DsRed, LAMP-1 and Stx3 showed that DsRed-FasL is found in large vesicles containing all three proteins (**Figure 4.3 C**). Similarly, transfected CTLL-2 cells also displayed DsRed-FasL in intracellular vesicles (**Figure 4.4 A**) and DsRed-FasL colocalized both with Stx3 as well as with LAMP-1 (**Figure 4.4 B**). Furthermore, as observed in transfected Clone 11 cells, transfected DsRed-FasL was found in $Stx3^{+}$ $LAMP\text{-}1^{+}$ vesicles (**Figure 4.4 C**). These results indicated that in Clone 11 and CTLL-2, exogenous FasL trafficked to an aberrant vesicle distinct from the

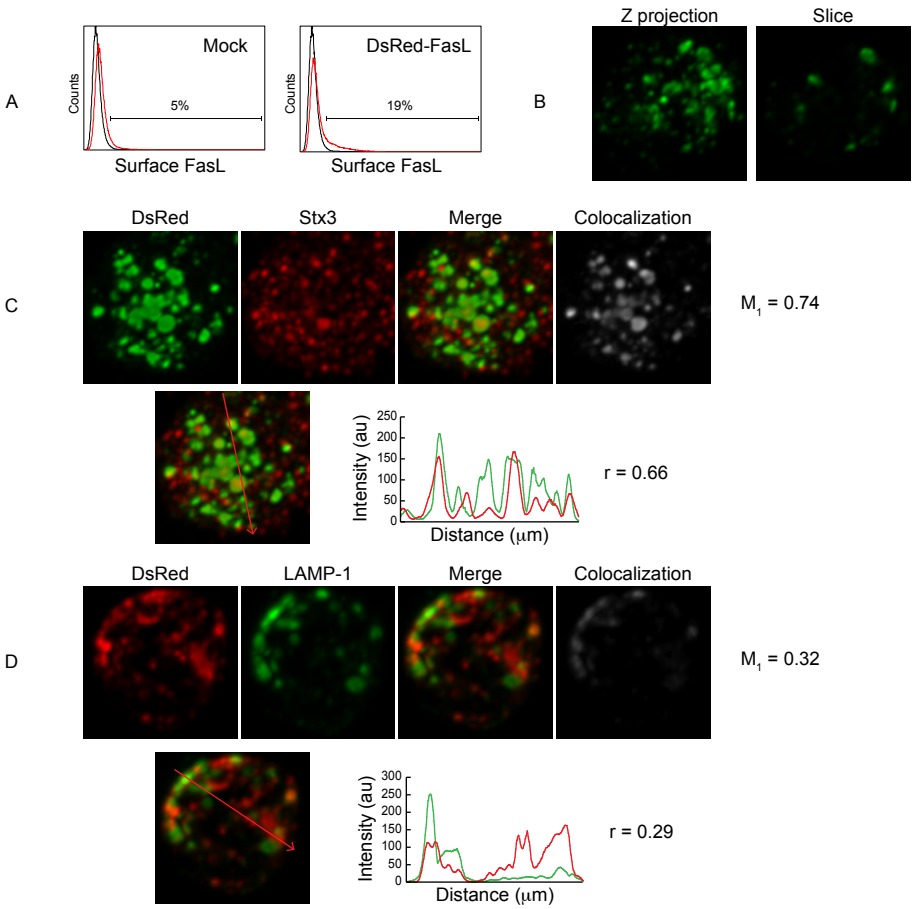

Figure 4.2. Transfected DsRed-FasL is located in Stx3$^+$ LAMP-1$^-$ intracellular vesicles in CTL Clone 3/4.
CTL Clone 3/4 cells were transfected with DsRed-FasL or mock-transfected **(A)** Surface FasL expression was determined by flow cytometry (red) and compared to isotype control (gray). **(B)** Transfected cells were stained with specific antibodies for DsRed and the corresponding secondary antibodies. Z-stack images were acquired (interval, 0.2μm) and subjected to deconvolution and three-dimensional reconstruction. Representative projections of the reconstructed images as well as a single optical slice are shown. **(C and D**) Clone 3/4 cells transfected with DsRed-FasL were stained with specific antibodies for DsRed and Stx3 **(C)** or DsRed and LAMP-1 **(D)**. After staining with the appropriate secondary antibodies, samples were analyzed by confocal microscopy. Z-stack images were acquired (interval, 0.2μm) and subjected to deconvolution and three-dimensional reconstruction. Representative projections of the reconstructed images are shown. Colocalization images were created displaying only the regions where the two channels colocalize and the corresponding Manders coefficients (M_1) were calculated. Lines were drawn across the merged images attempting to include maximums from all channels, the fluorescent intensity profiles over that line were graphed and Pearson coefficients (r) were calculated. Data is representative of at least 3 independent experiments corresponding to 11 and 15 cells.

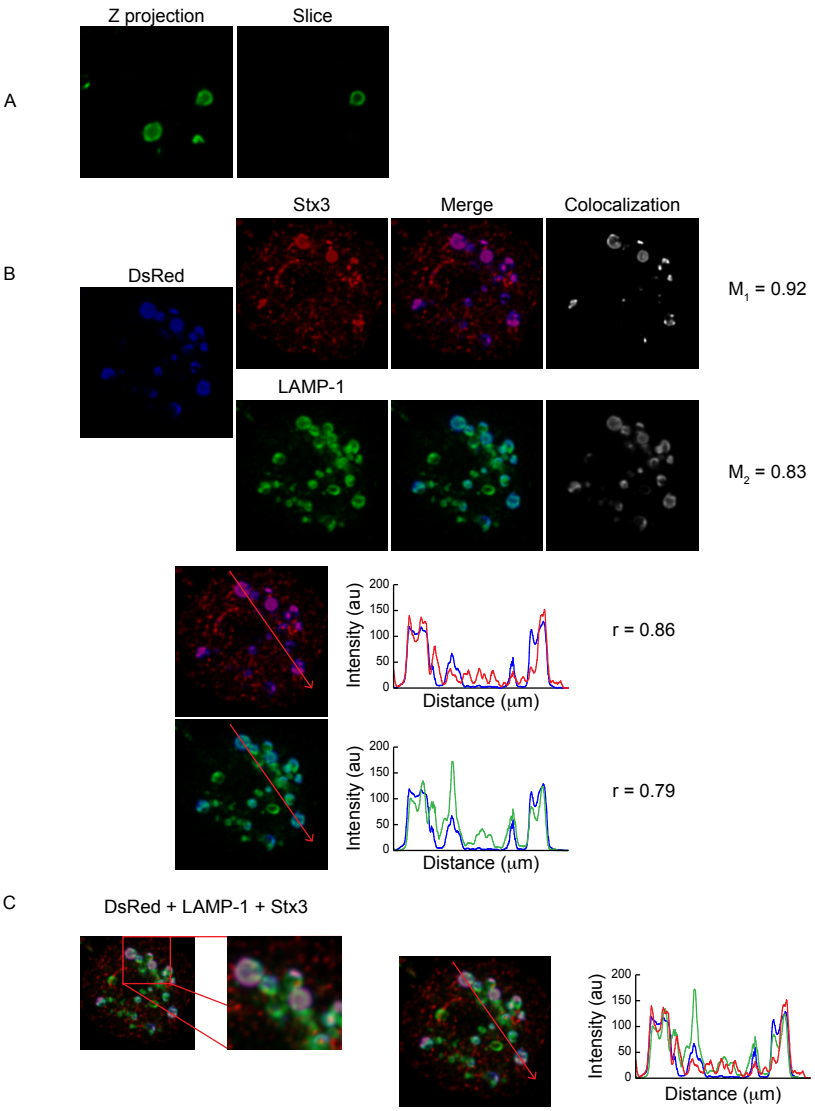

Figure 4.3. Transfected DsRed-FasL is located in Stx3$^+$ LAMP-1$^+$ intracellular vesicles in CTL Clone 11.

(A) CTL Clone 11 cells were transfected with DsRed-FasL and stained with specific antibodies for DsRed and the corresponding secondary antibodies. **(B and C)** Clone 11 cells transfected with DsRed-FasL were stained with specific antibodies for DsRed, Stx3 and LAMP-1. and the appropriate secondary antibodies. **(A, B and C)** Z-stack images were acquired (interval, 0.2μm) and subjected to deconvolution and three-dimensional reconstruction. Representative projections of the reconstructed images are shown. **(B)** Colocalization images were created displaying only the regions where the two channels colocalize and the corresponding Manders coefficients (M_1) were calculated. Lines were drawn across the merged images attempting to include maximums from both channels, the fluorescent intensity profiles over that line were graphed and Pearson coefficients (r) were calculated. **(C)** A three-color merged image and the corresponding fluorescent intensity profile is shown. Data is representative of three independent experiments corresponding to 16 cells.

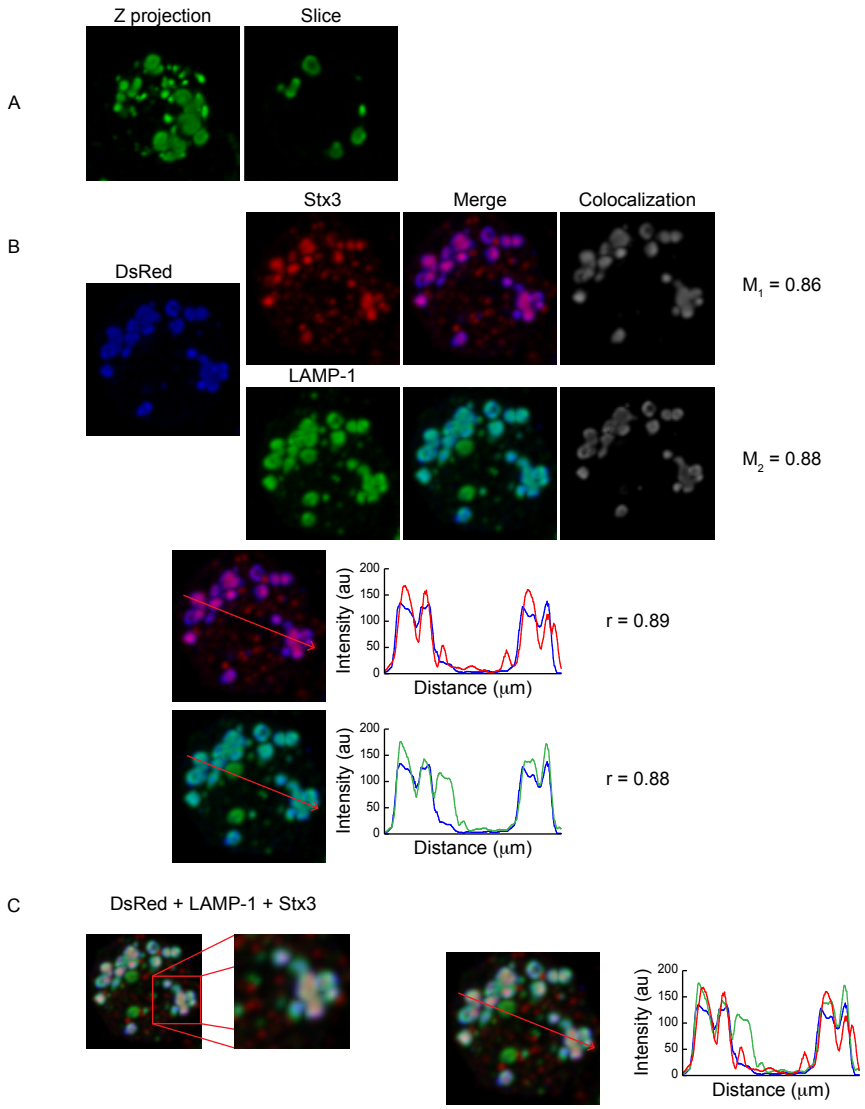

Figure 4.4. Transfected DsRed-FasL is located in Stx3$^+$ LAMP-1$^+$ intracellular vesicles in CTLL-2 cells.
(A) CTLL-2 cells were transfected with DsRed-FasL and stained with specific antibodies for DsRed and the corresponding secondary antibodies. **(B and C)** CTLL-2 cells transfected with DsRed-FasL were stained with specific antibodies for DsRed, Stx3 and LAMP-1 and the appropriate secondary antibodies. **(A, B and C)** Z-stack images were acquired (interval, 0.2μm) and subjected to deconvolution and three-dimensional reconstruction. Representative projections of the reconstructed images are shown. **(B)** Colocalization images were created displaying only the regions where the two channels colocalize and the corresponding Manders coefficients (M_1) were calculated. Lines were drawn across the merged images attempting to include maximums from both channels, the fluorescent intensity profiles over that line were graphed and Pearson coefficients (r) were calculated. **(C)** A three-color merged image and the corresponding fluorescent intensity profile is shown. Data is representative of three independent experiments corresponding to 49 cells.

$Stx3^+$ $LAMP\text{-}1^-$ endogenous FasL storage vesicle. It also demonstrated that DsRed-tagged FasL can only be used to study FasL trafficking in CTL Clone 3/4 cells, where it is targeted to the appropriate endogenous vesicle.

Despite the differences in intracellular targeting, the overall sum of results indicates FasL traffics with high efficiency to intracellular vesicles in all the CTL cell types studied and that, in contrast, in COS-1 cells, FasL is preferentially localized on the surface.

4.2.2. FasL is endocytosed from the cell surface

Proteins stored in cytolytic granules can reach this compartment through intracellular endocytic vesicle trafficking or by surface endocytosis and targeting of secreted proteins (Lettau et al. 2007). By analogy, I proposed two general alternatives for the trafficking of FasL in CTL. Upon synthesis in the ER, followed by transport to the Golgi, from the TGN the transmembrane FasL protein could either be A) intracellularly transported to the FSV or B) translocated to the cell surface, and later endocytosed and targeted to the FSV (**Figure 4.5**). Because FasL is expressed on the surface of COS-1 cells (Figure 4.1) and HeLa cells (Bossi and Griffiths 1999, Blott et al. 2001, Qian et al. 2006), I hypothesized that FasL was universally translocated to the surface as part of the constitutive secretion pathway and later specifically internalized into its FSV only in hematopoietic cells. In this hypothetical scenario, non-hematopoietic cells such as HeLa or COS-1 cells would lack the necessary machinery to allow the endocytosis, and FasL would thus remain on the surface.

To test my hypothesis, I conducted a confocal microscopy endocytosis assay. I incubated non-permeabilized CTL Clone 3/4 cells with specific anti-FasL antibodies at 37°C for 4 hours. This incubation allowed for the potential binding of antibodies to FasL molecules present on the surface and for their potential endocytosis, if it occurred. Then, I thoroughly washed away unbound antibodies, and permeabilized the cells before adding the appropriate secondary antibodies. Finally, confocal microscopy analysis allowed for the detection of FasL molecules

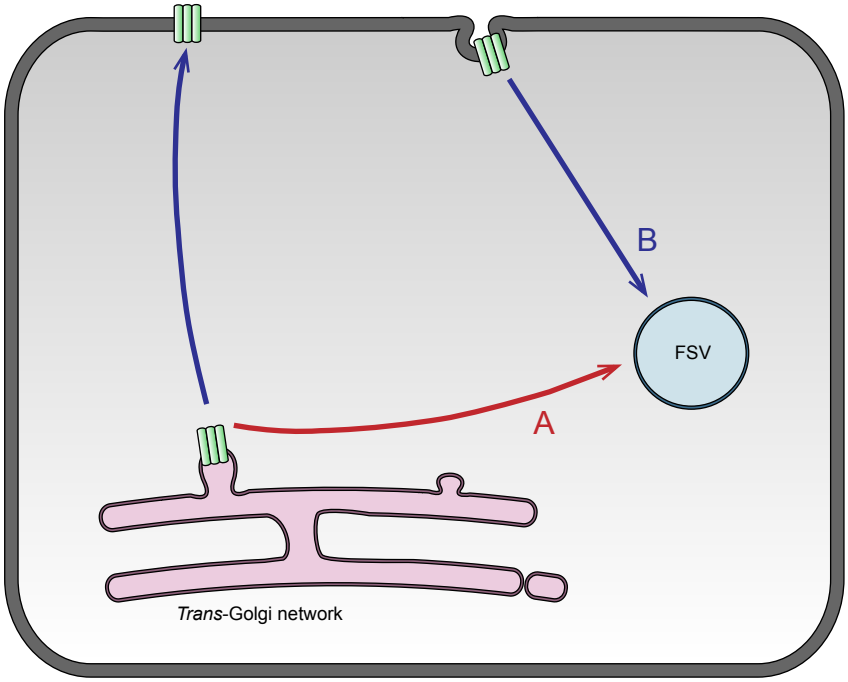

Figure 4.5. General alternatives for FasL trafficking in CTL.
After its synthesis and modification in ER and Golgi, FasL could either be A) intracellularly transported to the FSV or B) secreted to the cell surface and later endocytosed and targeted to the FSV.

endocytosed during the incubation. The first panel in **Figure 4.6 A** showed that FasL could be detected intracellularly in non-permeabilized cells. The intracellular distribution of FasL in the endocytosis assay was similar to that observed in cells stained for FasL after permeabilization (**Figure 4.6 A**, second panel). As a control, I performed the microscopy-based endocytosis assay using isotype control antibodies and detected no staining. I also analyzed cells incubated with antibodies against GM-130, a Golgi marker that does not traffic to the cell surface (Nakamura et al. 1995). In non-permeabilized cells the anti-GM-130 antibodies were washed away and no GM-130 could be detected, while in permeabilized cells, the expected GM-130 intracellular pattern was observed (**Figure 4.6 B**). This assay demonstrated that extracellular antibodies were able to bind FasL, indicating a surface trafficking route, and that FasL-bound antibodies could be internalized from the cell surface and detected intracellularly, indicating FasL was endocytosed from the plasma membrane.

To confirm that the FasL-bound antibodies detected in the endocytosis assay were targeted to the FSV, I stained CTL Clone 3/4 cells with anti-FasL in a confocal microscopy endocytosis assay, subsequently co-stained them with antibodies specific for Stx3 and analyzed their colocalization by confocal microscopy. The high degree of colocalization with the FSV marker Stx3 (**Figure 4.6 C**) confirmed that the intracellular destination of endocytosed FasL was in fact its $Stx3^+$ storage vesicle. Overall, these results demonstrate that FasL traffics to the cell surface, undergoes endocytosis and is targeted to its FSV. However, these observations do not exclude the possibility that additional mechanisms may be at play to target FasL to its vesicle.

4.2.3. Cycling of FasL between the surface and its storage vesicle

The next question I asked was whether FasL, after being endocytosed and targeted to its vesicle, remained static in the FSV in unstimulated conditions until the CTL received a stimulation signal. To evaluate this question, I used the protein inhibitor cyclohexamide (CHX) at 10 μg/ml. Previous results from our

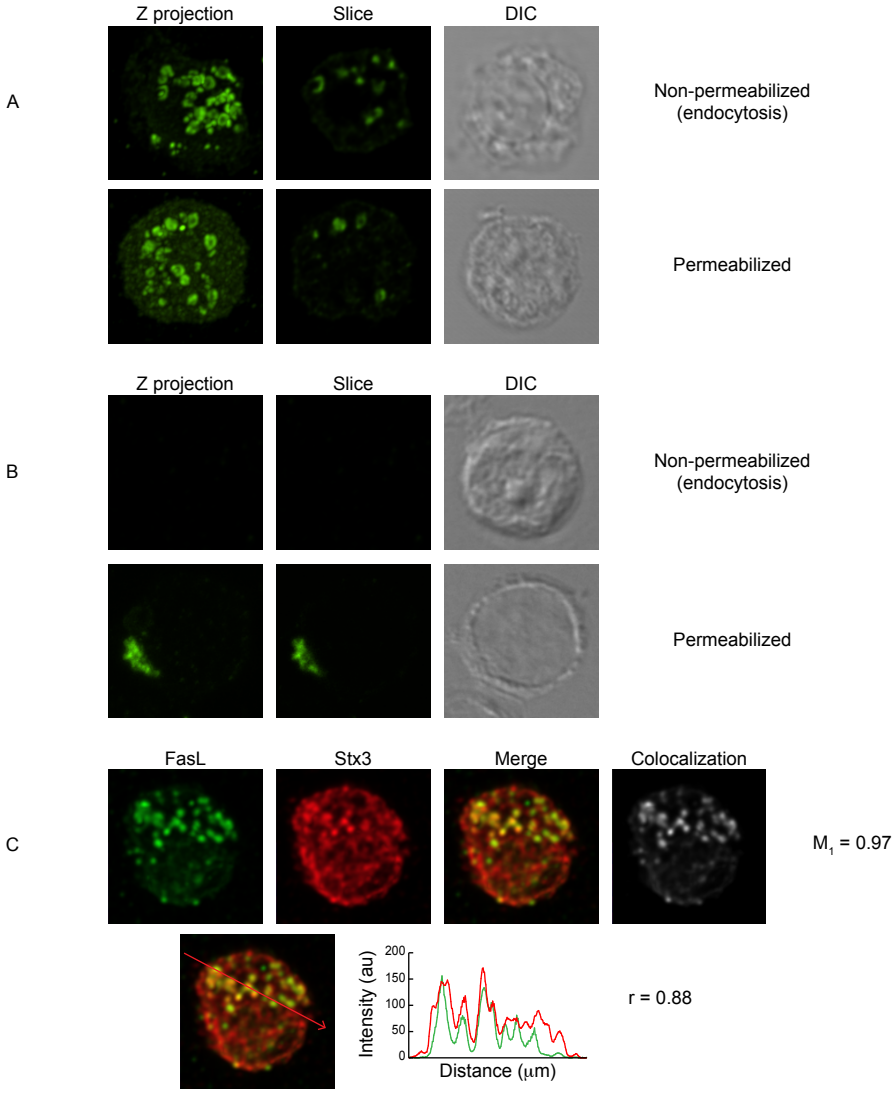

Figure 4.6. Antibodies against FasL are endocytosed from the cell surface. Non-permeabilized CTL Clone 3/4 CTL cells were incubated with antibodies specific for FasL **(A and C)** and GM130 **(B)** for 4 hours at 37°C. After washing the unbound antibodies, cells were permeabilized and incubated with the corresponding secondary antibodies **(C)** and costained with antibodies specific for Stx3. Z-stack images were acquired (interval, 0.2μm) and subjected to three-dimensional reconstruction. Representative projections of the reconstructed three-dimensional images are shown. **(A and B)** Single optical slices and DIC images are also shown. Additionally, images of permeabilized cells stained with the same antibodies are included as a control (right panels). **(C)** A colocalization image was created displaying only the regions where the two channels colocalize and the corresponding Manders coefficient (M_1) was calculated. A line was drawn across the merged image attempting to include maximums from both channels, the fluorescent intensity profile over that line was graphed and the Pearson coefficient (r) was calculated. Data is representative of 3 independent experiments corresponding to 30 cells.

laboratory showed that treatment of CTL clones with 10 μg/ml CHX completely blocked all new protein synthesis in a pulse chase experiment (Ostergaard, unpublished data). Moreover, I tested the effect of CHX on CTL Clone 3/4 cells stimulated with PMA and ionomycin for 2h. Consistent with previous studies (He and Ostergaard 2007), treatment with CHX at 10 μg/ml reduced FasL surface expression triggered after 2 hours of stimulation in CTL (**Figure 4.7 A**). I therefore pre-treated CTL Clone 3/4 cells with the protein synthesis inhibitor cyclohexamide (CHX) at 10 μg/ml for 210 min to stop the production of FasL molecules and conducted the same endocytosis assay described above in the presence of CHX. Confocal microscopy analysis of non-permeabilized cells previously treated with CHX, showed no detectable difference in the degree of endocytosis or colocalization with Stx3 compared to DMSO-treated cells, the carrier control (**Figure 4.7 B**). This indicated that protein synthesis was not necessary for FasL surface detection, endocytosis and FSV targeting.

In untreated cells, newly synthesized FasL molecules would traffic to the surface, become endocytosed and travel to the FSV. After the treatment with CHX, the production of new FasL molecules would be blocked. Thus, the antibodies used in the endocytosis assay would only be able to recognize and bind molecules synthesized prior to the CHX treatment. Thus, the fact that FasL was detected on the surface and observed intracellularly in CHX-treated cells, could suggest that FasL cycles between the surface and intracellular stores in unstimulated CTL.

4.2.4. FasL has no detectable association with components of the recycling pathway

Similarly to FasL, other proteins such as transferrin receptor (TfR) and CTLA-4 have been shown to continuously cycle between the surface and intracellular stores (Hopkins 1983, Hopkins and Trowbridge 1983, Linsley et al. 1996). TfR is endocytosed into $Rab5^+$ early endosomes, and is then recycled back to the surface, both directly from early endosomes as well as through recycling

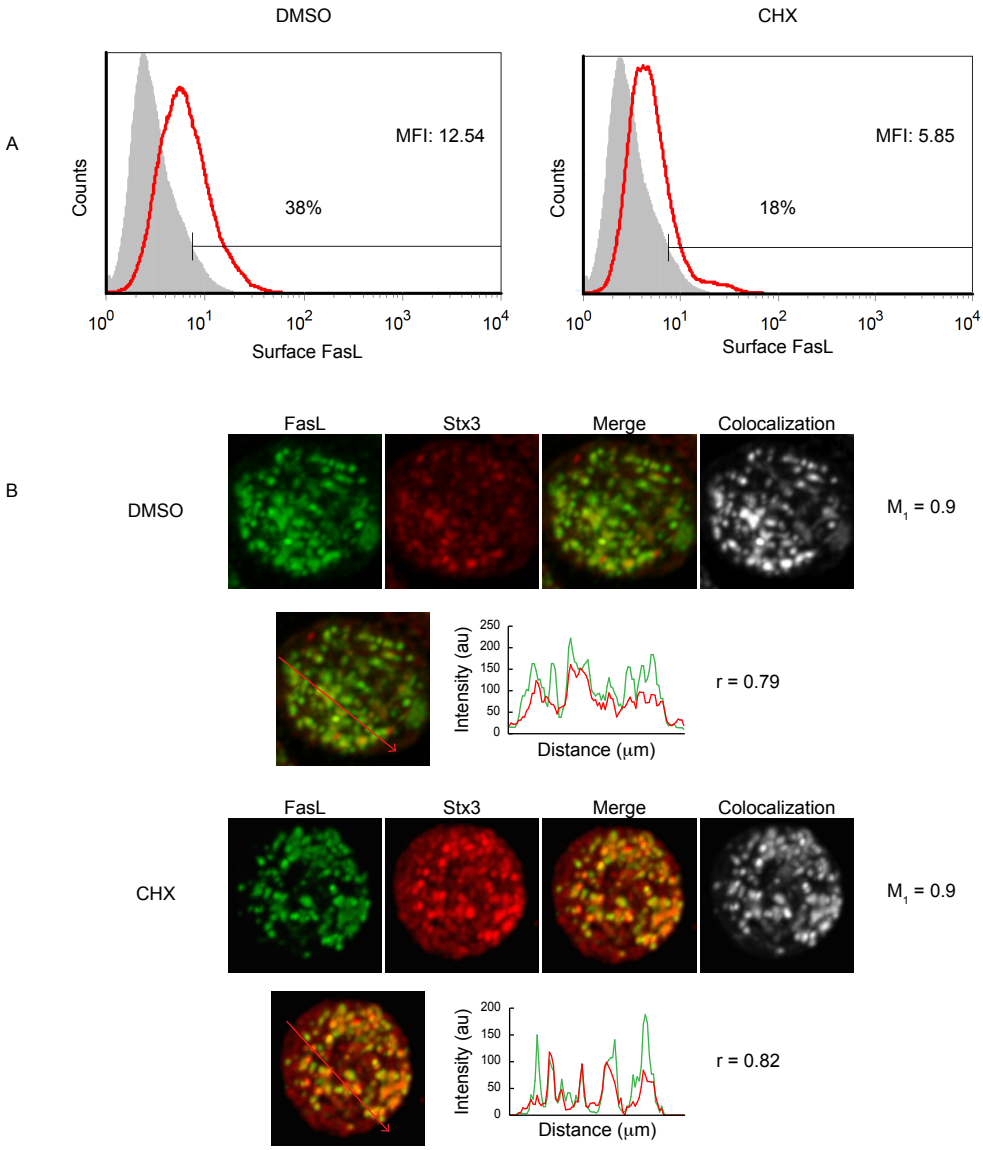

Figure 4.7. Protein synthesis is not necessary for FasL surface detection, endocytosis and FSV targeting.
(A) CTL Clone 3/4 cells were pre-incubated with CHX for 45 min and then stimulated with PMA and ionomycin for 2 hours in the presence of CHX. Surface FasL expression was determined by flow cytometry (red) and compared to isotype controls (gray) **(B)** Non-permeabilized CTL Clone 3/4 CTL cells were pre-incubated with CHX (or DMSO as a control) for 210 min and then FasL surface detection, endocytosis and Stx3 colocalization was determined as explained in Figure 4.6 C. Data is representative of 3 independent experiments corresponding to at least 27 cells.

endosomes in a process mediated by Rab8 and Rab11. Rab4 also affects TfR trafficking from early endosomes although it is unclear whether it is involved in its cycle back to the plasma membrane or its targeting to recycling endosomes (Mayle et al. 2012). Consistent with the notion that FasL cycles between the surface and its FSV, I postulated that FasL would colocalize with components of the endocytic recycling pathway. To test this hypothesis, I stained CTL Clone 3/4 cells for FasL and Rab4 and I conducted a colocalization microscopy analysis, as described in chapter 3. The low Manders (M_1) and Pearson (r) coefficients obtained supported the visual analysis and indicated that FasL did not have a strong colocalization with Rab4 (**Figure 4.8**). I also tried to examine the colocalization of FasL with Rab11 and Rab5 but was unable to detect staining for these proteins. Possible reasons for this failure of detection could be that the antibodies employed were not able to recognize and bind the proteins under the conditions used in this experiment, or that the amounts of endogenous Rab5 and Rab11 proteins expressed by CTL were insufficient for the detection by this method. I therefore transfected CTL Clone 3/4 cells with constructs containing GFP-tagged Rab4, GFP-Rab11, GFP-Rab5 or GFP-Rab8, separately, and stained the transfected cells for FasL and GFP. Confocal microscopy analysis of colocalization, allowed me to confirm that FasL did not colocalize with transfected Rab4 (**Figure 4.9 A**) and revealed that FasL did not colocalize with transfected Rab11 (**Figure 4.9 B**), transfected Rab5 (**Figure 4.9 C**) or transfected Rab8 (**Figure 4.9 D**). Lack of colocalization with the components of the endocytic system could indicate that the dynamic traffic of FasL between the surface and the FSV is highly efficient and/or that it only happens for a small percentage of molecules. This would result in very few molecules present in any vesicle different from the FSV at any given time and would make their detection unlikely.

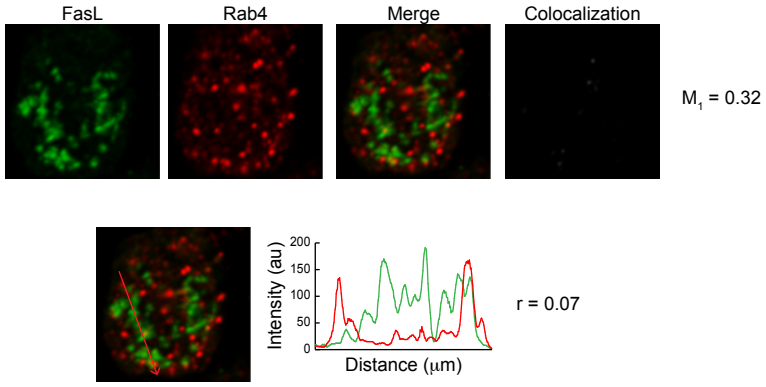

Figure 4.8. FasL does not colocalize with Rab4.
Clone 3/4 CTL cells were stained with antibodies specific for FasL and Rab4, as well as the appropriate secondary antibodies and analyzed by confocal microscopy. Z-stack images were acquired (interval, 0.2μm) and subjected to deconvolution and three-dimensional reconstruction. Representative projection of the reconstructed images is shown. A colocalization image was created displaying only the regions where the two channels colocalize and the corresponding Manders coefficients (M_1) was calculated. A line was drawn across the merged image attempting to include maximums from both channels, the fluorescent intensity profile over that line was graphed and Pearson coefficients (r) was calculated. Data is representative of 3 independent experiments corresponding to at least 27 cells.

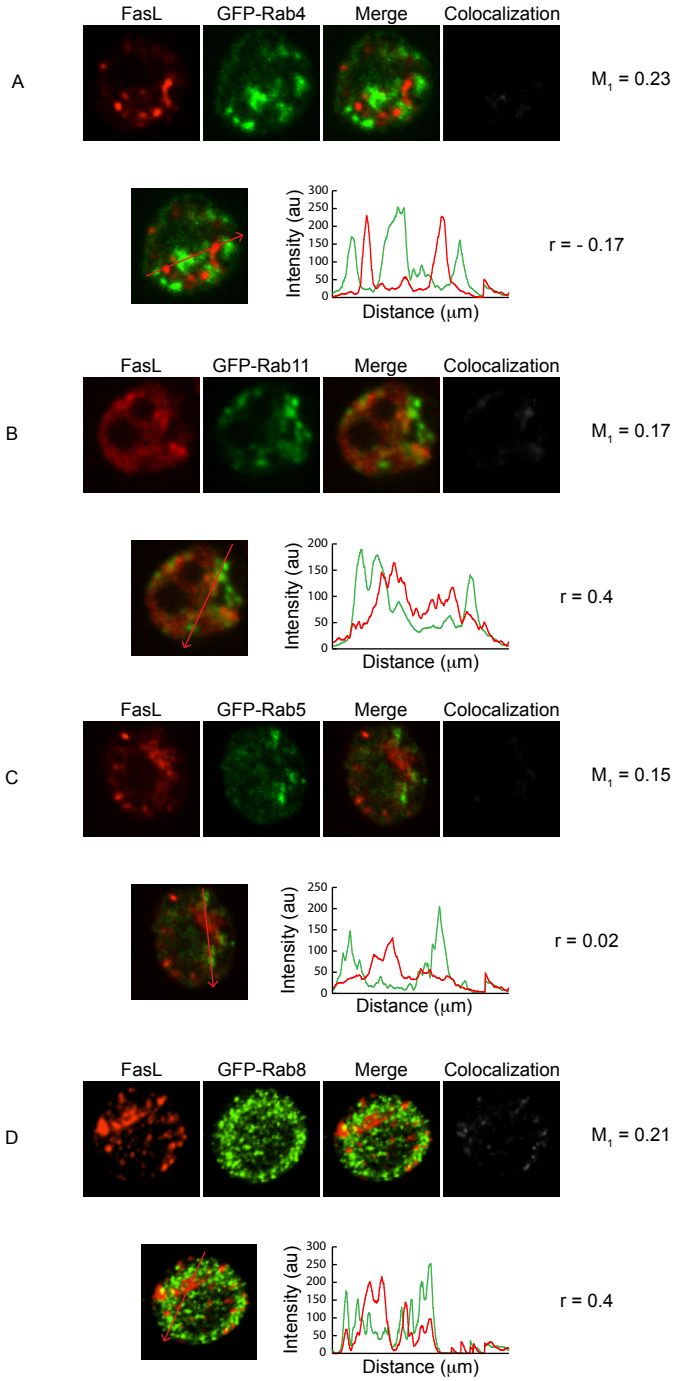

Figure 4.9. FasL does not colocalize with Rab4, Rab11, Rab5 and Rab8.
Clone 3/4 CTL cells were transfected with GFP-Rab4 **(A)** GFP-Rab11 **(B)** GFP-Rab5 **(C)** and GFP-Rab8 **(D)**. Transfected cells were stained with antibodies specific for FasL and GFP as well as the appropriate secondary antibodies and analyzed by confocal microscopy as explained in Figure 4.8. Data is representative of three independent experiments corresponding to 10 cells.

4.2.5. Syntaxin 3 affects FasL localization in COS-1 cells

Stx3 belongs to the SNARE family of proteins involved in the fusion event of protein trafficking (Teng et al. 2001). In particular, Stx3 is a target membrane SNARE, or t-SNARE, meaning that because of its structure it can be predicted to aid in the membrane fusion event from the side of the accepting compartment. t-SNAREs specifically pair with v-SNAREs on the donor vesicles and assemble to form trans-SNARE complexes that allow the fusion of the membranes in the two compartments by forcing them together (Jahn and Scheller 2006). In chapter 3 (Figure 3.8), I showed that Stx3 is found in the same vesicle with FasL indicating Stx3 may function as a t-SNARE on these vesicles to allow fusion of incoming vesicles with cargo destined to the FSV. Therefore, I hypothesized that Stx3 would affect the trafficking of FasL to the FSV. That is, after being endocytosed from the plasma membrane, endocytic vesicles containing FasL could fuse with FSVs in a process mediated by Stx3. To test this hypothesis I decided to first use COS-1 cells, where FasL is expressed mostly on the surface (Figure 4.1), transfected with exogenous Stx3. Overexpression of full-length SNAREs can be used to enhance trafficking in a variety of cells (Pagan et al. 2003, Murray et al. 2005). Therefore, I evaluated if the overexpression of Stx3 affected the localization of FasL, that is, whether the surface expression was reduced and the intracellular targeting increased.

For that purpose, I transfected COS-1 cells with DsRed-FasL and Stx3-Myc-Myc-His and with DsRed-FasL alone, I then stained them for surface FasL and analyzed them by flow cytometry. Overlap of their histograms did not reveal major differences (**Figure 4.10 A**) and analysis of the percentage of cells expressing surface FasL relative to isotype controls in COS-1 cells transfected with FasL and Stx3 versus cells transfected with FasL only, indicated there was no significant difference in the proportion of cells expressing surface FasL (**Figure 4.10 B**). Additionally, comparison of the mean fluorescence intensity for double transfected and single transfected cells showed that Stx3 had no significant effect on the level of expression of surface FasL (**Figure 4.10** C). Therefore I

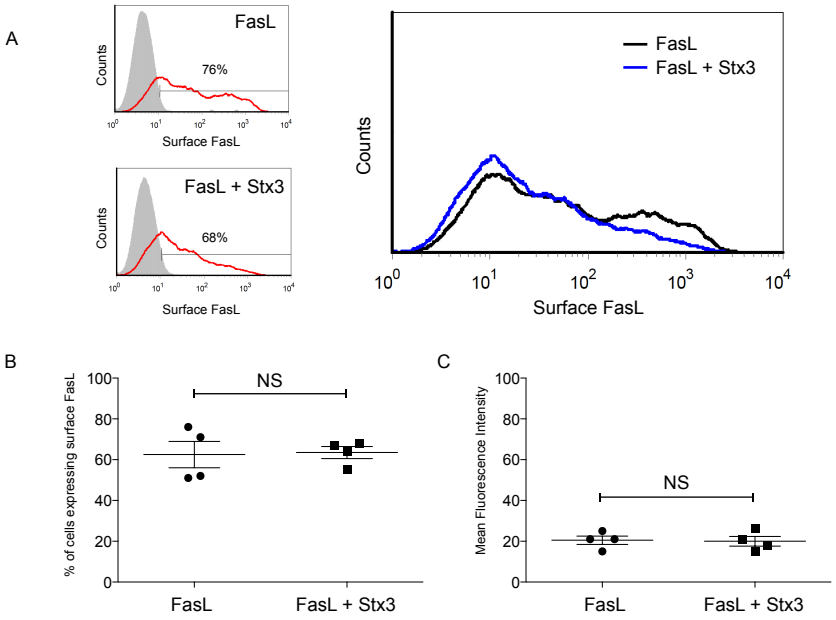

Figure 4.10. Stx3 has no detectable effect on surface FasL expression in COS-1 cells.

COS-1 cells were transfected with DsRed-FasL or DsRed-FasL and Stx3-Myc-Myc-His. **(A)** Surface FasL expression on transfected cells was analyzed by flow cytometry (red) and compared to isotype controls (gray). Histograms were overlapped for comparison and are shown on the right panel. The percentage of cells expressing surface FasL **(B)** and the MFI **(C)** were graphed and compared. Mean and standard error bars are indicated for each group. The unpaired Students *t*-test was used with significance set at a p value ≤ 0.05 where NS indicates not significant.

concluded there was no detectable effect of Stx3 on surface FasL expression. This could suggest that Stx3 does not affect FasL trafficking in COS-1 cells. However, I cannot be certain that all of the cells transfected with FasL also expressed the Stx3 construct. Gating on Stx3-transfected cells could exclude this possibility but was not feasible in this experiment since the antibody epitopes for His, Myc and Stx3 are intracellular and inaccessible in non-permeabilized cells.

Therefore, I decided to test the effect of Stx3 on intracellular FasL distribution by confocal microscopy focusing on Myc-expressing cells. I transfected COS-1 cells with DsRed-FasL and Stx3-Myc-Myc-His, stained them with antibodies specific for DsRed and Myc and analyzed them by confocal microscopy. There was a large number of cells expressing only FasL, further explaining the lack of a detectable Stx3 effect by flow cytometry (Figure 4.10). Acquisition of Z-stack images, deconvolution and three-dimensional reconstruction allowed me to evaluate the intracellular distribution of FasL in Myc^+ transfected cells. Interestingly, I observed two different phenotypes (**Figure 4.11 A**); some of the cells (42%) exhibited FasL simultaneously on the surface and in intracellular vesicles, the same phenotype observed for COS-1 cells transfected with DsRed-FasL alone (Figure 4.1 C), while the rest of the cells transfected with FasL and Stx3 displayed FasL exclusively in intracellular vesicles (**Figure 4.11 B**). To determine if these intracellular vesicles overlapped with the $Stx3^+$ intracellular vesicles, I analyzed the colocalization of Myc-tagged Stx3 and DsRed-tagged FasL in cells stained with DsRed and Myc. Unexpectedly, FasL did not colocalize with Stx3 in these intracellular vesicles (**Figure 4.11 C**).

These results demonstrated that the overexpression of Stx3 had an effect on the intracellular distribution of FasL in COS-1 cells, with 58% of the transfected cells expressing FasL in intracellular vesicles. However, the lack of colocalization of intracellular FasL with Stx3, suggested Stx3 did not enhance the fusion of FasL-containing vesicles with $Stx3^+$ vesicles. Because many of the mechanisms needed for FasL trafficking to its FSV are still unknown, an accurate

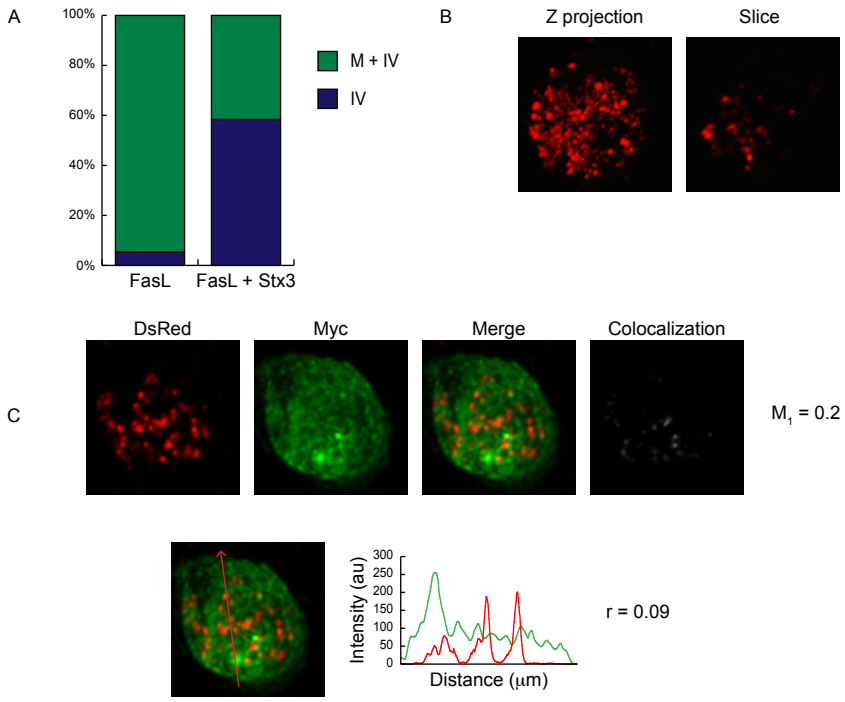

Figure 4.11. Stx3 affects the localization of FasL in COS-1 cells.
COS-1 cells were transfected with DsRed-FasL or DsRed-FasL and Stx3-Myc-Myc-His and stained with specific antibodies for DsRed and Myc and the corresponding secondary antibodies. Z-stack images were acquired (interval, 0.2μm) and subjected to deconvolution and three-dimensional reconstruction. **(A)** The localization of DsRed-FasL was scored in 19 cells transfected with FasL alone and 24 Myc^{+} cells transfected with FasL and Stx3. Scoring: Intracellular Vesicles (IV) and Membrane + Intracellular Vesicles (M + IV). Further details about the scoring system can be found in section 2.15. **(B)** Representative projections of the reconstructed three-dimensional images as well as single optical slices are shown for the IV phenotype of cells transfected with FasL and Stx3. **(C)** Colocalization images were created displaying only the regions where the two channels colocalize and the corresponding Manders coefficients (M_1) were calculated. Lines were drawn across the merged images attempting to include maximums from all channels, the fluorescent intensity profiles over that line were graphed and Pearson coefficients (r) were calculated. Data is representative of three independent experiments corresponding to 24 cells.

interpretation of these results may be difficult at this point. However, they strongly suggest Stx3 can influence FasL trafficking.

4.2.6. Syntaxin 3 affects FasL trafficking in CTL

Since COS-1 cells may lack the necessary machinery for FasL endocytosis or trafficking, I decided to assess the effect of Stx3 on FasL trafficking using CTL Clone 3/4 cells. As explained above, Stx3 is a t-SNARE and is stored in the FSVs in CTL (Figure 3.8). Thus, I hypothesized that Stx3 would influence the trafficking of FasL from the plasma membrane to its intracellular vesicle and decided to evaluate this possibility in CTL Clone 3/4 cells transfected with Stx3.

Staining of permeabilized, transfected cells and flow cytometry analysis indicated that the transfection resulted in higher levels of Stx3 expression compared to mock-transfected cells (**Figure 4.12 A**) confirming that the exogenous Stx3 protein was expressed in CTL. To evaluate the effect of Stx3 on FasL targeting to intracellular vesicles, I stimulated the transfected cells with PMA and ionomycin for 2h. This type of stimulation results in high levels of FasL surface expression (Figure 4.7 and He and Ostergaard 2007) and would allow me to observe a reduction in surface expression if Stx3 indeed affected FasL trafficking. After stimulation, I stained CTL Clone 3/4 cells transfected with Stx3 or mock transfected and analyzed surface FasL expression by flow cytometry. Overlap of the histograms indicated there was no significant difference in the level of surface FasL expression in Stx3-transfected cells compared to mock-transfected cells (**Figure 4.12 B**). Moreover, analysis of the percentage of cells expressing surface FasL relative to isotype controls in Clone 3/4 cells transfected with Stx3 versus mock-transfected, indicated there was no significant difference in the proportion of cells expressing surface FasL (**Figure 4.12 C**). In conclusion, Stx3 had no detectable effect on surface FasL expression in stimulated CTL. However, I cannot exclude the possibility that the effect of Stx3 on FasL is not detectable at the surface level. I attempted to analyze the subcellular distribution of FasL by confocal microscopy but was unable to detect staining for the Myc

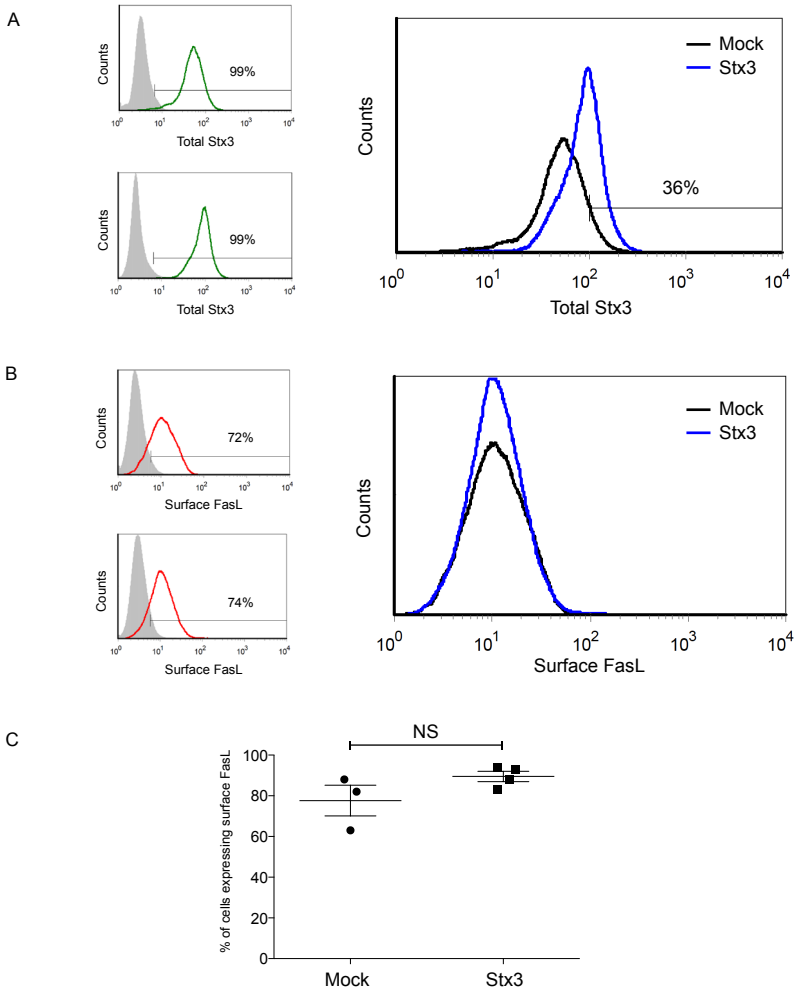

Figure 4.12. Stx3 has no detectable effect on surface FasL expression in stimulated CTL.

CTL Clone 3/4 cells were transfected with Stx3-Myc-Myc-His or mock-transfected. **(A)** Total Stx3 expression was assessed in permeabilized cells by flow cytometry (green) and compared to isotype control (gray). Histograms were overlapped for comparison and are shown on the right panel. **(B)** Transfected cells were stimulated with PMA and ionomycin for 2 hours and surface FasL expression was assessed by flow cytometry (red) and compared to isotype control (gray). Histograms were overlapped for comparison and are shown on the right panel. **(C)** The percentage of cells expressing surface FasL were graphed and compared. Mean and standard error bars are indicated for each group. The unpaired Students *t*-test was used with significance set at a p value ≤ 0.05 where NS indicates not significant.

antibody and thus incapable of distinguishing transfected from untransfected cells.

Surprisingly, however, analysis of unstimulated cells did show an effect of Stx3 on FasL. I stained CTL Clone 3/4 cells transfected with Stx3 or mock transfected and analyzed surface FasL expression by flow cytometry. Overlap of their histograms revealed an increase in surface FasL expression in Stx3-transfected cells (**Figure 4.13 A**). Moreover, analysis of the percentage of cells expressing surface FasL relative to isotype controls in Clone 3/4 cells transfected with Stx3 versus mock-transfected, indicated there was a significant increase in the proportion of cells expressing surface FasL (**Figure 4.13 B**). These results indicate Stx3 increases surface FasL expression in unstimulated cells.

4.2.7. Rab32 has no detectable effect on FasL trafficking

In addition to Stx3, I showed that FasL was also stored with Rab32 in chapter 3 (Figure 3.7). Rab32 is a Rab protein that has been shown to regulate the composition of mitochondria-associated membranes in HeLa cells (Bui et al. 2010). Rabs are a family of GTPases that oscillate between GTP and GDP bound conformations. The GTP-bound state is considered "active" as this is the form that interacts with soluble factors that act as "effectors" to transduce the signal of the Rab GTPases. This switch is controlled by guanine nucleotide exchange factors (GEFs) that promote dissociation of GDP (Stenmark and Olkkonen 2001). To determine if Rab32 affected the intracellular targeting of FasL, I used a GFP-tagged construct of Rab32 with a point mutation T39N that serves as a dominant negative (DN) (Bui et al. 2010). DN Rabs bind and titrate GEFs so that endogenous Rab proteins cannot bind them and are unable to become activated. Therefore, the rational of this experiment was that, in the presence of these mutants, if FasL targeting to the FSV was affected by Rab32, FasL would not be able to reach its storage compartment and would accumulate on the surface.

In order to test this hypothesis, I transfected CTL Clone 3/4 cells with a GFP-tagged Rab32 DN construct as well as with GFP-Rab32 WT and GFP empty vector as controls. I assessed surface expression of FasL by staining transfected

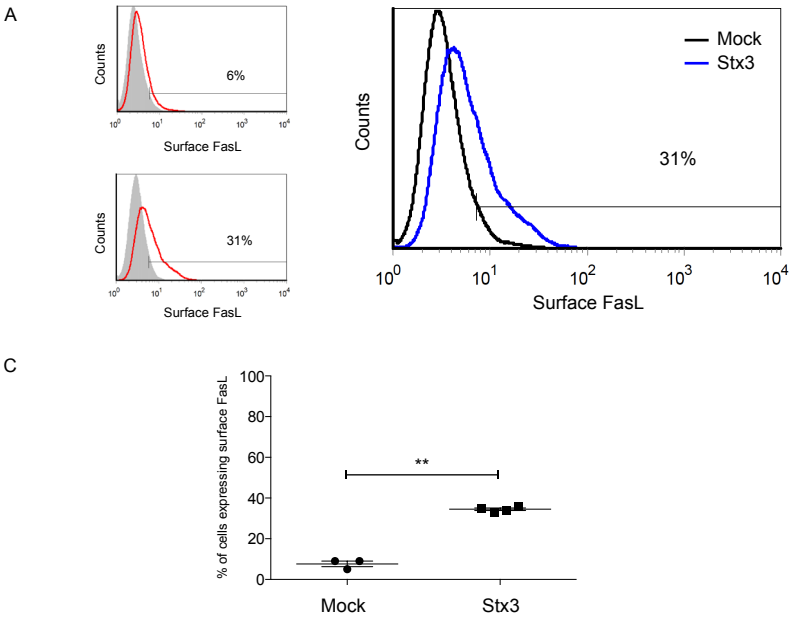

Figure 4.13. Stx3 increases surface FasL expression in unstimulated CTL. CTL Clone 3/4 cells were transfected with Stx3-Myc-Myc-His or mock-transfected. **(A)** Surface FasL expression was assessed by flow cytometry (red) and compared to isotype control (gray). Histograms were overlapped for comparison and are shown on the right panel. **(B)** The percentage of cells expressing surface FasL were graphed and compared. Mean and standard error bars are indicated for each group. The unpaired Students *t*-test was used with significance set at a p value ≤ 0.05 where ** indicates $p < 0.01$.

cells and flow cytometry analysis. Gating on GFP^+ cells allowed me to selectively look at FasL expression within transfected cells. Overlap of the resulting histograms showed no difference in the level of expression in Rab32 DN-transfected cells compared to the controls (**Figure 4.14 A**). Moreover, analysis of the percentage of cells expressing surface FasL indicated there was no significant difference for the expression of FasL in cells transfected with the Rab32 DN construct compared to the control WT or empty constructs (**Figure 4.14 B**). In conclusion I found no detectable effect of Rab32 on the surface expression of FasL. The caveat of this experiment, however, is the lack of a positive control. Unfortunately, Rab32 has not been studied extensively and what little is known about its role in trafficking is in epithelial cells, making it hard to find a suitable control for CTL. The lack of surface accumulation could indicate that: (1) the Rab32 mutant constructs are not expressed at high enough levels to act as dominant negatives (although selectively assessing surface FasL on GFP-expressing cells should reduce the probability of low expression); (2) that Rab32 has no effect on FasL trafficking; or that (3) Rab32 affects FasL trafficking to the FSV, but from an intermediate vesicle, such as an endocytic vesicle, instead of the surface. Nonetheless, preliminary data showed that Rab32 DN colocalized with FasL in a similar manner to the Rab32 WT construct (**Appendix Figure 1**), supporting the notion that Rab32 does not affect FasL localization.

Rab32 could also affect the trafficking of FasL to the cell surface after CTL stimulation. To assess this idea, I transfected CTL Clone 3/4 cells with GFP-Rab32 DN, as well as with GFP-Rab32 WT and empty vector as controls, and I stimulated the transfected cells for 15 min with PMA and ionomycin to trigger the translocation of stored FasL. I then evaluated surface expression of FasL by flow cytometry and compared the levels of expression in cells transfected with the different constructs. Overlap of the histograms for the stimulated cells after gating on GFP^+ transfected cells, showed no difference in surface expression of FasL (**Figure 4.15 A**). Moreover, analysis of the percentage of cells expressing surface FasL indicated no significant difference for cells transfected with Rab32 DN compared to the WT and empty vector controls (**Figure 4.15 B**). In conclusion,

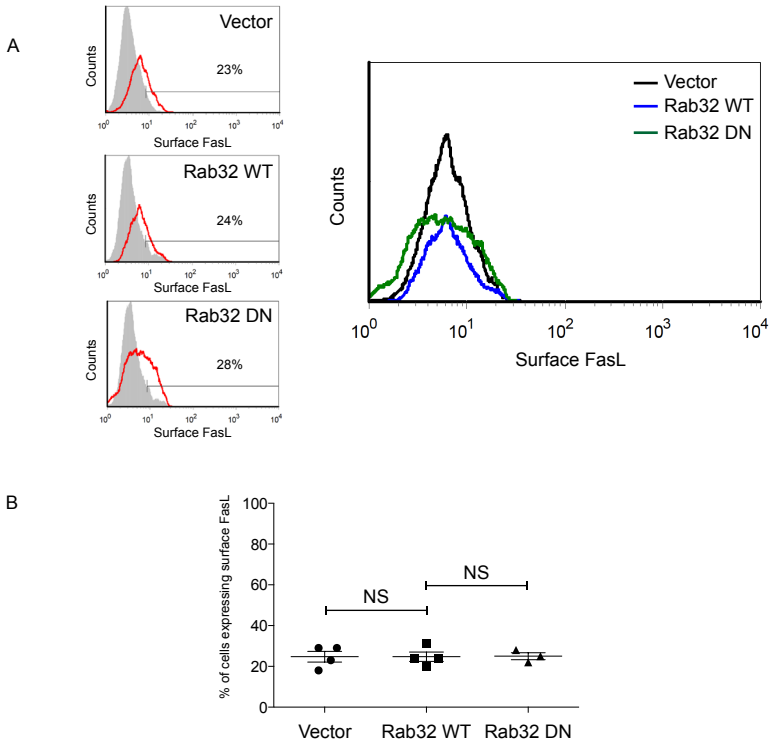

Figure 4.14. Rab32 has no detectable effect on surface FasL expression in unstimulated CTL.
CTL Clone 3/4 cells were transfected with GFP-Rab32 T39N, GFP-Rab32 WT or empty GFP vector **(A)** Surface FasL expression was assessed by flow cytometry (red) and compared to isotype control (gray). Histograms were overlapped for comparison and are shown on the right panel. **(B)** The percentage of cells expressing surface FasL were graphed and compared. Mean and standard error bars are indicated for each group. The unpaired Students *t*-test was used with significance set at a p value ≤ 0.05 where NS indicates not significant.

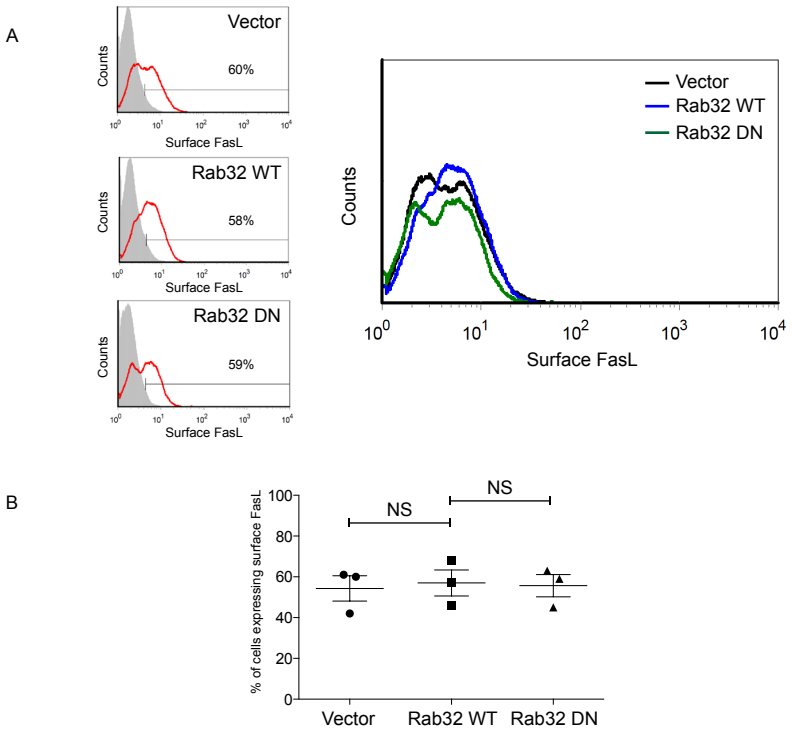

Figure 4.15. Rab32 has no detectable effect on surface FasL expression in stimulated CTL.
CTL Clone 3/4 cells were transfected with GFP-Rab32 T39N, GFP-Rab32 WT or empty GFP vector and later stimulated for 2 hours with PMA and ionomycin **(A)** Surface FasL expression was assessed by flow cytometry (red) and compared to isotype control (gray). Histograms were overlapped for comparison and are shown on the right panel. **(B)** The percentage of cells expressing surface FasL were graphed and compared. Mean and standard error bars are indicated for each group. The unpaired Students *t*-test was used with significance set at a p value ≤ 0.05 where ** indicates $p < 0.01$.

Rab32 showed no detectable effect on surface FasL expression in stimulated CTL. These results may suggest that Rab32 does not mediate FasL trafficking from the FSV to the surface after stimulation. However, I cannot exclude the possibility that the Rab32 T39N construct is not expressed at high enough levels to function as a dominant negative.

4.2.8. Myosin affects FasL translocation to the surface after stimulation

With the goal of identifying additional proteins that may assist FasL in its trafficking from the TGN to its storage vesicle, or from the FSV to the plasma membrane after stimulation, I attempted to find proteins that interacted with FasL. I decided to initially focus on proteins that would interact with the cytoplasmic tail of FasL, which would likely be present inside the cell and outside the FSV. For that purpose, I transformed *E. coli* with a truncated FasL construct containing the cytoplasmic tail fused with GST (GST-$FasL_{Cyto}$) and with a GST empty vector. I purified GST-$FasL_{Cyto}$ (and GST as a control) using glutathione sepharose beads and incubated them with cell lysates from COS-1 and CTL Clone 3/4 cells. I resolved the resulting precipitated proteins in an SDS-PAGE, including input lysates as controls, and visualized them by Coomasie Blue staining. Because COS-1 cells mostly express FasL on the surface (Figure 4.1), proteins that interacted with FasL intracellularly in the FSV would only be present in the CTL lysate. Using these criteria, two bands on the gel were selected, excised and sent for mass spectrometry analysis, resulting in the identification of myosin 9 and actin as the two proteins that were strongly and consistently present at 220 kDa and 42 kDa (**Figure 4.16 A**).

The association of FasL with myosin 9, which is the heavy chain component of the non-muscle myosin II protein (Berg et al. 2001), suggested this protein might affect FasL trafficking. When CTL encounter a target cell bearing the correct combination of peptide-MHC I, a stimulation signal is initiated by the TCR that results in the surface expression of FasL and the secretion of granule contents. Lytic granules move along microtubules to reach the plasma membrane

where they fuse and release their cytolytic factors (Stinchcombe and Griffiths 2007). However, FasL translocation to the surface has been shown to be microtubule independent (He and Ostergaard 2007). Myosin II belongs to the family of myosin proteins that bind to actin filaments and use energy derived from ATP hydrolysis to move along them (Wang et al. 2011). Many myosin proteins have been shown to carry membrane-enclosed organelles such as mitochondria or secretory vesicles (Wu et al. 1997). The results from the pull-down assay suggested FSVs may use myosin II as a molecular motor for actin-based movement. To test this hypothesis, I treated CTL Clone 3/4 cells with 50 uM blebbistatin (or DMSO as a control) for 30 min. Blebbistatin is an inhibitor of the myosin-actin interaction (Dou et al. 2007). I next stimulated blebbistatin pre-treated cells with PMA and ionomycin for 15 min or 2 hours in the continuous presence of blebbistatin and measured FasL surface expression by flow cytometry. Non-stimulated cells displayed no significant difference in the percentage of cells expressing surface FasL (**Figure 4.16 B**, first panel). However, the treatment with blebbistatin provoked a significant decrease in FasL surface expression in cells stimulated both for 15 min and 2 hours (**Figure 4.16 B**, second and third panels). These data suggest myosin affects FasL translocation to the cell surface after stimulation.

4.3. Discussion

The series of experiments shown in this chapter have provided insight into the trafficking route FasL follows after its synthesis to reach its storage vesicle. Using a confocal microscopy endocytosis assay, I demonstrated that FasL could be detected on the surface of non-permeabilized cells and that these antibody-bound surface molecules of FasL could be endocytosed and targeted to the $Stx3^{+}$ FSVs (Figures 4.6). Moreover, surface presence and endocytosis of FasL could be detected in the presence of CHX (Figure 4.7), suggesting FasL cycles between its storage vesicle and the plasma membrane. Taken together, these results open three possible alternatives for the trafficking route of FasL: (1) FasL is secreted to the

A

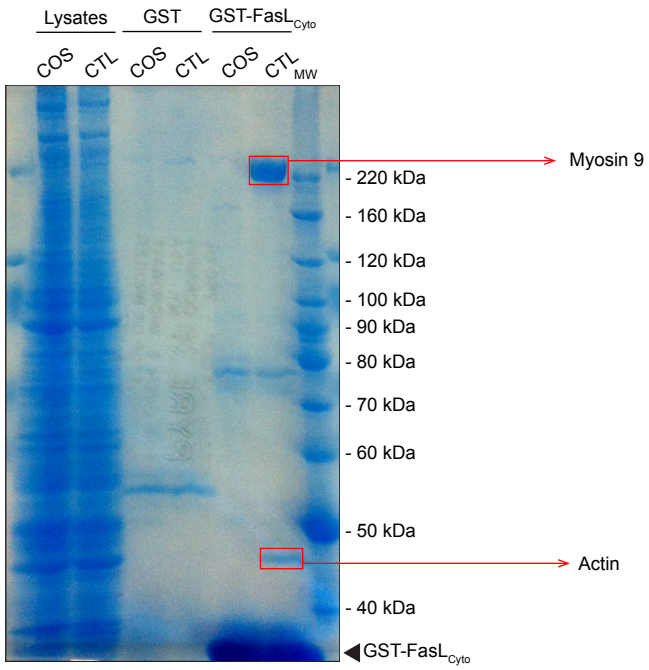
Lysates
GST
GST-FasL$_{Cyto}$
COS
CTL
COS
CTL
COS
CTL
MW
Myosin 9
- 220 kDa
- 160 kDa
- 120 kDa
- 100 kDa
- 90 kDa
- 80 kDa
- 70 kDa
- 60 kDa
- 50 kDa
Actin
- 40 kDa
GST-FasL$_{Cyto}$

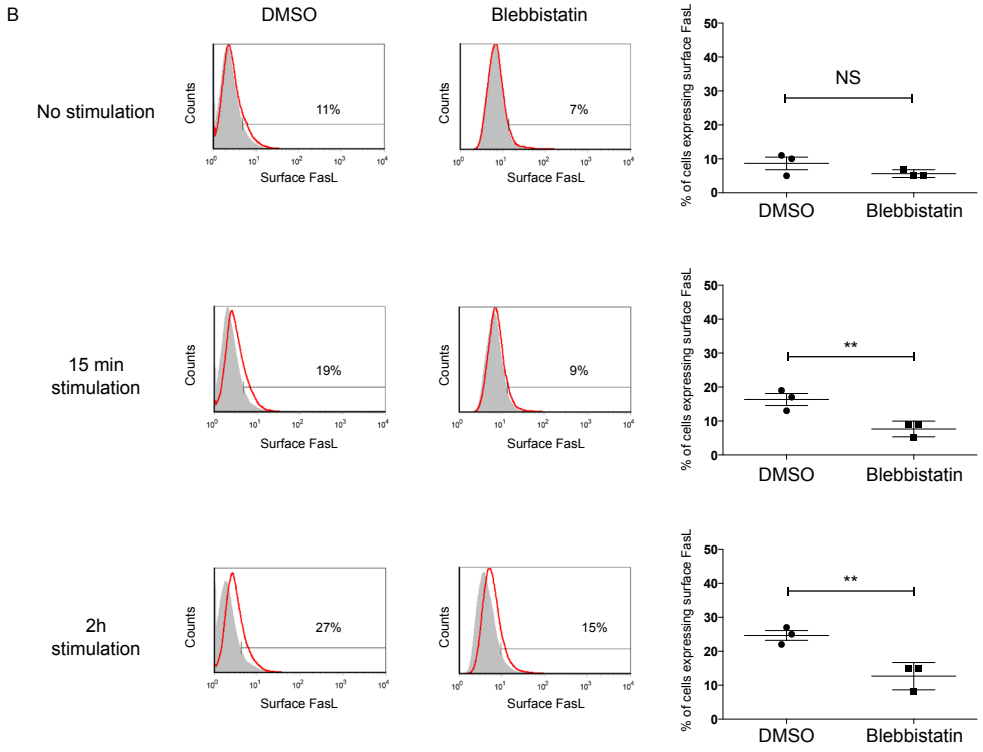

Figure 4.16. Myosin affects FasL surface expression after stimulation.
(A) CTL Clone 3/4 and COS-1 cell lysates were incubated with purified GST and GST-FasL$_{Cyto}$ and proteins precipitated with glutathione sepharose beads were resolved by SDS-PAGE and visualized by Coomasie Blue staining. Two bands present only on the CTL lysates incubated with GST-FasL$_{Cyto}$ were excised and sent for mass spectrophotometry analysis (shown with red rectangles). Proteins were identified as myosin 9 and actin. **(B)** CTL Clone 3/4 cells were incubated with blebbistatin or DMSO as a carrier control and stimulated with PMA and ionomycin for 15 min, 2 hours or not-stimulated. Surface FasL expression was assessed by flow cytometry (red) and compared to isotype control (gray). The percentage of cells expressing surface FasL were graphed and compared. Mean and standard error bars are indicated for each group. The unpaired Student *t*-test was used with significance set at a p value ≤ 0.05 where ** indicates $p < 0.01$.

surface from the TGN as part of the constitutive secretion pathway and from the surface, endocytosed and directed to its storage vesicle; (2) FasL is intracellularly targeted to FSVs from where it cycles to the surface and back; or (3) a combination of alternatives 1 and 2. Interestingly, proteins have been shown to traffic through each of these three options. CTLA-4 and BACE1 are transmembrane proteins that cycle through the surface. CTLA-4 is an inhibitory co-receptor expressed on T cells that downregulates T cell immune responses. However, despite having a surface function, it has mostly an intracellular distribution, similarly to what is observed for FasL, and it is thought to traffic to the surface only upon T cell activation (Valk et al. 2008). Studies of CTLA-4 trafficking have demonstrated that this protein is endocytosed from the plasma membrane, targeted to its intracellular stores and then recycled back to the surface (Linsley et al. 1996, Qureshi et al. 2012). β-site amyloid precursor protein-cleaving enzyme (BACE1) is a membrane-tethered protease that cleaves the amyloid precursor protein yielding a peptide that accumulates in the brain of patients with Alzheimer disease. Similarly to CTLA-4, BACE1 transits through the constitutive secretory pathway and is then endocytosed and stored in intracellular vesicles that colocalize with endosomal compartments. Moreover, BACE1 cycles between the plasma membrane and the endocytic compartments (Huse et al. 2000). In contrast, GLUT4 and M6PR are examples of direct intracellular trafficking. GLUT4 is a surface transporter protein that allows glucose uptake by fat and muscle cells. GLUT4 is targeted to endosomes directly from the TGN and is sequestered in intracellular insulin-responsive vesicles until insulin triggers the release of these vesicles (Verhey and Birnbaum 1994, Bogan and Kandror 2010). The mannose-6-phosphate receptor (M6PR) recognizes proteins modified with M6P and transports them to early endosomes, which later deliver their cargo to lysosomes. The M6PR is directly targeted from the TGN to late endosomes after which it cycles among the Golgi, the endosomes and the plasma membrane (Johnson and Kornfeld 1992). Finally, the lysosomal protein LAMP-1 has been shown to traffic through the cell surface and endocytic

pathway as well as directly to the lysosomes from the TGN (Carlsson and Fukuda 1992).

Additionally, I showed that transfected FasL was located mainly on the surface of COS-1 cells (Figure 4.1 A), consistent with previous results in HeLa cells (Bossi and Griffiths 1999, Blott et al. 2001, Qian et al. 2006). These results favor alternatives 1 and 3, described above. The fact that FasL is targeted to the surface in these cells suggests that FasL is probably translocated to the surface via the constitutive secretory pathway and specifically internalized only in hematopoietic cells, such as CTL, that may differentially posses the necessary machinery for signal recognition and/or targeting. In contrast to the surface localization in COS-1 and HeLa cells, FasL has been shown to localize in intracellular vesicles in CTL and NK cells (Bossi and Griffiths 1999, Kojima et al. 2002, Lettau et al. 2004, He and Ostergaard 2007, Kassahn et al. 2009). The drastic difference in trafficking between these cell types may be due to the specific presence in CTL and NK cells of proteins capable of recognizing and/or executing an endocytosis signal within FasL.

FasL may be endocytosed via a wide variety of possible mechanisms. Clathrin-dependent endocytosis is considered the classical pathway. The process is initiated when adaptor proteins bind to cargo proteins and to clathrin molecules. These form coated pits that bud and pinch off the membrane with the aid of the dynamin GTPase (Mousavi et al. 2004). Examples of proteins endocytosed by clathrin-mediated pathways in CTL are CTLA-4 and TfR (Mayle et al. 2012, Qureshi et al. 2012). Non-classical pathways are sometimes referred to as lipid raft-dependent pathways because all raft-associated proteins internalize through non-clathrin pathways, and also due to their sensitivity to cholesterol depletion (Le Roy and Wrana 2005). Within this pathway several routes have been described. The receptor for TGF-β can be endocytosed into caveolar membrane vesicles (Di Guglielmo et al. 2003), the β subunit of the IL-2 receptor is internalized by a clathrin and caveolin-independent mechanism that requires dynamin and the small GTPase RhoA (Lamaze et al. 2001) and ARF6 has been proposed to have a role in the endocytosis of MHC I (Radhakrishna and

Donaldson 1997). Future studies should focus on deciphering which of these pathways is involved in FasL endocytosis.

Blott et al. reported conflicting results in an endocytosis assay similar to the one I employed (Blott et al. 2001). They claimed FasL was directly targeted to its storage vesicle rather than transiting through the surface via endocytosis. These results can be explained by the YT NK cell line used in their experiments, which has been reported to exhibit very high constitutive surface expression of FasL (Montel et al. 1995). The surface localization resembles the phenotype observed in HeLa and COS-1 cells suggesting that these cells possibly also lack the necessary proteins for the endocytosis of FasL.

Overexpression of Stx3 in CTL resulted in an increase of surface FasL expression (Figure 4.13). This result was unexpected because Stx3 is a t-SNARE and it is consequently expected to regulate the fusion of incoming vesicles with the membrane of the compartment where it resides (Jahn and Scheller 2006). Because Stx3 is located in intracellular vesicles that colocalize with FasL (Figure 3.8), I anticipated that Stx3 overexpression would enhance the intracellular localization of FasL. One possible explanation would be that Stx3 mediates the FSV localization of another unknown protein that influences FasL translocation to the surface. However, the increase of surface FasL expression in CTL overexpressing Stx3, could also be explained by a compound exocytosis mechanism, which has been shown for Stx3 before. Compound exocytosis is the process where secretory vesicles interact with each other during fusion. It may proceed sequentially where an initial first line of vesicles fuse with the plasma membrane and become the target for fusion for additional vesicles, or multiple vesicles may fuse with each other before fusing with the membrane (Pickett and Edwardson 2006). Stx3 has been shown to mediate zymogen and insulin granule-to-granule fusion, as well as compound exocytosis in acinar cells and pancreatic beta cells respectively (Hansen 1999, Zhu et al. 2013). Therefore the overexpression of exogenous Stx3 may have bypassed or surpassed the mechanism that normally inhibits Stx3 action in unstimulated cells, resulting in FSV-FSV fusion and compound exocytosis of FasL onto the surface of CTL.

These results would then constitute the first indication for a compound exocytosis mechanism of FasL surface translocation, consistent with the compound exocytosis mechanisms used for secretory vesicles with cytotoxic contents in mast cells, neutrophils and eosinophils (Alvarez de Toledo and Fernandez 1990, Lollike et al. 2002, Hafez et al. 2003). It would be of great interest to explore this possibility in the future.

One of the most surprising results from this chapter was the colocalization pattern observed for transfected DsRed-tagged FasL in CTL Clone 11 and CTLL-2. In these cells, FasL colocalized both with Stx3 and LAMP-1 (Figures 4.3 and 4.4). Transfected FasL in CTL Clone 3/4, however, behaved like the endogenous protein showing high colocalization with Stx3 and poor colocalization with LAMP-1 (Figure 4.2). These results emphasize the importance of checking the correct localization of transfected FasL and provide a possible explanation for some of the controversy in the literature regarding FasL localization, indicating that overexpressed transfected FasL is not always stored in the right vesicle. Futures studies of FasL using transfected proteins could confirm their correct trafficking by testing its colocalization with the markers I described in chapter 3.

Lastly, I suggested a role for myosin II in the surface translocation of FasL (Figure 4.16). Myosins are a family of motor proteins that associate in complexes formed by one or two heavy chains and a variable number of light chains. The heavy chains allow binding to actin filaments and movement is powered by its ATPase activity, which is regulated by the light chain components (Wang et al. 2011). The non-muscle myosin II molecule (NM II) has been shown to have several functions in immune cells: it regulates T cell motility, the establishment of the immunological synapse between T cells and APCs, and NK cell degranulation (Maravillas-Montero and Santos-Argumedo 2012). In fact, Myosin 9 (one of the heavy chains of myosin II) is attached to the surface of lytic granules in NK cells indicating a direct role in granule transport (Sanborn et al. 2009). Consistent with these studies, I found that inhibition of myosin led to a decrease in surface FasL expression after stimulation. However, because inhibition of myosin has also been

shown to reduce intracellular Ca^{++} influx (Yu et al. 2012) I cannot exclude the possibility that myosin has an indirect effect on surface FasL. In future studies it would be interesting to evaluate if myosin II interacts with the FSVs and if it does, whether it binds directly to FasL or to the vesicle membrane (Li et al. 1994).

In summary, the results presented here provide a better understanding of FasL trafficking in CTL. I showed that FasL could be detected on the surface, endocytosed and targeted to the right vesicle. I indicated that Stx3 affected FasL trafficking and I provided evidence that myosin influenced FasL translocation to the surface after stimulation. Moreover, I demonstrated that overexpression of FasL can lead to incorrect targeting in certain CTL types stressing the importance of choosing an appropriate system when studying FasL trafficking.

CHAPTER 5: Identification of FasL sequences important for trafficking in Cytotoxic T Lymphocytes

5.1. Introduction

After its synthesis FasL is transported to its storage vesicle and from there to the surface of stimulated T cells. FasL localization in non-stimulated T cells is functionally important since apoptosis-inducing molecules such as FasL must not be expressed on the surface to avoid non-specific killing. To ensure its correct localization, FasL must be efficiently sorted to the right compartment, at the right time. In this chapter I endeavored to determine the identity of the FasL sequences responsible for its trafficking.

In chapter 4 I showed that FasL was endocytosed from the plasma membrane. Sequences important for signaling endocytosis are fairly well described for the classic clathrin-mediated pathway. In this pathway, adaptor-protein complexes bind to cargo proteins and to clathrin molecules and trigger their endocytosis. The adaptor complexes, such as AP-2, can recognize three distinct endocytosis signals in the cytoplasmic tails of transmembrane proteins: NPXY, YXXØ and di-leucine-based motives (Robinson and Bonifacino 2001). However, little is known about the signals that trigger non-classical endocytosis pathways. In proteins that lack cytoplasmic tails, specific clathrin-independent pathways have been proposed to show a preference for different lipid-based microdomains within the plasma membrane (Mayor and Pagano 2007). Endocytosis of proteins with cytoplasmic tails has been shown to be dependent on various sequences and modifications. Carboxypeptidase E contains a sequence SETLNF in its cytoplasmic tail that allows interaction with the ADP-ribosylation factor (ARF) 6 and triggers endocytosis by the ARF6-regulated pathway (Arnaoutova et al. 2003). Unknown sequences in the cytoplasmic tail of the IL-2 common γ chain receptor are required for its endocytosis (Morelon and Dautry-Varsat 1998). Moreover, ubiquitination of EGFR receptors prompts its clathrin-independent endocytosis and is important in the internalization of several other

proteins (d'Azzo et al. 2005, Sigismund et al. 2005). However, FasL lacks NPXY, YXXØ, di-leucine and SETLNF sequences in its cytoplasmic tail (**Figure 5.1**), indicating that non-typical endocytosis signals may be at play to ensure FasL removal from the plasma membrane.

The targeting of proteins to specific compartments is also mediated by sorting signals within the proteins. These sequences are recognized by transport mechanisms that can mediate retention, retrieval, or targeting. Transmembrane type II proteins have a di-arginine motif for ER retention within the positions 2-5 of their amino acid sequence (Schutze et al. 1994). Proteins destined for the Golgi usually have signals for retention, to avoid constitutive secretion, and/or for retrieval and targeting from the plasma membrane. For example, furin contains a YXXQ motif that interacts with AP-2 and allows its endocytosis, and an acidic cluster containing two serine residues that after phosphorylation, signal the transport of the protein from endosomes to the TGN (van Vliet et al. 2003). Targeting to endosomes and lysosomes can be achieved by the same signals used for classical endocytosis, that is, tyrosine and di-leucine based motifs. Additionally, ubiquitination of proteins signals their targeting to late endosomes (Piper and Lehner 2011). Lysosmal proteins are usually modified by mannose-6-phosphate (M6P) moieties, which are then recognized by M6P receptors. Lysosomal targeting of these proteins is accomplished by transport of the M6P receptor, which contains a YXXØ signal (Kornfeld and Mellman 1989). As discussed in chapters 3 and 4, after endocytosis, FasL is specifically stored in a compartment of unique composition. Therefore I hypothesized that FasL must contain specific targeting sequences to direct it to its FSV.

In this chapter I show that FasL contains sequences throughout its N-terminal cytoplasmic tail important for its endocytosis, as well as a triple-tyrosine motif that mediates its efficient targeting to FSVs. Moreover, I show that glycosylation and oligomerization are important for FasL trafficking to FSVs.

Figure 5.1. Sequence of the N-terminal end of mouse FasL.

5.2. Results

5.2.1. Both the N-terminal and C-terminal ends of FasL contain important trafficking sequences

To begin the study of FasL trafficking sequences I first evaluated the trafficking phenotype of FasL chimeric constructs where either the N-terminal cytoplasmic tail or the transmembrane (TM) and C-terminal external domains had been replaced with the corresponding domains of the unrelated protein Ly49A (**Figure 5.2**). Ly49A is a type II transmembrane receptor protein expressed on the surface of NK cells (Brennan et al. 1994) that was not expressed in the CTL clones I used. The resulting DsRed-tagged chimeras were labeled as: FasL/Ly49A, which had the cytoplasmic tail of FasL and the TM and external domains of Ly49A, and Ly49A/FasL, which had the N-terminal end of Ly49A and the TM and external domains of FasL. I decided to initially use COS-1 cells to determine if the chimeric constructs were properly expressed and localized in these cells. I thus transfected COS-1 cells with DsRed-FasL/Ly49A, DsRed-Ly49A/FasL as well as with DsRed-FasL and DsRed-Ly49A as controls. I then ran post-nuclear lysates of transfected cells in an SDS-PAGE and evaluated their expression by Western Blot using an antibody specific for DsRed. I concluded that all four constructs were expressed in COS-1 cells (**Figure 5.3 A**). Moreover, surface staining of unpermeabilized transfected cells with antibodies specific for FasL or Ly49A and subsequent flow cytometry analysis, revealed a high level of surface expression of the chimeric proteins similar to the WT protein (**Figure 5.3 B**). I also studied the ability of the Ly49A/FasL chimera to induce target cell killing. For this purpose I stained L.Fas cells (which express the Fas receptor on their surface) with a fluorescent dye and then incubated them with transfected COS-1 cells at 1:4 (target : killer) ratio for 90 min at 37°C. After breaking the conjugates and permeabilizing the cells, I assessed target-cell killing by staining with antibodies specific for active caspase 3 and analyzing by flow cytometry. Control untransfected COS-1 cells induced no killing (**Figure 5.3 C**, black lines)

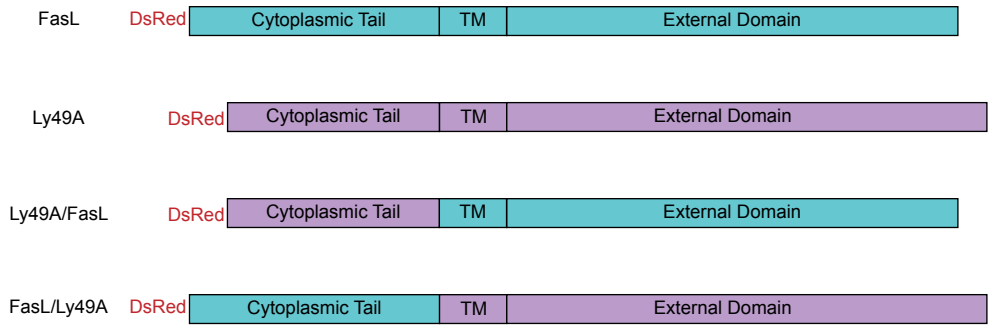

Figure 5.2. Structure of the DsRed-tagged chimeras of FasL and Ly49A.
The transmembrane (TM) and external domains of FasL were swapped for the corresponding domains of Ly49A to construct the FasL/Ly49A chimera. The cytoplasmic tail of FasL was swapped with the cytoplasmic tail of Ly49A to construct the Ly49A/FasL chimera.

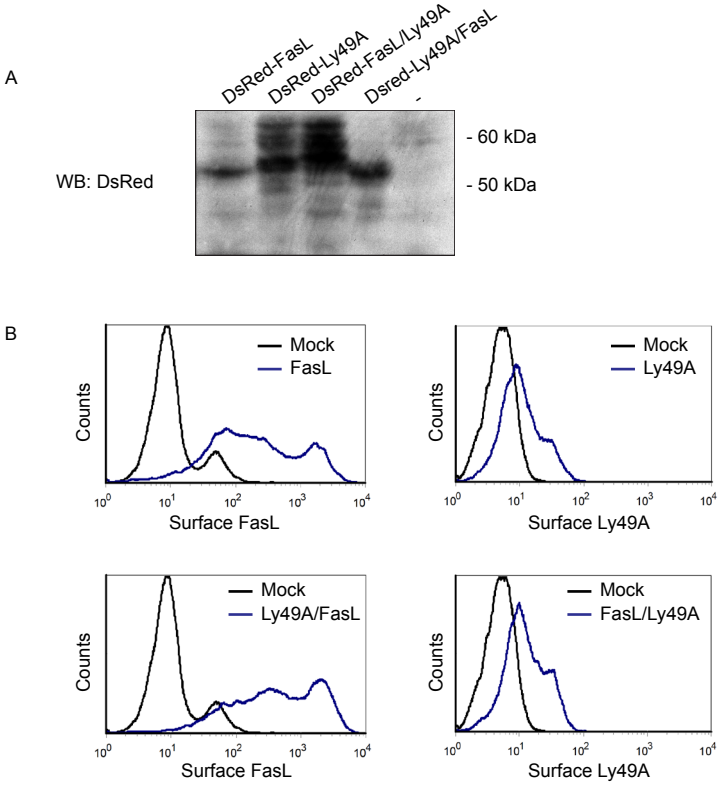
A
DsRed-FasL
DsRed-Ly49A
DsRed-FasL/Ly49A
Dsred-Ly49A/FasL
WB: DsRed
- 60 kDa
- 50 kDa
B
Mock
FasL
Counts
Surface FasL
Mock
Ly49A
Counts
Surface Ly49A
Mock
Ly49A/FasL
Counts
Surface FasL
Mock
FasL/Ly49A
Counts
Surface Ly49A

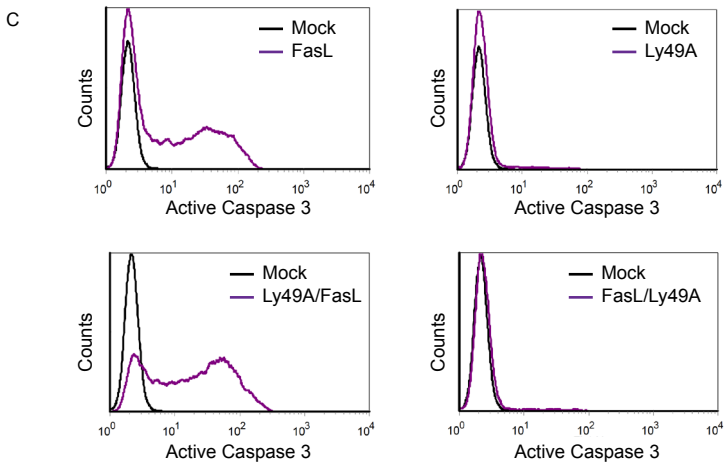

Figure 5.3. The FasL chimeras have no detectable defect in expression, localization or function in COS-1 cells.
COS-1 cells were transfected with DsRed-FasL, DsRed-Ly49A, DsRed-FasL/Ly49A or DsRed-Ly49A/FasL **(A)** Post-nuclear lysates corresponding to 1 x 10^6 transfected COS-1 cells were run in an SDS-PAGE and Western Blotting was performed using antibodies specific for DsRed. **(B)** Transfected cells were stained with antibodies specific for FasL (for DsRed-FasL and DsRed-Ly49A/FasL) or Ly49A (for DsRed-Ly49A and DsRed-FasL/Ly49A) and surface expression of the constructs was determined by flow cytometry. (C) Transfected cells were incubated for 2 hours at 37°C with previously stained L.Fas cells. After disrupting the conjugates, cells were permeabilized and stained with antibodies specific for active caspase 3. Target cell death was evaluated by flow cytometry after gating on the L.Fas population.

while FasL-transfected COS-1 cells induced a high level of active caspase 3 expression. Similarly, the Ly49A/FasL chimera also induced target cell killing (**Figure 5.3 C**). COS-1 cells transfected with the FasL/Ly49A chimera or the Ly49A protein displayed no active caspase 3 expression. Both of these constructs lack the Fas-binding motif on the C-terminal end of the FasL protein that triggers caspase 3 activation and apoptosis. In sum, the chimeric constructs had no detectable defects in expression, localization or function in COS-1 cells.

To evaluate FasL trafficking in CTL, I transfected Clone 3/4 cells with the DsRed-tagged chimeras as well as with the full-length FasL and Ly49A proteins. I then evaluated their surface expression by flow cytometry and their intracellular distribution by confocal microscopy. In chapter 4, I showed that in CTL Clone 3/4 cells, DsRed-FasL had almost no surface expression and was instead located in intracellular vesicles that colocalized with Stx3 and did not colocalize with LAMP-1 (Figure 4.2). In contrast, DsRed-Ly49A was expressed on the surface of transfected CTL (**Figure 5.4 A and B**) and showed no colocalization with the intracellular Stx3 and LAMP-1 proteins (**Figure 5.4 C and D**).

Interestingly, flow cytometry analysis using antibodies specific for the C-terminal end of Ly49A showed that the FasL/Ly49A chimera was expressed on the cell surface (**Figure 5.5 A**). Moreover, to evaluate the surface expression of the Ly49/FasL chimera, I stained transfected cells with antibodies specific for FasL and analyzed them by flow cytometry. I then compared FasL surface expression in cells transfected with Ly49A/FasL with mock-transfected cells. I assumed that both would have comparable levels of endogenous FasL expression and that the differences in surface FasL would only be due to the transfected proteins. DsRed-Ly49A/FasL was also expressed on the cell surface (**Figure 5.5 A**).

I then assessed the subcellular distribution of the chimeras by confocal microscopy and compared it with FasL WT. Unlike endogenous FasL, confocal microscopy analysis of transfected DsRed-FasL WT revealed that it was not always found in intracellular vesicles. In one of the cells analyzed, DsRed-FasL was observed on the plasma membrane as well as in intracellular vesicles within

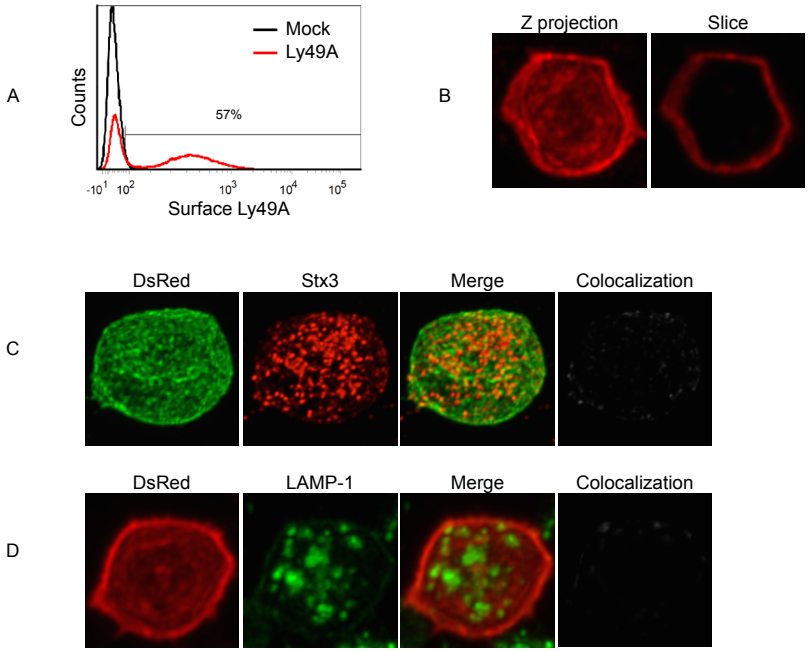

Figure 5.4. DsRed-Ly49A is located on the surface of CTL.
(A) Surface expression of Ly49A was determined by flow cytometry for cells transfected with DsRed-Ly49A (red) and compared to mock-transfected cells (black). Data is representative of 3 independent experiments. **(B)** Cells transfected with DsRed-Ly49A were stained with antibodies specific for DsRed and the corresponding secondary antibodies. Z-stack images were acquired (interval, 0.2µm) and subjected to deconvolution and three-dimensional reconstruction. Representative projection of the reconstructed image as well as a single optical slice are shown. **(C and D**) Clone 3/4 cells transfected with DsRed-Ly49A were stained with antibodies specific for DsRed and Stx3 **(C)** or DsRed and LAMP-1 **(D)**. After staining with the appropriate secondary antibodies, samples were analyzed by confocal microscopy. Z-stack images were acquired (interval, 0.2µm) and subjected to deconvolution and three-dimensional reconstruction. Representative projections of the reconstructed images are shown. Colocalization images were created displaying only the regions where the two channels colocalize. Data is representative of 6 independent experiments corresponding to 19 cells.

the same cell. I defined this phenotype as membrane + intracellular vesicles (M + IV) and I decided to score the distribution of DsRed-FasL within each analyzed cell as either: intracellular vesicles (IV), membrane (M) or M + IV. I employed these criteria for analyzing all of the FasL mutants shown in this chapter. Unlike FasL WT, which is found in intracellular vesicles in the majority (98%) of the cells analyzed, confocal microscopy analysis of the FasL/Ly49A and Ly49A/FasL chimeras indicated that these constructs were expressed on the surface as well as in intracellular vesicles within the same cell in 100% of the cells analyzed. This phenotype was drastically different from the IV phenotype and the M phenotype displayed by the majority of the cells transfected with FasL or Ly49A, respectively (**Figure 5.5 B**). This mixed distribution observed in **Figure 5.5 C** indicated that both the C-terminal and the N-terminal ends had a significant role in FasL trafficking.

To study if the transfected chimeras localized to the intracellular vesicles where endogenous FasL resides, I used the Stx3 marker for the FSV identified in chapter 3 and tested its colocalization with DsRed. Given the surface localization of these chimeras, the Manders colocalization coefficient and the intensity profiles described in chapter 3 were not as useful tools for evaluating colocalization as they were for intracellular endogenous FasL. The lack of surface Stx3 and LAMP-1 lowered overall colocalization and resulted in lower M_1 coefficients and affected intensity profiles over lines drawn across three-dimensional projections that display surface DsRed throughout the cells. Moreover, unlike endogenous FasL, the transfected DsRed-FasL proteins did not always have the same colocalization pattern with Stx3. In a few cells transfected with FasL WT, DsRed-FasL did not colocalize with Stx3 at all. I therefore decided to quantify the colocalization with Stx3 by individually assessing each transfected cell and then evaluating the trend observed for the majority of the analyzed cells. I characterized the colocalization of DsRed-FasL looking exclusively at the intracellular vesicles and using a stringent scoring system: *Complete colocalization*: all of the DsRed-FasL$^+$ vesicles are in Stx3$^+$ vesicles, *Partial colocalization*: some, but not all of the DsRed-FasL$^+$ vesicles are in Stx3$^+$

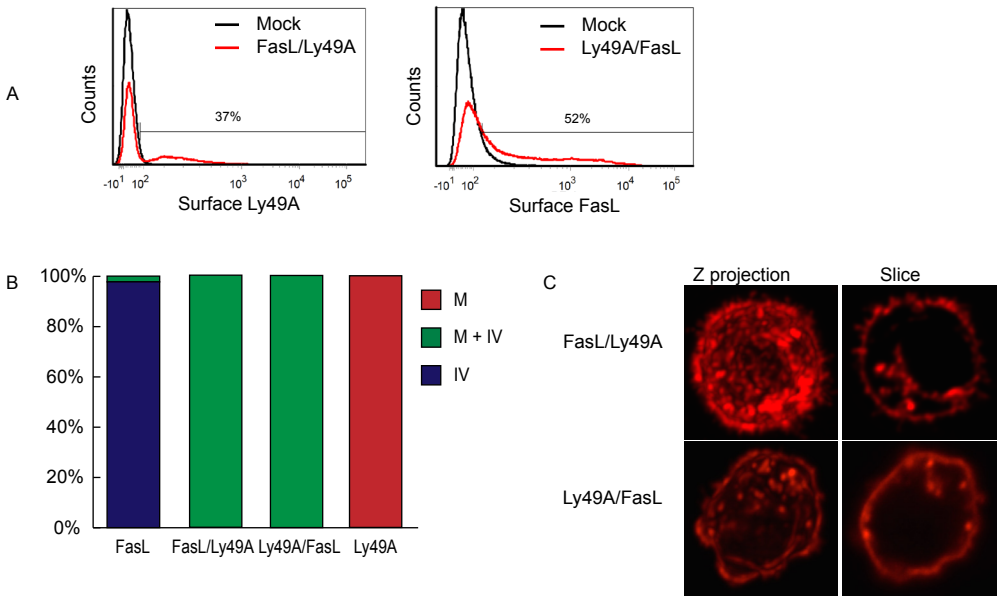

Figure 5.5. DsRed-FasL/Ly49A and DsRed-Ly49A/FasL are located on the surface and intracellular vesicles in CTL.
CTL Clone 3/4 cells were transfected with DsRed-FasL/Ly49A, DsRed-Ly49A/FasL or mock-transfected **(A)** Surface expression of Ly49A or FasL was determined by flow cytometry for cells transfected with DsRed-FasL/Ly49A or DsRed-Ly49A/FasL (red) and compared to mock-transfected cells (black). Data is representative of 3 independent experiments. **(B and C)** Cells transfected with DsRed-FasL/Ly49A or DsRed-Ly49A/FasL were stained with antibodies specific for DsRed and the corresponding secondary antibodies. Z-stack images were acquired (interval, 0.2µm) and subjected to deconvolution and three-dimensional reconstruction. **(B)** Localization was scored in 26 (for DsRed-FasL/Ly49A), 30 (for DsRed-Ly49A/FasL), 19 (for DsRed-Ly49A) and 40 (for DsRed-FasL WT) transfected cells. Scoring: Membrane (M), Intracellular Vesicles (IV) and Membrane + Intracellular Vesicles (M + IV). Further details about the scoring system can be found in section 2.15. **(C)** Representative projections of the reconstructed images as well as a single optical slice are shown.

vesicles, *No colocalization*: none of the DsRed-FasL$^+$ vesicles are in Stx3$^+$ vesicles (**Figure 5.6 A**). Although I performed the characterization using three-dimensional reconstructed images, examples of the corresponding Z-projection images corresponding to each of the three scoring phenotypes are shown in **Figure 5.6 B**. I applied these criteria for the colocalization analysis with Stx3 and LAMP-1 for all the FasL constructs in this chapter.

Analysis of Clone 3/4 cells stained for DsRed and Stx3 indicated that in 100% of the transfected cells, the FasL/Ly49A chimera exhibited no colocalization with Stx3 and that Ly49A/FasL did not colocalize with Stx3 in 81% of the cells (**Figure 5.7 A**). Confocal microscopy analysis of Clone 3/4 cells stained for DsRed and LAMP-1 showed that in 91% of the cells, DsRed-FasL/Ly49A had no colocalization with the cytolytic granule marker LAMP-1 either. However, the intracellular vesicles containing DsRed had either complete or partial colocalization with LAMP-1 in 89% of the cells transfected with DsRed-Ly49A/FasL (**Figure 5.7 B**). Representative examples of the cells analyzed for colocalization with Stx3 or LAMP-1 are shown in **Figure 5.7 C and D** respectively.

In summary, FasL/Ly49A was found on the surface and in Stx3$^-$ LAMP-1$^-$ vesicles and Ly49A/FasL can be found on the surface and in intracellular Stx3$^-$ LAMP-1$^+$ vesicles in CTL. These results suggest that both the C-terminal and the N-terminal ends of FasL contain important sequences that allow for the correct and efficient targeting of FasL to its intracellular Stx3$^+$ LAMP-1$^-$ FSV. Moreover, comparison of the results from the two chimeras, that had an aberrant but different phenotype, indicates that although both the external and the internal domains contain important sequences, they may have different functions in the trafficking of FasL.

I also intended to evaluate the effect of the chimeras on FasL translocation to the surface in transfected stimulated cells. Unfortunately, because the chimeras are expressed on the surface in non-stimulated cells, defects in translocation after stimulation would not be detectable.

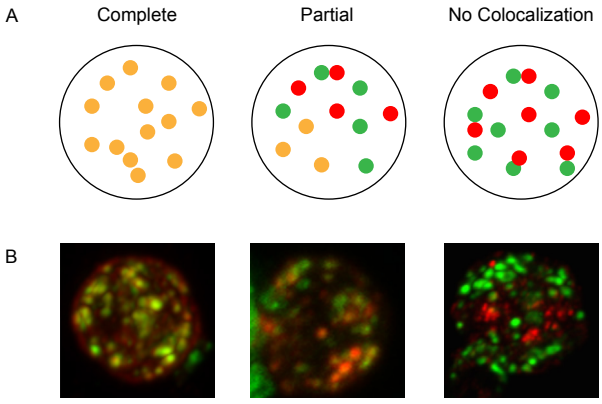

Figure 5.6. Colocalization scoring criteria.
(A) Colocalization with the different markers (Stx3 and LAMP-1) was characterized as *Complete colocalization*: all of the DsRed-FasL^{+} vesicles are in marker^{+} vesicles, *Partial colocalization*: some, but not all of the DsRed-FasL^{+} vesicles are in marker^{+} vesicles and *No colocalization*: nine of the DsRed-FasL^{+} vesicles are in marker^{+} vesicles. Further details are explained in section 2.15 **(B)** Examples for each of the colocalization phenotypes. *Complete*: Z-projection image corresponding to cells transfected with DsRed-FasL Δ3K and stained with DsRed (red) and LAMP-1 (green). *Partial*: Z-projection image corresponding to cells transfected with DsRed-FasL ΔSA and stained with DsRed (green) and Stx3 (red). *No colocalization*: Z-projection image corresponding to cells transfected with DsRed-FasL N117Q and stained with DsRed (red) and LAMP-1 (green).

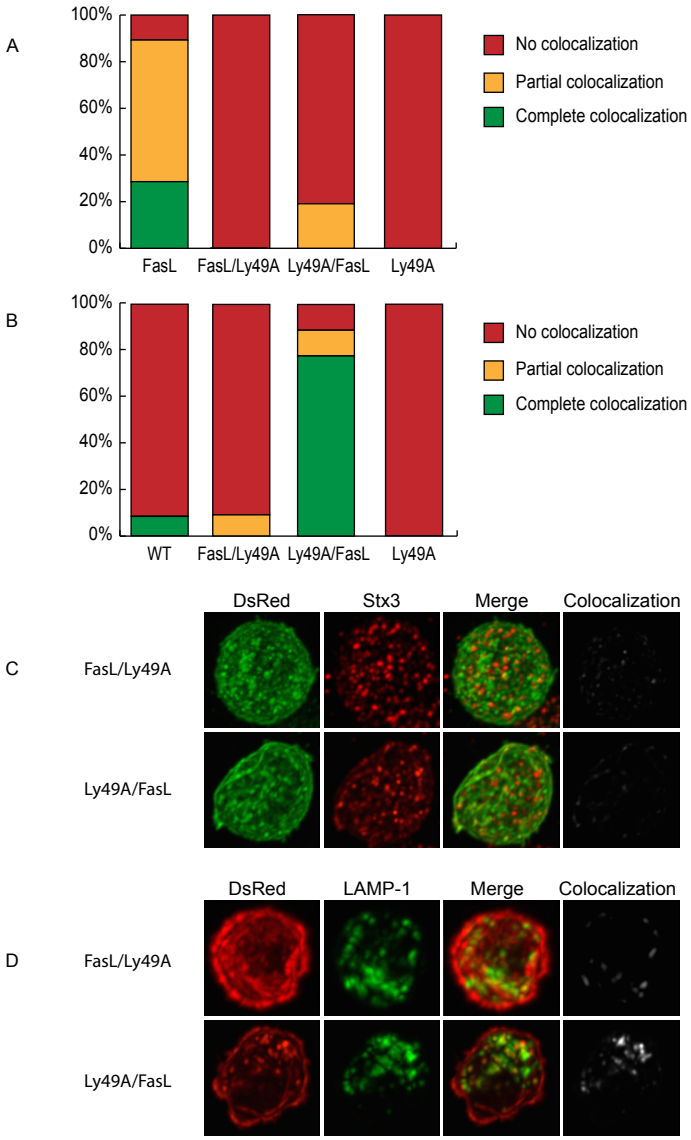

Figure 5.7. Intracellular DsRed-FasL/Ly49A is located in Stx3$^-$ LAMP-1$^-$ vesicles and DsRed-Ly49A/FasL is located in Stx3$^-$ LAMP-1$^+$ vesicles.
CTL Clone 3/4 cells transfected with DsRed-FasL/Ly49A and DsRed-Ly49A/FasL were stained with antibodies specific for DsRed and Stx3 **(A and C**) or LAMP-1 **(B and D)** and the corresponding secondary antibodies. Z-stack images were acquired (interval, 0.2μm) and subjected to deconvolution and three-dimensional reconstruction. **(A and B)** Colocalization was scored using the criteria depicted in Figure 5.6 using 12 (for Stx3) and 28 (for LAMP-1) cells transfected with DsRed-FasL, 15 (for Stx3) and 11 (for LAMP-1) cells transfected with DsRed-FasL/Ly49A, 21 (for Stx3) and 9 (for LAMP-1) cells transfected with DsRed-Ly49A/FasL and 9 (for Stx3) and 10 (for LAMP-1) cells transfected with DsRed-Ly49A. **(C and D)**. Representative projections of the reconstructed images for the majority colocalization phenotypes are shown.

5.2.2. The self-assembly domain is necessary for translocation after stimulation

Having shown that both the cytoplasmic and external domains of FasL contained important sequences for targeting FasL to its FSV, I attempted to identify specific sequences within these domains that contributed to FasL trafficking. I initially focused on the C-terminal end of FasL, specifically in its self-assembly (SA) domain and the N-glycosylation sites as moieties of potential relevance to trafficking. I thus decided to evaluate FasL trafficking using FasL mutant constructs with specific mutations in these regions (**Figure 5.8**).

The SA domain of human FasL was shown to be required for trimerization and cell-death induction (Orlinick et al. 1997a, Holler et al. 2003). However, whether trimerization is only needed for cell death signaling or if it also contributes to FasL trafficking has not been determined yet. I therefore transfected a deletion mutant of FasL that lacks the SA domain into CTL Clone 3/4 cells to study the effect of the SA domain on FasL trafficking. I stained transfected cells with antibodies specific for FasL and determined surface expression of the DsRed-FasL ΔSA construct with respect to mock-transfected cells. Flow cytometry analysis revealed almost no detectable surface expression (**Figure 5.9 A**) and no significant difference with the surface expression of FasL WT (**Figure 5.9 B**). Consistently, confocal microscopy analysis showed DsRed-FasL ΔSA was localized in intracellular vesicles (**Figure 5.9 C**) in 95% of the analyzed cells. This localization phenotype was comparable to the localization of FasL WT (**Figure 5.9 D**) and suggested the deletion had no effect on the localization of FasL. To evaluate if FasL ΔSA trafficked to the intracellular vesicles that harbor endogenous FasL, I analyzed the colocalization of DsRed-FasL ΔSA in CTL Clone 3/4 cells stained with antibodies specific for DsRed and Stx3 or LAMP-1, and compared it to the colocalization with Stx3 and LAMP-1 of DsRed-FasL WT. Similarly to FasL WT, the majority of the cells transfected with FasL ΔSA (92%) had either complete or partial colocalization with Stx3 (**Figure 5.9 E**). Also comparably to FasL WT, none of the cells transfected with FasL ΔSA exhibited

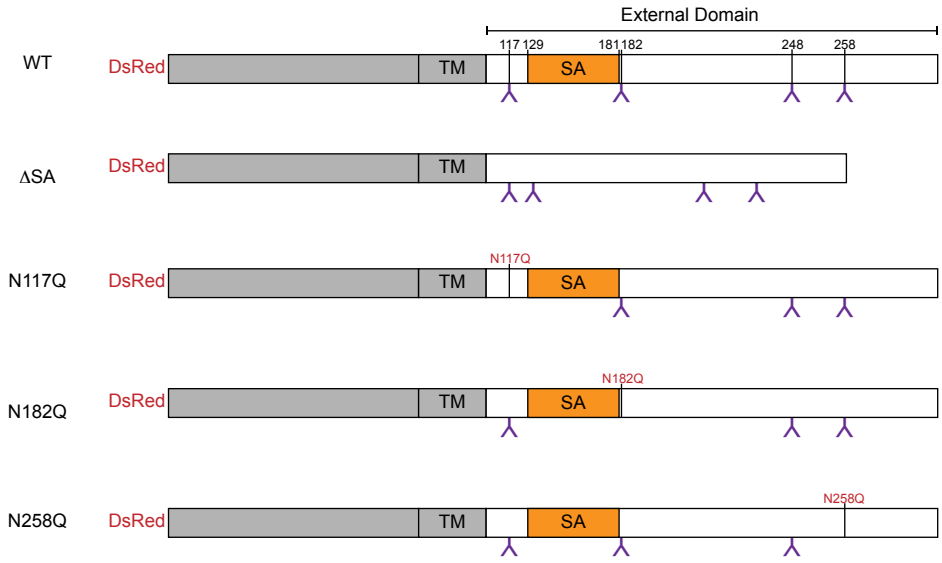

Figure 5.8. Structure of the DsRed-tagged FasL C-terminal mutant constructs.
The self-assembly (SA) domain was deleted to construct DsRed-FasL ΔSA. Point mutations replaced asparagines 117, 182 and 258 for glutamine to construct DsRed-FasL N117Q, DsRed-FasL N182Q and DsRed-FasL N1258Q.

colocalization with LAMP-1 (**Figure 5.9 F**). Examples of the colocalization analysis of DsRed-FasL ΔSA with Stx3 and LAMP-1 are shown in **Figures 5.9 G and H**, representing the colocalization phenotype displayed by the majority of the analyzed cells. In conclusion, DsRed-FasL ΔSA was found in intracellular $Stx3^{+}$ $LAMP\text{-}1^{-}$ vesicles. The sum of these results indicates the SA domain has no effect on the trafficking of FasL to its intracellular vesicle.

After 10-15 min of stimulation, pre-synthesized stored FasL is translocated to the surface of CTL (He and Ostergaard 2007). I therefore tested if transfected FasL WT and ΔSA also trafficked to the surface after stimulation. I stimulated transfected Clone 3/4 cells with PMA and ionomycin for 15 min and I analyzed the subcellular distribution of FasL by confocal microscopy with antibodies specific for DsRed. Three-dimensional reconstruction of Z stacks and subsequent Z projections of transfected cells showed that FasL WT is found on the surface as well as in intracellular vesicles (**Figure 5.10 A**). While the majority of the analyzed non-stimulated cells displayed FasL in intracellular vesicles, after stimulation, in 85% of the analyzed cells, FasL molecules were translocated to the surface (**Figure 5.10 B**). Interestingly, however, DsRed-FasL ΔSA was found in intracellular vesicles in stimulated cells (**Figure 5.10 C**) in 92% of the cells analyzed, displaying a similar phenotype to that of non-stimulated cells (**Figure 5.10 D**). In conclusion, even though the translocation of intracellular DsRed-FasL to the surface after stimulation could be detected by confocal microscopy, DsRed-FasL ΔSA could not be detected on the surface after stimulation. These results suggest that the SA domain is required for the efficient translocation of FasL to the surface after stimulation. However, I cannot exclude the possibility that the deletion may prevent the stable surface expression of FasL.

5.2.3. Glycosylation is important for FasL trafficking

Glycosylation has been shown to be important in the trafficking of several apical proteins in epithelial cells (Vagin et al. 2009), in the trafficking to lysosomes of the protein CLN5 in neurons (Moharir et al. 2013) and in the

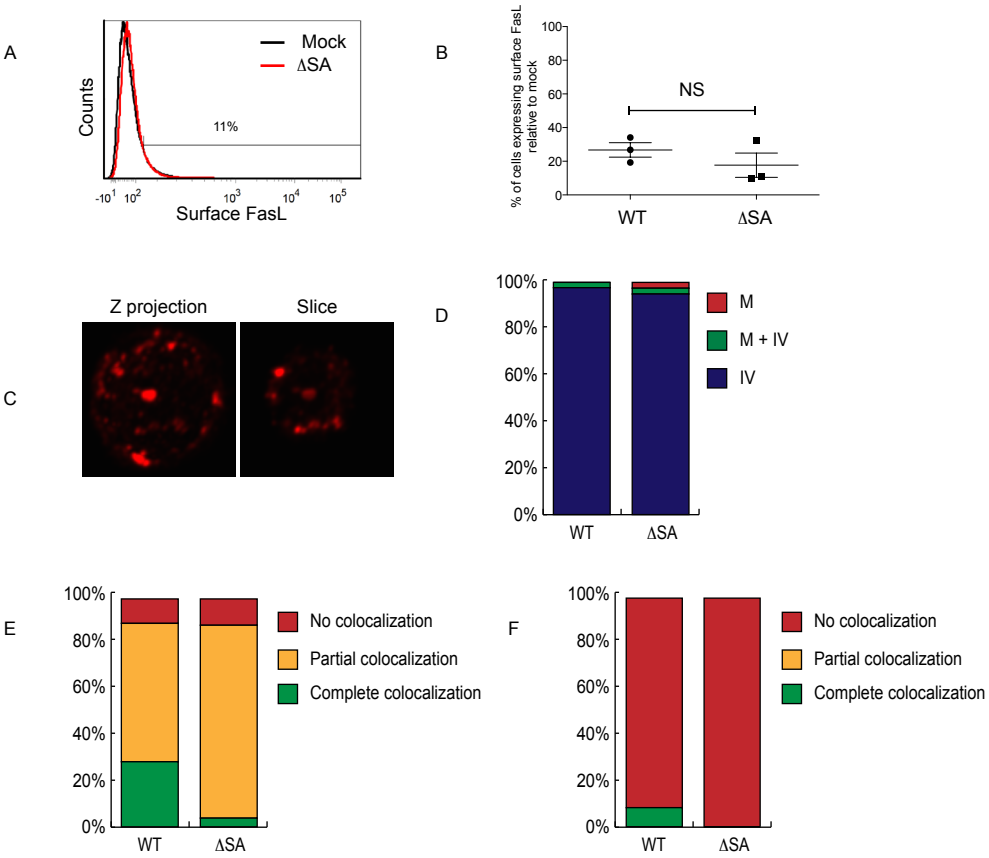
A
Mock
ΔSA
Counts
11%
Surface FasL
B
% of cells expressing surface FasL relative to mock
NS
WT
ΔSA
C
Z projection
Slice
D
M
M + IV
IV
WT
ΔSA
E
No colocalization
Partial colocalization
Complete colocalization
WT
ΔSA
F
No colocalization
Partial colocalization
Complete colocalization
WT
ΔSA

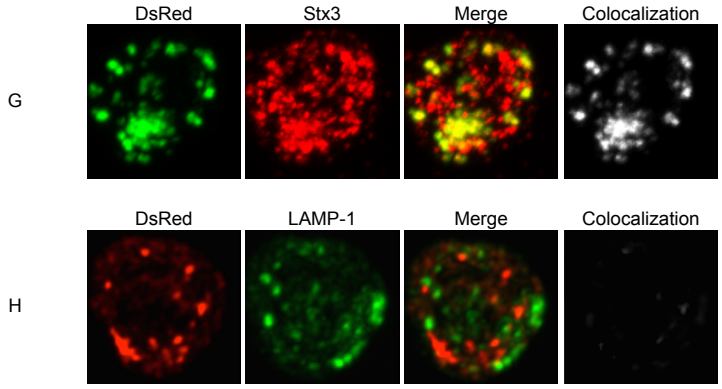

Figure 5.9. DsRed-FasL ΔSA is located in intracellular Stx3$^+$ LAMP-1$^-$ vesicles.
(A) Surface FasL expression was determined by flow cytometry for cells transfected with DsRed-FasL ΔSA (red) and compared to mock-transfected cells (black). **(B)** The percentage of cells expressing surface FasL relative to mock-transfected cells was graphed and compared to cells transfected with DsRed-FasL WT. Mean and standard error bars are indicated for each group. The unpaired Students *t*-test was used with significance set at a p value ≤ 0.05 where NS indicates not significant. **(C and D)** Cells transfected with DsRed-FasL ΔSA were stained with antibodies specific for DsRed and the corresponding secondary antibodies. Z-stack images were acquired (interval, 0.2μm) and subjected to deconvolution and three-dimensional reconstruction. **(C)** Representative projections of the reconstructed images as well as a single optical slice are shown. **(D)** Localization was scored in 38 (for DsRed-FasL ΔSA) and 40 (for DsRed-FasL WT) transfected cells. Scoring: Membrane (M), Intracellular Vesicles (IV) and Membrane + Intracellular Vesicles (M + IV). Further details about the scoring system can be found in section 2.15. **(E-H)** CTL Clone 3/4 cells transfected with DsRed-FasL ΔSA were stained with Rfor DsRed and Stx3 **(E and G**) or LAMP-1 **(F and H)** and the corresponding secondary antibodies. Colocalization was scored using the criteria depicted in Figure 5.6 using 12 (for Stx3) and 28 (for LAMP-1) cells transfected with DsRed-FasL, and 12 (for Stx3) and 26 (for LAMP-1) cells transfected with DsRed-FasL ΔSA. **(G and H)**. Representative projections of the reconstructed images for the majority colocalization phenotypes are shown.

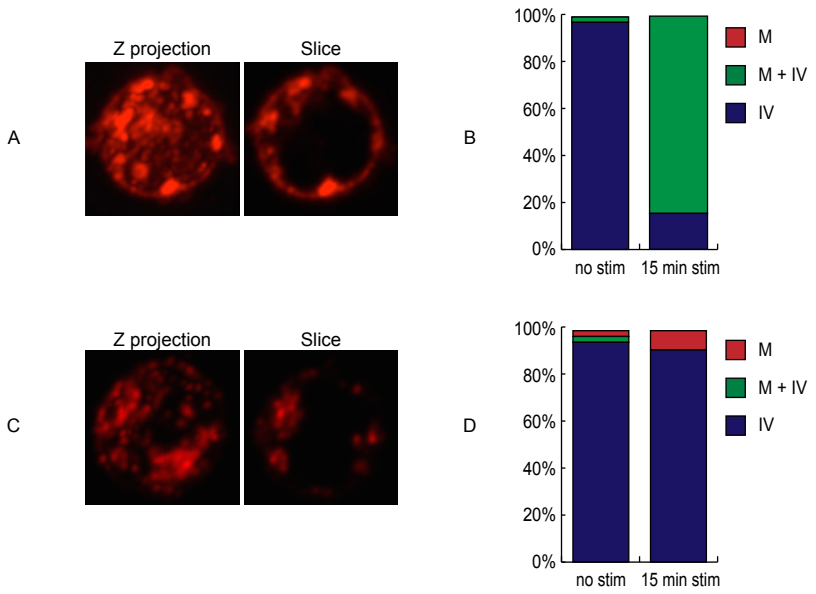

Figure 5.10. DsRed-FasL ΔSA is not translocated to the surface after stimulation.
CTL Clone 3/4 cells were transfected with DsRed-FasL **(A and B)** or DsRed-FasL ΔSA **(C and D)** and stimulated with PMA and Ionomycin for 2 hours. Transfected cells were stained with antibodies specific for DsRed and the corresponding secondary antibodies. Z-stack images were acquired (interval, 0.2μm) and subjected to deconvolution and three-dimensional reconstruction. **(A and C)** Representative projections of the reconstructed images as well as a single optical slice are shown. **(B and D)** Localization in stimulated cells was scored in 12 (for DsRed-FasL ΔSA) and 13 (for DsRed-FasL WT) transfected cells. Scoring: Membrane (M), Intracellular Vesicles (IV) and Membrane + Intracellular Vesicles (M + IV). Further details about the scoring system can be found in section 2.15.

transport of the glucose transporter GLUT4 (Haga et al. 2011) to its intracellular storage vesicle, among others. I therefore hypothesized that glycosylation of FasL would be important in its trafficking to FSVs. To test this hypothesis I used FasL constructs with point mutations in three of the four putative sites for glycosylation in which asparagine residues were replaced for structurally similar glutamine residues that are not glycosylated (Figure 5.8). I transfected the mutated FasL constructs into CTL Clone 3/4 cells and evaluated their surface expression and intracellular distribution.

I stained transfected cells with antibodies specific for FasL and determined surface expression of the DsRed-FasL N117Q, N182Q and N258Q constructs with respect to mock-transfected cells. Flow cytometry analysis revealed low surface expression for FasL N182Q and N258Q but high frequency of FasL surface expression in cells transfected with FasL N182Q (**Figure 5.11 A**). Analysis of the percentage of cells expressing surface FasL after transfection indicated there was no significant difference in the proportion of cells expressing surface FasL N117Q and N258Q but a statistically significant increase in cells transfected with FasL N182Q compared to cells transfected with FasL WT (**Figure 5.11 B**). Consistent with these findings, confocal microscopy analysis of transfected cells stained with DsRed antibodies showed that DsRed-FasL N117Q was localized in intracellular vesicles in 91% of the analyzed cells and that FasL N258Q is stored in intracellular vesicles in all the analyzed cells (**Figure 5.11 C**). These localization phenotypes were comparable to the localization of FasL WT (**Figure 5.11 D**). Interestingly, however, confocal microscopy analysis of cells transfected with FasL N182Q and stained for DsRed showed that the mutant proteins were found simultaneously in intracellular vesicles and on the cell surface (**Figure 5.11 C**). This mixed phenotype was observed for 76% of the analyzed cells and was drastically different from the IV phenotype of FasL WT (**Figure 5.11 D**). These results indicated that FasL N182Q accumulated on the surface. However, some FasL molecules were still transported to intracellular vesicles.

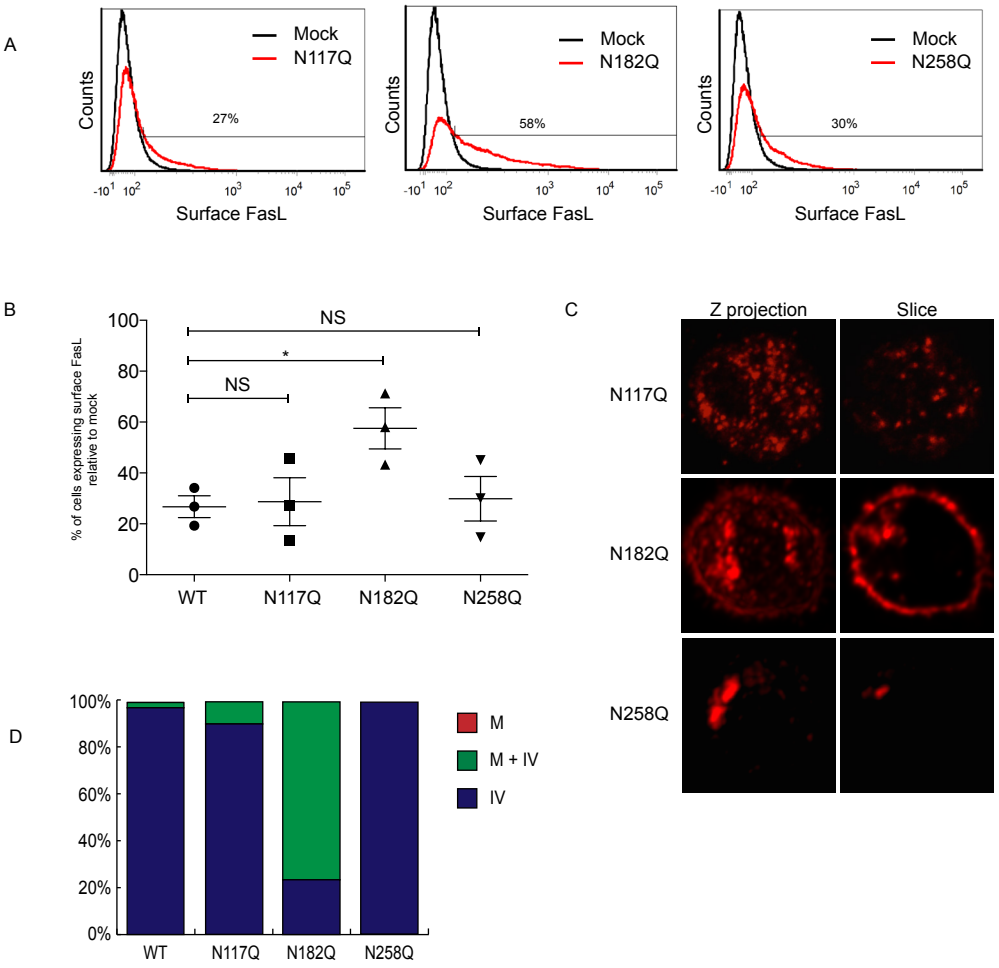

Figure 5.11. DsRed-FasL N117Q and N258Q are in intracellular vesicles while DsRed-FasL N182Q is located on the surface and intracellular vesicles. **(A)** Surface FasL expression was determined by flow cytometry for cells transfected with DsRed-FasL N117Q, N182Q and N258Q (red) and compared to mock-transfected cells (black). **(B)** The percentage of cells expressing surface FasL relative to mock-transfected cells was graphed and compared to cells transfected with DsRed-FasL WT. Mean and standard error bars are indicated for each group. The unpaired Students *t*-test was used with significance set at a *p* value ≤ 0.05 where NS means not significant and * indicates $p < 0.05$. **(C and D)** Cells transfected with DsRed-FasL N117Q, N182Q and N258Q were stained with antibodies specific for DsRed and the corresponding secondary antibodies. Z-stack images were acquired (interval, 0.2µm) and subjected to deconvolution and three-dimensional reconstruction. **(C)** Representative projections of the reconstructed images as well as a single optical slice are shown. **(D)** Localization was scored in 21 (for DsRed-FasL N117Q), 29 (for DsRed-FasL N182Q), 33 (for DsRed-FasL N258Q) and 40 (for DsRed-FasL WT) transfected cells. Scoring: Membrane (M), Intracellular Vesicles (IV) and Membrane + Intracellular Vesicles (M + IV). Further details about the scoring system can be found in section 2.15.

To evaluate if the mutations affected the localization of FasL to the endogenous FSVs, I analyzed the colocalization of $DsRed^+$ vesicles with Stx3 and LAMP-1 in cells transfected with DsRed-FasL N117Q, N182Q and N258Q. All of the analyzed cells transfected with FasL N117Q exhibited either complete or partial colocalization with Stx3, similar to FasL WT. Similarly, in 91% of the transfected cells analyzed for colocalization with Stx3, DsRed-FasL N258Q displayed partial colocalization with Stx3. In contrast, 90% of the cells analyzed for colocalization with Stx3 showed that intracellular DsRed-FasL N182Q was not localized in $Stx3^+$ vesicles (**Figure 5.12 A**). After performing the confocal microscopy colocalization analysis with LAMP-1, I determined that, like FasL WT, 90% and 86% of the analyzed cells transfected with FasL N117Q and N128Q respectively, had no colocalization with LAMP-1. Conversely, in 90% of the cells analyzed for colocalization with LAMP-1, intracellular FasL N182Q had either complete or partial colocalization with LAMP-1 (**Figure 5.12 B**). The most prevalent colocalization phenotypes are shown in **Figures 5.12 C and D.** These results suggested glycosylation in asparagines 117 and 258 was not important for FasL trafficking to the FSV in CTL. However, I concluded that glycosylation in arginine 182 was important for FasL trafficking. In chapter 4 I showed that FasL was endocytosed from the surface, therefore, the surface accumulation observed by flow cytometry and confocal microscopy could result from deficient endocytosis from the plasma membrane, suggesting glycosylation in N182 may be important for efficient endocytosis. Additionally, mutant FasL molecules could be detected in intracellular vesicles different from the FSV. These results indicate that glycosylation in N182 may also affect the targeting to FSVs.

Previous results from our laboratory had indicated that FasL is differentially modified in CTL clones and COS-1 cells, as evidenced from different electrophoretic mobilities in SDS-PAGE (He and Ostergaard, unpublished results). Because differences in protein glycosylation could account for differences in electrophoretic mobilities and would be interesting candidates to explain the differences observed in FasL trafficking in CTL and COS-1 cells (discussed in chapter 4), I decided to study the localization of the different

A

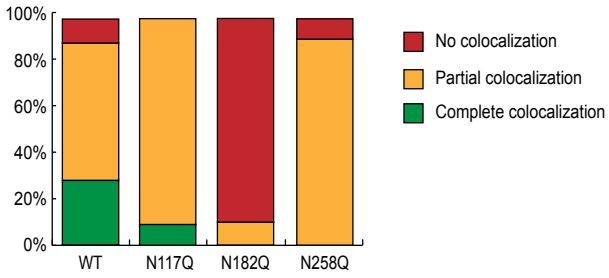
100%
80%
60%
40%
20%
0%
WT
N117Q
N182Q
N258Q
No colocalization
Partial colocalization
Complete colocalization

B

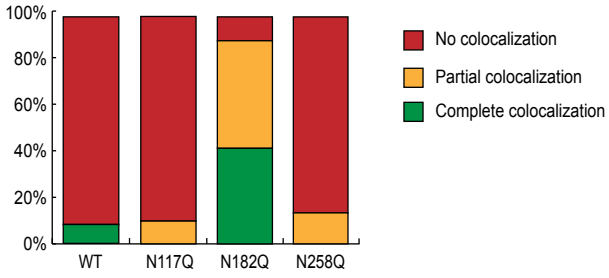
100%
80%
60%
40%
20%
0%
WT
N117Q
N182Q
N258Q
No colocalization
Partial colocalization
Complete colocalization

C

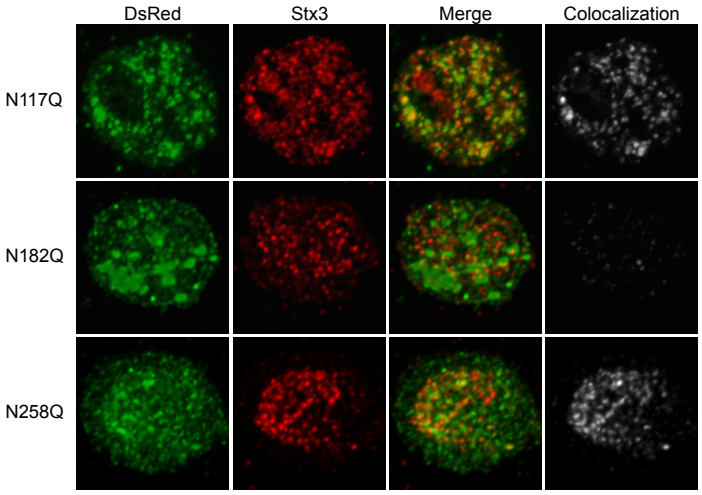
DsRed
Stx3
Merge
Colocalization
N117Q
N182Q
N258Q

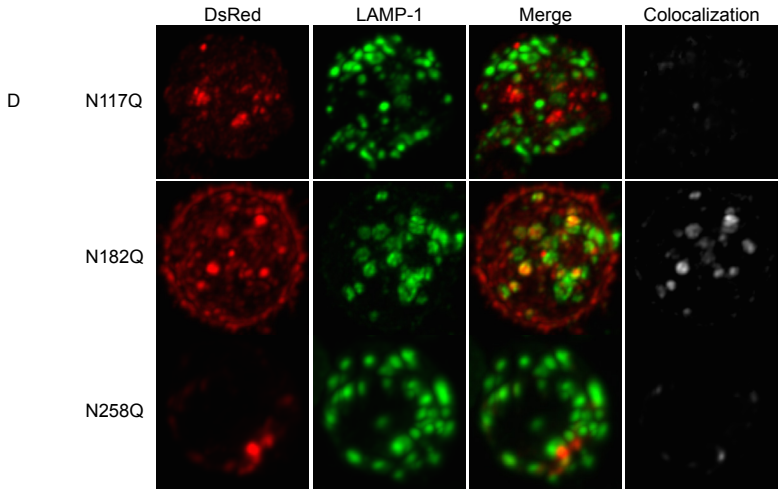

Figure 5.12. DsRed-FasL N117Q and N258Q are in Stx3^{+} LAMP-1^{-} vesicles while intracellular DsRed-FasL N182Q is located in Stx3^{-} LAMP-1^{+} vesicles. CTL Clone 3/4 cells transfected with DsRed-FasL N117Q, N182Q and N258Q were stained with antibodies specific for DsRed and Stx3 **(A and C**) or LAMP-1 **(B and D)** and the corresponding secondary antibodies. Z-stack images were acquired (interval, 0.2μm) and subjected to deconvolution and three-dimensional reconstruction. **(A and B)** Colocalization was scored using the criteria depicted in Figure 5.6 using 12 (for Stx3) and 28 (for LAMP-1) cells transfected with DsRed-FasL, 11 (for Stx3) and 10 (for LAMP-1) cells transfected with DsRed-FasL N117Q, 10 (for Stx3) and 19 (for LAMP-1) cells transfected with DsRed-FasL N182Q and 11 (for Stx3) and 22 (for LAMP-1) cells transfected with DsRed-FasL N258Q. **(C and D)** Representative projections of the reconstructed images for the majority colocalization phenotypes are shown.

glycosylation mutants in COS-1 cells. I stained transfected cells with antibodies for FasL and determined surface expression by flow cytometry analysis. As shown in chapter 4, FasL WT was expressed at a high frequency on the surface of COS-1 cells. Although FasL N117Q and FasL N182Q had high and comparable expression, FasL N258Q was expressed on the surface of a lower percentage of cells (**Figure 5.13 A**). Analysis of the percentage of cells expressing surface FasL relative to WT indicated that the decrease in surface expression of FasL N258Q was statistically significant (**Figure 5.13 B**). To exclude the possibility that this construct may not be stably expressed in COS-1 cells, post-nuclear lysates from COS-1 cells transfected with DsRed-FasL WT, DsRed-FasL N117Q, DsRed-FasL N182Q, DsRed-FasL N258Q and untransfected controls were immunoprecipitated with antibodies against DsRed and run with lysate controls in an SDS-PAGE. Western Blot analysis with antibodies specific for FasL showed that all of the FasL constructs were comparably expressed in COS-1 cells (**Figure 5.13 C**). In sum, these results indicate glycosylation in arginine 258 is important for trafficking in COS-1 cells. Interestingly, glycosylation at this site had no detectable effect in CTL (Figure 5.11 and 5.12) supporting the importance of differential glycosylation for FasL trafficking in different cells.

5.2.4. N-terminal domain of FasL is important for endocytosis and targeting to FSVs in CTL

While DsRed-FasL was found in intracellular vesicles, and DsRed-Ly49A was found on the surface, the DsRed-Ly49A/FasL chimera was found to localize both in the membrane and in intracellular vesicles (Figure 5.5), indicating that the N-terminal end of FasL contained important sequences that directed its trafficking. I therefore decided to study the contribution of the N-terminal end to the trafficking of FasL using deletion mutants that lacked the N-terminal end of the cytoplasmic tail (Δ2-43), the proline-rich domain (ΔPRD) or three lysines near the transmembrane domain (Δ3K) (**Figure 5.14**). I transfected CTL Clone 3/4 cells with the FasL N-terminal deletion mutant constructs and stained them with

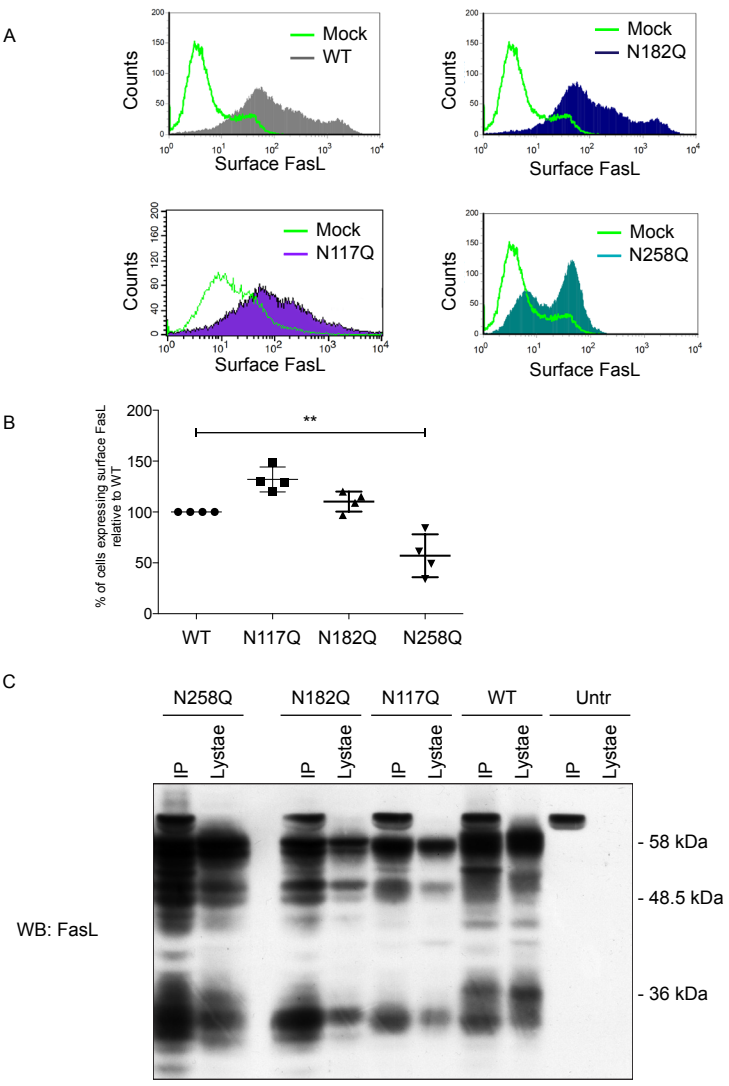

Figure 5.13. Glycosylation in N258 affects FasL surface expression in COS-1 cells.

COS-1 cells were transfected with DsRed-FasL, DsRed-FasL N117Q, DsRed-FasL N182Q and DsRed-FasL N258Q. **(A)** Transfected cells were stained with antibodies specific for FasL. Surface expression was determined by flow cytometry and compared to the expression on mock-transfected cells (green lines). **(B)** The percentage of cells expressing surface FasL relative to WT was graphed and compared to DsRed-FasL WT. Mean and standard error bars are indicated for each group. The unpaired Students *t*-test was used with significance set at a p value $\leq$ 0.05 where ** indicates $p < 0.01$. Data is representative of at least three independent experiments. **(C)** Post-nuclear lysates corresponding to 1 x 10^6 transfected (and untransfected) COS-1 cells were immunoprecipitated with antibodies specific for DsRed and run in an SDS-PAGE. Western Blotting was performed using antibodies specific for DsRed. *Colleen Reid contributed to the collection of data in this figure.*

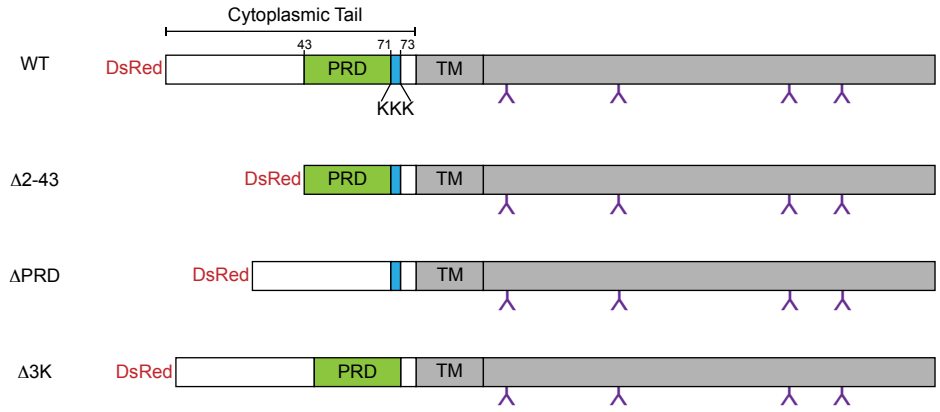

Figure 5.14. Structure of the DsRed-tagged FasL N-terminal deletion mutant constructs.
The proline-rich domain (PRD) domain was deleted to construct DsRed-FasL ΔPRD, residues 2-43 were deleted to construct DsRed-FasL Δ2-43 and lysines 71, 72 and 73 were deleted to construct DsRed-FasL Δ3K.

antibodies specific for FasL. Flow cytometry analysis of their surface expression showed that all three constructs exhibited high frequency of surface expression (**Figure 5.15 A**). Comparison of the percentage of cells expressing surface FasL relative to mock-transfected cells indicated surface expression of the N-terminal mutant proteins was significantly higher compared to the surface expression of FasL WT (**Figure 5.15 B**). Additionally, I examined their subcellular distribution in CTL Clone 3/4 cells by confocal microscopy. The single-plane slice images emphasize the membrane localization displayed by all three deletion mutants (**Figure 5.15 C**). In contrast to FasL WT, analysis of FasL localization in cells transfected with the Δ2-43, ΔPRD or Δ3K constructs, revealed that DsRed-FasL was found on the membrane as well as in intracellular vesicles within the majority of the analyzed cells (**Figure 5.15 D**). In summary, these results indicated that all of the tested deletions in the N-terminal end of FasL result in surface accumulation of FasL. This surface accumulation is indicative of inefficient surface endocytosis suggesting the cytoplasmic tail of FasL contains important sequences for FasL endocytosis.

However, microscopy images also showed that some FasL molecules did become internalized, and localized to intracellular vesicles. To determine whether the mutations had an effect on the correct targeting of those FasL proteins, I stained transfected cells with antibodies specific for DsRed and Stx3 and tested the colocalization of DsRed-FasL with Stx3 by confocal microscopy. Similarly to FasL WT, the majority of the cells transfected with FasL Δ2-43 or FasL ΔPRD exhibited either a complete or partial colocalization of their intracellular $DsRed^{+}$ vesicles with Stx3. However, 75% of the cells transfected with FasL Δ3K showed no colocalization of DsRed with Stx3 (**Figure 5.16 A**). This can be observed in the example images in **Figure 5.16 B** where the partial colocalization of FasL Δ2-43 and ΔPRD, and the poor colocalization of FasL Δ3K with Stx3 are represented. From these experiments I concluded that FasL Δ3K was not targeted to the right vesicle. To determine whether it was directed to lysosomal granules I stained Clone 3/4 cells transfected with FasL Δ2-43, FasL ΔPRD or FasL Δ3K with antibodies specific for DsRed and LAMP-1 and analyzed their colocalization by

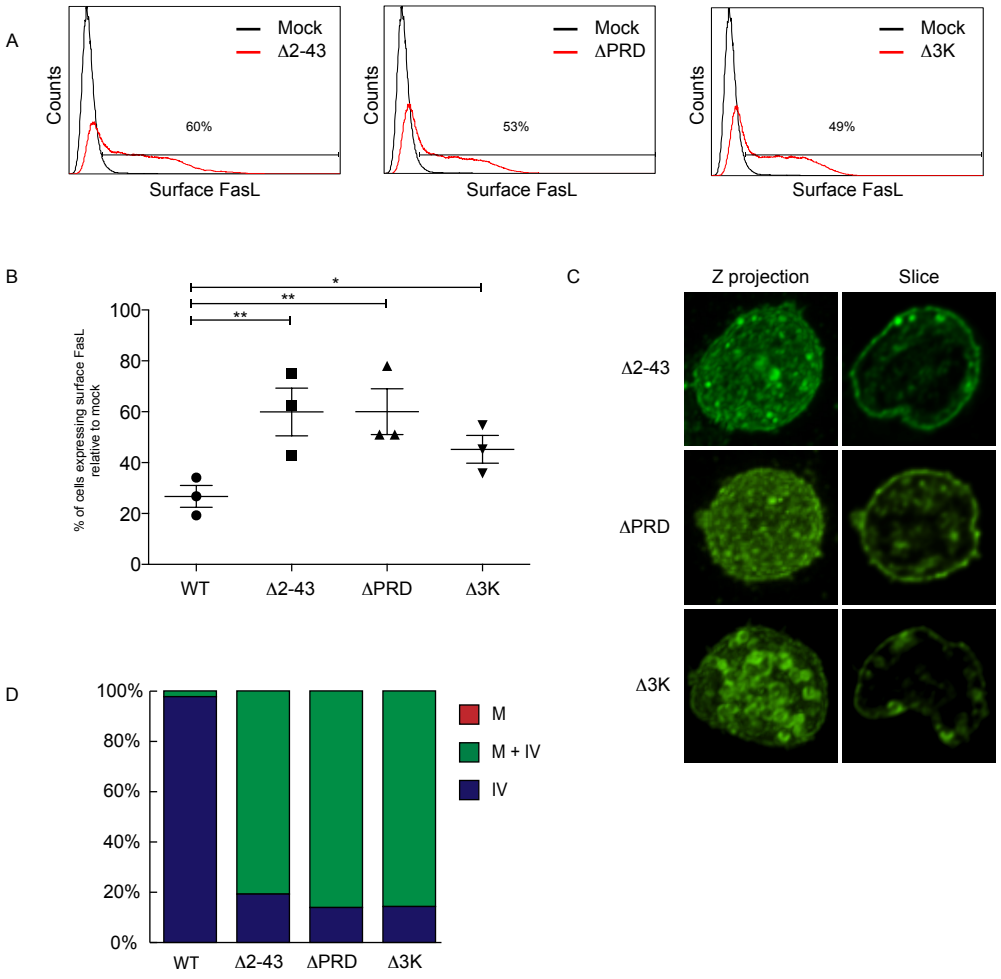

Figure 5.15. DsRed-FasL Δ2-43, ΔPRD, and Δ3K are located on the surface and intracellular vesicles in CTL.

CTL Clone 3/4 cells were transfected with DsRed-FasL Δ2-43, ΔPRD and Δ3K or mock-transfected **(A)** Surface expression of transfected cells was determined by flow cytometry (red) and compared to mock-transfected cells (black). **(B)** The percentage of cells expressing surface FasL relative to mock-transfected cells was graphed and compared to cells transfected with DsRed-FasL WT. Mean and standard error bars are indicated for each group. The unpaired Students *t*-test was used with significance set at a p value $\leq$ 0.05 where * indicates $p < 0.05$ and ** indicates $p < 0.01$. **(C and D)** Transfected cells were stained with antibodies specific for DsRed and the corresponding secondary antibodies. Z-stack images were acquired (interval, 0.2µm) and subjected to deconvolution and three-dimensional reconstruction. **(C)** Representative projections of the reconstructed images as well as a single optical slice are shown. **(D)** Localization was scored in 47 (for DsRed-FasL Δ2-43), 34 (for DsRed-FasL ΔPRD), 31 for DsRed-FasL Δ3K and 40 (for DsRed-FasL WT) transfected cells. Scoring: Membrane (M), Intracellular Vesicles (IV) and Membrane + Intracellular Vesicles (M + IV). Further details about the scoring system can be found in section 2.15.

confocal microscopy. While the majority of the cells transfected with FasL Δ2-43 or FasL ΔPRD displayed no colocalization with LAMP-1, 90% of the cells transfected with FasL Δ3K had either complete or partial colocalization of their intracellular vesicles with LAMP-1. Strikingly, in 84% of those cells, the intracellular vesicles where FasL Δ3K was stored exhibited a perfect colocalization with LAMP-1 (**Figure 5.16 C**). Representative images for the colocalization of each of the three mutants with LAMP-1 are shown in **Figure 5.16 D**. These results suggested that while deletion mutants Δ2-43 and ΔPRD were transported to the correct vesicle, deletion of lysines 71, 72 and 73 resulted in aberrant localization to LAMP-1^+ $Stx3^-$ vesicles indicating a role for these lysines in targeting FasL to FSVs.

5.2.5. Lysines 71, 72 and 73 are important for FasL targeting to FSVs

Deletion of lysines 71, 72 and 73 led to mistargeting to LAMP-1^+ $Stx3^-$ vesicles suggesting these residues direct FasL to the FSVs. I therefore evaluated which of the three lysines was required for the correct targeting of FasL. I tested the subcellular localization of DsRed-FasL K71A, K72A and K73A point mutation constructs (**Figure 5.17**) where the positively charged lysines were replaced by alanines. I transfected CTL Clone 3/4 cells with FasL K71A, FasL K72A and FasL K73A and stained them with antibodies specific for FasL. Flow cytometry analysis of their surface expression showed that cells transfected with each of the three constructs exhibited high frequency of FasL surface expression (**Figure 5.18 A**). Comparison of the percentage of cells expressing surface FasL relative to mock-transfected cells indicated surface expression of the lysine mutant proteins was significantly higher compared to the surface expression of FasL WT (**Figure 5.18 B**). Additionally, I examined their subcellular distribution in CTL Clone 3/4 stained with DsRed antibodies. Confocal microscopy analysis revealed that all three mutants displayed membrane localization in addition to intracellular vesicles (**Figure 5.18 C**). In fact, in 71%, 83% and 81% of the cells

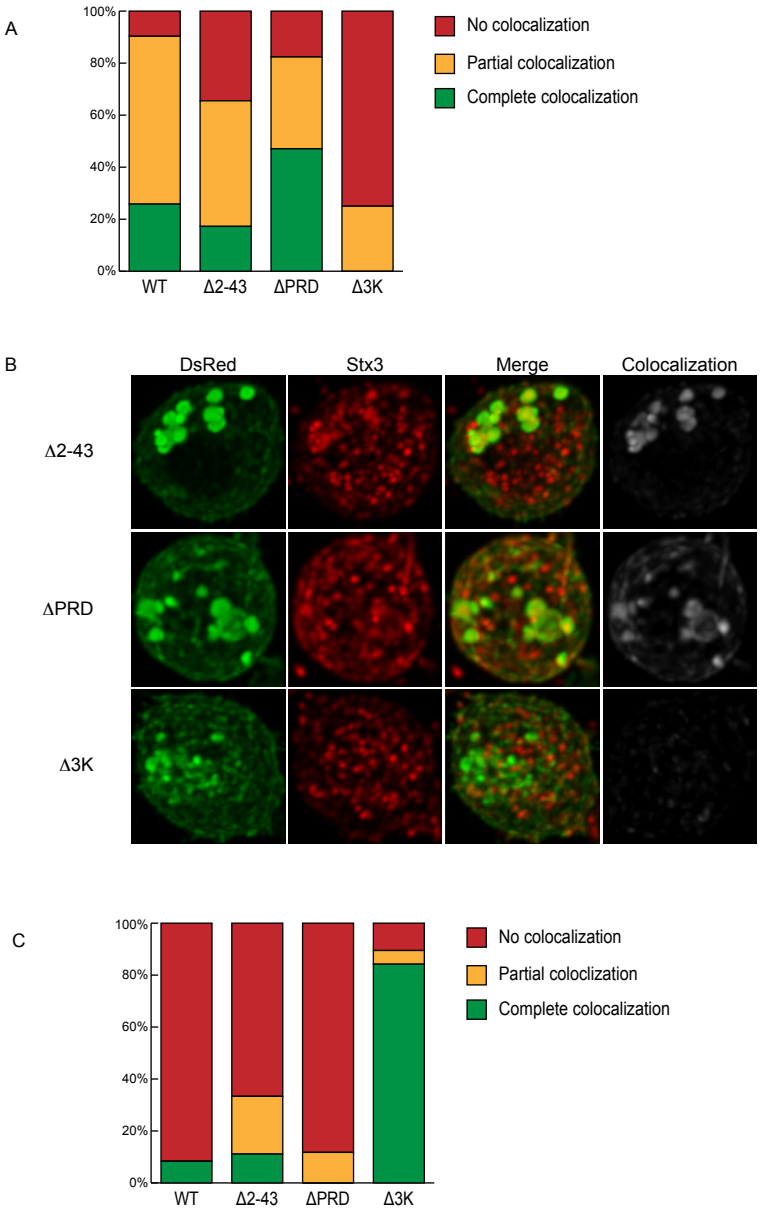
A
100%
80%
60%
40%
20%
0%
WT
Δ2-43
ΔPRD
Δ3K
No colocalization
Partial colocalization
Complete colocalization
B
DsRed
Stx3
Merge
Colocalization
Δ2-43
ΔPRD
Δ3K
C
100%
80%
60%
40%
20%
0%
WT
Δ2-43
ΔPRD
Δ3K
No colocalization
Partial coloclization
Complete colocalization

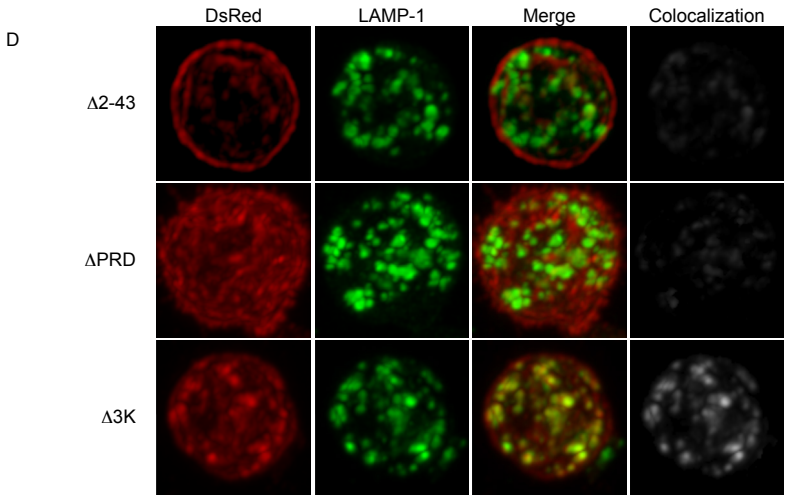

Figure 5.16. Intracellular DsRed-FasL Δ2-43 and ΔPRD are located in Stx3$^+$ LAMP-1$^-$ vesicles while Δ3K is found in Stx3$^-$ LAMP-1$^+$ vesicles.
CTL Clone 3/4 cells transfected with DsRed-FasL Δ2-43, ΔPRD and Δ3K were stained with antibodies specific for DsRed and Stx3 **(A and B**) or LAMP-1 **(C and D)** and the corresponding secondary antibodies. Z-stack images were acquired (interval, 0.2μm) and subjected to deconvolution and three-dimensional reconstruction. **(A and C)** Colocalization was scored using the criteria depicted in Figure 5.6 using 29 (for Stx3) and 18 (for LAMP-1) cells transfected with DsRed-FasL Δ2-43, 17 (for Stx3) and 17 (for LAMP-1) cells transfected with DsRed-FasL ΔPRD, 12 (for Stx3) and 19 (for LAMP-1) cells transfected with DsRed-FasL Δ3K and 12 (for Stx3) and 28 (for LAMP-1) cells transfected with DsRed-FasL. **(B and D)** Representative projections of the reconstructed images for the majority colocalization phenotypes are shown.

transfected with FasL K71A, K72A and K73A respectively, FasL was found on the membrane as well as in intracellular vesicles (**Figure 5.18 D**). In summary, replacing any of the three lysines resulted in surface accumulation of FasL in addition to intracellular vesicles localization.

To evaluate whether the intracellular vesicles where the K71A, K72A and K73A mutant molecules are stored were FSVs or LAMP-1^+ vesicles, I initially stained transfected Clone 3/4 cells with DsRed and Stx3. I analyzed their colocalization by confocal microscopy and determined that the majority of the cells transfected with FasL K71A, FasL K72A or FasL K73A exhibited poor colocalization with Stx3 (**Figures 5.19 A and B**). However, analysis of their colocalization with LAMP-1 revealed that in most of the analyzed transfected cells, intracellular DsRed-FasL colocalized either partially or completely with LAMP-1 (**Figure 5.19 C and D**). These results indicated that all three lysines 71, 72 and 73 were required for targeting FasL to its $Stx3^+$ storage vesicle. It is interesting to notice that while the trend was comparable, none of the point mutations generated the same striking phenotype observed for FasL Δ3K in which most of the intracellular vesicles had a perfect colocalization with LAMP-1. This probably suggests that even though all three lysines might be needed for the correct targeting of FasL, partial and inefficient targeting could be accomplished with two of the three.

5.2.6. FasL has no detectable ubiquitin or SUMO modifications

Protein modification via the addition of ubiquitin (Uq) polypeptides has been shown to signal endocytosis from the plasma membrane, lysosomal targeting for degradation and intracellular sorting to endosomal compartments (Piper and Lehner 2011). Ubiquitination of target proteins is accomplished by the formation of isopeptide bonds that bind the C-terminal glycine of Uq to the ε-amino group of a lysine residue on the ubiquitinated protein (Welchman et al. 2005). Because I found that lysines are important for FasL trafficking in CTL, I hypothesized that

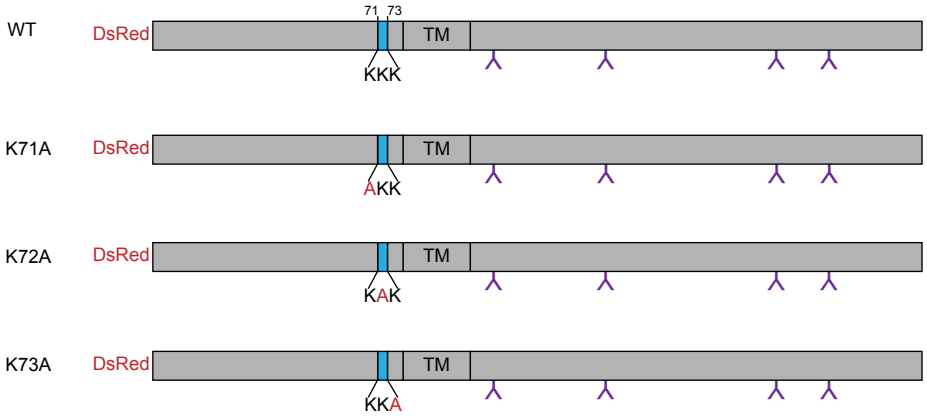

Figure 5.17. Structure of the DsRed-tagged FasL lysine mutant constructs. Lysines 71, 72 or 73 were replaced by alanine to construct DsRed-FasL N71A, DsRed-FasL K72A and DsRed-FasL K73A.

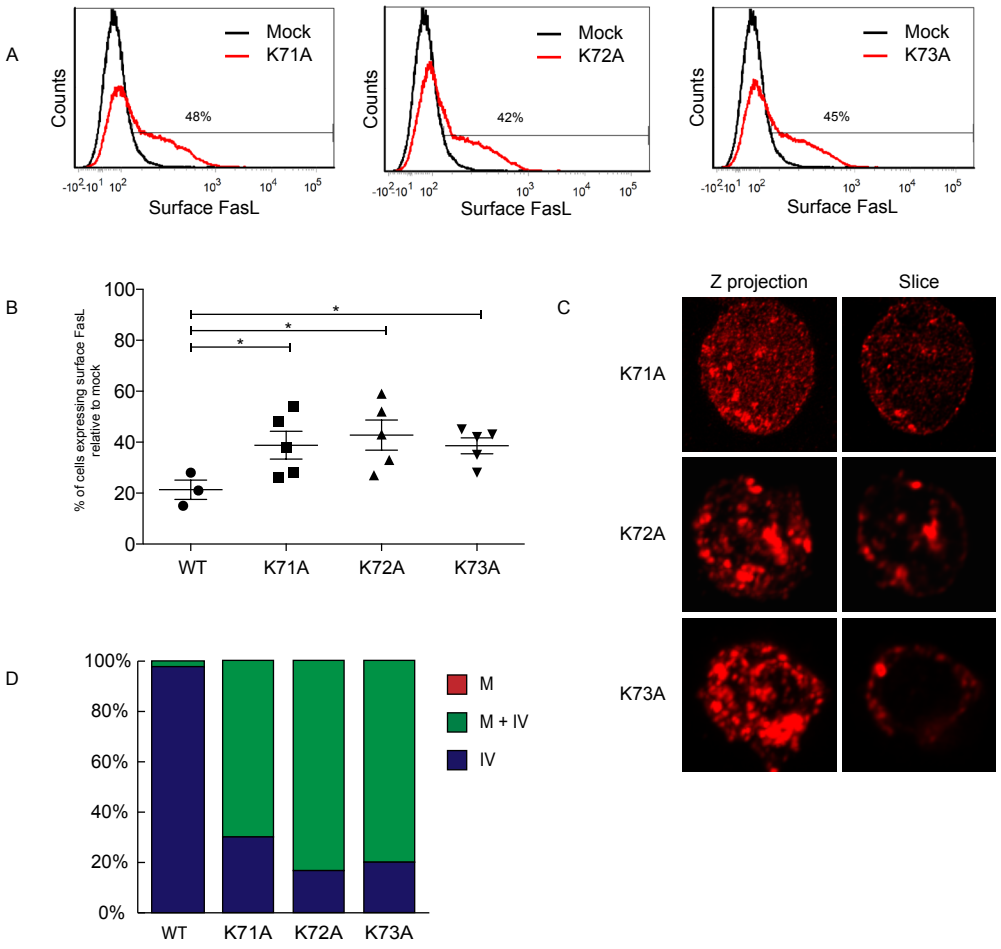

Figure 5.18. DsRed-FasL K71A, K72A and K73A are located on the surface and in intracellular vesicles in CTL.
CTL Clone 3/4 cells were transfected with DsRed-FasL K71A, K72A and K73A or mock-transfected **(A)** Surface expression of transfected cells was determined by flow cytometry (red) and compared to mock-transfected cells (black). **(B)** The percentage of cells expressing surface FasL relative to mock-transfected cells was graphed and compared to cells transfected with DsRed-FasL WT. Mean and standard error bars are indicated for each group. The unpaired Students *t*-test was used with significance set at a p value $\leq$ 0.05 where * indicates $p < 0.05$. **(C and D)** Transfected cells were stained with antibodies specific for DsRed and the corresponding secondary antibodies. Z-stack images were acquired (interval, 0.2µm) and subjected to deconvolution and three-dimensional reconstruction. **(C)** Representative projections of the reconstructed images as well as a single optical slice are shown. **(D)** Localization was scored in 21 (for DsRed-FasL K71A), 18 (for DsRed-FasL K72A), 21 for DsRed-FasL K73A and 40 (for DsRed-FasL WT) transfected cells. Scoring: Membrane (M), Intracellular Vesicles (IV) and Membrane + Intracellular Vesicles (M + IV). Further details about the scoring system can be found in section 2.15.

A

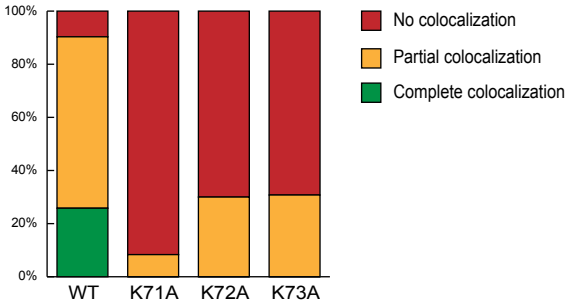
100%
80%
60%
40%
20%
0%
WT
K71A
K72A
K73A
No colocalization
Partial colocalization
Complete colocalization

B

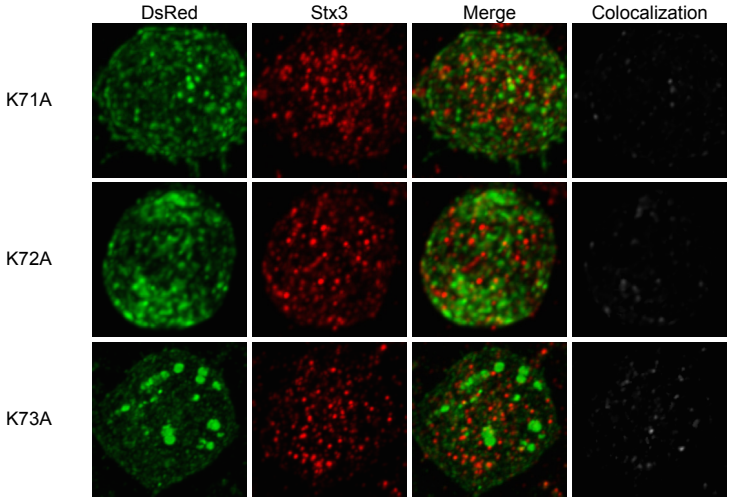
DsRed
Stx3
Merge
Colocalization
K71A
K72A
K73A

C

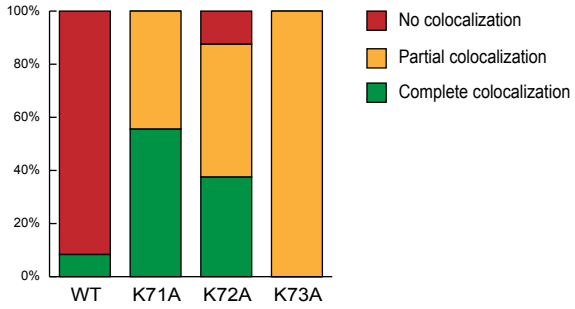
100%
80%
60%
40%
20%
0%
WT
K71A
K72A
K73A
No colocalization
Partial colocalization
Complete colocalization

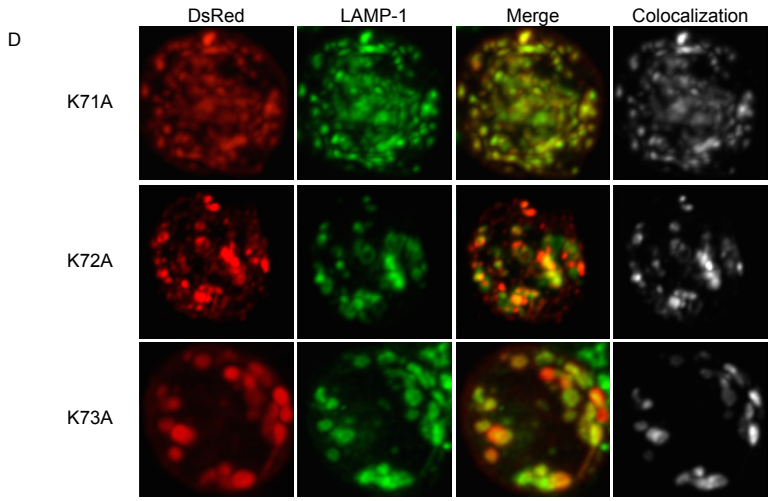

Figure 5.19. Intracellular DsRed-FasL K71A, K72A and K73A are located in Stx3$^-$ LAMP-1$^+$ vesicles.
CTL Clone 3/4 cells transfected with DsRed-FasL Δ2-43, ΔPRD and Δ3K were stained with antibodies specific for DsRed and Stx3 **(A and B**) or LAMP-1 **(C and D)** and the corresponding secondary antibodies. Z-stack images were acquired (interval, 0.2μm) and subjected to deconvolution and three-dimensional reconstruction. **(A and C)** Colocalization was scored using the criteria depicted in Figure 5.6 using 12 (for Stx3) and 9 (for LAMP-1) cells transfected with DsRed-FasL K71A, 10 (for Stx3) and 8 (for LAMP-1) cells transfected with DsRed-FasL K72A, 13 (for Stx3) and 8 (for LAMP-1) cells transfected with DsRed-FasL K73A and 12 (for Stx3) and 28 (for LAMP-1) cells transfected with DsRed-FasL. **(B and D)** Representative projections of the reconstructed images for the majority colocalization phenotypes are shown.

ubiquitination of FasL in lysines 71, 72 and/or 73 would mediate FasL trafficking from the plasma membrane to its storage vesicle. In fact, ubiquitination of FasL has been demonstrated for human FasL (Zuccato et al. 2007). To test this hypothesis I transfected CTL Clone 3/4 cells with a construct containing HA-tagged Uq and I immunoprecipitated FasL from post-nuclear lysates of 2 x 10^7 transfected cells. I ran the immunoprecipitates and lysate controls in an SDS-PAGE and analyzed them by Western Blot. As a control, to confirm that the FasL antibodies used for immunoprecipitation were able to recover the protein, I probed the samples against FasL and observed a set of bands corresponding to FasL in the lanes corresponding to cells transfected with HA-Uq and mock-transfected. However, I did not detect HA-Uq in transfected or mock-transfected cells after probing with antibodies against HA (**Figure 5.20 A**). Although this result could suggest that FasL is not ubiquitinated in CTL Clone 3/4, the absence of the typical Uq ladder on the lysate controls suggested the expression levels of the HA-Uq construct in Clone 3/4 cells was not high enough for detection by this method. I therefore assessed if FasL was ubiquitinated using CTLL-2 cells. Because these cells are more amenable to double-transfection, I also evaluated if overexpressed transfected FasL could be ubiquitinated. I transfected CTLL-2 cells with DsRed-FasL and HA-Uq, with each construct individually or mock-transfected them and immunoprecipitated FasL from post-nuclear lysates. I subjected the immunoprecipitates and the corresponding lysate controls to Western Blot analysis to evaluate the association of Uq with FasL. Probing with FasL antibodies confirmed that DsRed-FasL and endogenous FasL could be detected in the immunoprecipitates. However, HA-Uq could not be detected in FasL immunoprecipitates from cells transfected with HA-Uq alone or FasL and HA-Uq together (**Figure 5.20 B**). Nonetheless, a typical ubiquitin ladder pattern was observed in the lysate control lanes of cells transfected with HA-Uq. Thus, even though the expression level of HA-Uq was high enough for detection in lysates corresponding to 0.8 x 10^6 cells, it could not be detected in FasL immunoprecipitates. These results suggested that neither endogenous nor transfected FasL associated with HA-Uq in CTL. However, I cannot exclude the

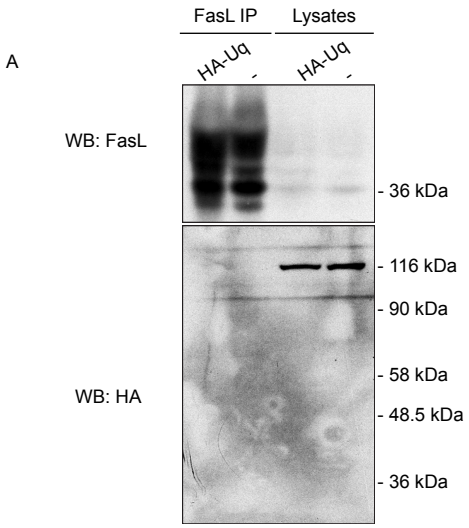
A
FasL IP
Lysates
HA-Ub
-
HA-Ub
-
WB: FasL
- 36 kDa
- 116 kDa
- 90 kDa
WB: HA
- 58 kDa
- 48.5 kDa
- 36 kDa

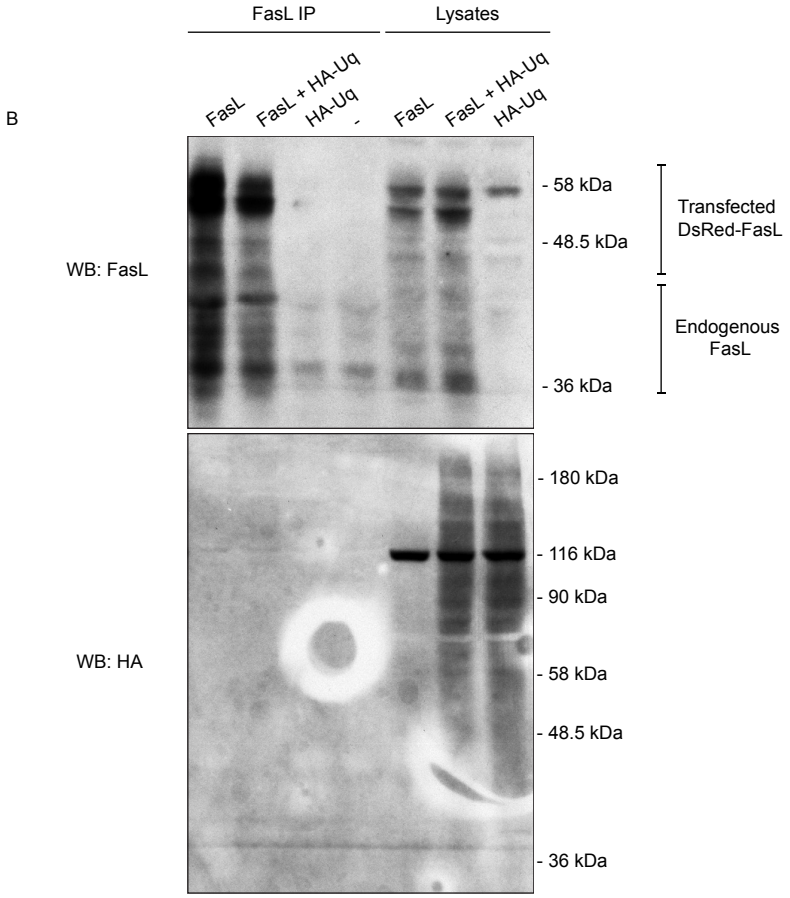

Figure 5.20. Ubiquitination of FasL was not detected in CTL Clone 3/4 or CTLL-2 cells.
(A) CTL Clone 3/4 cells were transfected with HA-Uq or mock-transfected. **(B)** CTLL-2 cells were transfected with DsRed-FasL, HA-Uq, both or mock-transfected. Post-nuclear lysates corresponding to 2 x 10^7 cells were immunoprecipitated with antibodies specific for FasL and run in an SDS-PAGE. Non-immunoprecipitated lysate controls corresponding to 0.8 x10^6 cells were also included. Immunoblotting was performed using antibodies specific for FasL (top panel) and HA (bottom panel).

possibility that only a few Uq molecules associate with FasL and that this level of association is below the threshold of detection by this method.

SUMO is a protein that, like Uq, can also be covalently attached to target proteins and alter their trafficking. For example, SUMOylation of the glutamate receptor subunit 6 (GluR6) leads to its endocytosis from the plasma membrane of neurons (Martin et al. 2007). Moreover GLUT4 sorting into glucose transporter vesicles is a SUMO-dependent process (Liu et al. 2007). Because SUMO peptides are also attached to lysine residues (Geiss-Friedlander and Melchior 2007), I decided to study if FasL was SUMOylated in CTL. For this purpose, I immunoprecipitated FasL from post-nuclear lysates of CTL Clone 3/4 cells and determined its association with SUMO by SDS-PAGE and Western Blot. I ran the FasL and control immunoprecipitates together with lysate controls in duplicate within the same gel and evaluated specific FasL immunoprecipitation using FasL antibodies. FasL was detected in the lanes corresponding to FasL immunoprecipitates but not in the ones corresponding to control immunoprecipitates. Subsequent division of the membrane yielded two equal copies of samples that I probed with antibodies specific for SUMO that had (or not) been pre-incubated with purified SUMO peptides for 2 hours. The purpose of pre-incubating with SUMO peptides is to block binding of SUMO-specific antibodies to SUMOylated proteins. Comparison with membranes blotted with antibodies not pre-incubated, highlights *bona fide* over non-specific detection of SUMOylation. The SUMO antibodies were able to detect SUMOylated proteins, as evidenced by the bands present on the lysate lane of the SUMO Western Blot, which are not observed when using antibodies pre-incubated with SUMO peptides. In the Western Blot using antibodies not pre-incubated with SUMO, I observed a band present only on the lane corresponding to FasL immunoprecipitates. However, the electrophoretic mobility of this protein was too high compared to FasL. Moreover, the same band was present in the Western Blot using pre-incubated SUMO antibodies, which suggested it corresponded to non-specific antibody binding (**Figure 5.21 A**). No further bands were detected in the FasL immunoprecipitates, suggesting FasL may not be SUMOylated in CTL

Clone 3/4 cells. Additionally I evaluated if FasL associated with SUMO in CTLL-2 cells using the same methodology employed for Clone 3/4 cells. Similarly, I was unable to detect SUMO in FasL immunoprecipitates (**Figure 5.21 B**) suggesting that FasL might not be SUMOylated in CTLL-2 cells. However, I cannot exclude the possibility that the levels of SUMO association are too low for detection with this method.

5.3. Discussion

In this chapter I have described the characterization of multiple FasL mutant constructs that have provided insight into the sections of the FasL protein that are important for its trafficking. After being synthesized, FasL is first transported to its storage vesicle where it is safely kept from inducing non-specific apoptosis. After CTL encounter target cells, FasL is quickly translocated from its FSV to the surface to exert its killing function (He and Ostergaard 2007). Because most of the mutants analyzed in this chapter led to surface accumulation, I was not able to evaluate the effect of most of the mutations on surface translocation after stimulation. Nonetheless, my results suggested that the self-assembly domain, needed for the trimerization of the protein, may be required for efficient surface translocation of FasL after CTL stimulation (Figure 5.10). Oligomerization of FasL is required for its apoptosis-inducing function (Holler et al. 2003). Likewise, oligomerization of other ligands of the TNF superfamily is essential for their activity. Only the oligomeric form of BAFF can bind to its receptor TACI on B cells (Bossen et al. 2008) and costimulation of B cell proliferation by APRIL can only be achieved upon APRIL oligomerization (Ingold et al. 2005). Similarly, oligomerization of 4-1BBL is required for its costimulatory effect on T lymphocytes (Rabu et al. 2005) and the costimulatory activity of OX40 ligand is enhanced by its oligomerization (Muller et al. 2008). Oligomerization of the TNF ligands TRAIL, CD40L, GITRL and CD27L has also been shown to be essential for their activity (Muhlenbeck et al. 2000, Wyzgol et al. 2009). To my knowledge, however, oligomerization-dependent trafficking has

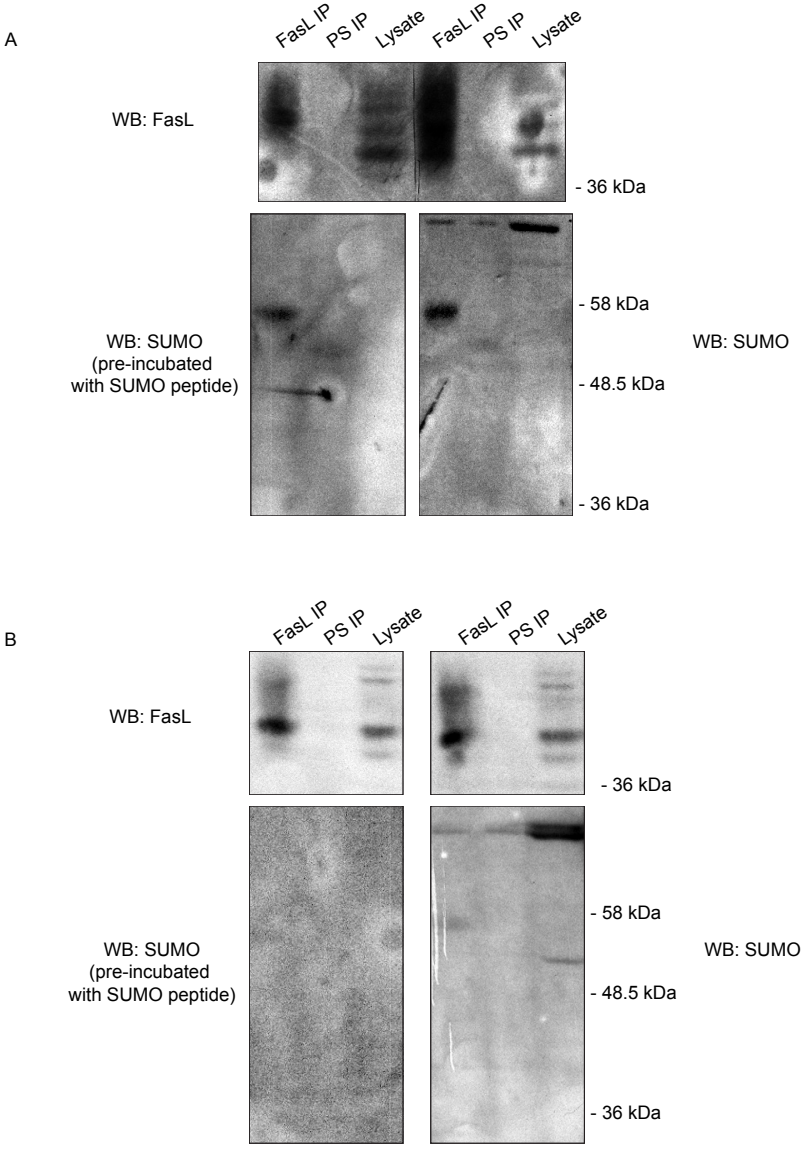

Figure 5.21. SUMOylation of endogenous FasL was not detected in CTL Clone 3/4 or CTLL-2 cells.

Post-nuclear lysates from Clone 3/4 **(A)** and CTLL-2 **(B)** cells were immunoprecipitated with antibodies specific for FasL and run in an SDS-PAGE in duplicates. Non-immunoprecipitated lysate controls corresponding to 0.8 $x10^6$ cells were also included. Immunoblotting was performed using antibodies specific for FasL (top panel) and after excising the membrane in two, each set of samples was probed with antibodies specific for SUMO that had (left bottom panel) or not (right bottom panel) been pre-incubated for 2 hours with SUMO peptides.

never been described for any TNF family member, making this the first report to suggest its importance. Interestingly, oligomer formation has been shown to be essential for trafficking of the neurotransmitter sodium symporter family of proteins. The effect on trafficking is thought to be due to conformational changes induced by the association that either hide or expose sorting signals (Sitte et al. 2004). In the future it would be interesting to evaluate whether the same is true for FasL.

Using chimeric constructs where the N-terminal or the C-terminal ends of FasL had been replaced with the corresponding domains of the unrelated Ly49A protein, I found that both ends of the protein contained relevant sequences that allowed for FasL correct trafficking to its FSV (Figures 5.5 and 5.7). Within the C-terminal external domain, I showed mutation of asparagine 182 to glutamine, affected FasL trafficking. Mutating this single amino acid resulted in surface accumulation and mistargeting of FasL to $Stx3^{-}$ $LAMP\text{-}1^{+}$ vesicles (Figures 5.11 and 5.12). Because this residue is a putative site for N-glycosylation of FasL, these findings suggest glycosylation of FasL has a severe effect on its trafficking. A strikingly similar situation is observed for the glucose transporter protein GLUT4 in adipocytes. GLUT4 is glycosylated on residue N57 and a mutant lacking this N-glycosylation site displays increased surface expression and lack of colocalization with IRAP, a component of the GLUT4 storage vesicles (Haga et al. 2011). Interestingly, mutation of FasL asparagines 117 and 258, also putative sites for glycosylation, exhibited no apparent defect in FasL localization (Figures 5.11 and 5.12) suggesting only glycosylation in N182 affects FasL trafficking in CTL. A related case has been reported for CLN5, a protein of unknown function but relevant in causing neurodegenerative disorders, that has eight glycosylation sites. Mutation of a single one of those residues (N401) results in mislocalization (Moharir et al. 2013). Similarly, the lysosomal tripeptidyl-peptidase I has five N-glycosylation sites, of which only the asparagine 286-linked glycan is critical for lysosomal targeting (Wujek et al. 2004).

The mechanisms by which N-glycans facilitate sorting of proteins to specific locations are not completely understood. Lysosomal proteins modified

with mannose-6-phosphate (M6P) groups are recognized by M6P receptors and carried to lysosomes (Kornfeld and Mellman 1989). The galactose-binding lectin galectin-3 promotes apical sorting of lactase-phlorizin hydrolase, transmembrane neurotrophin receptor p75 and gp114 in MDCK cells (Delacour et al. 2006) and the high-mannose-binding lectin VIP36 binds to and promotes apical sorting of clusterin and α-amylase (Hara-Kuge et al. 2002). However, in many cases glycosylation may affect protein transport by providing an optimal three-dimensional conformation that facilitates the recognition of other sorting signals in the protein (Vagin et al. 2009). An interesting alternative indicates that N-glycosylation has a role in trafficking to lipid rafts. Consistent with this, VIP36, which was originally isolated from lipid rafts, has been proposed to cluster glycoproteins in lipid rafts for subsequent targeting to apical surfaces (Vagin et al. 2009). Glycosylation-mediated trafficking to lipid rafts has been described for various proteins. Mutation of N934 of the TRPM8, a thermosensible channel expressed on the surface of neurons, results in elimination of N-glycosylation and drastic reduction in the association of the protein with lipid rafts (Morenilla-Palao et al. 2009). Glycosylation of the urea transporter UT-A1 was shown to be important for its transport to lipid rafts and subsequent targeting to the apical membrane of polarized epithelial cells (Chen et al. 2011). Similarly, disruption of the N-glycosylation of the adenylyl cyclase AC8 results in its exclusion from lipid rafts (Pagano et al. 2009). FasL has been shown to accumulate in lipid rafts in transfected non-hematopoietic cells and in stimulated primary T cells (Cahuzac et al. 2006, Nachbur et al. 2006). The authors claim FasL is targeted to these motifs as a result of T cell stimulation. However, a more encompassing explanation could be that FasL is normally targeted to lipid rafts (possibly by its N182 glycan), both after stimulation and in steady-state conditions as part of its trafficking route to the internal FSV. It would be interesting to evaluate if FasL N182Q fails to localize to lipid rafts in CTL.

The experiments shown in this chapter indicate that glycosylation in N182 permits efficient endocytosis and correct targeting to FSVs. Although I cannot fully explain how glycosylation on the external domain of FasL would signal both

of these processes, if glycosylation proved to mediate the trafficking of FasL to lipid rafts, FasL may be endocytosed via a lipid raft-dependent pathway, as discussed in chapter 4. In this hypothetical scenario, mutation of N182 would abrogate glycosylation, reducing lipid raft targeting and lipid raft-mediated endocytosis of FasL. As a result FasL N182Q would be endocytosed by less efficient methods, resulting in surface accumulation. Also, endocytosis through a different mechanism might preclude the recognition of FSV sorting sequences resulting in default targeting to LAMP-1^+ lysosomes.

Surprisingly, although normal localization of FasL was also affected by glycosylation in transfected COS-1 cells, in these cells, it was glycosylation in N258 that had a significant effect. FasL N258Q exhibited reduced surface expression compared to FasL WT (Figure 5.13) which was mostly expressed on the surface of non-hematopoietic COS-1 cells (Figure 4.1). Western Blot analysis suggested this protein was expressed at levels comparable to WT indicating the mutation did not affect its stability, however, its subcellular distribution was not evaluated. Glycosylation in this N1258 may affect protein folding or ER-to-Golgi trafficking, since these are typical functions of glycans (van Vliet et al. 2003). However, the fact that FasL N258Q was found in FSVs instead of trapped in the biosynthetic pathway, clearly suggests glycosylation in N258 has different functions in Clone 3/4 versus COS-1 cells further emphasizing the differences in trafficking mechanisms between these cells.

In chapter 4 I showed that FasL is endocytosed from the plasma membrane and then targeted to its FSV. The surface accumulation exhibited by the N-terminal Δ2-43, ΔPRD and Δ3K deletion mutants (Figure 5.15) allowed me to determine that the signal within the FasL protein that triggers its endocytosis is probably present in the N-terminal end of the protein. The fact that all the N-terminal mutants displayed a similar surface localization phenotype could indicate that different residues separated in the amino acid sequence of the N-terminal domain are required for the endocytosis signal. Consistently, residues throughout the cytoplasmic tail of P-selectin were required for its endocytosis (Setiadi et al. 1995). Moreover, several regions in the cytoplasmic tail of the γc and of the

prolactin receptors are involved in the endocytosis of these proteins (Vincent et al. 1997, Morelon and Dautry-Varsat 1998). These distant residues could either come together as a result of three-dimensional folding or they could be involved in sequential events necessary for efficient endocytosis. Future analysis with deletions of narrower segments will be necessary to distinguish between these scenarios for the mechanism of FasL efficient endocytosis. Interestingly, even though all the mutants accumulate on the surface, they were still able to become endocytosed to a small degree. This could be due to low-rate basal endocytic membrane trafficking, as it has previously been described for CD4 and the Fc receptor (Pelchen-Matthews et al. 1991, Miettinen et al. 1992). Also relevant to mention is that the FasL/Ly49A chimera exhibited surface accumulation that suggested similar inefficient endocytosis. This could indicate that the endocytosis signal is not limited to the N-terminal domain, with relevant sequences present on the C-terminal domain. The challenge with this possibility would be to identify the mechanism by which cytosolic constituents recognize external motifs. The deficient endocytosis observed for the FasL/Ly49A chimera could be explained by the same hypothetical scenario proposed for FasL N182Q, where glycosylation in the N182 residue of the C-terminal end targets FasL to specific sections of the plasma membrane (such as lipid rafts) in which the endocytosis signal present in the cytoplasmic tail would be specifically recognized.

Deletion or point mutation of K71, K72 and K73 led to aberrant localization to $Stx3^{-}$ LAMP-1^{+} vesicles (Figures 5.16 and 5.19). These results indicated that after being endocytosed, K71, K72 and K73 provide the necessary signal to target FasL to its storage vesicle. A contradicting study using transfected human FasL and conducted on a rat basophil RBL cell line (Zuccato et al. 2007) claims that phosphorylation and ubiquitination of the N-terminal cytoplasmic tail of FasL are both necessary for its transport to cytolytic granules. However, their results could not explain how mouse FasL (which lacks the N-terminal tyrosines thought to be phosphorylated and essential for its trafficking) is efficiently targeted to its storage vesicle. Moreover, I could not detect ubiquitination or SUMOylation of endogenous FasL in Clone 3/4 or CTLL-2 cells (Figure 5.20 and

5.21). I hypothesize that these 3 lysines interact with an unidentified protein or group of proteins that direct FasL towards its storage vesicle. It would be interesting to investigate if their polar nature is important for the targeting function of lysines 71, 72 and 73. If the replacement of these lysines for arginine residues restored the correct targeting of FasL to its FSV, it would indicate that the positive charge in these positions is important for FasL trafficking. It has been previously shown that positively charged amino acids can serve as sorting signals to specialized vesicles (Baerends 2000, Mullen and Trelease 2000, Cabrera et al. 2012) and even though their trafficking has not yet been studied, other members of the TNF ligand superfamily (LIGHT and TWEAK) also contain 3-4 positively charged amino acids in a similar position of their cytoplasmic tails. In fact, identically to FasL, LIGHT has been shown to localize to intracellular vesicles in *ex vivo* T cells from where it is transported to the cell surface upon T cell stimulation (Morel et al. 2000).

In summary in this chapter I showed that oligomerization is required for FasL translocation to the surface after stimulation and I demonstrated the importance of glycosylation in the trafficking of FasL in CTL and non-hematopoietic COS-1 cells. Furthermore, the major contributions from this chapter were the identification of the sorting signals that mediate FasL endocytosis and targeting to its FSV.

I have proposed models for the trafficking of the FasL mutants employed in this thesis (**Figure 5.22**). DsRed-FasL WT, N117Q and N258Q use a signal in the cytoplasmic tail to promote their active endocytosis from the plasma membrane. However, I postulate that the endocytic machinery in these CTL expressing endogenous as well as transfected FasL becomes overloaded explaining why some FasL proteins are detected by flow cytometry on the surface of these transfected CTL. I hypothesize that because FasL Δ2-43 and ΔPRD are missing the endocytosis signal, they cannot be recognized by the specialized endocytosis machinery and therefore are not efficiently internalized. Instead, basal endocytosis allows for low rate endocytosis and once inside, lysines 71, 72 and 73

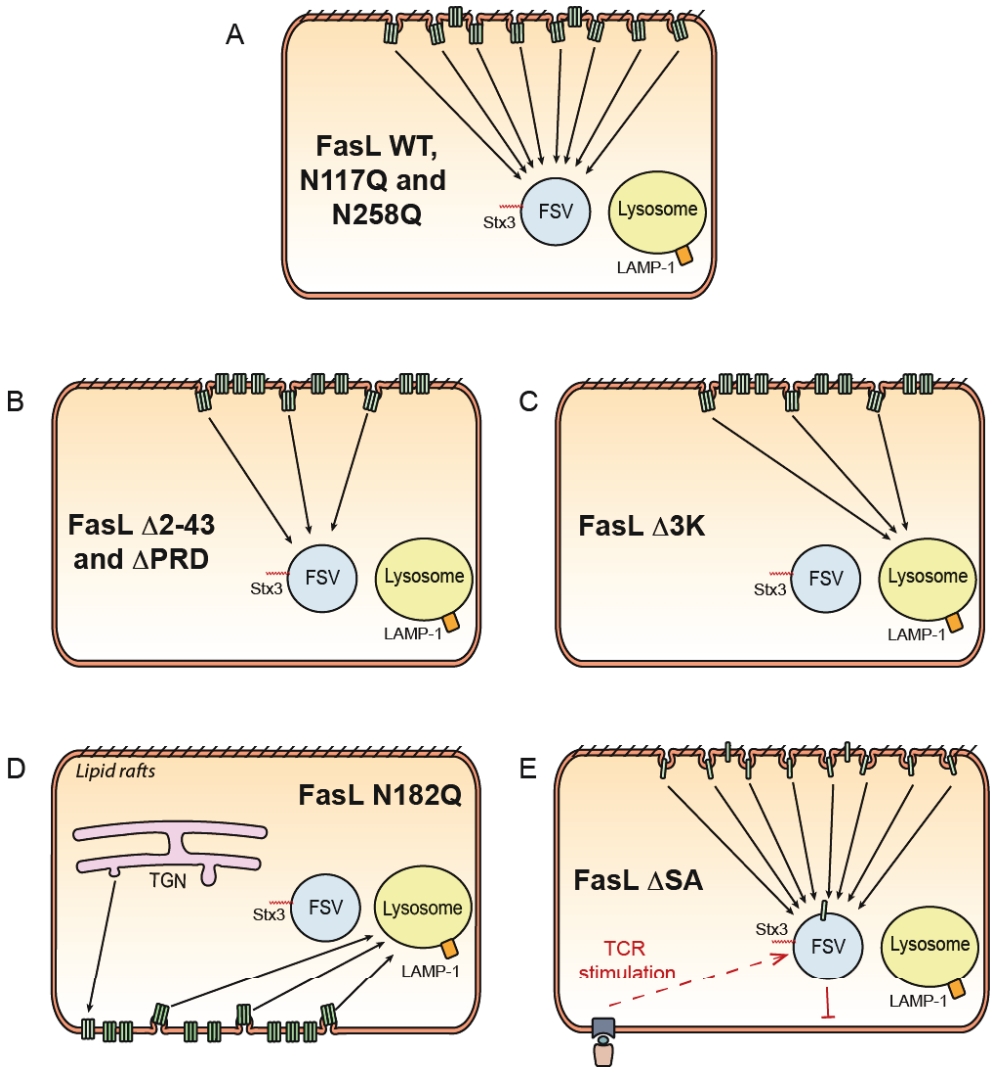

Figure 5.22. Model for trafficking of FasL mutant constructs in CTL.
A) FasL WT, N117Q and N258Q are actively endocytosed and targeted to the FSV. The FasL molecules detected by flow cytometry could be explained by the saturation of the endocytic machinery, which would have to internalize the overexpressed DsRed-tagged proteins as well as the endogenous FasL molecules. **B)** FasL Δ2-43 and ΔPRD are missing the endocytosis signal and cannot be recognized by the specialized endocytic machinery. I hypothesize that basal endocytosis allows for low rate endocytosis and once inside the cells, lysines 71, 72 and 73 signal their targeting to FSVs. **C)** FasL Δ3K is also inefficiently endocytosed and those protein internalized by basal non-specific endocytosis cannot signal their trafficking to the FSV are and instead destine to the default lysosomal location. **D)** I postulate that N-glycosylation in N182 delivers FasL to lipid raft sections of the plasma membrane where the specific endocytosis and targeting machinery is present. Therefore, FasL N182 is inefficiently endocytosed and mistargeted to lysosomes. **E)** FasL ΔSA is normally targeted to FSV but being unable to trimerize it cannot be translocated to the surface upon TCR stimulation of CTL.

signal their trafficking to FSVs. I posit that transfected FasL Δ3K is also inefficiently endocytosed and that the few proteins internalized by basal non-specific endocytosis cannot signal their trafficking to the FSV and are destined to the default lysosomal destination. I hypothesize that DsRed-FasL N182Q affects the targeting of FasL to lipid rafts which results in reduced endocytosis and mistargeting to lysosomes, possibly because the machinery that recognized these signals is only present in lipid raft areas. And lastly, FasL ΔSA, which would be unable to trimerize, is normally targeted to its FSV but cannot be translocated to the surface upon stimulation.

CHAPTER 6: General Discussion

6.1. Summary of Results

FasL is a protein expressed by CTL, which may be employed to induce apoptosis in target cells. In unstimulated conditions it is found stored in intracellular storage vesicles but upon TCR stimulation after encountering a target cell, or as a response to artificial chemical PMA and ionomycin stimulation, FasL can be detected on the surface of CTL. The major focus of my research was to decipher the identity of the FasL storage vesicle and to understand the trafficking mechanisms that take FasL to its vesicle after its biosynthesis and from there to the surface after stimulation.

CTL contain other apoptosis-inducing molecules, mainly perforin and granzymes, which are also stored in intracellular lysosome-derived granules. After CTL become stimulated, these granules are transported to the point of contact with the target cell and they fuse with the plasma membrane. Because the cytolytic molecules contained in the granules are soluble, instead of transmembrane like FasL, this results in their secretion. Although some authors claim FasL, perforin and granzymes are stored within the same granules and are thus subject to the same trafficking cues, other authors and previous results from our laboratory maintain that the localization of FasL is distinct and must therefore have a specific trafficking mechanism to direct it to its storage vesicle and to the plasma membrane after stimulation.

I characterized the storage vesicle of FasL in unstimulated CTL analyzing its colocalization by confocal microscopy. FasL did not colocalize with markers of ER, Golgi, late endosomes, early endosomes or recycling endosomes, suggesting FasL must be stored in a specialized vesicle. It also failed to colocalize with PD-1 or TNF-α, and most relevantly it did not colocalize with perforin and LAMP-1, supporting the hypothesis that FasL is stored in a separate compartment. However, it displayed a high degree of colocalization with the proteins Stx3, Munc18-2 and Rab32 in three different CTL types. Moreover, these proteins

exhibited a high degree of colocalization among them but failed to colocalize with perforin and LAMP-1 further reinforcing the notion that FasL is stored in a vesicle distinct from the lysosomal granules. My colocalization studies also revealed partial colocalization of FasL with cytochrome c, resident of the mitochondria, and with Grp78, an ER chaperone enriched in the mitochondria-associated membranes. Together with the high colocalization with Rab32, a Rab protein involved in the trafficking of proteins to MAMs, I inferred that the FSV may be near the MAMs.

Overall these results demonstrated that FasL was stored in a compartment distinct from the lysosomal granules, found near the MAMs and with a composition that included Stx3, Rab32 and Munc18-2, three proteins that until this report had not been described to reside in the same vesicles. I therefore reasoned that FasL must follow a specific trafficking route to reach its unique storage vesicle. I first attempted to determine if FasL, after its biosynthesis in the ER and Golgi, trafficked to its FSV via the surface or thorough a direct intracellular pathway. Using a microscopy-based endocytosis assay I showed that FasL can be transiently detected by specific antibodies on the surface of non-stimulated CTL from where it is endocytosed to reach its intracellular location. Moreover, because FasL was still internalized from the surface in the presence of a protein synthesis inhibitor, I concluded that FasL might cycle continuously between the plasma membrane and its FSV.

Given the colocalization of FasL with Stx3 (a SNARE protein) and Rab32 (a Rab protein), both of which are involved in vesicle trafficking, I then studied the effect of these proteins on FasL trafficking. I showed that overexpression of Stx3 affected the localization of FasL resulting in increased surface expression in CTL, although the mechanism for this Stx3-mediated surface FasL translocation is still not well understood. However, Rab32 had no detectable effect on FasL trafficking in unstimulated or stimulated CTL.

Using a purified GST-tagged polypeptide of the cytoplasmic tail of FasL, I precipitated proteins from CTL lysates and identified myosin 9 as one of the proteins that consistently and specifically associated with FasL. Myosin 9 is the

heavy chain component of the non-muscle myosin II motor protein that binds to actin filaments and uses energy to move along them, suggesting myosin may be involved in FasL trafficking. Consistently, inhibition of myosin interaction with actin using blebbistatin, led to reduced surface FasL expression after CTL stimulation, indicating myosin affects FasL translocation to the cell surface after stimulation.

FasL seems to traffic through the plasma membrane after its biosynthesis and it is apparently continuously cycling through the surface. Because of the deadly effect of surface FasL expression, there must be an efficient endocytosis mechanism of FasL to avoid non-specific killing. I thus attempted to determine the sorting signals within the FasL sequence that are responsible for its efficient internalization and correct transport using FasL mutant constructs. I started by testing the effect of swapping the N-terminal or the C-terminal ends of FasL with the corresponding domains of the unrelated type II transmembrane protein Ly49A. Evaluation of the surface expression and intracellular distribution of these FasL chimeras by flow cytometry and confocal microscopy first revealed that both ends of the protein contain important sequences for its proper trafficking. Moreover, the surface accumulation of several N-terminal deletion mutants of FasL indicated the sequences that signal the endocytosis of FasL are found on its cytoplasmic tail. Additionally, I found that three lysines within that tail provide the signal needed for its posterior targeting to the FSV since their deletion or point mutation led to mistargeting to LAMP-1^{+} $Stx3^{-}$ vesicles. Within the C-terminal end, I showed that N-glycosylation in arginine 182 had an effect on the trafficking of FasL. Mutation to glutamine, which would abolish glycosylation at that site, resulted in surface accumulation and aberrant targeting to $Stx3^{-}$ LAMP-1^{+} vesicles. Interestingly, a deletion mutant of FasL lacking the self-assembly domain was not detected on the surface upon CTL stimulation. These results indicate oligomerization of FasL may be required for its surface trafficking.

I also showed that in COS-1 cells, which do not express endogenous FasL, transfected DsRed-FasL is expressed on the surface, highlighting the existence of different trafficking mechanisms in these cells. Consistent with the notion that

FasL traffics differently in non-hematopoietic COS-1 cells and CTL, I found that glycosylation in arginine 258, which had no effect in CTL, affected trafficking of FasL in COS-1 cells. Moreover, I showed that overexpression of Stx3 increased the intracellular localization of transfected FasL in COS-1 cells.

6.2. Components of the FasL storage vesicle

My confocal microscopy studies demonstrated that FasL colocalized with Stx3, Munc18-2 and Rab32, indicating these three proteins are components of the FasL storage vesicle. Even though their overall functions have been described before, they had not been associated with FasL prior to this report. Moreover, I showed that none of these proteins or FasL colocalized with the lysosomal granule components, stressing the difference of composition between these two vesicles.

6.2.1. Syntaxin 3

Stx3, a SNARE protein, is classified as a Q-SNARE and as a t-SNARE. It is a transmembrane protein anchored to the membrane by its C-terminal end with its N-terminal end facing the cytoplasm. In its cytoplasmic tail, proximal to the membrane it contains the SNARE motif that allows it to interact with other t-SNAREs and with a v-SNARE to form the trans-SNARE complex. This complex provides the necessary force to fuse the vesicle and target lipid membranes. On the N-terminal end of the cytoplasmic tail it contains another characteristic domain, denominated H_{abc}, which is thought to fold as an auto-inhibitory regulatory domain. By folding back onto the membrane-proximal SNARE motif, the molecule adopts a "closed" conformation that prevents the formation of SNARE complexes and membrane fusion (Teng et al. 2001). Additionally, on the N-terminal extreme it contains an unstructured peptide, shown to be important for the regulation of the SNARE motif by MS proteins (Sudhof and Rothman 2009).

Stx3 has been shown to participate in the fusion step of a number of different processes, such as neurotransmitter receptor exocytosis in neuronal cells (Jurado et al. 2013), degranulation in mast cells (Tadokoro et al. 2007, Brochetta et al. 2014), protein traffic to melanosomes in melanocytes (Yatsu et al. 2013), insulin secretion from pancreatic beta cells (Zhu et al. 2013), chemokine release by mast cells (Frank et al. 2011), targeting of apical proteins in epithelial cells (Sharma et al. 2006), zymogen release from pancreatic acinar cells (Hansen 1999) and phagosomal maturation in macrophages (Hackam et al. 1996).

Because of its role as membrane fusion-mediator, after demonstrating its colocalization with FasL, I hypothesized that Stx3 would affect FasL trafficking. Since Stx3 is a t-SNARE and is found on the FSVs, I further hypothesized that it would mediate the fusion event that allowed the delivery of FasL to its storage vesicle. However, overexpression of Stx3, which is typically used to enhance trafficking, failed to decrease surface expression of FasL in stimulated CTL, which was the expected outcome of increased intracellular targeting to the FSV. Instead, I showed that overexpression of Stx3 affected the localization of FasL in unstimulated CTL resulting in increased surface expression. Although at first these results were surprising, given that Stx3 is a t-SNARE, its overexpression could increase the homotypic fusion of $Stx3^{+}$ vesicles resulting in enhanced FSV-FSV fusion. Such vesicle-vesicle fusion events have been shown to enhance exocytosis, in a process known as compound exocytosis. Therefore, a possible explanation for my results would involve a compound exocytosis mechanism for FasL translocation to the surface that is exacerbated with the gain of function overexpression of Stx3. Although this would be the first time such a mechanism has been indicated for FasL, there is evidence in the literature to support it. For instance, overexpression of Stx3 in pancreatic beta cells results in enhanced homotypic fusion of insulin-containing granules and increased exocytosis of insulin (Zhu et al. 2013). Compound exocytosis has also been described for mast cells, eosinophils and neutrophils (Alvarez de Toledo and Fernandez 1990, Lollike et al. 2002, Hafez et al. 2003) highlighting the importance of this mechanism for secretory vesicles in immune cells.

The functional advantages for a compound exocytosis could be in the efficient and specific surface display of FasL molecules at the immunological synapse. FasL surface expression could be accomplished in shorter time since not all of the FSVs have to fuse directly to the plasma membrane to discharge its contents and fewer vesicles directly fusing with the membrane would allow for a more discrete secretion specifically at the site of contact with the target cell (Pickett and Edwardson 2006).

6.2.2. Munc18-2

Munc18-2 belongs to the family of Sec/Munc-like (SM) proteins. The crystal structure of Munc18-1, the most studied member of the family, indicates that these proteins are composed of a conserved sequence of approximately 600 amino acids with three domains that form an arch or clasp with a large cavity on one side and a deep groove on the opposite side (Misura et al. 2000). Although they are essential for membrane fusion to occur, their function is not fully understood, possibly because they perform more than one role (Rizo and Sudhof 2012). Firstly, they can bind to the closed conformation of syntaxins, when the H_{abc} domain is contacting the SNARE motif. Binding of Munc18-1 to Syntaxin 1 has been shown to stabilize this closed conformation and hinder SNARE-complex formation (Chen et al. 2008). This allows then a regulatory role in which Munc18 proteins inhibit membrane fusion. Additionally, the N-terminal end of Munc18-3 has been shown to bind to the N-terminal peptide of Syntaxin 4 leaving the arch-shaped domain free to interact with the four-helix bundle of the trans-SNARE complex (Hu et al. 2007). This association is proposed to prevent the dissociation of the complex and promote membrane fusion (Rizo and Sudhof 2012).

Munc18-2 can interact with Syntaxins 1, 2, 3 and 11 (Hata and Sudhof 1995, Martin-Verdeaux 2002, Cote et al. 2009, zur Stadt et al. 2009). Specifically, Munc18-2 has been shown to interact with the conserved N-peptide of Stx3, providing a positive regulatory role, as well as with its closed conformation

encompassing the H_{abc} and the SNARE motif, to inhibit membrane fusion (Peng et al. 2010).

Consistent with a positive role promoting vesicle fusion, Munc18-2 has been shown to affect several processes that are regulated by Syntaxin 3, such as neurotransmitter receptor exocytosis in neuronal cells (Jurado et al. 2013), apical membrane trafficking in epithelial cells (Al Hawas et al. 2012) or insulin secretion from pancreatic beta cells (Mandic et al. 2011). Similarly, knock down of Munc18-2 led to reduced degranulation from mast cells (Tadokoro et al. 2007) while treatment with antibodies specific for Munc18-2 reduced degranulation from neutrophils (Brochetta et al. 2008). Moreover, platelets from FLH5 patients deficient in Munc18-2 exhibit defective secretion of the contents of their granules (Al Hawas et al. 2012).

It would be intriguing to study the effect of Munc18-2 on FasL trafficking. Given its proven association with Stx3 (confirmed by my microscopy studies that reflected colocalization between the two proteins in CTL) and my results showing an effect of Stx3 on FasL trafficking, it would not be surprising that Stx3-mediated membrane fusion, which somehow enables FasL trafficking, is regulated by Munc18-2.

Interestingly, mutations in Munc18-2 that impair its binding to Stx11 have been recently described to cause familial hemophagocytic lymphohistiocytosis type 5 (FHL5) and cytotoxicity defects in NK and T cells (Cote et al. 2009, zur Stadt et al. 2009). However, the effect of this deficiency on FasL surface expression was not tested. It is also unknown whether defects in Stx11 yield a reduced surface FasL expression. It may prove of interest to study the possibility that the plasma membrane resident Stx11 mediates the fusion of FSVs and that Munc18-2 stabilizes the trans-SNARE complex promoting this fusion.

6.2.3. Rab32

Rab32 belongs to the family of Rab GTPases. As other Rab proteins it can alternate between an inactive GDP-bound conformation and an active GTP-bound

conformation. GTP hydrolysis is necessary for their role in tethering vesicles to the correct target membranes. Rabs in their GTP-bound active state can bind to its effector(s), embedded on the destination membranes, providing specificity to vesicle trafficking. Rab32 localizes specifically to MAMs in HeLa cells and regulates its composition (Bui et al. 2010). Because of its colocalization with FasL, I hypothesized that it may affect FasL trafficking, either to the FSV after endocytosis, or from the storage vesicle to the membrane after stimulation. However, overexpression of a Rab32 dominant negative construct in CTL resulted in no detectable difference on FasL localization and surface expression.

Nonetheless, the colocalization with Rab32 provided additional evidence to support the notion that the FSVs are near the MAMs. MAMs allow for the efficient exchange of Ca^{++} ions from the ER to the mitochondria. Therefore, close proximity to these membranes would allow rapid sensing of intracellular calcium release after TCR engagement and CTL stimulation resulting in efficient triggering of FasL surface translocation. This would explain why the surface expression of stored FasL is not affected by the extracellular Ca^{++} chelator EGTA, as opposed to newly synthesized FasL and degranulation (He et al. 2010).

6.2.4. Markers of the FSV

FasL colocalized with Stx3, Munc18-2 and Rab32 in unstimulated and stimulated CTL, as well as in three different types of non-transformed CTL. These results strongly suggest Stx3, Munc18-2 and Rab32 reside with FasL in the FSV. I propose that these proteins are used henceforth as markers of the FSV to study if different treatments or mutations affect the localization of FasL, as I used them in chapters 4 and 5 of this thesis. These tools might be more needed than originally anticipated. For example, DsRed-FasL transfected in Clone 11 and CTLL-2 cells did not colocalize with Stx3, as endogenous FasL did, suggesting the overexpressed tagged protein accumulated in an aberrant localization and indicating these cell types could not be used to study the trafficking of transfected FasL. Fortunately, DsRed-FasL was transported to $Stx3^{+}$ $LAMP\text{-}1^{-}$ vesicles in

CTL Clone 3/4 cells and I was able to employ these cells for my studies. However, GFP-FasL did not colocalize with Stx3 or Rab32 in transfected Clone 3/4 cells (**Appendix Figure 2**), underlying the need to use these markers to test the correct localization of transfected FasL. In fact, many of the controversial reports stating that FasL is stored within granules have used overexpressed transfected constructs (Bossi and Griffiths 1999, Qian et al. 2006). My results would warrant re-assessing if in their experiments the transfected FasL proteins are trafficking normally.

6.2.5. FSVs are distinct from lysosomal granules

Some authors claim that FasL is stored with granzymes and perforin in lysosomal granules (Bossi and Griffiths 1999, Lettau et al. 2004, Qian et al. 2006, Schmidt et al. 2011b). However, my results showed no colocalization of FasL, Stx3 or Rab32 with perforin or the granule marker LAMP-1. These results strongly indicate that the FSVs and lysosomal granules are two separate compartments characterized by different markers. My results support previous observations made in our laboratory and by others (He and Ostergaard 2007, Kassahn et al. 2009, Schmidt et al. 2011a) and they explain the differences in regulation described for the FasL-mediated and degranulation pathways (He et al. 2010).

These opposing results regarding the storage compartment for FasL suggest there may be certain conditions where both arguments are true. That is, depending on the cell type, the position on the cell growth cycle, the differentiation status of the CTL, the nature and strength of the signals that led to its activation, among many other possibilities, FSVs and granules may traffic to the plasma membrane through an intermediate vesicle containing proteins from both. Consistently, it has been shown that Rab27a and Munc13-4 are stored in separate compartments and only fuse with the lysosomal granules at the immunological synapse. Rab27a allows the tethering of incoming cytolytic granules to the plasma membrane by binding to SLP1 and SLP2 (Holt et al. 2008,

Menasche et al. 2008). Munc13-4 is thought to "prime" Syntaxin 11, the t-SNARE on the plasma membrane, to take it from a closed conformation to an open conformation that enables binding to other SNAREs and formation of the trans-SNARE complex that mediates the fusion of the docked granules (Hong 2005). These two proteins have been shown to reside in a endosomal vesicle separate from the cytolytic granules in unstimulated CTL and to only colocalize with perforin and granzyme B at the immunological synapse after stimulation (Menager et al. 2007). Their trafficking to the surface has even been shown to be responsive to different signals, suggesting Rab27a and Munc13-4 may also be stored separately from each other (Wood et al. 2009). Furthermore, Stx11 has also been shown to reside on yet a separate endosomal compartment in resting NK cells which traffics to the plasma membrane after stimulation to deliver its cargo to the surface (Dabrazhynetskaya et al. 2012). Overall, these results indicate that stimulation of CTL triggers the trafficking of multiple vesicles towards the immunological synapse and that some of them likely fuse before reaching the membrane. It is therefore possible that, depending on the conditions, FasL-containing vesicles could also fuse with some of these vesicles involved in the trafficking of granules, which could result in colocalization with components of the lysosomal granules.

6.3. Trafficking of FasL in CTL

6.3.1. Targeting to FSVs

Antibodies specific for FasL incubated with non-permeabilized resting CTL could be detected inside the cells in FSVs after confocal microscopy analysis. These results suggested that FasL travels to the plasma membrane and is then endocytosed and transported to its storage vesicle. This could indicate that after its biosynthesis FasL is transported to the surface, probably via the constitutive default secretion pathway, and then directed to its vesicle from the membrane. However, the protein synthesis inhibitor cyclohexamide did not affect

this process, indicating the antibodies used in the endocytosis assay detected the presence of surface proteins synthesized prior to the treatment. Therefore, an alternative trafficking route may be proposed: FasL could be intracellularly targeted to its FSV and then transported to the plasma membrane from where it would be recycled back to the FSV.

Although I have no evidence to distinguish between these two possibilities, or from a third alternative encompassing both mechanisms, the surface expression of transfected FasL in COS-1 cells favors the first option. These results suggest that FasL is probably secreted via the constitutive secretion pathway both in fibroblasts and T cells, but that the latter posses specialized machinery that allows them to either recognize and/or execute the N-terminal endocytosis signals of FasL.

FasL mutants with deletions in the N-terminal end of the cytoplasmic tail (Δ2-43), in the proline-rich domain (ΔPRD) or that lacked three lysines near the transmembrane domain (Δ3K), showed accumulation on the surface when transfected into CTL. These results suggest that the cytoplasmic tail contains sequences necessary for the efficient endocytosis of FasL from the plasma membrane. These three deletions could not define the specific amino acids involved in signaling endocytosis suggesting the signal may be distributed throughout the tail. These could come together as a result of three-dimensional folding or they may play separate but cooperative functions regulating the endocytosis of FasL.

Point mutation of asparagine 182, on the external domain of FasL, also led to FasL surface accumulation when transfected into CTL. This site is a putative site for N-glycosylation so this result indicated glycosylation of FasL is also important for its efficient endocytosis. Although I cannot exclude the possibility that glycosylation may be somehow recognized by a surface endocytic machinery, I favor a scenario in which glycosylation directs FasL to lipid rafts in the plasma membrane. In support of this alternative, N-glycosylation has been shown to promote lipid raft localization of other proteins (Morenilla-Palao et al. 2009, Pagano et al. 2009, Chen et al. 2011) and FasL has been shown to accumulate in

lipid rafts (Cahuzac et al. 2006, Nachbur et al. 2006). Within lipid rafts, FasL may then be endocytosed using a non-classical lipid raft-dependent mechanism. According to this theory, abrogation of glycosylation in N182 would result in mistargeting of FasL to non-lipid raft sections of the membrane and inefficient non-lipid raft-dependent endocytosis. More experiments are needed to establish the way glycosylation affects endocytosis of FasL.

It is important to note that although the mutations decrease FasL endocytosis, they do not completely abolish it, since some FasL molecules can still be detected in intracellular vesicles. This could be due to low-rate basal endocytic membrane trafficking, previously described for CD4 and the Fc receptor in immune cells (Pelchen-Matthews et al. 1991, Miettinen et al. 1992).

After being endocytosed from the surface, FasL is transported to its FSV. Deletion or point mutation of lysines 71, 72 and 73 led to mistargeting of FasL to $Stx3^{-}$ $LAMP\text{-}1^{+}$ vesicles. Thus, these three amino acids provide the necessary signal to target FasL to the right vesicle. Since I could not detect evidence of ubiquitination or SUMOylation, I hypothesize that these residues serve as a binding motif for an unidentified protein that direct FasL to its vesicle. Consistently, three-dimensional modeling of the cytoplasmic tail of FasL predicts solvent accessibility of these residues (**Figure 6.1**). It would be interesting to determine if the positive charge of these amino acids has a role in FasL trafficking. Intriguingly, other members of the TNF ligand superfamily, LIGHT and TWEAK, also contain 3-4 positively charged residues in their cytoplasmic tail in a position near to the membrane, similar to FasL (**Figure 6.2**). Moreover, positively charged amino acids have been shown to mediate trafficking to specialized intracellular compartments, such as peroxisomes (Baerends 2000, Mullen and Trelease 2000).

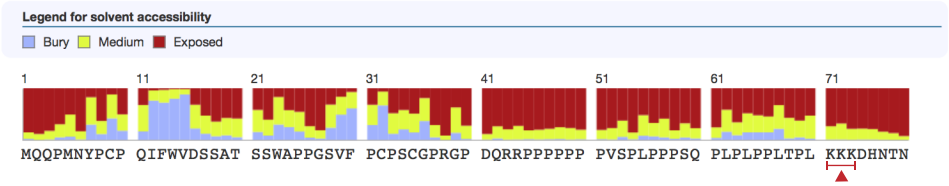

Figure 6.1. Lysines 71, 72 and 73 are exposed to the solvent.
Three-dimensional structure and solvent accessibility were predicted for the cytoplasmic tail of FasL using the Raptor X web server (Peng and Xu 2011a, Peng and Xu 2011b, Kallberg et al. 2012, Ma et al. 2013)

FasL

MQQPMNYPCPQIFWVDSSATSSWAPPGSVFPCPSCGPRGPDQRRPPPPPPPVSPLPPPS
QPLPLPPLTPLKKKDHNTNLWLPVVFFMVLVALVGMGLGMYQLFHLQKELAELREFTNQ
SLKVSSFEKQIANPSTPSEKKEPRSVAHLTGNPHSRSIPLEWEDTYGTALISGVKYKKG
GLVINETGLYFVYSKVYFRGQSCNNQPLNHKVYMRNSKYPEDLVLMEEKRLNYCTTGQI
WAHSSYLGAVFNLTSADHLYVNISQLSLINFEESKTFFGLYKL

LIGHT

MESVVQPSVFVVDGQTDIPFRRLEQNHRRRRCGTVQVSLALVLLLGAGLATQGWFLLRL
HQRLGDIVAHLPDGGKGSWEKLIQDQRSHQANPAAHLTGANASLIGIGGPLLWETRLGL
AFLRGLTYHDGALVTMEPGYYYVYSKVQLSGVGCPQGLANGLPITHGLYKRTSRYPKEL
ELLVSRRSPCGRANSSRVWWDSSFLGGVVHLEAGEEVVVRVPGNRLVRPRDGTRSYFGA
FMV

TWEAK

MAARRSQRRRGRRGEPGTALLAPLVLSLGLALACLGLLLVVVSLGSWATLSAQEPSQEE
LTAEDRREPPELNPQTEESQDVVPFLEQLVRPRRSAPKGRKARPRRAIAAHYEVHPRPG
QDGAQAGVDGTVSGWEETKINSSSPLRYDRQIGEFTVIRAGLYYLYCQVHFDEGKAVYL
KLDLLVNGVLALRCLEEFSATAASSPGPQLRLCQVSGLLPLRPGSSLRIRTLPWAHLKA
APFLTYFGLFQVH

Figure 6.2. LIGHT and TWEAK contain 3-4 positively charged residues near the transmembrane domain, similar to FasL.
The transmembrane domains of FasL, LIGHT and TWEAK were predicted using the DAS web server (Cserzo et al. 1997) and were depicted with red font on the protein sequences. The positively charged residues are highlighted on blue.

6.3.2. Trafficking to the surface upon stimulation

After stimulation of CTL, FasL is expressed on the surface where it exerts its function. Although much research has been done, the mechanisms involved in FasL surface trafficking are still largely unknown. In my thesis, I showed that inhibition of myosin by blebbistatin led to reduced surface FasL expression after CTL stimulation. These results indicated myosin might regulate the trafficking of the FasL-containing vesicles, in a similar manner as they have been shown to promote the last steps of lytic granule mobilization in NK cells (Sanborn et al. 2009). Nonetheless, since blebbistatin has been shown to affect the intracellular Ca^{++} flux after TCR stimulation (Yu et al. 2012), it may also have an indirect effect by blocking the Ca^{++} signal that triggers the surface translocation of FasL. Furthermore, as discussed above, my results could provide the first indication of a Stx3-mediated compound exocytosis mechanism for the translocation of FasL after stimulation, although further research is needed to confirm this hypothesis.

Nonetheless, my findings also suggested that FasL traffics through the surface and may continuously cycle between the plasma membrane and the FSV in non-stimulated CTL. These results indicate two general alternatives for the trafficking of FasL to the surface after stimulation. The first assumes that stimulation-triggered FasL surface expression activates a previously dormant mechanism that either releases or stops the retention of FasL to mobilize the FSVs to the surface. If this option were true, it would indicate there are two independent ways FasL can reach the membrane: steady-state recycling and regulated release upon TCR stimulation. In the second scenario, surface FasL expression after stimulation could be the result of endocytosis blockage (for example by receptor binding) or saturation of the endocytic machinery due to large numbers of FasL molecules on the surface. The rapid accumulation of surface FasL observed after stimulation and the directionality towards the point of contact with the target cell (He et al. 2010) favor the first option, although my findings do not fully support or negate either alternative.

6.4. Model of FasL trafficking

In light of the results from chapter 3, 4 and 5 discussed above, I propose the model depicted in **Figure 6.3** for FasL trafficking in CTL. After its biosynthesis in the ER and Golgi, FasL would be translocated to the cell surface from the *trans*-Golgi network as part of the default constitutive secretion pathway. N-glycosylation in asparagine 182 might direct the protein towards lipid raft areas of the plasma membrane. On the surface, the cytoplasmic tail of FasL would signal its endocytosis and lysines 71, 72 and 73 would target it to the FSV composed of Stx3, Munc18-2 and Rab32. When CTL encounter a target cell bearing the correct peptide-MHC, the TCR triggers a signaling cascade that results in the release of Ca^{++} ions from the ER. Being in close proximity to the MAMs, this flux of Ca^{++} would be readily sensed and FasL would be transported to the surface possibly aided by myosin II and using a Stx3-mediated compound exocytosis mechanism.

Additionally, **Figure 6.4** depicts a model for trafficking of transfected FasL in COS-1 cells. I propose that FasL is translocated to the surface of these cells via the constitutive secretion pathway, for which N-glycosylation in asparagine 258 is required, but because these cells lack the specialized endocytic machinery to recognize and/or to mediate active endocytosis of FasL, most of the FasL molecules are accumulated on the surface. Basal non-specific endocytosis would allow for inefficient endocytosis into the default endocytic destination, i.e. $LAMP\text{-}1^{+}$ lysosomes, accounting for the few intracellular molecules observed in transfected COS-1 cells.

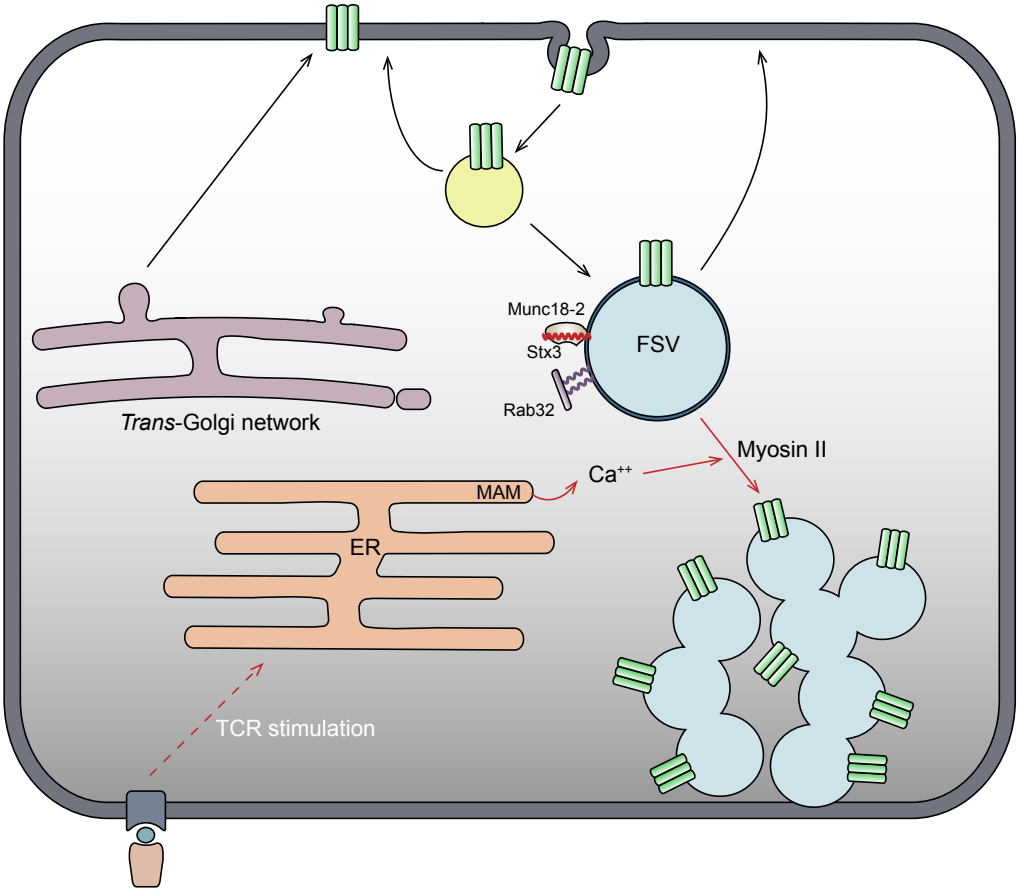

Figure 6.3. Model for trafficking of FasL in CTL.
After its biosynthesis FasL would be secreted from the *trans*-Golgi network as part of the default constitutive pathway. On the surface, the cytoplasmic tail of FasL would signal its endocytosis and lysines 71, 72 and 73 would target it to the FSV composed of Stx3, Munc18-2 and Rab32. Membrane recycling of FasL molecules could happen from endosomes or FSVs. When CTL encounter a target cell bearing the correct peptide-MHC, the TCR triggers a signaling cascade that results in the release of Ca^{++} ions from the ER. Being in close proximity to the MAMs, this flux of Ca^{++} would be readily sensed and FasL would be transported to the surface possibly aided by myosin II and using a Stx3-mediated compound exocytosis mechanism.

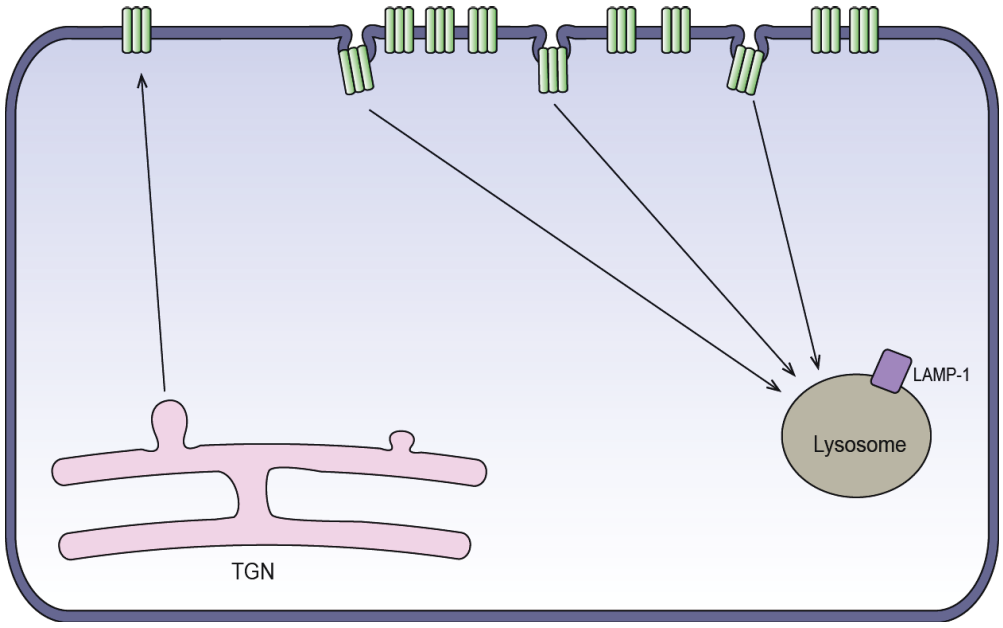

Figure 6.4. Model for trafficking of FasL in COS-1 cells.
FasL is translocated to the surface of these cells via the constitutive secretion pathway, for which N-glycosylation in asparagine 258 is required, but because these cells lack the specialized endocytic machinery to recognize and/or to mediate active endocytosis of FasL, most of the FasL molecules are accumulated on the surface. Basal non-specific endocytosis would allow for inefficient endocytosis into the default endocytic destination, i.e. LAMP-1^{+} lysosomes.

6.5. Future directions

6.5.1. Trafficking to FSVs

Although I showed FasL traffics through the surface, I could not determine whether it reached the plasma membrane after being secreted from the TGN, as part of the default constitutive secretion pathway, or if it was recycled to the surface after being intracellularly targeted to its FSV. In the future, it would be important to determine which route(s) FasL follows after its biosynthesis. To determine this, one could use *fasl* KO CTL transfected with a plasmid expressing FasL under an inducible promoter. Endocytosis could then be blocked at the same time that expression is induced and the resulting localization of the newly-synthesized FasL proteins could be determined by confocal microscopy. If they accumulate on the surface, it would indicate that they are secreted from the Golgi after their biosynthesis and if they accumulate in intracellular $Stx3^+$ vesicles, it would indicate an intracellular targeting mechanism is at play.

To block endocytosis, it would first be necessary to determine which endocytosis mechanism is responsible for FasL internalization in CTL. There are several mechanisms for surface endocytosis. The classical pathway involves the coat protein clathrin and is thus known as clathrin-dependent. Many other adaptor proteins, such as AP-2, Epsin or Eps15, are involved in the recognition of endocytosis motifs within the cargo proteins and the recruitment of clathrin coats. Moreover, coated pits pinch off from the plasma membrane with the assistance of dynamin, a GTPase that provides the energy to promote membrane fission (Mousavi et al. 2004). Non-classical pathways, or lipid-raft-dependent, encompass a number of different pathways that occur within the lipid rafts areas of the plasma membrane. The most studied one is the caveolae-mediated endocytosis characterized by vesicles containing the protein caveolin. This pathway also depends on the dynamin protein for its separation from the membrane (Mayor and Pagano 2007). Other lipid raft-dependent and caveolin-independent mechanisms are also possible but are less understood. For example,

the β subunit of the IL-2 receptor is internalized by a clathrin and caveolin-independent mechanism that requires dynamin and the small GTPase RhoA (Lamaze et al. 2001). Additionally, two dynamin-independent endocytosis mechanisms have been described to use the GTPases Cdc42 or ARF6 (Mayor and Pagano 2007).

To study which of these mechanisms mediates FasL endocytosis, it would be important to test the effect of K^+ depletion or the transfection of dominant-negative mutants of Eps15, which block clathrin-dependent endocytosis (Di Guglielmo et al. 2003). The effect of depleting cholesterol would indicate if FasL is endocytosed via a lipid-raft dependent mechanism and co-staining with caveolin could suggest that it uses a caveolae-mediated pathway. Additional classification could be achieved by studying FasL endocytosis in cells treated with genistein (a general tyrosine kinase inhibitor), PP2 (a Src family kinase inhibitor) or *Clostridium* toxin B, or in cells transfected with dominant-negative mutants of RhoA, Cdc42 or ARF6, as it has been described before (Mayor and Pagano 2007).

The FasL mutant that replaced asparagine 182 for glutamine accumulated on the surface and in intracellular LAMP-1^+ vesicles. I hypothesized that this mistargeting could be explained by abrogated N-glycosylation and defective delivery to lipid raft areas of the membrane, followed by ineffective endocytosis and inadequate targeting. If lipid raft-dependent mechanisms prove to mediate FasL endocytosis, it would support this hypothesis. Moreover, it would be interesting to evaluate if FasL N182Q fails to localize to lipid rafts and what type of mechanism facilitates its inefficient endocytosis.

Furthermore, it would be interesting to specifically map the sequences in the cytoplasmic tail that signal the endocytosis of FasL. With this purpose, mutant constructs with smaller deletions could be used in experiments similar to those described in chapter 5. Additionally, future studies should focus on understanding if the polar nature of the three cytoplasmic lysines is important for their role in targeting FasL to FSVs. It would be interesting to transfect a FasL mutant construct that replaces these residues for arginines and evaluate if the protein is correctly targeted to Stx3^+ vesicles. If the positive charge in these residues serves

as a signal for targeting, it would also be of interest to evaluate if LIGHT and TWEAK are targeted to FSVs. Consistently, LIGHT has been shown to localize to intracellular vesicles in *ex vivo* T cells from where it is transported to the cell surface upon T cell stimulation (Morel et al. 2000).

6.5.2. Trafficking to the surface upon stimulation

When CTL encounter a target cell, the expression of surface FasL is rapidly detected on the surface. I hypothesized that a mechanism of compound exocytosis mediates the transport of FasL-containing vesicles to the surface. Compound exocytosis is traditionally evaluated using time-resolved capacitance measurements that follow the step increases in surface area that result from the fusion of secretory granules with the plasma membrane. The size of the steps can determine the size of the granule and large steps indicate compound exocytosis (Alvarez de Toledo 1990). It would be necessary to inhibit degranulation (via Ca^{++} chelation) to specifically determine the mechanism of FasL trafficking. The aggregation of FSVs prior or during exocytosis could be further corroborated by using electron microscopy. I also hypothesized that Stx3 would allow for FSV-FSV fusion events. Thus, knockdown of Stx3 or inhibition using the Botulinum toxin serotype C, should be useful to corroborate its effect on FasL surface trafficking.

It would be of great interest to identify the v-SNARE present on the FSV that mediates its fusion, both in the SNARE complex with Stx3 for FSV-FSV fusion events, if FasL is translocated using a compound exocytosis mechanism, and/or with the plasma membrane for those vesicles that fuse with the surface to deliver FasL. Stx3 has been shown to form trans-SNARE complexes with the t-SNARE SNAP-23 and the v-SNAREs VAMP-7 and VAMP-8 (Pombo et al. 2003, Cosen-Binker et al. 2008, Frank et al. 2011, Yatsu et al. 2013). Future studies should therefore analyze the colocalization of FasL with VAMP-7 and VAMP-8, which are expressed in CTL (Pattu et al. 2012). These studies may provide an additional marker for the FSV. Moreover, knock down of these

proteins would interfere with the fusion of FasL-containing vesicles thus confirming their role in FasL surface translocation.

My results showed that inhibition of myosin led to reduced FasL surface expression after stimulation. This could indicate that myosin II is involved in promoting the movement of FSVs after stimulation. However, because myosin inhibition has been shown to disrupt the intracellular Ca^{++} flux after TCR stimulation (Yu et al. 2012), using inhibitors may prove inefficient to distinguish between a direct or indirect effect on FasL. Evaluating the colocalization of myosin II and FasL in CTL treated or not with blebbistatin could indicate whether myosin has a direct role in the transport of FSVs.

The final step on the traffic of FSVs to the surface would involve the fusion of these vesicles with the plasma membrane. The major proteins involved in this step would be: a Rab protein on the vesicle, tethering factors on the membrane, a v-SNARE on the FSVs, t-SNAREs on the membrane, and possibly Munc18 proteins to promote the formation of the SNARE complex and Munc13 proteins to "prime" the t-SNAREs. None of these components have been identified yet. For the membrane fusion of lysosomal granules, exocytic vesicles containing Rab27 and Munc13-4 fuse with the granules after TCR stimulation near the immunological synapse and provide them with part of these necessary proteins (Menager et al. 2007). Colocalization of FasL with Munc13-4 and Rab27a before and after target cell stimulation has not been yet tested and could indicate whether these proteins also mediate the tethering and priming for FSV fusion to the membrane. Moreover, Syntaxin 11 is also transported to the surface upon stimulation to serve as the t-SNARE in the trans-SNARE complex that fuses the granules with the surface (Dabrazhynetskaya et al. 2012). It would be interesting to investigate if Stx11, and its associated protein Munc18-2, also mediates the fusion of FSVs with the plasma membrane. These results would suggest that stimulation of CTL triggers the activation of a common mechanism that facilitates the fusion of its two distinct cytolytic vesicles: granules and FSVs.

REFERENCES

Acuto, O. and D. Cantrell (2000). "T cell activation and the cytoskeleton." Annu Rev Immunol **18**: 165-184.

Al Hawas, R., Q. Ren, S. Ye, Z. A. Karim, A. H. Filipovich and S. W. Whiteheart (2012). "Munc18b/STXBP2 is required for platelet secretion." Blood **120**(12): 2493-2500.

Alvarez de Toledo, G. and J. M. Fernandez (1990). "Compound versus multigranular exocytosis in peritoneal mast cells." J Gen Physiol **95**(3): 397-409.

Andreola, G. (2002). "Induction of Lymphocyte Apoptosis by Tumor Cell Secretion of FasL-bearing Microvesicles." Journal of Experimental Medicine **195**(10): 1303-1316.

Appelqvist, H., P. Waster, I. Eriksson, I. Rosdahl and K. Ollinger (2013). "Lysosomal exocytosis and caspase-8-mediated apoptosis in UVA-irradiated keratinocytes." J Cell Sci **126**(Pt 24): 5578-5584.

Arnaoutova, I., C. L. Jackson, O. S. Al-Awar, J. G. Donaldson and Y. P. Loh (2003). "Recycling of Raft-associated prohormone sorting receptor carboxypeptidase E requires interaction with ARF6." Mol Biol Cell **14**(11): 4448-4457.

Baerends, R. J. S. (2000). "A Stretch of Positively Charged Amino Acids at the N Terminus of Hansenula polymorpha Pex3p Is Involved in Incorporation of the Protein into the Peroxisomal Membrane." Journal of Biological Chemistry **275**(14): 9986-9995.

Baker, S. J. and E. P. Reddy (1998). "Modulation of life and death by the TNF receptor superfamily." Oncogene **17**(25): 3261-3270.

Barry, M. and R. C. Bleackley (2002). "Cytotoxic T lymphocytes: all roads lead to death." Nat Rev Immunol **2**(6): 401-409.

Bellgrau, D., D. Gold, H. Selawry, J. Moore, A. Franzusoff and R. C. Duke (1995). "A role for CD95 ligand in preventing graft rejection." Nature **377**(6550): 630-632.

Beresford, P. J., D. Zhang, D. Y. Oh, Z. Fan, E. L. Greer, M. L. Russo, M. Jaju and J. Lieberman (2001). "Granzyme A activates an endoplasmic reticulum-associated caspase-independent nuclease to induce single-stranded DNA nicks." J Biol Chem **276**(46): 43285-43293.

Berg, J. S., B. C. Powell and R. E. Cheney (2001). "A millennial myosin census." Mol Biol Cell **12**(4): 780-794.

Berrebi, G., H. Takayama and M. V. Sitkovsky (1987). "Antigen-receptor interaction requirement for conjugate formation and lethal-hit triggering by cytotoxic T lymphocytes can be bypassed by protein kinase C activators and Ca2+ ionophores." Proc Natl Acad Sci U S A **84**(5): 1364-1368.

Black, R. A., C. T. Rauch, C. J. Kozlosky, J. J. Peschon, J. L. Slack, M. F. Wolfson, B. J. Castner, K. L. Stocking, P. Reddy, S. Srinivasan, N. Nelson, N. Boiani, K. A. Schooley, M. Gerhart, R. Davis, J. N. Fitzner, R. S. Johnson, R. J. Paxton, C. J. March and D. P. Cerretti (1997). "A metalloproteinase disintegrin that releases tumour-necrosis factor-alpha from cells." Nature **385**(6618): 729-733.

Blott, E. J., G. Bossi, R. Clark, M. Zvelebil and G. M. Griffiths (2001). "Fas ligand is targeted to secretory lysosomes via a proline-rich domain in its cytoplasmic tail." J Cell Sci **114**(Pt 13): 2405-2416.

Blott, E. J. and G. M. Griffiths (2002). "Secretory lysosomes." Nat Rev Mol Cell Biol **3**(2): 122-131.

Bodmer, J. L., P. Schneider and J. Tschopp (2002). "The molecular architecture of the TNF superfamily." Trends Biochem Sci **27**(1): 19-26.

Bodor, J., J. Bodorova, C. Bare, D. L. Hodge, H. A. Young and R. E. Gress (2002). "Differential inducibility of the transcriptional repressor ICER and its role in modulation of Fas ligand expression in T and NK lymphocytes." Eur J Immunol **32**(1): 203-212.

Bogan, J. S. and K. V. Kandror (2010). "Biogenesis and regulation of insulin-responsive vesicles containing GLUT4." Curr Opin Cell Biol **22**(4): 506-512.

Bonifacino, J. S. and B. S. Glick (2004). "The mechanisms of vesicle budding and fusion." Cell **116**(2): 153-166.

Bossen, C., T. G. Cachero, A. Tardivel, K. Ingold, L. Willen, M. Dobles, M. L. Scott, A. Maquelin, E. Belnoue, C. A. Siegrist, S. Chevrier, H. Acha-Orbea, H. Leung, F. Mackay, J. Tschopp and P. Schneider (2008). "TACI, unlike BAFF-R, is solely activated by oligomeric BAFF and APRIL to support survival of activated B cells and plasmablasts." Blood **111**(3): 1004-1012.

Bossi, G. and G. M. Griffiths (1999). "Degranulation plays an essential part in regulating cell surface expression of Fas ligand in T cells and natural killer cells." Nat Med **5**(1): 90-96.

Boursalian, T. E. and P. J. Fink (2003). "Mutation in fas ligand impairs maturation of thymocytes bearing moderate affinity T cell receptors." J Exp Med **198**(2): 349-360.

Brennan, A. J., J. Chia, K. A. Browne, A. Ciccone, S. Ellis, J. A. Lopez, O. Susanto, S. Verschoor, H. Yagita, J. C. Whisstock, J. A. Trapani and I. Voskoboinik (2011). "Protection from endogenous perforin: glycans and the C terminus regulate exocytic trafficking in cytotoxic lymphocytes." Immunity **34**(6): 879-892.

Brennan, J., D. Mager, W. Jefferies and F. Takei (1994). "Expression of different members of the Ly-49 gene family defines distinct natural killer cell subsets and cell adhesion properties." J Exp Med **180**(6): 2287-2295.

Brochetta, C., R. Suzuki, F. Vita, M. R. Soranzo, J. Claver, L. C. Madjene, T. Attout, J. Vitte, N. Varin-Blank, G. Zabucchi, J. Rivera and U. Blank (2014). "Munc18-2 and syntaxin 3 control distinct essential steps in mast cell degranulation." J Immunol **192**(1): 41-51.

Brochetta, C., F. Vita, N. Tiwari, L. Scandiuzzi, M. R. Soranzo, C. Guerin-Marchand, G. Zabucchi and U. Blank (2008). "Involvement of Munc18 isoforms in the regulation of granule exocytosis in neutrophils." Biochim Biophys Acta **1783**(10): 1781-1791.

Brunner, T. (2003). "Fas (CD95/Apo-1) ligand regulation in T cell homeostasis, cell-mediated cytotoxicity and immune pathology." Seminars in Immunology **15**(3): 167-176.

Bryceson, Y. T., E. Rudd, C. Zheng, J. Edner, D. Ma, S. M. Wood, A. G. Bechensteen, J. J. Boelens, T. Celkan, R. A. Farah, K. Hultenby, J. Winiarski, P. A. Roche, M. Nordenskjold, J. I. Henter, E. O. Long and H. G. Ljunggren (2007). "Defective cytotoxic lymphocyte degranulation in syntaxin-11 deficient familial hemophagocytic lymphohistiocytosis 4 (FHL4) patients." Blood **110**(6): 1906-1915.

Brzezinska, A. A., J. L. Johnson, D. B. Munafo, K. Crozat, B. Beutler, W. B. Kiosses, B. A. Ellis and S. D. Catz (2008). "The Rab27a effectors JFC1/Slp1 and Munc13-4 regulate exocytosis of neutrophil granules." Traffic **9**(12): 2151-2164.

Bucci, C., P. Thomsen, P. Nicoziani, J. McCarthy and B. van Deurs (2000). "Rab7: a key to lysosome biogenesis." Mol Biol Cell **11**(2): 467-480.

Bui, M., S. Y. Gilady, R. E. Fitzsimmons, M. D. Benson, E. M. Lynes, K. Gesson, N. M. Alto, S. Strack, J. D. Scott and T. Simmen (2010). "Rab32 modulates apoptosis onset and mitochondria-associated membrane (MAM) properties." J Biol Chem **285**(41): 31590-31602.

Burgess, T. L. and R. B. Kelly (1987). "Constitutive and regulated secretion of proteins." Annu Rev Cell Biol **3**: 243-293.

Burkhardt, J. K., S. Hester, C. K. Lapham and Y. Argon (1990). "The lytic granules of natural killer cells are dual-function organelles combining secretory and pre-lysosomal compartments." J Cell Biol **111**(6 Pt 1): 2327-2340.

Cabrera, A., S. Herrmann, D. Warszta, J. M. Santos, A. T. John Peter, M. Kono, S. Debrouver, T. Jacobs, T. Spielmann, C. Ungermann, D. Soldati-Favre and T. W. Gilberger (2012). "Dissection of minimal sequence requirements for rhoptry membrane targeting in the malaria parasite." Traffic **13**(10): 1335-1350.

Cahuzac, N., W. Baum, V. Kirkin, F. Conchonaud, L. Wawrezinieck, D. Marguet, O. Janssen, M. Zornig and A. O. Hueber (2006). "Fas ligand is localized

to membrane rafts, where it displays increased cell death-inducing activity." Blood **107**(6): 2384-2391.

Caldwell, S. A., M. H. Ryan, E. McDuffie and S. I. Abrams (2003). "The Fas/Fas ligand pathway is important for optimal tumor regression in a mouse model of CTL adoptive immunotherapy of experimental CMS4 lung metastases." J Immunol **171**(5): 2402-2412.

Carlsson, S. R. and M. Fukuda (1992). "The lysosomal membrane glycoprotein lamp-1 is transported to lysosomes by two alternative pathways." Arch Biochem Biophys **296**(2): 630-639.

Carlsson, S. R., J. Roth, F. Piller and M. Fukuda (1988). "Isolation and characterization of human lysosomal membrane glycoproteins, h-lamp-1 and h-lamp-2. Major sialoglycoproteins carrying polylactosaminoglycan." J Biol Chem **263**(35): 18911-18919.

Carr, C. M. and J. Rizo (2010). "At the junction of SNARE and SM protein function." Curr Opin Cell Biol **22**(4): 488-495.

Catalfamo, M. and P. A. Henkart (2003). "Perforin and the granule exocytosis cytotoxicity pathway." Current Opinion in Immunology **15**(5): 522-527.

Catalfamo, M., T. Karpova, J. McNally, S. V. Costes, S. J. Lockett, E. Bos, P. J. Peters and P. A. Henkart (2004). "Human CD8+ T cells store RANTES in a unique secretory compartment and release it rapidly after TcR stimulation." Immunity **20**(2): 219-230.

Chen, G., A. G. Howe, G. Xu, O. Frohlich, J. D. Klein and J. M. Sands (2011). "Mature N-linked glycans facilitate UT-A1 urea transporter lipid raft compartmentalization." FASEB J **25**(12): 4531-4539.

Chen, X., J. Lu, I. Dulubova and J. Rizo (2008). "NMR analysis of the closed conformation of syntaxin-1." J Biomol NMR **41**(1): 43-54.

Chen, Y. A. and R. H. Scheller (2001). "SNARE-mediated membrane fusion." Nat Rev Mol Cell Biol **2**(2): 98-106.

Chinnaiyan, A. M., C. G. Tepper, M. F. Seldin, K. O'Rourke, F. C. Kischkel, S. Hellbardt, P. H. Krammer, M. E. Peter and V. M. Dixit (1996).

"FADD/MORT1 is a common mediator of CD95 (Fas/APO-1) and tumor necrosis factor receptor-induced apoptosis." J Biol Chem **271**(9): 4961-4965.

Cippitelli, M., C. Fionda, D. Di Bona, F. Di Rosa, A. Lupo, M. Piccoli, L. Frati and A. Santoni (2002). "Negative Regulation of CD95 Ligand Gene Expression by Vitamin D3 in T Lymphocytes." The Journal of Immunology **168**(3): 1154-1166.

Cosen-Binker, L. I., M. G. Binker, C. C. Wang, W. Hong and H. Y. Gaisano (2008). "VAMP8 is the v-SNARE that mediates basolateral exocytosis in a mouse model of alcoholic pancreatitis." J Clin Invest **118**(7): 2535-2551.

Cote, M., M. M. Menager, A. Burgess, N. Mahlaoui, C. Picard, C. Schaffner, F. Al-Manjomi, M. Al-Harbi, A. Alangari, F. Le Deist, A. R. Gennery, N. Prince, A. Cariou, P. Nitschke, U. Blank, G. El-Ghazali, G. Menasche, S. Latour, A. Fischer and G. de Saint Basile (2009). "Munc18-2 deficiency causes familial hemophagocytic lymphohistiocytosis type 5 and impairs cytotoxic granule exocytosis in patient NK cells." J Clin Invest **119**(12): 3765-3773.

Croft, M. (2003). "Costimulation of T cells by OX40, 4-1BB, and CD27." Cytokine & Growth Factor Reviews **14**(3-4): 265-273.

Cronin, S. J. and J. M. Penninger (2007). "From T-cell activation signals to signaling control of anti-cancer immunity." Immunol Rev **220**: 151-168.

Cserzo, M., E. Wallin, I. Simon, G. von Heijne and A. Elofsson (1997). "Prediction of transmembrane alpha-helices in prokaryotic membrane proteins: the dense alignment surface method." Protein Eng **10**(6): 673-676.

Curtsinger, J. M. and M. F. Mescher (2010). "Inflammatory cytokines as a third signal for T cell activation." Curr Opin Immunol **22**(3): 333-340.

D'Angelo, M. E., P. I. Bird, C. Peters, T. Reinheckel, J. A. Trapani and V. R. Sutton (2010). "Cathepsin H is an additional convertase of pro-granzyme B." J Biol Chem **285**(27): 20514-20519.

d'Azzo, A., A. Bongiovanni and T. Nastasi (2005). "E3 ubiquitin ligases as regulators of membrane protein trafficking and degradation." Traffic **6**(6): 429-441.

D'Souza-Schorey, C. and P. Chavrier (2006). "ARF proteins: roles in membrane traffic and beyond." Nat Rev Mol Cell Biol **7**(5): 347-358.

Dabrazhynetskaya, A., J. Ma, A. O. Guerreiro-Cacais, Z. Arany, E. Rudd, J. I. Henter, K. Karre, J. Levitskaya and V. Levitsky (2012). "Syntaxin 11 marks a distinct intracellular compartment recruited to the immunological synapse of NK cells to colocalize with cytotoxic granules." J Cell Mol Med **16**(1): 129-141.

de Saint Basile, G., G. Menasche and A. Fischer (2010). "Molecular mechanisms of biogenesis and exocytosis of cytotoxic granules." Nat Rev Immunol **10**(8): 568-579.

Del-Rey, M., J. Ruiz-Contreras, A. Bosque, S. Calleja, J. Gomez-Rial, E. Roldan, P. Morales, A. Serrano, A. Anel, E. Paz-Artal and L. M. Allende (2006). "A homozygous Fas ligand gene mutation in a patient causes a new type of autoimmune lymphoproliferative syndrome." Blood **108**(4): 1306-1312.

Delacour, D., C. I. Cramm-Behrens, H. Drobecq, A. Le Bivic, H. Y. Naim and R. Jacob (2006). "Requirement for galectin-3 in apical protein sorting." Curr Biol **16**(4): 408-414.

Dell'Angelica, E. C., C. Mullins, S. Caplan and J. S. Bonifacino (2000). "Lysosome-related organelles." FASEB J **14**(10): 1265-1278.

Di Guglielmo, G. M., C. Le Roy, A. F. Goodfellow and J. L. Wrana (2003). "Distinct endocytic pathways regulate TGF-beta receptor signalling and turnover." Nat Cell Biol **5**(5): 410-421.

Dobrzanski, M. J., J. B. Reome, J. A. Hollenbaugh, J. C. Hylind and R. W. Dutton (2004). "Effector cell-derived lymphotoxin alpha and Fas ligand, but not perforin, promote Tc1 and Tc2 effector cell-mediated tumor therapy in established pulmonary metastases." Cancer Res **64**(1): 406-414.

Dou, Y., P. Arlock and A. Arner (2007). "Blebbistatin specifically inhibits actin-myosin interaction in mouse cardiac muscle." Am J Physiol Cell Physiol **293**(3): C1148-1153.

Dressel, R., S. M. Raja, S. Honing, T. Seidler, C. J. Froelich, K. von Figura and E. Gunther (2004). "Granzyme-mediated cytotoxicity does not involve

the mannose 6-phosphate receptors on target cells." J Biol Chem **279**(19): 20200-20210.

Dulubova, I., S. Sugita, S. Hill, M. Hosaka, I. Fernandez, T. C. Sudhof and J. Rizo (1999). "A conformational switch in syntaxin during exocytosis: role of munc18." EMBO J **18**(16): 4372-4382.

Dustin, M. L. and E. O. Long (2010). "Cytotoxic immunological synapses." Immunol Rev **235**(1): 24-34.

Faris, M., K. M. Latinis, S. J. Kempiak, G. A. Koretzky and A. Nel (1998). "Stress-induced Fas ligand expression in T cells is mediated through a MEK kinase 1-regulated response element in the Fas ligand promoter." Mol Cell Biol **18**(9): 5414-5424.

Feldmann, J., I. Callebaut, G. Raposo, S. Certain, D. Bacq, C. Dumont, N. Lambert, M. Ouachee-Chardin, G. Chedeville, H. Tamary, V. Minard-Colin, E. Vilmer, S. Blanche, F. Le Deist, A. Fischer and G. de Saint Basile (2003). "Munc13-4 is essential for cytolytic granules fusion and is mutated in a form of familial hemophagocytic lymphohistiocytosis (FHL3)." Cell **115**(4): 461-473.

Frangsmyr, L., V. Baranov, O. Nagaeva, U. Stendahl, L. Kjellberg and L. Mincheva-Nilsson (2005). "Cytoplasmic microvesicular form of Fas ligand in human early placenta: switching the tissue immune privilege hypothesis from cellular to vesicular level." Mol Hum Reprod **11**(1): 35-41.

Frank, S. P., K. P. Thon, S. C. Bischoff and A. Lorentz (2011). "SNAP-23 and syntaxin-3 are required for chemokine release by mature human mast cells." Mol Immunol **49**(1-2): 353-358.

Gao, Y. s. (1998). "Molecular Cloning, Characterization, and Dynamics of Rat Formiminotransferase Cyclodeaminase, a Golgi-associated 58-kDa Protein." Journal of Biological Chemistry **273**(50): 33825-33834.

Gasser, O., A. Missiou, C. Eken and C. Hess (2005). "Human CD8+ T cells store CXCR1 in a distinct intracellular compartment and up-regulate it rapidly to the cell surface upon activation." Blood **106**(12): 3718-3724.

Geiss-Friedlander, R. and F. Melchior (2007). "Concepts in sumoylation: a decade on." Nat Rev Mol Cell Biol **8**(12): 947-956.

Gilady, S. Y., M. Bui, E. M. Lynes, M. D. Benson, R. Watts, J. E. Vance and T. Simmen (2010). "Ero1alpha requires oxidizing and normoxic conditions to localize to the mitochondria-associated membrane (MAM)." Cell Stress Chaperones **15**(5): 619-629.

Giorgi, C., D. De Stefani, A. Bononi, R. Rizzuto and P. Pinton (2009). "Structural and functional link between the mitochondrial network and the endoplasmic reticulum." Int J Biochem Cell Biol **41**(10): 1817-1827.

Glass, A., C. M. Walsh, D. H. Lynch and W. R. Clark (1996). "Regulation of the Fas lytic pathway in cloned CTL." J Immunol **156**(10): 3638-3644.

Green, D. R., N. Droin and M. Pinkoski (2003). "Activation-induced cell death in T cells." Immunol Rev **193**: 70-81.

Griffith, T. S., T. Brunner, S. M. Fletcher, D. R. Green and T. A. Ferguson (1995). "Fas ligand-induced apoptosis as a mechanism of immune privilege." Science **270**(5239): 1189-1192.

Griffiths, G. M. and S. Isaaz (1993). "Granzymes A and B are targeted to the lytic granules of lymphocytes by the mannose-6-phosphate receptor." J Cell Biol **120**(4): 885-896.

Guidotti, L. G., T. Ishikawa, M. V. Hobbs, B. Matzke, R. Schreiber and F. V. Chisari (1996). "Intracellular inactivation of the hepatitis B virus by cytotoxic T lymphocytes." Immunity **4**(1): 25-36.

Guizetti, J., L. Schermelleh, J. Mantler, S. Maar, I. Poser, H. Leonhardt, T. Muller-Reichert and D. W. Gerlich (2011). "Cortical constriction during abscission involves helices of ESCRT-III-dependent filaments." Science **331**(6024): 1616-1620.

Hackam, D. J., O. D. Rotstein, M. K. Bennett, A. Klip, S. Grinstein and M. F. Manolson (1996). "Characterization and subcellular localization of target membrane soluble NSF attachment protein receptors (t-SNAREs) in macrophages. Syntaxins 2, 3, and 4 are present on phagosomal membranes." J Immunol **156**(11): 4377-4383.

Haddad, E. K., X. Wu, J. A. Hammer, 3rd and P. A. Henkart (2001). "Defective granule exocytosis in Rab27a-deficient lymphocytes from Ashen mice." J Cell Biol **152**(4): 835-842.

Hafez, I., A. Stolpe and M. Lindau (2003). "Compound exocytosis and cumulative fusion in eosinophils." J Biol Chem **278**(45): 44921-44928.

Haga, Y., K. Ishii and T. Suzuki (2011). "N-glycosylation is critical for the stability and intracellular trafficking of glucose transporter GLUT4." J Biol Chem **286**(36): 31320-31327.

Halimani, M., V. Pattu, M. R. Marshall, H. F. Chang, U. Matti, M. Jung, U. Becherer, E. Krause, M. Hoth, E. C. Schwarz and J. Rettig (2013). "Syntaxin11 serves as a t-SNARE for the fusion of lytic granules in human cytotoxic T lymphocytes." Eur J Immunol.

Hansen, N. J. (1999). "Identification of SNAREs Involved in Regulated Exocytosis in the Pancreatic Acinar Cell." Journal of Biological Chemistry **274**(32): 22871-22876.

Hara-Kuge, S., T. Ohkura, H. Ideo, O. Shimada, S. Atsumi and K. Yamashita (2002). "Involvement of VIP36 in intracellular transport and secretion of glycoproteins in polarized Madin-Darby canine kidney (MDCK) cells." J Biol Chem **277**(18): 16332-16339.

Harris, J. L., E. P. Peterson, D. Hudig, N. A. Thornberry and C. S. Craik (1998). "Definition and redesign of the extended substrate specificity of granzyme B." J Biol Chem **273**(42): 27364-27373.

Hasilik, A., U. Klein, A. Waheed, G. Strecker and K. von Figura (1980). "Phosphorylated oligosaccharides in lysosomal enzymes: identification of alpha-N-acetylglucosamine(1)phospho(6)mannose diester groups." Proc Natl Acad Sci U S A **77**(12): 7074-7078.

Hata, Y. and T. C. Sudhof (1995). "A novel ubiquitous form of Munc-18 interacts with multiple syntaxins. Use of the yeast two-hybrid system to study interactions between proteins involved in membrane traffic." J Biol Chem **270**(22): 13022-13028.

He, J. S., D. E. Gong and H. L. Ostergaard (2010). "Stored Fas ligand, a mediator of rapid CTL-mediated killing, has a lower threshold for response than degranulation or newly synthesized Fas ligand." J Immunol **184**(2): 555-563.

He, J. S. and H. L. Ostergaard (2007). "CTLs contain and use intracellular stores of FasL distinct from cytolytic granules." J Immunol **179**(4): 2339-2348.

Hengartner, M. O. (2000). "The biochemistry of apoptosis." Nature **407**(6805): 770-776.

Hohlbaum, A. M., S. Moe and A. Marshak-Rothstein (2000). "Opposing effects of transmembrane and soluble Fas ligand expression on inflammation and tumor cell survival." J Exp Med **191**(7): 1209-1220.

Holler, N., A. Tardivel, M. Kovacsovics-Bankowski, S. Hertig, O. Gaide, F. Martinon, A. Tinel, D. Deperthes, S. Calderara, T. Schulthess, J. Engel, P. Schneider and J. Tschopp (2003). "Two Adjacent Trimeric Fas Ligands Are Required for Fas Signaling and Formation of a Death-Inducing Signaling Complex." Molecular and Cellular Biology **23**(4): 1428-1440.

Holt, O., E. Kanno, G. Bossi, S. Booth, T. Daniele, A. Santoro, M. Arico, C. Saegusa, M. Fukuda and G. M. Griffiths (2008). "Slp1 and Slp2-a localize to the plasma membrane of CTL and contribute to secretion from the immunological synapse." Traffic **9**(4): 446-457.

Hong, W. (2005). "Cytotoxic T lymphocyte exocytosis: bring on the SNAREs!" Trends Cell Biol **15**(12): 644-650.

Hopkins, C. R. (1983). "Intracellular routing of transferrin and transferrin receptors in epidermoid carcinoma A431 cells." Cell **35**(1): 321-330.

Hopkins, C. R. and I. S. Trowbridge (1983). "Internalization and processing of transferrin and the transferrin receptor in human carcinoma A431 cells." J Cell Biol **97**(2): 508-521.

Hu, S. H., C. F. Latham, C. L. Gee, D. E. James and J. L. Martin (2007). "Structure of the Munc18c/Syntaxin4 N-peptide complex defines universal features of the N-peptide binding mode of Sec1/Munc18 proteins." Proc Natl Acad Sci U S A **104**(21): 8773-8778.

Hunt, J. S., D. Vassmer, T. A. Ferguson and L. Miller (1997). "Fas ligand is positioned in mouse uterus and placenta to prevent trafficking of activated leukocytes between the mother and the conceptus." J Immunol **158**(9): 4122-4128.

Huppa, J. B. and M. M. Davis (2003). "T-cell-antigen recognition and the immunological synapse." Nat Rev Immunol **3**(12): 973-983.

Huse, J. T., D. S. Pijak, G. J. Leslie, V. M. Lee and R. W. Doms (2000). "Maturation and endosomal targeting of beta-site amyloid precursor protein-cleaving enzyme. The Alzheimer's disease beta-secretase." J Biol Chem **275**(43): 33729-33737.

Igney, F. H. and P. H. Krammer (2005). "Tumor counterattack: fact or fiction?" Cancer Immunol Immunother **54**(11): 1127-1136.

Ingold, K., A. Zumsteg, A. Tardivel, B. Huard, Q. G. Steiner, T. G. Cachero, F. Qiang, L. Gorelik, S. L. Kalled, H. Acha-Orbea, P. D. Rennert, J. Tschopp and P. Schneider (2005). "Identification of proteoglycans as the APRIL-specific binding partners." J Exp Med **201**(9): 1375-1383.

Iwasaki, A. and R. Medzhitov (2004). "Toll-like receptor control of the adaptive immune responses." Nat Immunol **5**(10): 987-995.

Jahn, R. and R. H. Scheller (2006). "SNAREs--engines for membrane fusion." Nat Rev Mol Cell Biol **7**(9): 631-643.

Janeway, C. A., Jr. and R. Medzhitov (2002). "Innate immune recognition." Annu Rev Immunol **20**: 197-216.

Johnson, K. F. and S. Kornfeld (1992). "The cytoplasmic tail of the mannose 6-phosphate/insulin-like growth factor-II receptor has two signals for lysosomal enzyme sorting in the Golgi." J Cell Biol **119**(2): 249-257.

Jurado, S., D. Goswami, Y. Zhang, A. J. Molina, T. C. Sudhof and R. C. Malenka (2013). "LTP requires a unique postsynaptic SNARE fusion machinery." Neuron **77**(3): 542-558.

Kallberg, M., H. Wang, S. Wang, J. Peng, Z. Wang, H. Lu and J. Xu (2012). "Template-based protein structure modeling using the RaptorX web server." Nat Protoc **7**(8): 1511-1522.

Kane, K. P. and M. F. Mescher (1993). "Activation of CD8-dependent cytotoxic T lymphocyte adhesion and degranulation by peptide class I antigen complexes." J Immunol **150**(11): 4788-4797.

Kane, K. P., L. A. Sherman and M. F. Mescher (1989). "Molecular interactions required for triggering alloantigen-specific cytolytic T lymphocytes." J Immunol **142**(12): 4153-4160.

Karray, S., C. Kress, S. Cuvellier, C. Hue-Beauvais, D. Damotte, C. Babinet and M. Levi-Strauss (2004). "Complete loss of Fas ligand gene causes massive lymphoproliferation and early death, indicating a residual activity of gld allele." J Immunol **172**(4): 2118-2125.

Kassahn, D., U. Nachbur, S. Conus, O. Micheau, P. Schneider, H. U. Simon and T. Brunner (2009). "Distinct requirements for activation-induced cell surface expression of preformed Fas/CD95 ligand and cytolytic granule markers in T cells." Cell Death Differ **16**(1): 115-124.

Kessler, B., D. Hudrisier, M. Schroeter, J. Tschopp, J. C. Cerottini and I. F. Luescher (1998). "Peptide modification or blocking of CD8, resulting in weak TCR signaling, can activate CTL for Fas- but not perforin-dependent cytotoxicity or cytokine production." J Immunol **161**(12): 6939-6946.

Kiener, P. A., P. M. Davis, B. M. Rankin, S. J. Klebanoff, J. A. Ledbetter, G. C. Starling and W. C. Liles (1997). "Human monocytic cells contain high levels of intracellular Fas ligand: rapid release following cellular activation." J Immunol **159**(4): 1594-1598.

Kishimoto, H., C. D. Surh and J. Sprent (1998). "A role for Fas in negative selection of thymocytes in vivo." J Exp Med **187**(9): 1427-1438.

Kobayashi, T., U. M. Vischer, C. Rosnoblet, C. Lebrand, M. Lindsay, R. G. Parton, E. K. Kruithof and J. Gruenberg (2000). "The tetraspanin CD63/lamp3 cycles between endocytic and secretory compartments in human endothelial cells." Mol Biol Cell **11**(5): 1829-1843.

Koguchi, Y., J. L. Gardell, T. J. Thauland and D. C. Parker (2011). "Cyclosporine-resistant, Rab27a-independent mobilization of intracellular

preformed CD40 ligand mediates antigen-specific T cell help in vitro." J Immunol **187**(2): 626-634.

Kojima, Y., A. Kawasaki-Koyanagi, N. Sueyoshi, A. Kanai, H. Yagita and K. Okumura (2002). "Localization of Fas ligand in cytoplasmic granules of CD8+ cytotoxic T lymphocytes and natural killer cells: participation of Fas ligand in granule exocytosis model of cytotoxicity." Biochem Biophys Res Commun **296**(2): 328-336.

Koncz, G., A. Hancz, K. Chakrabandhu, P. Gogolak, K. Kerekes, E. Rajnavolgyi and A. O. Hueber (2012). "Vesicles released by activated T cells induce both Fas-mediated RIP-dependent apoptotic and Fas-independent nonapoptotic cell deaths." J Immunol **189**(6): 2815-2823.

Kornfeld, S. and I. Mellman (1989). "The biogenesis of lysosomes." Annu Rev Cell Biol **5**: 483-525.

Krammer, P. H. (2000). "CD95's deadly mission in the immune system." Nature **407**(6805): 789-795.

LA, O. R., L. Tai, L. Lee, E. A. Kruse, S. Grabow, W. D. Fairlie, N. M. Haynes, D. M. Tarlinton, J. G. Zhang, G. T. Belz, M. J. Smyth, P. Bouillet, L. Robb and A. Strasser (2009). "Membrane-bound Fas ligand only is essential for Fas-induced apoptosis." Nature **461**(7264): 659-663.

Lacy, P. (2006). "Mechanisms of degranulation in neutrophils." Allergy Asthma Clin Immunol **2**(3): 98-108.

Lamaze, C., A. Dujeancourt, T. Baba, C. G. Lo, A. Benmerah and A. Dautry-Varsat (2001). "Interleukin 2 receptors and detergent-resistant membrane domains define a clathrin-independent endocytic pathway." Mol Cell **7**(3): 661-671.

Le Roy, C. and J. L. Wrana (2005). "Clathrin- and non-clathrin-mediated endocytic regulation of cell signalling." Nat Rev Mol Cell Biol **6**(2): 112-126.

Lee, M. O., H. J. Kang, Y. M. Kim, J. H. Oum and J. Park (2002). "Repression of FasL expression by retinoic acid involves a novel mechanism of inhibition of transactivation function of the nuclear factors of activated T-cells." Eur J Biochem **269**(4): 1162-1170.

Lee, R. K., J. Spielman, D. Y. Zhao, K. J. Olsen and E. R. Podack (1996). "Perforin, Fas ligand, and tumor necrosis factor are the major cytotoxic molecules used by lymphokine-activated killer cells." J Immunol **157**(5): 1919-1925.

Lettau, M., M. Paulsen, H. Schmidt and O. Janssen (2011). "Insights into the molecular regulation of FasL (CD178) biology." Eur J Cell Biol **90**(6-7): 456-466.

Lettau, M., J. Qian, D. Kabelitz and O. Janssen (2004). "Activation-dependent FasL expression in T lymphocytes and Natural Killer cells." Signal Transduction **4**(5-6): 206-211.

Lettau, M., H. Schmidt, D. Kabelitz and O. Janssen (2007). "Secretory lysosomes and their cargo in T and NK cells." Immunol Lett **108**(1): 10-19.

Leung, H. T., J. Bradshaw, J. S. Cleaveland and P. S. Linsley (1995). "Cytotoxic T lymphocyte-associated molecule-4, a high-avidity receptor for CD80 and CD86, contains an intracellular localization motif in its cytoplasmic tail." J Biol Chem **270**(42): 25107-25114.

Li, D., M. Miller and P. D. Chantler (1994). "Association of a cellular myosin II with anionic phospholipids and the neuronal plasma membrane." Proc Natl Acad Sci U S A **91**(3): 853-857.

Li, J. H., D. Rosen, D. Ronen, C. K. Behrens, P. H. Krammer, W. R. Clark and G. Berke (1998). "The regulation of CD95 ligand expression and function in CTL." J Immunol **161**(8): 3943-3949.

Li, P., D. Nijhawan, I. Budihardjo, S. M. Srinivasula, M. Ahmad, E. S. Alnemri and X. Wang (1997). "Cytochrome c and dATP-dependent formation of Apaf-1/caspase-9 complex initiates an apoptotic protease cascade." Cell **91**(4): 479-489.

Li-Weber, M. and P. H. Krammer (2003). "Function and regulation of the CD95 (APO-1/Fas) ligand in the immune system." Seminars in Immunology **15**(3): 145-157.

Linsley, P. S., J. Bradshaw, J. Greene, R. Peach, K. L. Bennett and R. S. Mittler (1996). "Intracellular trafficking of CTLA-4 and focal localization towards sites of TCR engagement." Immunity **4**(6): 535-543.

Liu, L. B., W. Omata, I. Kojima and H. Shibata (2007). "The SUMO conjugating enzyme Ubc9 is a regulator of GLUT4 turnover and targeting to the insulin-responsive storage compartment in 3T3-L1 adipocytes." Diabetes **56**(8): 1977-1985.

Lollike, K., M. Lindau, J. Calafat and N. Borregaard (2002). "Compound exocytosis of granules in human neutrophils." J Leukoc Biol **71**(6): 973-980.

Lopez, J. A., A. J. Brennan, J. C. Whisstock, I. Voskoboinik and J. A. Trapani (2012). "Protecting a serial killer: pathways for perforin trafficking and self-defence ensure sequential target cell death." Trends Immunol **33**(8): 406-412.

Luo, X., I. Budihardjo, H. Zou, C. Slaughter and X. Wang (1998). "Bid, a Bcl2 interacting protein, mediates cytochrome c release from mitochondria in response to activation of cell surface death receptors." Cell **94**(4): 481-490.

Ma, J., S. Wang, F. Zhao and J. Xu (2013). "Protein threading using context-specific alignment potential." Bioinformatics **29**(13): i257-265.

Magerus-Chatinet, A., M. C. Stolzenberg, N. Lanzarotti, B. Neven, C. Daussy, C. Picard, N. Neveux, M. Desai, M. Rao, K. Ghosh, M. Madkaikar, A. Fischer and F. Rieux-Laucat (2013). "Autoimmune lymphoproliferative syndrome caused by a homozygous null FAS ligand (FASLG) mutation." J Allergy Clin Immunol **131**(2): 486-490.

Mandic, S. A., M. Skelin, J. U. Johansson, M. S. Rupnik, P. O. Berggren and C. Bark (2011). "Munc18-1 and Munc18-2 proteins modulate beta-cell Ca2+ sensitivity and kinetics of insulin exocytosis differently." J Biol Chem **286**(32): 28026-28040.

Maravillas-Montero, J. L. and L. Santos-Argumedo (2012). "The myosin family: unconventional roles of actin-dependent molecular motors in immune cells." J Leukoc Biol **91**(1): 35-46.

Martin, S., A. Nishimune, J. R. Mellor and J. M. Henley (2007). "SUMOylation regulates kainate-receptor-mediated synaptic transmission." Nature **447**(7142): 321-325.

Martin-Verdeaux, S. (2002). "Evidence of a role for Munc18-2 and microtubules in mast cell granule exocytosis." Journal of Cell Science **116**(2): 325-334.

Martinez-Lorenzo, M. J., A. Anel, S. Gamen, I. Monle n, P. Lasierra, L. Larrad, A. Pineiro, M. A. Alava and J. Naval (1999). "Activated human T cells release bioactive Fas ligand and APO2 ligand in microvesicles." J Immunol **163**(3): 1274-1281.

Maxfield, F. R. and T. E. McGraw (2004). "Endocytic recycling." Nat Rev Mol Cell Biol **5**(2): 121-132.

Mayle, K. M., A. M. Le and D. T. Kamei (2012). "The intracellular trafficking pathway of transferrin." Biochim Biophys Acta **1820**(3): 264-281.

Mayor, S. and R. E. Pagano (2007). "Pathways of clathrin-independent endocytosis." Nat Rev Mol Cell Biol **8**(8): 603-612.

Medema, J. P., C. Scaffidi, F. C. Kischkel, A. Shevchenko, M. Mann, P. H. Krammer and M. E. Peter (1997). "FLICE is activated by association with the CD95 death-inducing signaling complex (DISC)." EMBO J **16**(10): 2794-2804.

Melino, G., F. Bernassola, M. V. Catani, A. Rossi, M. Corazzari, S. Sabatini, F. Vilbois and D. R. Green (2000). "Nitric oxide inhibits apoptosis via AP-1-dependent CD95L transactivation." Cancer Res **60**(9): 2377-2383.

Mellman, I. and G. Warren (2000). "The road taken: past and future foundations of membrane traffic." Cell **100**(1): 99-112.

Menager, M. M., G. Menasche, M. Romao, P. Knapnougel, C. H. Ho, M. Garfa, G. Raposo, J. Feldmann, A. Fischer and G. de Saint Basile (2007). "Secretory cytotoxic granule maturation and exocytosis require the effector protein hMunc13-4." Nat Immunol **8**(3): 257-267.

Menasche, G., M. M. Menager, J. M. Lefebvre, E. Deutsch, R. Athman, N. Lambert, N. Mahlaoui, M. Court, J. Garin, A. Fischer and G. de Saint Basile (2008). "A newly identified isoform of Slp2a associates with Rab27a in cytotoxic T cells and participates to cytotoxic granule secretion." Blood **112**(13): 5052-5062.

Menasche, G., E. Pastural, J. Feldmann, S. Certain, F. Ersoy, S. Dupuis, N. Wulffraat, D. Bianchi, A. Fischer, F. Le Deist and G. de Saint Basile (2000). "Mutations in RAB27A cause Griscelli syndrome associated with haemophagocytic syndrome." Nat Genet **25**(2): 173-176.

Miettinen, H. M., K. Matter, W. Hunziker, J. K. Rose and I. Mellman (1992). "Fc receptor endocytosis is controlled by a cytoplasmic domain determinant that actively prevents coated pit localization." J Cell Biol **116**(4): 875-888.

Misura, K. M., R. H. Scheller and W. I. Weis (2000). "Three-dimensional structure of the neuronal-Sec1-syntaxin 1a complex." Nature **404**(6776): 355-362.

Mogensen, T. H. (2009). "Pathogen recognition and inflammatory signaling in innate immune defenses." Clin Microbiol Rev **22**(2): 240-273, Table of Contents.

Moharir, A., S. H. Peck, T. Budden and S. Y. Lee (2013). "The role of N-glycosylation in folding, trafficking, and functionality of lysosomal protein CLN5." PLoS One **8**(9): e74299.

Monks, C. R., B. A. Freiberg, H. Kupfer, N. Sciaky and A. Kupfer (1998). "Three-dimensional segregation of supramolecular activation clusters in T cells." Nature **395**(6697): 82-86.

Monleon, I., M. J. Martinez-Lorenzo, L. Monteagudo, P. Lasierra, M. Taules, M. Iturralde, A. Pineiro, L. Larrad, M. A. Alava, J. Naval and A. Anel (2001). "Differential Secretion of Fas Ligand- or APO2 Ligand/TNF-Related Apoptosis-Inducing Ligand-Carrying Microvesicles During Activation-Induced Death of Human T Cells." The Journal of Immunology **167**(12): 6736-6744.

Montel, A. H., M. R. Bochan, J. A. Hobbs, D. H. Lynch and Z. Brahmi (1995). "Fas involvement in cytotoxicity mediated by human NK cells." Cell Immunol **166**(2): 236-246.

Morel, Y., J. M. Schiano de Colella, J. Harrop, K. C. Deen, S. D. Holmes, T. A. Wattam, S. S. Khandekar, A. Truneh, R. W. Sweet, J. A. Gastaut, D. Olive and R. T. Costello (2000). "Reciprocal expression of the TNF family receptor

herpes virus entry mediator and its ligand LIGHT on activated T cells: LIGHT down-regulates its own receptor." J Immunol **165**(8): 4397-4404.

Morelon, E. and A. Dautry-Varsat (1998). "Endocytosis of the common cytokine receptor gammac chain. Identification of sequences involved in internalization and degradation." J Biol Chem **273**(34): 22044-22051.

Morenilla-Palao, C., M. Pertusa, V. Meseguer, H. Cabedo and F. Viana (2009). "Lipid raft segregation modulates TRPM8 channel activity." J Biol Chem **284**(14): 9215-9224.

Motyka, B., G. Korbutt, M. J. Pinkoski, J. A. Heibein, A. Caputo, M. Hobman, M. Barry, I. Shostak, T. Sawchuk, C. F. Holmes, J. Gauldie and R. C. Bleackley (2000). "Mannose 6-phosphate/insulin-like growth factor II receptor is a death receptor for granzyme B during cytotoxic T cell-induced apoptosis." Cell **103**(3): 491-500.

Mousavi, S. A., L. Malerod, T. Berg and R. Kjeken (2004). "Clathrin-dependent endocytosis." Biochem J **377**(Pt 1): 1-16.

Muhlenbeck, F., P. Schneider, J. L. Bodmer, R. Schwenzer, A. Hauser, G. Schubert, P. Scheurich, D. Moosmayer, J. Tschopp and H. Wajant (2000). "The tumor necrosis factor-related apoptosis-inducing ligand receptors TRAIL-R1 and TRAIL-R2 have distinct cross-linking requirements for initiation of apoptosis and are non-redundant in JNK activation." J Biol Chem **275**(41): 32208-32213.

Mullen, R. T. and R. N. Trelease (2000). "The sorting signals for peroxisomal membrane-bound ascorbate peroxidase are within its C-terminal tail." J Biol Chem **275**(21): 16337-16344.

Muller, N., A. Wyzgol, S. Munkel, K. Pfizenmaier and H. Wajant (2008). "Activity of soluble OX40 ligand is enhanced by oligomerization and cell surface immobilization." FEBS J **275**(9): 2296-2304.

Murray, R. Z., J. G. Kay, D. G. Sangermani and J. L. Stow (2005). "A role for the phagosome in cytokine secretion." Science **310**(5753): 1492-1495.

Muzio, M., A. M. Chinnaiyan, F. C. Kischkel, K. O'Rourke, A. Shevchenko, J. Ni, C. Scaffidi, J. D. Bretz, M. Zhang, R. Gentz, M. Mann, P. H. Krammer, M. E. Peter and V. M. Dixit (1996). "FLICE, a novel FADD-

homologous ICE/CED-3-like protease, is recruited to the CD95 (Fas/APO-1) death--inducing signaling complex." Cell **85**(6): 817-827.

Nachbur, U., D. Kassahn, S. Yousefi, D. F. Legler and T. Brunner (2006). "Posttranscriptional regulation of Fas (CD95) ligand killing activity by lipid rafts." Blood **107**(7): 2790-2796.

Nagasawa, R., J. Gross, O. Kanagawa, K. Townsend, L. L. Lanier, J. Chiller and J. P. Allison (1987). "Identification of a novel T cell surface disulfide-bonded dimer distinct from the alpha/beta antigen receptor." J Immunol **138**(3): 815-824.

Nakamura, N., C. Rabouille, R. Watson, T. Nilsson, N. Hui, P. Slusarewicz, T. E. Kreis and G. Warren (1995). "Characterization of a cis-Golgi matrix protein, GM130." J Cell Biol **131**(6 Pt 2): 1715-1726.

Neeft, M., M. Wieffer, A. S. de Jong, G. Negroiu, C. H. Metz, A. van Loon, J. Griffith, J. Krijgsveld, N. Wulffraat, H. Koch, A. J. Heck, N. Brose, M. Kleijmeer and P. van der Sluijs (2005). "Munc13-4 is an effector of rab27a and controls secretion of lysosomes in hematopoietic cells." Mol Biol Cell **16**(2): 731-741.

O'Connell, J., M. W. Bennett, G. C. O'Sullivan, J. K. Collins and F. Shanahan (1999). "The Fas counterattack: cancer as a site of immune privilege." Immunol Today **20**(1): 46-52.

Oprins, A., R. Duden, T. E. Kreis, H. J. Geuze and J. W. Slot (1993). "Beta-COP localizes mainly to the cis-Golgi side in exocrine pancreas." J Cell Biol **121**(1): 49-59.

Orlinick, J. R., K. B. Elkon and M. V. Chao (1997a). "Separate domains of the human fas ligand dictate self-association and receptor binding." J Biol Chem **272**(51): 32221-32229.

Orlinick, J. R., A. Vaishnaw, K. B. Elkon and M. V. Chao (1997b). "Requirement of cysteine-rich repeats of the Fas receptor for binding by the Fas ligand." J Biol Chem **272**(46): 28889-28894.

Ostergaard, H. L., K. P. Kane, M. F. Mescher and W. R. Clark (1987). "Cytotoxic T lymphocyte mediated lysis without release of serine esterase." Nature **330**(6143): 71-72.

Ottonello, L., G. Tortolina, M. Amelotti and F. Dallegri (1999). "Soluble Fas ligand is chemotactic for human neutrophilic polymorphonuclear leukocytes." J Immunol **162**(6): 3601-3606.

Pagan, J. K., F. G. Wylie, S. Joseph, C. Widberg, N. J. Bryant, D. E. James and J. L. Stow (2003). "The t-SNARE syntaxin 4 is regulated during macrophage activation to function in membrane traffic and cytokine secretion." Curr Biol **13**(2): 156-160.

Pagano, M., M. A. Clynes, N. Masada, A. Ciruela, L. J. Ayling, S. Wachten and D. M. Cooper (2009). "Insights into the residence in lipid rafts of adenylyl cyclase AC8 and its regulation by capacitative calcium entry." Am J Physiol Cell Physiol **296**(3): C607-619.

Pattu, V., B. Qu, E. C. Schwarz, B. Strauss, L. Weins, S. S. Bhat, M. Halimani, M. Marshall, J. Rettig and M. Hoth (2012). "SNARE protein expression and localization in human cytotoxic T lymphocytes." Eur J Immunol **42**(2): 470-475.

Pelchen-Matthews, A., J. E. Armes, G. Griffiths and M. Marsh (1991). "Differential endocytosis of CD4 in lymphocytic and nonlymphocytic cells." J Exp Med **173**(3): 575-587.

Peng, J. and J. Xu (2011a). "A multiple-template approach to protein threading." Proteins **79**(6): 1930-1939.

Peng, J. and J. Xu (2011b). "RaptorX: exploiting structure information for protein alignment by statistical inference." Proteins **79 Suppl 10**: 161-171.

Peng, R. W., C. Guetg, E. Abellan and M. Fussenegger (2010). "Munc18b regulates core SNARE complex assembly and constitutive exocytosis by interacting with the N-peptide and the closed-conformation C-terminus of syntaxin 3." Biochem J **431**(3): 353-361.

Pentcheva-Hoang, T., L. Chen, D. M. Pardoll and J. P. Allison (2007). "Programmed death-1 concentration at the immunological synapse is determined

by ligand affinity and availability." Proc Natl Acad Sci U S A **104**(45): 17765-17770.

Peter, M. E. and P. H. Krammer (2003). "The CD95(APO-1/Fas) DISC and beyond." Cell Death Differ **10**(1): 26-35.

Peters, P. J., J. Borst, V. Oorschot, M. Fukuda, O. Krahenbuhl, J. Tschopp, J. W. Slot and H. J. Geuze (1991). "Cytotoxic T lymphocyte granules are secretory lysosomes, containing both perforin and granzymes." J Exp Med **173**(5): 1099-1109.

Pfeffer, S. and D. Aivazian (2004). "Targeting Rab GTPases to distinct membrane compartments." Nat Rev Mol Cell Biol **5**(11): 886-896.

Pham, C. T. and T. J. Ley (1999). "Dipeptidyl peptidase I is required for the processing and activation of granzymes A and B in vivo." Proc Natl Acad Sci U S A **96**(15): 8627-8632.

Pickett, J. A. and J. M. Edwardson (2006). "Compound exocytosis: mechanisms and functional significance." Traffic **7**(2): 109-116.

Pinkoski, M. J., N. M. Droin, T. Lin, L. Genestier, T. A. Ferguson and D. R. Green (2002). "Nonlymphoid Fas ligand in peptide-induced peripheral lymphocyte deletion." Proc Natl Acad Sci U S A **99**(25): 16174-16179.

Piper, R. C. and P. J. Lehner (2011). "Endosomal transport via ubiquitination." Trends Cell Biol **21**(11): 647-655.

Pivot-Pajot, C., F. Varoqueaux, G. de Saint Basile and S. G. Bourgoin (2008). "Munc13-4 regulates granule secretion in human neutrophils." J Immunol **180**(10): 6786-6797.

Podack, E. R., J. D. Young and Z. A. Cohn (1985). "Isolation and biochemical and functional characterization of perforin 1 from cytolytic T-cell granules." Proc Natl Acad Sci U S A **82**(24): 8629-8633.

Pombo, I., J. Rivera and U. Blank (2003). "Munc18-2/syntaxin3 complexes are spatially separated from syntaxin3-containing SNARE complexes." FEBS Lett **550**(1-3): 144-148.

Price, G. E., L. Huang, R. Ou, M. Zhang and D. Moskophidis (2005). "Perforin and Fas cytolytic pathways coordinately shape the selection and

diversity of CD8+-T-cell escape variants of influenza virus." J Virol **79**(13): 8545-8559.

Puri, N. and P. A. Roche (2008). "Mast cells possess distinct secretory granule subsets whose exocytosis is regulated by different SNARE isoforms." Proc Natl Acad Sci U S A **105**(7): 2580-2585.

Qian, J., W. Chen, M. Lettau, G. Podda, M. Zornig, D. Kabelitz and O. Janssen (2006). "Regulation of FasL expression: a SH3 domain containing protein family involved in the lysosomal association of FasL." Cell Signal **18**(8): 1327-1337.

Qureshi, O. S., S. Kaur, T. Z. Hou, L. E. Jeffery, N. S. Poulter, Z. Briggs, R. Kenefeck, A. K. Willox, S. J. Royle, J. Z. Rappoport and D. M. Sansom (2012). "Constitutive clathrin-mediated endocytosis of CTLA-4 persists during T cell activation." J Biol Chem **287**(12): 9429-9440.

Rabu, C., A. Quemener, Y. Jacques, K. Echasserieau, P. Vusio and F. Lang (2005). "Production of recombinant human trimeric CD137L (4-1BBL). Cross-linking is essential to its T cell co-stimulation activity." J Biol Chem **280**(50): 41472-41481.

Radhakrishna, H. and J. G. Donaldson (1997). "ADP-ribosylation factor 6 regulates a novel plasma membrane recycling pathway." J Cell Biol **139**(1): 49-61.

Ratner, A. and W. R. Clark (1993). "Role of TNF-alpha in CD8+ cytotoxic T lymphocyte-mediated lysis." J Immunol **150**(10): 4303-4314.

Reich, A., H. Korner, J. D. Sedgwick and H. Pircher (2000). "Immune down-regulation and peripheral deletion of CD8 T cells does not require TNF receptor-ligand interactions nor CD95 (Fas, APO-1)." Eur J Immunol **30**(2): 678-682.

Riento, K. (2000). "Munc18-2, a Functional Partner of Syntaxin 3, Controls Apical Membrane Trafficking in Epithelial Cells." Journal of Biological Chemistry **275**(18): 13476-13483.

Rieux-Laucat, F., F. Le Deist and A. Fischer (2003). "Autoimmune lymphoproliferative syndromes: genetic defects of apoptosis pathways." Cell Death Differ **10**(1): 124-133.

Rizo, J. and T. C. Sudhof (2012). "The membrane fusion enigma: SNAREs, Sec1/Munc18 proteins, and their accomplices--guilty as charged?" Annu Rev Cell Dev Biol **28**: 279-308.

Robinson, M. S. and J. S. Bonifacino (2001). "Adaptor-related proteins." Curr Opin Cell Biol **13**(4): 444-453.

Rode, M., S. Balkow, V. Sobek, R. Brehm, P. Martin, A. Kersten, T. Dumrese, T. Stehle, A. Mullbacher, R. Wallich and M. M. Simon (2004). "Perforin and Fas act together in the induction of apoptosis, and both are critical in the clearance of lymphocytic choriomeningitis virus infection." J Virol **78**(22): 12395-12405.

Roose, J. P., M. Mollenauer, V. A. Gupta, J. Stone and A. Weiss (2005). "A diacylglycerol-protein kinase C-RasGRP1 pathway directs Ras activation upon antigen receptor stimulation of T cells." Mol Cell Biol **25**(11): 4426-4441.

Rouvier, E., M. F. Luciani and P. Golstein (1993). "Fas involvement in Ca(2+)-independent T cell-mediated cytotoxicity." J Exp Med **177**(1): 195-200.

Sabri, F., F. Chiodi, J. P. Piret, C. H. Wei, E. Major, B. Westermark, M. G. Masucci and V. Levitsky (2003). "Soluble factors released by virus specific activated cytotoxic T-lymphocytes induce apoptotic death of astroglioma cell lines." Brain Pathol **13**(2): 165-175.

Samelson, L. E. (2002). "Signal transduction mediated by the T cell antigen receptor: the role of adapter proteins." Annu Rev Immunol **20**: 371-394.

Sanborn, K. B., G. D. Rak, S. Y. Maru, K. Demers, A. Difeo, J. A. Martignetti, M. R. Betts, R. Favier, P. P. Banerjee and J. S. Orange (2009). "Myosin IIA associates with NK cell lytic granules to enable their interaction with F-actin and function at the immunological synapse." J Immunol **182**(11): 6969-6984.

Scaffidi, C., S. Fulda, A. Srinivasan, C. Friesen, F. Li, K. J. Tomaselli, K. M. Debatin, P. H. Krammer and M. E. Peter (1998). "Two CD95 (APO-1/Fas) signaling pathways." EMBO J **17**(6): 1675-1687.

Schmidt, H., C. Gelhaus, M. Nebendahl, M. Lettau, R. Lucius, M. Leippe, D. Kabelitz and O. Janssen (2011a). "Effector granules in human T lymphocytes: proteomic evidence for two distinct species of cytotoxic effector vesicles." J Proteome Res **10**(4): 1603-1620.

Schmidt, H., C. Gelhaus, M. Nebendahl, M. Lettau, R. Lucius, M. Leippe, D. Kabelitz and O. Janssen (2011b). "Effector granules in human T lymphocytes: the luminal proteome of secretory lysosomes from human T cells." Cell Commun Signal **9**(1): 4.

Schneider, P., N. Holler, J. L. Bodmer, M. Hahne, K. Frei, A. Fontana and J. Tschopp (1998). "Conversion of membrane-bound Fas(CD95) ligand to its soluble form is associated with downregulation of its proapoptotic activity and loss of liver toxicity." J Exp Med **187**(8): 1205-1213.

Schutze, M. P., P. A. Peterson and M. R. Jackson (1994). "An N-terminal double-arginine motif maintains type II membrane proteins in the endoplasmic reticulum." EMBO J **13**(7): 1696-1705.

Seino, K., K. Iwabuchi, N. Kayagaki, R. Miyata, I. Nagaoka, A. Matsuzawa, K. Fukao, H. Yagita and K. Okumura (1998). "Chemotactic activity of soluble Fas ligand against phagocytes." J Immunol **161**(9): 4484-4488.

Seki, N., A. D. Brooks, C. R. Carter, T. C. Back, E. M. Parsoneault, M. J. Smyth, R. H. Wiltrout and T. J. Sayers (2002). "Tumor-specific CTL kill murine renal cancer cells using both perforin and Fas ligand-mediated lysis in vitro, but cause tumor regression in vivo in the absence of perforin." J Immunol **168**(7): 3484-3492.

Setiadi, H., M. Disdier, S. A. Green, W. M. Canfield and R. P. McEver (1995). "Residues throughout the cytoplasmic domain affect the internalization efficiency of P-selectin." J Biol Chem **270**(45): 26818-26826.

Sharma, N., S. H. Low, S. Misra, B. Pallavi and T. Weimbs (2006). "Apical targeting of syntaxin 3 is essential for epithelial cell polarity." J Cell Biol **173**(6): 937-948.

Shi, L., S. Mai, S. Israels, K. Browne, J. A. Trapani and A. H. Greenberg (1997). "Granzyme B (GraB) autonomously crosses the cell membrane and perforin initiates apoptosis and GraB nuclear localization." J Exp Med **185**(5): 855-866.

Shrestha, B. and M. S. Diamond (2007). "Fas ligand interactions contribute to CD8+ T-cell-mediated control of West Nile virus infection in the central nervous system." J Virol **81**(21): 11749-11757.

Sidman, C. L., J. D. Marshall and H. Von Boehmer (1992). "Transgenic T cell receptor interactions in the lymphoproliferative and autoimmune syndromes of lpr and gld mutant mice." Eur J Immunol **22**(2): 499-504.

Sigismund, S., T. Woelk, C. Puri, E. Maspero, C. Tacchetti, P. Transidico, P. P. Di Fiore and S. Polo (2005). "Clathrin-independent endocytosis of ubiquitinated cargos." Proc Natl Acad Sci U S A **102**(8): 2760-2765.

Singer, G. G. and A. K. Abbas (1994). "The fas antigen is involved in peripheral but not thymic deletion of T lymphocytes in T cell receptor transgenic mice." Immunity **1**(5): 365-371.

Sitte, H. H., H. Farhan and J. A. Javitch (2004). "Sodium-dependent neurotransmitter transporters: oligomerization as a determinant of transporter function and trafficking." Mol Interv **4**(1): 38-47.

Smith, A. J., J. R. Pfeiffer, J. Zhang, A. M. Martinez, G. M. Griffiths and B. S. Wilson (2003). "Microtubule-dependent transport of secretory vesicles in RBL-2H3 cells." Traffic **4**(5): 302-312.

Sneller, M. C., J. Wang, J. K. Dale, W. Strober, L. A. Middelton, Y. Choi, T. A. Fleisher, M. S. Lim, E. S. Jaffe, J. M. Puck, M. J. Lenardo and S. E. Straus (1997). "Clincal, immunologic, and genetic features of an autoimmune lymphoproliferative syndrome associated with abnormal lymphocyte apoptosis." Blood **89**(4): 1341-1348.

Stenmark, H. and V. M. Olkkonen (2001). "The Rab GTPase family." Genome Biol **2**(5): REVIEWS3007.

Stepp, S. E. (1999). "Perforin Gene Defects in Familial Hemophagocytic Lymphohistiocytosis." Science **286**(5446): 1957-1959.

Stinchcombe, J., G. Bossi and G. M. Griffiths (2004). "Linking albinism and immunity: the secrets of secretory lysosomes." Science **305**(5680): 55-59.

Stinchcombe, J. C., D. C. Barral, E. H. Mules, S. Booth, A. N. Hume, L. M. Machesky, M. C. Seabra and G. M. Griffiths (2001a). "Rab27a is required for regulated secretion in cytotoxic T lymphocytes." J Cell Biol **152**(4): 825-834.

Stinchcombe, J. C., G. Bossi, S. Booth and G. M. Griffiths (2001b). "The immunological synapse of CTL contains a secretory domain and membrane bridges." Immunity **15**(5): 751-761.

Stinchcombe, J. C. and G. M. Griffiths (1999). "Regulated secretion from hemopoietic cells." J Cell Biol **147**(1): 1-6.

Stinchcombe, J. C. and G. M. Griffiths (2007). "Secretory mechanisms in cell-mediated cytotoxicity." Annu Rev Cell Dev Biol **23**: 495-517.

Straus, D. B. and A. Weiss (1992). "Genetic evidence for the involvement of the lck tyrosine kinase in signal transduction through the T cell antigen receptor." Cell **70**(4): 585-593.

Suda, T., H. Hashimoto, M. Tanaka, T. Ochi and S. Nagata (1997). "Membrane Fas ligand kills human peripheral blood T lymphocytes, and soluble Fas ligand blocks the killing." J Exp Med **186**(12): 2045-2050.

Suda, T., T. Takahashi, P. Golstein and S. Nagata (1993). "Molecular cloning and expression of the Fas ligand, a novel member of the tumor necrosis factor family." Cell **75**(6): 1169-1178.

Sudhof, T. C. and J. E. Rothman (2009). "Membrane fusion: grappling with SNARE and SM proteins." Science **323**(5913): 474-477.

Suk, K., S. Kim, Y. H. Kim, K. A. Kim, I. Chang, H. Yagita, M. Shong and M. S. Lee (2001). "IFN-gamma/TNF-alpha synergism as the final effector in autoimmune diabetes: a key role for STAT1/IFN regulatory factor-1 pathway in pancreatic beta cell death." J Immunol **166**(7): 4481-4489.

Sun, M., K. T. Ames, I. Suzuki and P. J. Fink (2006). "The Cytoplasmic Domain of Fas Ligand Costimulates TCR Signals." The Journal of Immunology **177**(3): 1481-1491.

Sun, M., S. Lee, S. Karray, M. Levi-Strauss, K. T. Ames and P. J. Fink (2007). "Cutting edge: two distinct motifs within the Fas ligand tail regulate Fas ligand-mediated costimulation." J Immunol **179**(9): 5639-5643.

Suzuki, I. and P. J. Fink (2000). "The dual functions of fas ligand in the regulation of peripheral CD8+ and CD4+ T cells." Proc Natl Acad Sci U S A **97**(4): 1707-1712.

Suzuki, I., S. Martin, T. E. Boursalian, C. Beers and P. J. Fink (2000). "Fas Ligand Costimulates the In Vivo Proliferation of CD8+ T Cells." The Journal of Immunology **165**(10): 5537-5543.

Tadokoro, S., T. Kurimoto, M. Nakanishi and N. Hirashima (2007). "Munc18-2 regulates exocytotic membrane fusion positively interacting with syntaxin-3 in RBL-2H3 cells." Mol Immunol **44**(13): 3427-3433.

Takahashi, T., M. Tanaka, C. I. Brannan, N. A. Jenkins, N. G. Copeland, T. Suda and S. Nagata (1994). "Generalized lymphoproliferative disease in mice, caused by a point mutation in the Fas ligand." Cell **76**(6): 969-976.

Tanaka, M., T. Itai, M. Adachi and S. Nagata (1998). "Downregulation of Fas ligand by shedding." Nat Med **4**(1): 31-36.

Teng, F. Y., Y. Wang and B. L. Tang (2001). "The syntaxins." Genome Biol **2**(11): REVIEWS3012.

Thiery, J., D. Keefe, S. Boulant, E. Boucrot, M. Walch, D. Martinvalet, I. S. Goping, R. C. Bleackley, T. Kirchhausen and J. Lieberman (2011). "Perforin pores in the endosomal membrane trigger the release of endocytosed granzyme B into the cytosol of target cells." Nat Immunol **12**(8): 770-777.

Trambas, C. M. and G. M. Griffiths (2003). "Delivering the kiss of death." Nat Immunol **4**(5): 399-403.

Trenn, G., H. Takayama and M. V. Sitkovsky (1987). "Exocytosis of cytolytic granules may not be required for target cell lysis by cytotoxic T-lymphocytes." Nature **330**(6143): 72-74.

Tuvim, M. J., R. Adachi, S. Hoffenberg and B. F. Dickey (2001). "Traffic control: Rab GTPases and the regulation of interorganellar transport." News Physiol Sci **16**: 56-61.

Vagin, O., J. A. Kraut and G. Sachs (2009). "Role of N-glycosylation in trafficking of apical membrane proteins in epithelia." Am J Physiol Renal Physiol **296**(3): F459-469.

Valk, E., C. E. Rudd and H. Schneider (2008). "CTLA-4 trafficking and surface expression." Trends Immunol **29**(6): 272-279.

van Vliet, C., E. C. Thomas, A. Merino-Trigo, R. D. Teasdale and P. A. Gleeson (2003). "Intracellular sorting and transport of proteins." Progress in Biophysics and Molecular Biology **83**(1): 1-45.

Verhey, K. J. and M. J. Birnbaum (1994). "A Leu-Leu sequence is essential for COOH-terminal targeting signal of GLUT4 glucose transporter in fibroblasts." J Biol Chem **269**(4): 2353-2356.

Vignaux, F., E. Vivier, B. Malissen, V. Depraetere, S. Nagata and P. Golstein (1995). "TCR/CD3 coupling to Fas-based cytotoxicity." J Exp Med **181**(2): 781-786.

Vincent, V., V. Goffin, M. Rozakis-Adcock, J. P. Mornon and P. A. Kelly (1997). "Identification of cytoplasmic motifs required for short prolactin receptor internalization." J Biol Chem **272**(11): 7062-7068.

Voss, M., M. Lettau, M. Paulsen and O. Janssen (2008). "Posttranslational regulation of Fas ligand function." Cell Commun Signal **6**: 11.

Wada, I., D. Rindress, P. H. Cameron, W. J. Ou, J. J. Doherty, 2nd, D. Louvard, A. W. Bell, D. Dignard, D. Y. Thomas and J. J. Bergeron (1991). "SSR alpha and associated calnexin are major calcium binding proteins of the endoplasmic reticulum membrane." J Biol Chem **266**(29): 19599-19610.

Walsh, C. M., A. A. Glass, V. Chiu and W. R. Clark (1994). "The role of the Fas lytic pathway in a perforin-less CTL hybridoma." J Immunol **153**(6): 2506-2514.

Wang, A., X. Ma, M. A. Conti and R. S. Adelstein (2011). "Distinct and redundant roles of the non-muscle myosin II isoforms and functional domains." Biochem Soc Trans **39**(5): 1131-1135.

Watanabe-Fukunaga, R., C. I. Brannan, N. G. Copeland, N. A. Jenkins and S. Nagata (1992a). "Lymphoproliferation disorder in mice explained by defects in Fas antigen that mediates apoptosis." Nature **356**(6367): 314-317.

Watanabe-Fukunaga, R., C. I. Brannan, N. Itoh, S. Yonehara, N. G. Copeland, N. A. Jenkins and S. Nagata (1992b). "The cDNA structure, expression, and chromosomal assignment of the mouse Fas antigen." J Immunol **148**(4): 1274-1279.

Watts, A. D., N. H. Hunt, Y. Wanigasekara, G. Bloomfield, D. Wallach, B. D. Roufogalis and G. Chaudhri (1999). "A casein kinase I motif present in the cytoplasmic domain of members of the tumour necrosis factor ligand family is implicated in 'reverse signalling'." Embo J **18**(8): 2119-2126.

Welchman, R. L., C. Gordon and R. J. Mayer (2005). "Ubiquitin and ubiquitin-like proteins as multifunctional signals." Nat Rev Mol Cell Biol **6**(8): 599-609.

Wohlleber, D., H. Kashkar, K. Gartner, M. K. Frings, M. Odenthal, S. Hegenbarth, C. Borner, B. Arnold, G. Hammerling, B. Nieswandt, N. van Rooijen, A. Limmer, K. Cederbrant, M. Heikenwalder, M. Pasparakis, U. Protzer, H. P. Dienes, C. Kurts, M. Kronke and P. A. Knolle (2012). "TNF-induced target cell killing by CTL activated through cross-presentation." Cell Rep **2**(3): 478-487.

Wood, S. M., M. Meeths, S. C. Chiang, A. G. Bechensteen, J. J. Boelens, C. Heilmann, H. Horiuchi, S. Rosthoj, O. Rutynowska, J. Winiarski, J. L. Stow, M. Nordenskjold, J. I. Henter, H. G. Ljunggren and Y. T. Bryceson (2009). "Different NK cell-activating receptors preferentially recruit Rab27a or Munc13-4 to perforin-containing granules for cytotoxicity." Blood **114**(19): 4117-4127.

Wu, X., B. Bowers, Q. Wei, B. Kocher and J. A. Hammer, 3rd (1997). "Myosin V associates with melanosomes in mouse melanocytes: evidence that myosin V is an organelle motor." J Cell Sci **110 (Pt 7)**: 847-859.

Wujek, P., E. Kida, M. Walus, K. E. Wisniewski and A. A. Golabek (2004). "N-glycosylation is crucial for folding, trafficking, and stability of human tripeptidyl-peptidase I." J Biol Chem **279**(13): 12827-12839.

Wyzgol, A., N. Muller, A. Fick, S. Munkel, G. U. Grigoleit, K. Pfizenmaier and H. Wajant (2009). "Trimer stabilization, oligomerization, and antibody-mediated cell surface immobilization improve the activity of soluble trimers of CD27L, CD40L, 41BBL, and glucocorticoid-induced TNF receptor ligand." J Immunol **183**(3): 1851-1861.

Xiao, S., K. Matsui, A. Fine, B. Zhu, A. Marshak-Rothstein, R. L. Widom and S. T. Ju (1999). "FasL promoter activation by IL-2 through SP1 and NFAT but not Egr-2 and Egr-3." Eur J Immunol **29**(11): 3456-3465.

Yang, B., M. Steegmaier, L. C. Gonzalez, Jr. and R. H. Scheller (2000). "nSec1 binds a closed conformation of syntaxin1A." J Cell Biol **148**(2): 247-252.

Yatsu, A., N. Ohbayashi, K. Tamura and M. Fukuda (2013). "Syntaxin-3 is required for melanosomal localization of Tyrp1 in melanocytes." J Invest Dermatol **133**(9): 2237-2246.

Yin, X. M., K. Wang, A. Gross, Y. Zhao, S. Zinkel, B. Klocke, K. A. Roth and S. J. Korsmeyer (1999). "Bid-deficient mice are resistant to Fas-induced hepatocellular apoptosis." Nature **400**(6747): 886-891.

Yu, Y., N. C. Fay, A. A. Smoligovets, H. J. Wu and J. T. Groves (2012). "Myosin IIA modulates T cell receptor transport and CasL phosphorylation during early immunological synapse formation." PLoS One **7**(2): e30704.

Zelinskyy, G., S. Balkow, S. Schimmer, K. Schepers, M. M. Simon and U. Dittmer (2004). "Independent roles of perforin, granzymes, and Fas in the control of Friend retrovirus infection." Virology **330**(2): 365-374.

Zheng, L., U. Baumann and J. L. Reymond (2004). "An efficient one-step site-directed and site-saturation mutagenesis protocol." Nucleic Acids Res **32**(14): e115.

Zhu, D., E. Koo, E. Kwan, Y. Kang, S. Park, H. Xie, S. Sugita and H. Y. Gaisano (2013). "Syntaxin-3 regulates newcomer insulin granule exocytosis and compound fusion in pancreatic beta cells." Diabetologia **56**(2): 359-369.

Zimmermann, C., M. Rawiel, C. Blaser, M. Kaufmann and H. Pircher (1996). "Homeostatic regulation of CD8+ T cells after antigen challenge in the absence of Fas (CD95)." Eur J Immunol **26**(12): 2903-2910.

Zuccato, E., E. J. Blott, O. Holt, S. Sigismund, M. Shaw, G. Bossi and G. M. Griffiths (2007). "Sorting of Fas ligand to secretory lysosomes is regulated by mono-ubiquitylation and phosphorylation." J Cell Sci **120**(Pt 1): 191-199.

zur Stadt, U., J. Rohr, W. Seifert, F. Koch, S. Grieve, J. Pagel, J. Strauss, B. Kasper, G. Nurnberg, C. Becker, A. Maul-Pavicic, K. Beutel, G. Janka, G. Griffiths, S. Ehl and H. C. Hennies (2009). "Familial hemophagocytic lymphohistiocytosis type 5 (FHL-5) is caused by mutations in Munc18-2 and impaired binding to syntaxin 11." Am J Hum Genet **85**(4): 482-492.

APPENDIX

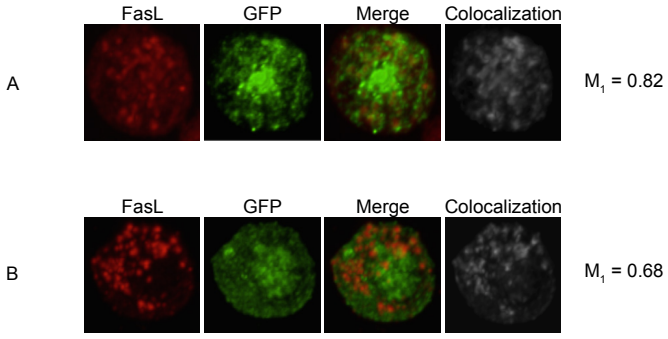

Appendix Figure 1. Rab32 has no detectable effect on FasL localization.
CTL Clone 3/4 cells were transfected with GFP-Rab32 WT **(A)** or GFP-Rab32 T39N **(B)** and stained with specific antibodies for GFP and FasL and the corresponding secondary antibodies. Z-stack images were acquired (interval, 0.4μm) and subjected to three-dimensional reconstruction. Representative projections of the reconstructed three-dimensional images are shown. Colocalization images were created displaying only the regions where the two channels colocalize and the corresponding Manders coefficients (M_1) were calculated.

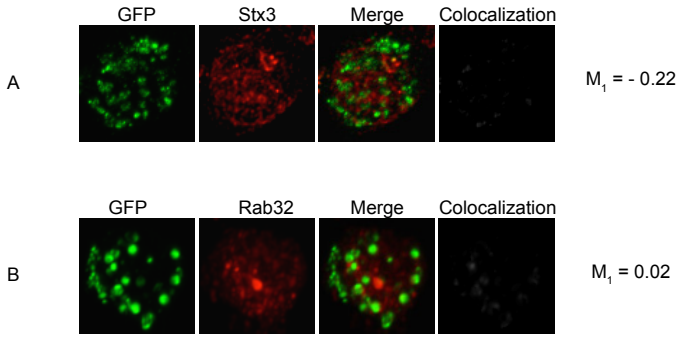

Appendix Figure 2. GFP-FasL is not stored in Stx3$^+$ vesicles.
CTL Clone 3/4 cells transfected with GFP-FasL WT were stained with antibodies specific for GFP and Stx3 **(A)** or Rab32 **(B)** and the corresponding secondary antibodies. Z-stack images were acquired (interval, 0.2μm) and subjected to three-dimensional reconstruction. Representative projections of the reconstructed three-dimensional images are shown. Colocalization images were created displaying only the regions where the two channels colocalize and the corresponding Manders coefficients (M_1) were calculated.